DESIGN, SYNTHESIS OF FLAVOKAWAIN B DERIVATIVE AND THEIR CYTOTOXIC EFFECTS ON MCF-7 AND MDA-MB-231 CELL LINES

ADDILA BINTI ABU BAKAR

Master of Science

UNIVERSITI MALAYSIA PAHANG

UNIVERSITI MALAYSIA PAHANG

DECLARATION OF THESIS AND COPYRIGHT

Author's Full Name : ADDILA BINTI ABU BAKAR

Date of Birth : 26 AUGUST 1992

Title : DESIGN, SYNTHESIS OF FLAVOKAWAIN B DERIVATIVE AND THEIR CYTOTOXIC EFFECTS ON MCF-7 AND MDA-MB-231 CELL LINES

Academic Session : 2015

I declare that this thesis is classified as:

☐	CONFIDENTIAL	(Contains confidential information under the Official Secret Act 1997)*
☐	RESTRICTED	(Contains restricted information as specified by the organization where research was done)*
☑	OPEN ACCESS	I agree that my thesis to be published as online open access (Full Text)

I acknowledge that Universiti Malaysia Pahang reserve the right as follows:

1. The Thesis is the Property of Universiti Malaysia Pahang
2. The Library of Universiti Malaysia Pahang has the right to make copies for the purpose of research only.
3. The Library has the right to make copies of the thesis for academic exchange.

Certified by:

_____ _____

(Student's Signature) (Supervisor's Signature)

_____ _____

New IC/Passport Number Name of Supervisor

Date: Date:

SUPERVISOR'S DECLARATION

We hereby declare that we have checked this thesis and in our opinion, this thesis is adequate in terms of scope and quality for the award of the degree of Master of Science.

_____

(Supervisor's Signature)

Full Name :DR. MUHAMMAD NADEEM AKHTAR

Position : ASSOCIATE PROFESSOR

Date :

_____

(Co-supervisor's Signature)

Full Name : DR. SAIFUL NIZAM BIN TAJUDDIN

Position : ASSOCIATE PROFESSOR

Date :

STUDENT'S DECLARATION

I hereby declare that the work in this thesis is based on my original work except for quotations and citation which have been duly acknowledged. I also declare that it has not been previously or concurrently submitted for any other degree at Universiti Malaysia Pahang or any other institutions.

_____

(Student's Signature)

Full Name : ADDILA BINTI ABU BAKAR

ID Number : MKD15002

Date :

DESIGN, SYNTHESIS OF FLAVOKAWAIN B DERIVATIVE AND THEIR CYTOTOXIC EFFECTS ON MCF-7 AND MDA-MB-231 CELL LINES

ADDILA BINTI ABU BAKAR

Thesis submitted in fulfillment of the requirements
for the award of the degree of
Master of Science

Faculty of Industrial Sciences and Technology

UNIVERSITI MALAYSIA PAHANG

2018

ACKNOWLEDGEMENT

First and foremost, I am very grateful to God the Almighty, the Most Gracious and the Most Merciful for giving me this chance and guiding me through.

I am extremely grateful and would like to express my sincere gratitude to my supervisor, Assoc. Prof. Dr. Muhammad Nadeem Akhtar for his creative ideas, invaluable guidance, continued encouragement, constant support and time spent in making this project possible.

I would also like to express my sincere gratitude to my Co-supervisor, Assoc. Prof. Dr. Saiful Nizam bin Tajuddin for his guidance, constant support and encouragement throughout this project.

I would like to express my sincere appreciation towards my colleague, Siti Noor Hajar binti Zamrus for her continued support and motivation throughout my research project. I would also like to thank all administrative and laboratory staff of Faculty of Industrial Sciences & Technology for their enormous help in any way needed to complete this research project.

I am very thankful to Assoc. Prof. Dr. Noorjahan Banu Alitheen, and her master's students, Nurul Fattin binti Che Rahim, Muhammad Nazirul Mubin bin Aziz and Yazmin binti Hussin from Faculty of Biotechnology and Biomolecular Science, Universiti Putra Malaysia for their generous help, particularly in the study of biological activities.

I would also like to express my gratitude to Dr. Seema Zareen as well as Universiti Malaysia Pahang and Ministry of Higher Education for their trust and financial support, which have helped me completing my master's degree.

Last but not least, I am grateful to my parents for their understanding, financial support and prayers. My appreciation also goes to everyone who has either directly or indirectly involved in this project.

ABSTRAK

Kanser adalah antara punca kematian di mana kanser payudara merupakan kanser yang kedua terbanyak di kalangan wanita di seluruh dunia. Rawatan kanser dengan ubat kanser, kemoterapi dan radiasi yang biasa digunakan telah menyebabkan kesan yang tidak diingini pada pesakit. Oleh itu, kalkon dengan pelbagai manfaat farmakologi seperti anti-kanser, anti-mitosis, dan lain-lain, telah mendapat perhatian sebagai subjek penyelidikan. Derivatif kalkon flavokawain B yang mengandungi kumpulan metoksi, dimetoksi, trimetoksi, bromo, kloro, floro, metil, metiltio, nitro, hidroksil dan dimetilamino pada benzaldehida telah disintesis melalui kaedah kondensasi Claisen-Schmidt menggunakan pemangkin alkali; sebatian yang disintesis dicirikan dengan menggunakan spektrofotometri Ultraungu-Nampak (UV-Vis), spektroskopi Infrared (FTIR), Kromatografi Gas-Spektrometri Jisim (GC-MS) dan spektroskopi Resonans Magnetik Nuklear (NMR); dan dinilai untuk kesitotoksikan mereka terhadap sel kanser payudara dengan menggunakan asai MTT. Antara 22 sebatian yang disintesis, dua sebatian **80** dan **91** telah ditemui sebagai analog flavokawain B yang baru dan beberapa sebatian menunjukkan aktiviti anti-kanser yang bagus berikutan had nilai, IC_{50} adalah kurang daripada 30 μg/mL. Sebatian tersebut adalah kalkon **4** (7.70 ± 0.30 μg/mL), **5** (8.90 ± 0.60 μg/mL), **75** (12.30 ± 1.40 μg/mL), **79** (6.50 ± 0.40 μg/mL), **80** (7.12 ± 0.80 μg/mL), **82** (9.70 ± 0.70 μg/mL), **84** (5.50 ± 0.35 μg/mL), **85** (8.43 ± 0.40 μg/mL), **44** (13.30 ± 3.10 μg/mL) dan **90** (6.50 ± 0.35 μg/mL) yang menunjukkan aktiviti anti-kanser yang baik terhadap MCF-7. Kalkon **4** (5.90 ± 0.30 μg/mL), **5** (6.80 ± 0.45 μg/mL), **75** (18.10 ± 1.10 μg/mL), **79** (4.12 ± 0.20 μg/mL), **80** (4.04 ± 0.30 μg/mL), **81** (9.50 ± 0.60 μg/mL), **82** (8.30 ± 0.56 μg/mL), **84** (5.50 ± 0.40 μg/mL), **85** (7.22 ± 0.70 μg/mL) dan **44** (17.10 ± 2.15 μg/mL) yang menunjukkan aktiviti anti-kanser yang baik terhadap MDA-MB-231, serta sebatian **79** dan **80** didapati lebih aktif daripada ubat rujukan doksorubisin (5.05 ± 0.20 μg/mL). Kajian perhubungan struktur-aktiviti menunjukkan bahawa sitotoksik yang bertambah baik ditunjukkan oleh derivatif flavokawain B dengan kumpulan halogen, diikuti oleh derivatif flavokawain B dengan kumpulan metoksi terutamanya ketika penggantian terjadi pada kedudukan 2 dan 3 di cincin aromatik B.

ABSTRACT

Cancer is among the cause of death whereof breast cancer is the second leading cause of cancer death among women worldwide. Cancer treatment with standard anti-cancer drug, chemotherapy and radiation have caused unwanted side effects in the patient. Therefore chalcone with many pharmacological benefits such as anti-cancer, anti-mitotic, etc., has gained attention as a subject of research. Flavokawain B derivative chalcones bearing methoxy, dimethoxy, trimethoxy, bromo, chloro, fluoro, methyl, methylthio, nitro, hydroxyl and dimethylamino groups on benzaldehyde were synthesized via Claisen-Schmidt condensation method using base catalyst; the synthesized compounds were characterized by using UV-Visible, Fourier Transform Infrared spectrophotometry (FTIR), Gas Chromatography-Mass Spectrometry (GC-MS) and Nuclear Magnetic Resonance (NMR) spectrometry and evaluated for their cytotoxicity against breast cancer cell line by using 3-(4,5-dimethylthiazol-2-yl)-2,5-diphenyltetrazolium bromide (MTT) assay *in vitro*. Among 22 synthesized compounds, two compounds, **80** and **91** have been discovered as new flavokawain B analogs and some compounds showed good anti-cancer activity following the cut-off point value, IC_{50} is less than 30 μg/mL. The compounds are chalcone **4** (7.70 ± 0.30 μg/mL), **5** (8.90 ± 0.60 μg/mL), **75** (12.30 ± 1.40 μg/mL), **79** (6.50 ± 0.40 μg/mL), **80** (7.12 ± 0.80 μg/mL), **82** (9.70 ± 0.70 μg/mL), **84** (5.50 ± 0.35 μg/mL), **85** (8.43 ± 0.40 μg/mL), **44** (13.30 ± 3.10 μg/mL) and **91** (6.50 ± 0.35 μg/mL) that exhibited good anti-cancer activity against MCF-7. Chalcone **4** (5.90 ± 0.30 μg/mL), **5** (6.80 ± 0.45 μg/mL), **75** (18.10 ± 1.10 μg/mL), **79** (4.12 ± 0.20 μg/mL), **80** (4.04 ± 0.30 μg/mL), **81** (9.50 ± 0.60 μg/mL), **82** (8.30 ± 0.56 μg/mL), **84** (5.50 ± 0.40 μg/mL), **85** (7.22 ± 0.70 μg/mL) and **44** (17.10 ± 2.15 μg/mL) showed good anti-cancer activity against MDA-MB-231 as well as compound **79** and **80** was discovered to be more active than the reference drug doxorubicin (5.05 ± 0.20 μg/mL). Structure-activity relationship study suggested that significantly improved cytotoxicity was shown by halogenated flavokawain B, followed by methoxylated flavokawain B, particularly when substitution occurred at position 2 and 3 in ring B.

TABLE OF CONTENT

LIST OF TABLES

LIST OF FIGURES

LIST OF SYMBOLS

s	Singlet
d	Doublet
t	Triplet
m	Multiplet
J	Coupling constant
W	Watt
MHz	Mega Hertz
mg/mL	Milligram per millilitre
U/mL	Unit per millilitre
m/z	Mass to charge ratio
µM	Micromolar
µg/mL	Microgram per millilitre
α	Alpha
β	Beta
λ_{max}	Maximum wavelength
δ	Delta

LIST OF ABBREVIATIONS

^{13}C-NMR	Carbon Nuclear Magnetic Resonance
^{1}H-NMR	Proton Nuclear Magnetic Resonance
ABCG2	ATP-binding cassette sub-family G member 2
BCRP	Breast cancer resistance protein
BF_3-Et_2O	Boron trifluoride diethyl etherate
CC	Column chromatography
$CDCl_3$	Deuterated chloroform
CF_3	Trifluoromethyl
CO_2	Carbon dioxide
CuTC	Copper(I)-thiophene-2-carboxylate
DMEM	Dulbecco's Modified Eagle Medium
DMF	Dimethylformamide
DMSO	Dimethyl sulfoxide
ED_{50}	Median effective dose
FBS	Fetal Bovine Serum
FTIR	Fourier Transform Infrared spectroscopy
GC-MS	Gas Chromatography-Mass Spectrometry
GI_{50}	50% growth inhibition
Hep-G2	Liver hepatocelular carcinoma
IC_{50}	Concentration for 50% inhibition
K_2CO_3	Potassium carbonate
KOH	Potassium hydroxide
LU	Lung adenocarcinoma
MCF-7	Human breast adenocarcinoma cell line
MDA-MB-231	Human breast adenocarcinoma cell line
MDR	Multi-drug resistance

MIC	Minimum inhibitory concentration
MTT	3-(4,5-dimethylthiazol-2-yl)-2,5-diphenyltetrazolium bromide
NaOH	Sodium hydroxide
NMR	Nuclear Magnetic Resonance spectroscopy
OCH_3	Methoxy
P338	Leukemia
PARP	Poly (ADP ribose) polymerase
PBS	Phosphate buffer saline
Pd	Palladium
$Pd(dba)_2$	Bis(dibenzylideneacetone)palladium(0)
$PdCl_2$	Palladium(II) chloride
p-gp	Permeability glycoprotein
PPh_3	Triphenylphospine
RPMI	Roswell Park Medium Institute
$S\text{-}CH_3$	Thio-methyl
$SOCl_2$	Thionyl Chloride
SSG	Sodium stigluconate
SW480	Colon adenocarcinoma
TLC	Thin Layer Chromatography
UV-Vis	Ultraviolet-visible spectroscopy
VRP	Verapamil

CHAPTER 1

INTRODUCTION

1.1 Background of Research

Chalcone (1,3-diphenyl-2-propene-1-one), also known as benzylidene-acetophenone, consists of two aromatic rings that are linked by a three carbon α,β-unsaturated carbonyl system. It is an aromatic ketone that acts as a precursor of flavonoids and isoflavonoids, which are widely present in edible plants (Rahman, 2011). Chalcone is in flavonoid family and they are one of major class of natural products which are widely distributed in fruit, vegetables, tea, soy-based food and spices (Nowakowska, 2007). Flavonoid structure was formed due to the closure of hydroxychalcone structure. Flavonoids are responsible in pigments for hue of autumn and floral colors of yellow, orange and red (Carlo et al., 1999); and they are extensively distributed secondary metabolites with diverse metabolic functions in plants (Ferreyra et al., 2012). The main factor contributed to its biologically active nature is the presence of α,β-unsaturated carbonyl system of chalcone (Yerragunta et al., 2013). They are believed to exhibit multiple pharmacological activities such as anti-inflammatory, anti-infective, anti-cancer, anti-oxidant, anti-bacterial, anti-malarial, anti-proliferative and anti-invasive (Coşkun et al., 2016; Mai et al., 2014). Flavokawain A, B and C are among chalcones that are widely found in the extract of kava-kava plant, whereof flavokawain A and flavokawain B are known to have anti-cancer property (Abu et al., 2016; Abu et al., 2014).

Cancer is an environmental disease with 90-95% of cases are attributed to environmental factors such as exposure to different types of chemical and radiation, and another 5-10% of cases are due to genetic mutations which is inherited in some families. Worldwide, breast cancer is the most common cancer among women after skin cancer, and it is also the second leading cause of cancer death in women after lung cancer. Studies in 2016 have reported that there were 2,600 new cases of breast cancer

in men, 246,660 new cases in women and about 61,000 cases of carcinoma *in situ* of female breast diagnosed in United States (Siegel et al., 2016).

Chalcones are regarded as promising anti-cancer agents against most of the human cancers. Previous literature suggested that chalcones are capable of inducing apoptosis and also have the ability to uncouple mitochondrial respiration, resulting collapse mitochondrial membrane potential (Mai et al., 2014). Hence, chalcones and its derivatives are the interesting subject for research to be investigate about the potent anti-cancer effects of these compounds against the breast cancer cell lines.

There are several methods used to synthesize chalcones and three major synthesis pathways are being extensively used. The three pathways are (1) Claisen-Schmidt condensation reaction between the corresponding acetophenone and the corresponding aromatic aldehyde in the presence of base catalyst such as potassium hydroxide or sodium hydroxide, (2) Suzuki coupling reaction between cinnamoyl chloride and phenylboronic acids and (3) palladium-catalyzed carbonylative vinylation. Among these methods, Claisen-Schmidt condensation reaction are the most commonly used method to synthesize chalcones due to its simple operation, high reaction yields and eco-friendly nature.

1.2 Problem Statement

Cancer is the third leading cause of death after heart disease and stroke in the developing countries and the second leading cause of death (after heart disease) globally. Worldwide, breast cancer is the most common cancer among women after skin cancer and also the second leading cause of cancer death in women. Studies have shown that in 2017, there were 600,920 cases of cancer death and 63,410 cases of female breast carcinoma *in situ* reported in United States (Siegel et al., 2017). In Malaysia, breast cancer is the most common cancer and frequently diagnosed disease, affecting Malaysian women from all ethnic groups (Loganathan et al., 2015).

Many anti-cancer drugs for instance doxorubicin have solubility and resistance problems. Multi-drug resistance (MDR) is a major problem for the success of cancer chemotherapy and closely associated with treatment failure in cases of most common cancer types, as lung, colon, breast, and cervical cancer. Although the chemotherapy and radiation for breast cancer destroy the constantly dividing breast cancer cells, these

treatments can also attack the healthy cells. Many patients that undergo these treatment suffer from side effects such as nausea, vomiting, lethargy, cachexia and poor oral consumption (Mai et al., 2014). Moreover, many conventional drugs cannot effectively bind to receptors in target cells due to poor drug efficacy which response to the side effects.

There are several methods that can be used to synthesize chalcone and its derivatives. Challenges in the synthesis of chalcone and its derivatives includes the possibility that the reaction may not occur, uncertainty in reaction yield, and the production of unwanted by-products. Different reactants may require the use of different synthesis methods. The reaction with the presence of hydroxyl substituent in the aromatic aldehyde retards the base-catalyzed aldol reaction. Basic catalysts decrease the activity of aldehyde component by causing delocalization of the anion (Dhar, 1981).

1.3 Objectives

1. To synthesize and characterize flavokawain B derivative.
2. To investigate the cytotoxic properties of flavokawain B derivative.
3. To establish the structure-activity relationship between different substituted flavokawain B derivative.

1.4 Scope of Study

The aim of this research is to determine the new potential drug that potential for breast cancer cell line. This research has focused on flavokawain B and its derivative due to their significant pharmacological activity. Flavokawain B derivative have been synthesized via Claisen-Schmidt condensation reaction by using basic catalyst. The synthesized compounds were purified by column chromatography (CC), followed by crystallization and purity of the compounds have been monitored by using Thin Layer Chromatography (TLC) technique. The structure of synthesized compounds have been characterized by using UV-Visible, Fourier Transform Infrared spectrophotometry (FTIR), Gas Chromatography-Mass Spectrometry (GC-MS), and Nuclear Magnetic Resonance (NMR). Finally, the synthesized compounds have been tested for their cytotoxicity against breast cancer cell line, MCF-7 and MDA-MB-231 by using 3-(4,5-

dimethylthiazol-2-yl)-2,5-diphenyltetrazolium bromide (MTT) assay and the structure-activity relationship of different substituted benzaldehyde used in the synthesis have been studied.

CHAPTER 2

LITERATURE REVIEW

2.1 Overview of Chalcone

Chalcone comes from the flavonoid family and known as benzylidene-acetophenone or 1,3-diphenyl-2-propene-1-one. It consists of two aromatic ring linked by a three carbon α,β-unsaturated carbonyl system and contains conjugated double bonds. It has π-electron system that is completely delocalized on benzene ring A and B (Yerragunta et al., 2013). Chalcones are widely found in fruit and vegetables and responsible for pigments of color ranged from yellow to orange in flower and diverse tissues of plants (Aksöz et al., 2011). Chalcone, which is in flavonoid family act as the precursor of flavonoid and isoflavonoid and play an important role in the growth, development of plant. It exists as secondary metabolites with multiple metabolic functions in plants (Ferreyra et al., 2012). Flavonoid protect the leaf cells from photo-oxidative damages and enhances the nutrient retrieval during senescence (Feild et al., 2001).

2.2 Synthesis of Chalcone

Chalcone has been identified as an interesting compound with multiple biological activities and the discovery has led to development of various methods for synthesis of chalcone.

2.2.1 Claisen-Schmidt Condensation Method

Chalcone and its derivatives have been synthesized by Claisen-Schmidt base-catalyzed condensation of acetophenone and aromatic aldehyde in the presence of sodium hydroxide (NaOH) in ethanol (EtOH) as shown in Figure 2.1. Similar reaction have been carried out in the presence of potassium hydroxide (KOH) in methanol

(MeOH) as reported in (Aksöz et al., 2011) and shown in Figure 2.2. The reaction mixture was stirred for 18 hr at room temperature (rt) (Weldon et al., 2014). The residue was purified by column chromatography equipped with silica gel in mixture of 10% ethyl acetate and 90% hexane as eluent and the products were characterized using different types of spectroscopic techniques (Bandgar et al., 2010a). Chalcone and its derivatives in Figure 2.3 were the example product from reaction using Claisen-Schmidt condensation method.

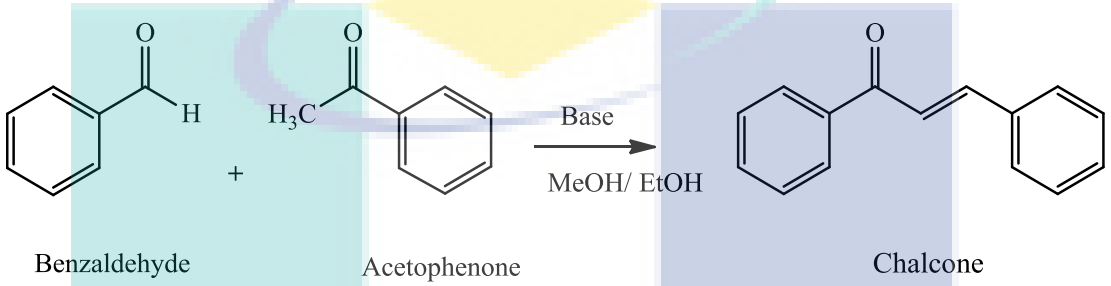

Figure 2.1 Synthesis of chalcone via Claisen-Schmidt condensation

Source: Yerragunta (2013)

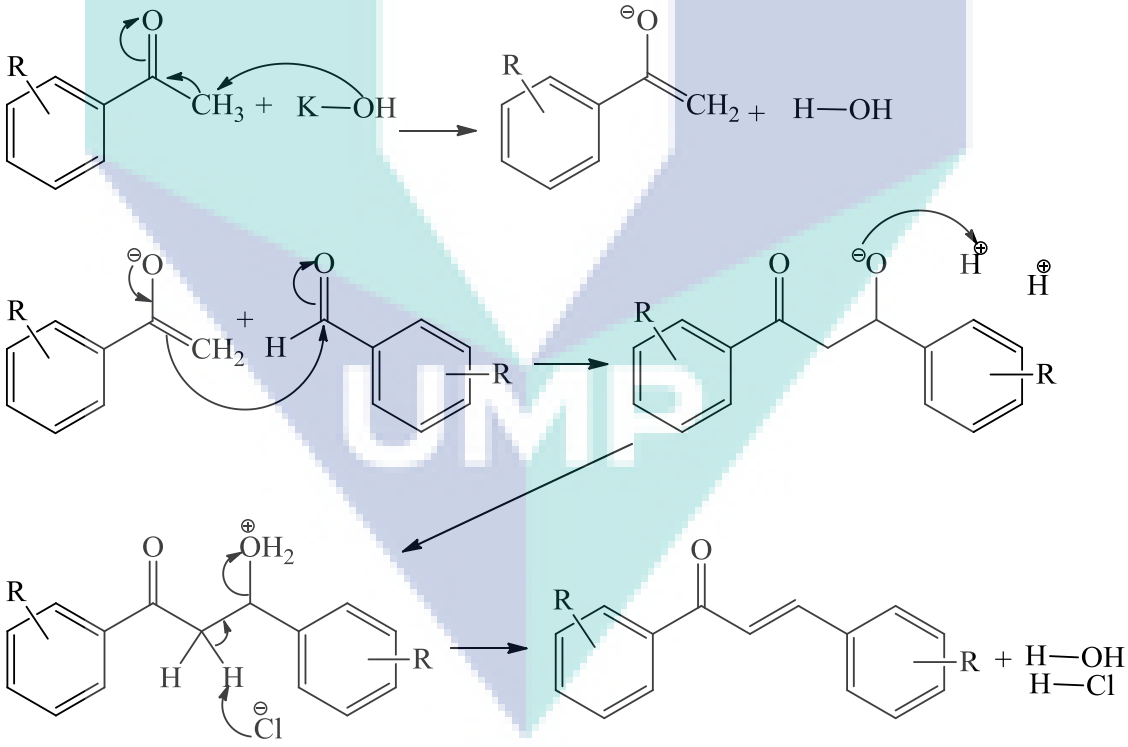

Figure 2.2 Mechanism in synthesis of chalcone via base-catalyzed Claisen-Schmidt condensation

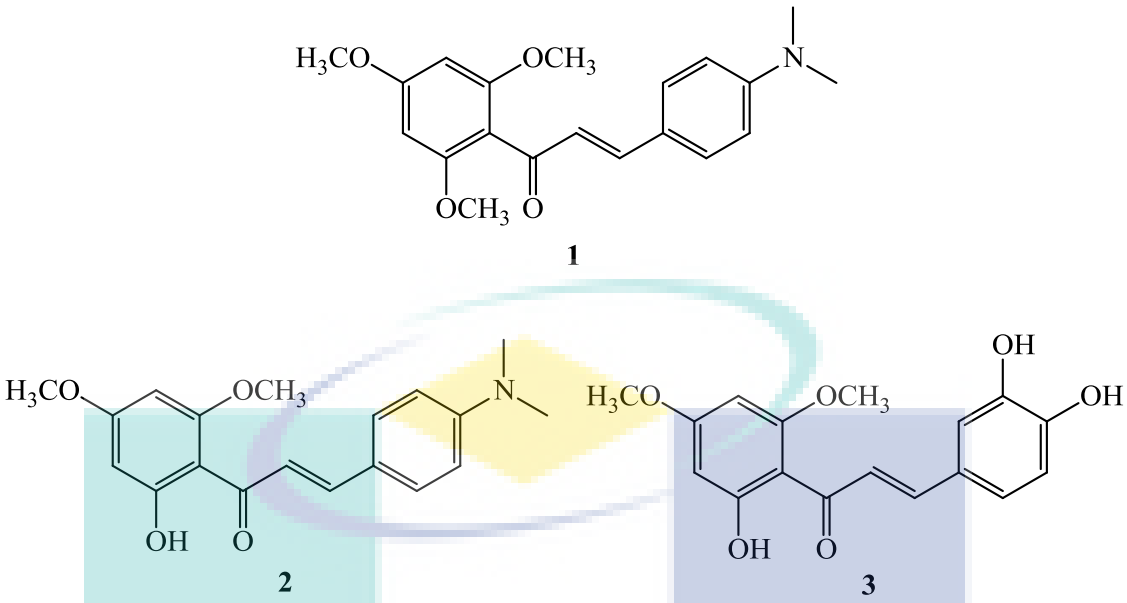

Figure 2.3 Chalcones derivatives (**1-3**) synthesized via Claisen-Schmidt condensation method

Source: Akhtar (2015)

2.2.2 Acid Catalyzed Aldol Reaction

One of the most commonly used method for the synthesis of chalcones is Claisen-Schmidt condensation carried out in basic aqueous alkaline solutions. However, the presence of hydroxyl substituent on aromatic aldehyde has been found to retard the base-catalyzed aldol reaction. Basic catalysts decrease the activity of aldehyde component by causing delocalization of the anion. It is necessary to use protective groups for the preparation of the hydroxychalcones under basic conditions, and thus acid catalyzed aldol reaction has been the preferred method for such purposes (Go et al., 2005).

Acetophenone and benzaldehyde in absolute ethanol (abs. EtOH) were mixed together and thionyl chloride ($SOCl_2$) was added dropwise as shown in Figure 2.4. The reaction mixture was stirred for 2 hr at room temperature (rt) and left standing for 12 hr before precipitated by the addition of water. The product was filtered, washed with cold ethanol and dried to form yellow crystals. (Petrov et al., 2008).

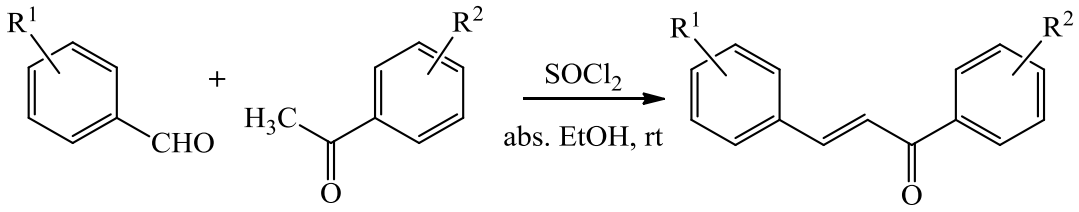

Figure 2.4 Synthesis of chalcone via Aldol reaction with acid catalyst

Source: Petrov (2008)

2.2.3 Microwave Irradiation Method

Chalcone has also been synthesized by using microwave irradiation (MWI) method. Figure 2.5 shows the condensation of both *ortho*-hydroxyacetophenone and aromatic aldehyde in the presence of potassium carbonate (K_2CO_3) was carried out under microwave irradiations within 3-5 min (Jayapal et al., 2010). Another procedure for synthesis of chalcone using microwave irradiation method is the reaction between 2-acetyl hetero cyclic derivatives and respective aldehydes. Both reactants were mixed and dissolved in minimum amount of alcohol. Then, aqueous potassium hydroxide solution was slowly added and mixed well. The entire reaction mixture was subjected to microwave irradiation for about 2–6 min at 180 watts (W) (Ahmad et al., 2011)

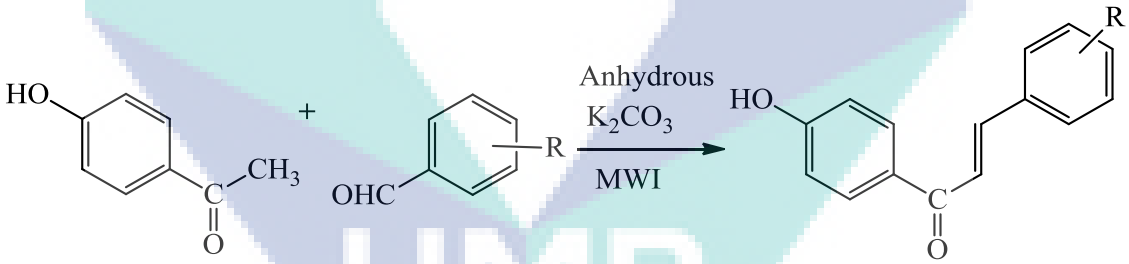

Figure 2.5 Synthesis of chalcone derivatives by using microwave irradiation

Source: Jayapal (2010)

2.2.4 Synthesis of Chalcone by Using Boron Trifluoride Etherate

Several chalcones have been synthesized by reacting substituted acetophenone with substituted benzaldehyde by using boron trifluoride etherate (BF_3–Et_2O). The reaction in Figure 2.6 was conducted for 15-150 min at room temperature. The solution was washed with moist ether and water to discharge the color and the BF_3–Et_2O complex. The ethereal solution obtained from the extraction was then dried over anhydrous sodium sulphate (Na_2SO_4) and evaporated under reduced pressure (Narender et al., 2007).

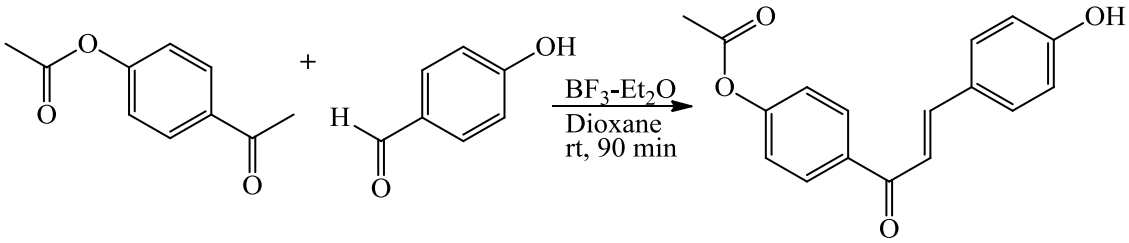

Figure 2.6 Examples of chalcone derivatives synthesized by using Boron trifluoride etherate

Source: Narender (2007)

2.2.5 Palladium-Catalyzed Chalcone Synthesis

2.2.5.1 Cross-coupling Reaction of Aryl or Alkenylboronic Acids with Acid Chlorides

The chalcone can be synthesized by cross-coupling reaction of aryl or alkenyl-boronic acid with acid chlorides catalyzed by palladium using bis(dibenzylidene-acetone)palladium(0) ($Pd(dba)_2$) at room temperature, in the presence of copper(I) thiophene-2-carboxylate (CuTC) and triphenylphospine (PPh_3) which act as the activators in diethyl ether (Et_2O) as shown in Figure 2.7 and Figure2.8. This reaction has been performed under non-basic conditions. (Ogawa et al., 2013).

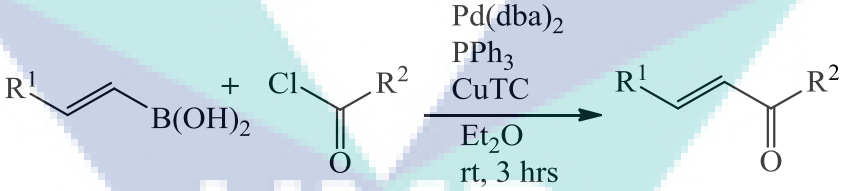

Figure 2.7 Cross-coupling reaction of alkenylboronic acids with acid chlorides

Source: Ogawa (2013)

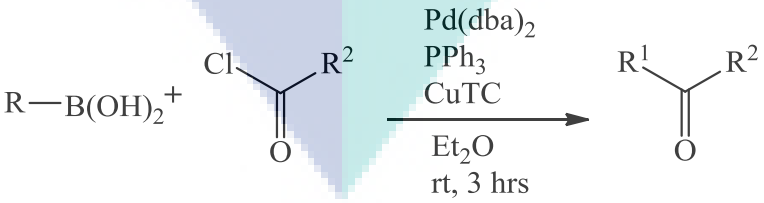

Figure 2.8 Cross-coupling reaction of arylboronic acids with acid chlorides

Source: Ogawa (2013)

2.2.5.2 General Procedure for Reaction of 3-benzoylacrylic Acid with Arylboronic Acid

The synthesis of chalcone derivatives can be achieved by reaction of 3-benzoylacrylic acids that undergo decarboxylative arylation with arylboronic acids or aryl halides, catalyzed by palladium in the presence of copper salt oxidant as shown in Figure 2.9. The mixture of starting materials and catalyst were stirred under nitrogen at 120°C (bath temperature) for 4−5 hr. After being cooled, the reaction mixture was quenched with water and extracted with ethyl acetate. The combined organic layer was dried over sodium sulphate (Na_2SO_4) (Unoh. et al., 2013).

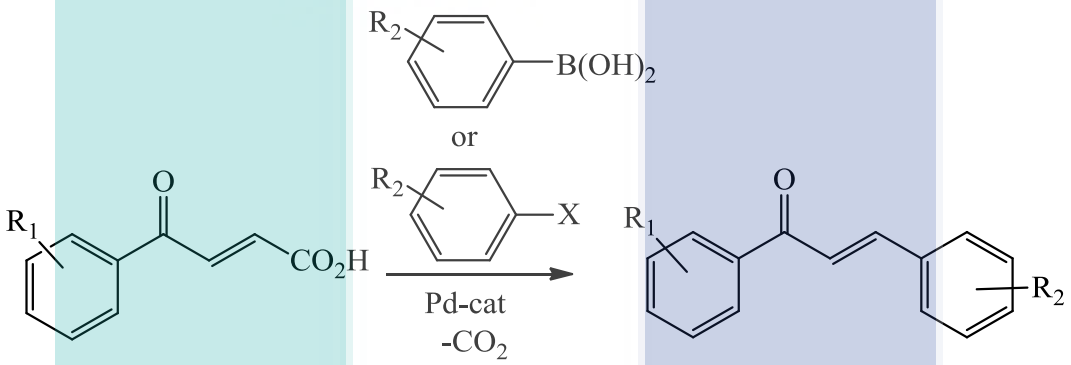

Figure 2.9 General reaction of 3-benzoylacrylic acid with arylboronic acid or aryl halides

Source: Unoh (2013)

2.2.5.3 Cross-coupling reaction of benzoyl chlorides with potassium styryltrifluoroborate

Synthesis of chalcone has been achieved through the cross-coupling reaction of potassium styryltrifluoroborate and benzoyl chloride with palladium(II) chloride ($PdCl_2$) as catalyst in a microwave (MW) tube. The reactants were flushed with argon for 1-2 min to prevent the presence of air triggering the decomposition of the palladium catalyst followed by the addition of dry 1,4-dioxane from a sure-seal bottle. The resulting mixture in the microwave tube was then inserted into the microwave and heated at 140°C for 30 min at 300 W as shown in Figure 2.10 (Al-Masum et al., 2011).

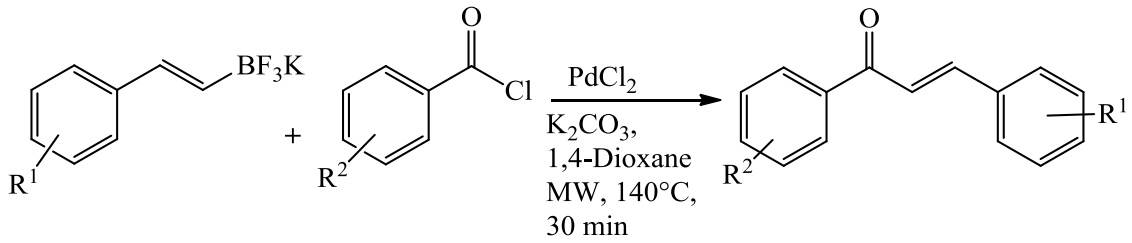

Figure 2.10 Cross-coupling reaction of benzoyl chlorides with potassium styryltrifluoroborate

Source: Al-Masum (2011)

2.2.6 Suzuki Coupling Reaction

As phenols are very sensitive to autoxidation under even slightly basic conditions, there is a need for protecting group that is cleavable under neutral or slightly acidic conditions. The mild conditions of Suzuki coupling reaction has allowed the use of methoxymethylether (MOM) as a protecting group for phenolic compounds (Eddarir et al., 2003).

There are two pathways that are readily available for the synthesis of chalcones: Pathway A that involved the coupling between activated cinnamic acids and phenylboronic acids diluted with absolute toluene, catalyzed by tetrakis(triphenyl-phospine)palladium(0) ($(PPh_3)_4Pd$) in the presence of base cesium carbonate (Cs_2CO_3) as shown in Figure 2.11; Pathway B that involved the coupling between activated benzoic acids and phenylvinylboronic acids using toluene as a solvent, catalyzed by tetrakis(triphenylphospine)palladium(0) in the presence of base cesium carbonate as shown in Figure 2.12.

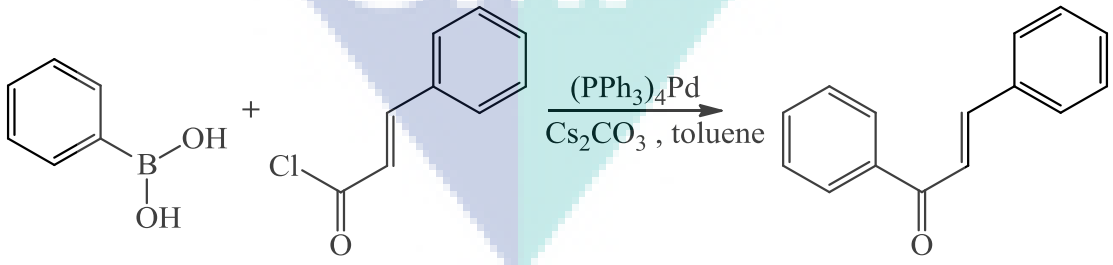

Figure 2.11 Pathway A, the coupling between activated cinnamic acids and phenylboronic acids

Source: Eddarir (2003)

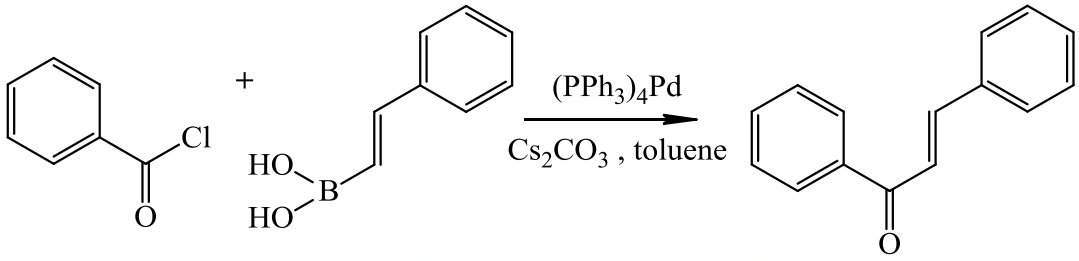

Figure 2.12 Pathway B, the coupling between activated benzoic acids and phenylvinylboronic acids

Source: Eddarir (2003)

2.3 Pharmacological Activities of Chalcones

Chalcones are among the important compounds which are mostly obtained from natural sources and the examples include flavokawain A, B and C. Chalcones have exhibited multiple pharmacological activities including anti-leishmanial where stated in previous research by Ruiz (2011), natural chalcone derivative extracted from leaves of *Piper hispidum* exhibited anti-leishmanial activity with an IC_{50} value of 0.8 µM when tested against *Leishmanial amazonensis* axenic amastigotes (Ruiz et al., 2011); anti-cancer where according to Jin (2013), some chalcone derivatives with pyrimidinyl group has showed anti-cancer against several human cancer cell line better than curcumin and Fluorouracil (5-FU) such as oral carcinoma cell (KB) with IC_{50} 5.55 µM, nasopharyngeal carcinoma cell (CNE2) with IC_{50} value 10.7 µM, against gastric carcinoma (MGC-803) with IC_{50} value 12.5 µM, breast carcinoma with IC_{50} value 15.9 µM, leukemia cell with IC_{50} value 18.6 µM (C. Jin et al., 2013). Study by Chinthala (2015) stated that the chalcone-triazole derivatives showed anti-cancer activity against A549 (lung adenocarcinoma) cell line with range of IC_{50} value 35.81-65.86 µM in comparison with doxorubicin IC_{50} value of 69.30 µM, and one compound from these chalcone-triazole derivatives exhibited promising anti-cancer against human cancer cell lines A-549 (lung adenocarcinoma), MCF-7 (breast adenocarcinoma), DU-145 (prostate carcinoma), IMR-32 (neuroblastoma) and Hep-G2 (hepatoma) with IC_{50} value range of 17.11-69.90 µM (Chinthala et al., 2015); Chalcone have anti-inflammatory where in study by Herencia 2002 where chalcone derivatives has exhibited NO-scavenging properties (Herencia et al., 2002); anti-fungal activity by substituted oxathiolone fused chalcone against *Candida albicans* with IC_{50} value of 62.5 µg/mL (Konieczny et al., 2007); anti-invasive where chalcones help to inhibit the invasive of the human MCF-7/6 mammary carcinoma cell line onto normal embryonic chick heart (Mukherjee et al.,

2001); anti-tuberculosis when chalcone derivatives at concentration 12.5 µg/mL screened on *Mvcobacterium tuberculosis* H_{37}Rv exhibited greater than 90% inhibition of tuberculosis bacteria, (Y.-M. Lin et al., 2002); anti-malarial where in research by M Liu (2001) and Hans (2010) , chalcones show growth inhibition against the strain of *Plasmodium falciparum* (Hans et al., 2010); (M Liu et al., 2001), immunosuppressive (Luo et al., 2012); anti-mitotic (Boumendjel. et al., 2008.); and anti-oxidant (Gopi et al., 2016). Chalcones have also been found to act as anti-fibrogenic and modulate the p-glycoprotein-mediated multi-drug resistance (Go et al., 2005) and play a role as cysteinyl leukotriene receptor-1 antagonist (Zwaagstra et al., 1998).

Chemically, chalcones consist of two aromatic rings joined by a three carbon α,β-unsaturated carbonyl group. Chalcones have been found to be the precursor of flavonoids and isoflavonoids, abundantly available in edible plants and have also been known to display a various array of pharmacological activities. Among the flavonoids, chalcones are the most interesting compounds, which have been extensively investigated for their broad range of biological activities that include anti-inflammatory, anti-invasive, anti-tumor and anti-bacterial (Abu et al., 2015; Ahmad et al., 2011; Roman et al., 2012; Won et al., 2005).

Recent reports have suggested that chalcones have exhibited anti-microbial (anti-bacterial and anti-fungal) activity which screened against *Escheria coli*, *Pseudomonas aeruginosa*, *Aspergillus niger* and *Aspergillus flavus* (Prasad et al., 2008b; Tiwari et al., 2010), anti-malarial when screened against *Plasmodium falciparum* chloroquine sensitive strain 3D7 and K1 that give low cytotoxicity with minimum inhibitory concentration in range 0.25-1.19 µM, (Tadigoppula et al., 2012), anti-inflammatory activities against TNF-α (tumor necrosis factor alpha) and IL-6 (interleukin 6) with 90-100% inhibition at 10 µM concentration (Bandgar et al., 2010a). Flavokawain B (**4**), flavokawain A (**5**) and flavokawain C (**6**) in Figure 2.13 are among the naturally occurred chalcones that have been extracted from kava-kava plant, *Piper methsyticum*, which has been traditionally known as the tonic of Pacific islands. The compounds play a vital role through their wide range of biological activities (Abu et al., 2014; Dharmaratne et al., 2002). The extract from the roots of this plant contains a variety of interesting molecules including chalcone **4** and **5** which have been known for their anti-cancer property (Abu et al., 2016; Abu et al., 2014).

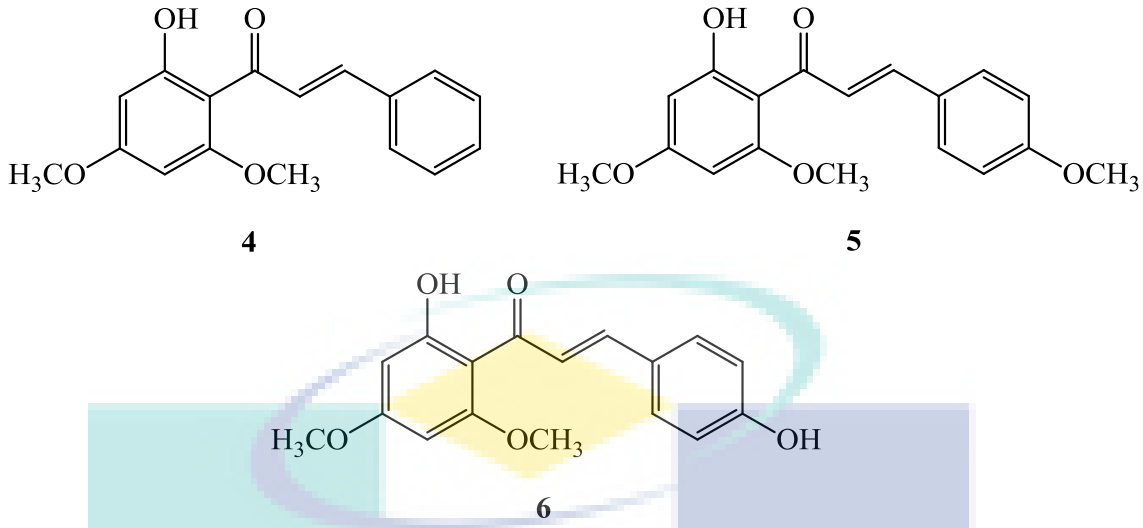

Figure 2.13 Natural chalcone Flavokawain B (**4**), A (**5**) and C (**6**) from kava-kava plant

Source: Dharmaratne (2002)

2.3.1 Anti-cancer Properties

Anti-cancer drug refer to any drug that works effectively in the treatment of malignant or cancerous disease. (Gu et al., 2012). Permeability-glycoprotein (P-gp) is an ATP-binding cassette transporter that functions as a biological barrier by releasing toxins and xenobiotics out of cells, plays an important role in drug absorption and disposition (J. H. Lin et al., 2003). Permeability-glycoprotein is also known as multi-drug resistance protein 1 that act as an efflux pump by translocating the substrate from the intracellular to the extracellular compartment (Kim, 2002). Over-expression of po-glycoprotein can interrupt the efficacy of anti-cancer drug and become major problem to the successful cancer chemotherapy (Gu et al., 2012). Several studies of chalcones have showed that chalcones could act as P-gp and breast cancer resistance protein (BCRP) inhibitor, thus reversing P-gp and BCRP mediated-MDR (Juvale et al., 2013). Chalcones, especially bifendate-chalcone hybrids could reverse permeability-glycoprotein (P-gp) mediated multidrug resistance (MDR) more potently than verapamil (VRP) by inhibiting P-gp efflux function with the very low intrinsic cytotoxicity where the IC_{50} value more than 200 μM.

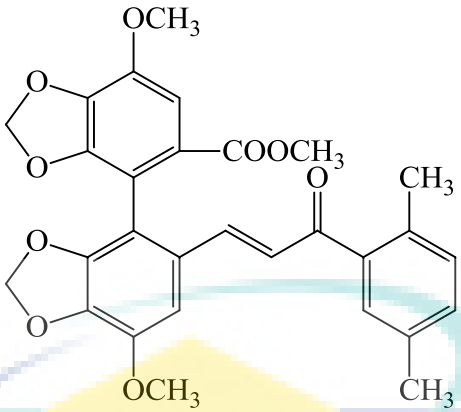

7

Figure 2.14 Bifendate-chalcone hybrid as permeability-glycoprotein (P-gp) and breast cancer resistance protein (BCRP) inhibitor

Source: Gu (2012)

Bifendate-chalcone hybrid, **7** with methyl substituent at *ortho* and *meta* position in ring A as shown in Figure 2.14; has exhibited remarkable inhibitory effect on BCRP thus reversing P-gp and BCRP mediated-MDR (Gu et al., 2012). Chalcone has exhibited cytotoxic activity related with tubulin inhibition and the ability to interfere with microtubule formation. Dihalogenated chalcones series **8** and **9** with electron-rich 4-diethylaminophenyl group, compound **10-11** with unsubstituted aromatic ring and compound **12** with elongated styryl group at position 3 on chalcone structure from Figure 2.15 have been found to inhibit the tubulin polymerization. Compound **13** shown in Figure 2.15 is a dienone derivative which has been found to stabilize the tubulin to the same extent of doxatacel, anti-cancer drug. Compound **8-13** exhibit cytotoxic activities towards individual cancer cells such as NCI-H69 (small-cell lung cancer), U937-GTB (lymphoma), RPMI 8226 (myeloma) and CCRF-CEM (leukemia) with IC_{50} value ranged from 5.2-20.0 μM, 8.2-49.0 μM, 18.7-119 μM, and 14.8-280 μM, respectively for each cancer cell. (Dyrager et al., 2011).

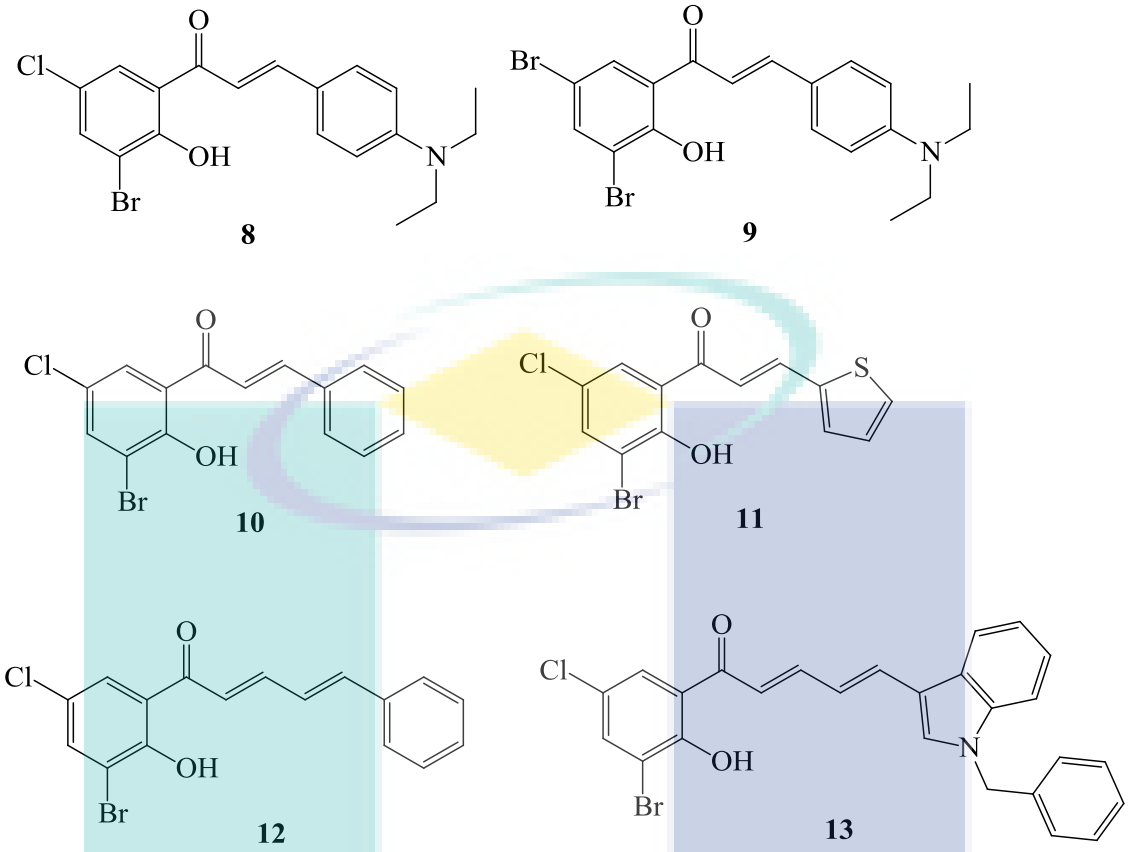

Figure 2.15 Dihalogenated chalcones and dienone derivative that inhibit tubulin polymerization, stabilize the tubulin and exhibit cytotoxicity against RPMI 8226 (myeloma), CCRF-CEM (leukemia), U937-GTB (lymphoma) and NCI-H69 (small-cell lung cancer) cell line

Source: Dyrager (2011)

Additionally, compounds **14-15** as series of chalcones linked imidazolones with methoxy and hydroxyl substituents at position 3 and 4 in ring B, and phenyl and 4-chloro phenyl substituent at imidazolones ring shown in Figure 2.16 have demonstrated good anti-cancer activity. Compound **14-15** with GI_{50} value, the concentration values ranged from 1.26 to 10.5 µM were able inhibit 50% of cell growth against 53 human cancer cell lines derived from leukemia, lung, colon, central nervous system (CNS), melanoma, ovarian, renal, prostate and breast cancer. These compounds have induced apoptotic cell death via caspase dependent pathway. These compounds also exhibited significant cell cycle arrest at G2/M phase on MCF-7 cell at 10 µM, concentration with 48.85% and 31.65% of G2/M arrest, respectively compared to the positive control CA-4 that give 68.8% of G2/M arrest (Kamal et al., 2010). The compound **16** shown in Figure 2.17 has exhibited a potent selective cytotoxicity against human breast adenocarcinoma cells MCF-7 with ED_{50} value (median effective dose) of 0.16 µg/mL. The compound

has induced cell death by apoptosis as observed through the accumulation of sub G1 DNA contents in cells and analyzed by flow cytometer (Won et al., 2005).

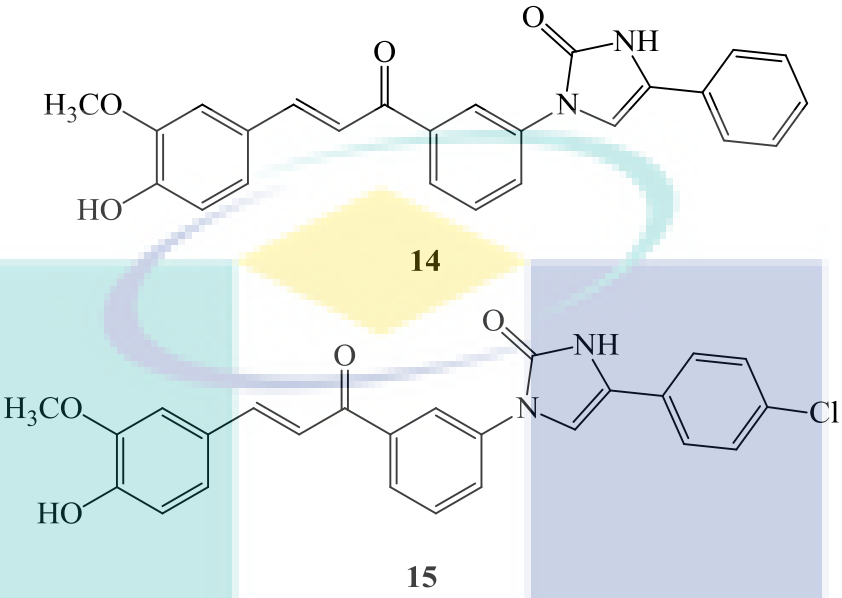

Figure 2.16 Chalcones linked imidazolones with potent anti-cancer activity towards cancer cell lines derived from leukemia, long, colon, central nervous system (CNS), melanoma, ovarian, renal, prostate and breast cancer and exhibited cell cycle arrest at G2/M phase.

Source: Kamal (2010)

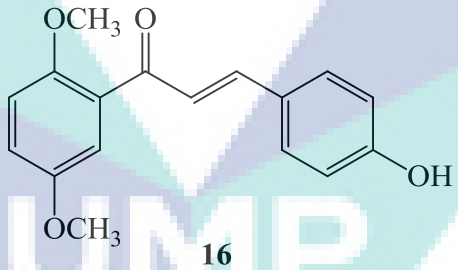

Figure 2.17 Potent chalcone derivative with selective cytotoxicity against MCF-7 cancer cell and induced cell death by apoptosis

Source: Won (2005)

2.3.2 Anti-oxidant Properties

Anti-oxidant agent is a molecule that inhibits the oxidation of other molecules thus preventing cell damages that occur due to exposure to free radicals (Shenvi et al., 2013). Free radicals such as hydroxyl, superoxide, hydrogen peroxide and lipid peroxide radicals have been involved in a variety of diseases such as cancer, asthma, cardiovascular, diabetes, gastrointestinal inflammation, and other inflammatory

processes. Anti-oxidant properties of chalcones are greatly influenced by the presence of two aryl groups and the patterns of substitution and hydroxyl is one of the key groups that could improve the anti-oxidant activity of chalcones due to its easy conversion to phenoxy radical through hydrogen transfer mechanism (Bandgar et al., 2010a) and methoxy group also plays a part in anti-oxidant properties of chalcones. Chalcones derivatives **17-20** with hydroxyl and methoxy substituents shown in Figure 2.18, Figure 2.19 and Figure 2.20 have demonstrated good anti-oxidant properties, granted by the presence of electron-releasing atom that has improved anti-oxidant activity of these compounds (Doan et al., 2011; Shenvi et al., 2013); (Bandgar et al., 2010a). Anti-oxidant of compound was determined by DPPH free radical scavenging activity where it was measured in % anti-oxidant activity. Chalcone **17** and **18** exhibited anti-oxidant activity through DPPH radical scavenging method with value 41.00% and 40.90%, respectively compared to Vitamin C as the standard with value 97.92% (Doan et al., 2011). Compound **19** exhibited good anti-oxidant activity with IC_{50} value of 2.563 µg/mL 2.444 µg/mL and 2.103 µg/mL in comparison with the standard molecule, α-topocole with IC_{50} 3.039 µg/mL, 2.632 µg/mL and 3.685 µg/mL evaluated by DPPH free radical scavenging activity, nitric oxide scavenging and $PhNHNH_2$ assay, respectively (Shenvi et al., 2013). Compound **20** has showed anti-oxidant activity when evaluated by DPPH free radical scavenging activity with value of 52.00 ± 0.43% inhibition in comparison to standard BHA with value 74.00 ± 0.53% (Bandgar et al., 2010a).

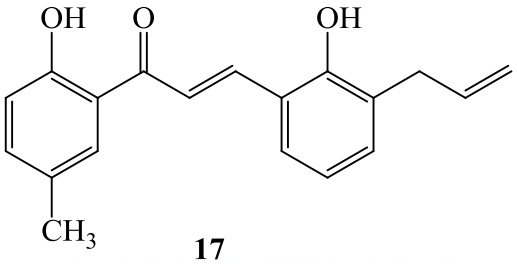

17

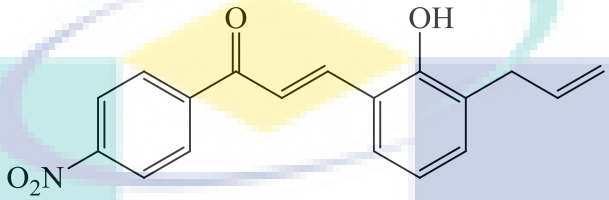

18

Figure 2.18 Compound **17** and **18** with promising anti-oxidant activity compared with standard Vitamin C, determined through DPPH free radical scavenging method with good anti-oxidant activity

Source: Doan (2011)

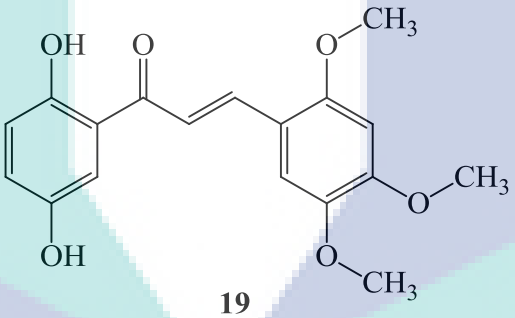

19

Figure 2.19 Methoxy and hydroxy substituted chalcone with comparable anti-oxidant activity with standard molecule α-topocole, evaluated by DPPH free radical scavenging activity, nitric oxide scavenging and $PhNHNH_2$ assay

Source: Shenvi (2013)

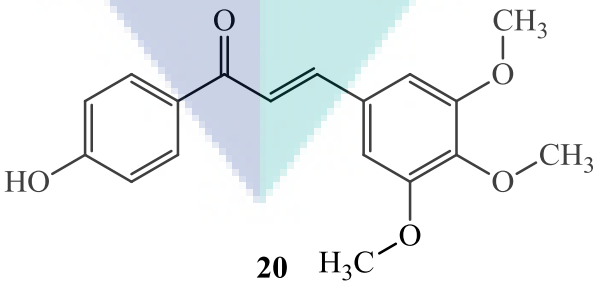

20

Figure 2.20 Chalcone derivative (**20**) with potent anti-oxidant properties in comparison with standard anti-oxidant BHA

Source: Bandgar (2010)

2.3.3 Anti-inflammatory Properties

Nitric oxide (NO) is a strong vasodilator that accelerates leukocyte migration and formation of edema, as well as leukocyte activity and cytokine production. In addition, NO could also react with superoxide anion to form peroxynitrite, a potent oxidizing molecule that has contributed to tissue injury during inflammatory responses (Rojas et al., 2002). Research have found that chalcones with trimethoxy substituents at ring B possess substantial anti-inflammatory properties (Bandgar et al., 2010a). Previous study showed that dimethoxy and trimethoxychalcone derivatives series **21** and **22** shown in Figure 2.21 are the effective anti-inflammatory agents with IC_{50} value of 24.4 ± 8.1 and 46.8 ± 5.3, respectively. The value for constant second order rate of these compounds are 8.1 ± 2.2 $\times 10^7$ M^{-1} s^{-1} and 4.0 ± 0.8 $\times 10^7$ M^{-1} s^{-1}, respectively by means the reaction rate that are used to evaluate the biological relevance of chalcone reactivity toward NO (Herencia et al., 2002).

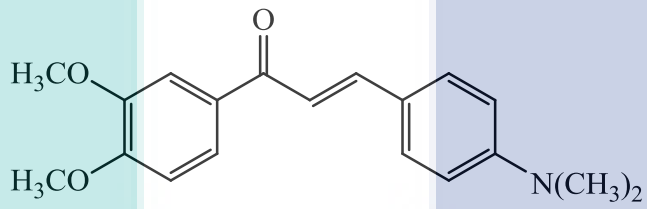

21

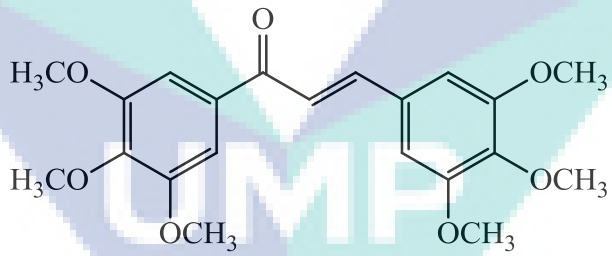

22

Figure 2.21 Chalcone with effective anti-inflammatory activitity in NO scavenging activity

Source: Herencia (2002)

Improved inhibition activity against nitrite production has been observed in chalcone derivatives with fluoro substitution at C4′. Trifluoromethyl group positioned at C2′ in dimethoxychalcones and trimethoxychalcones has been reported to possess potent inhibitory effects on nitrite accumulation.

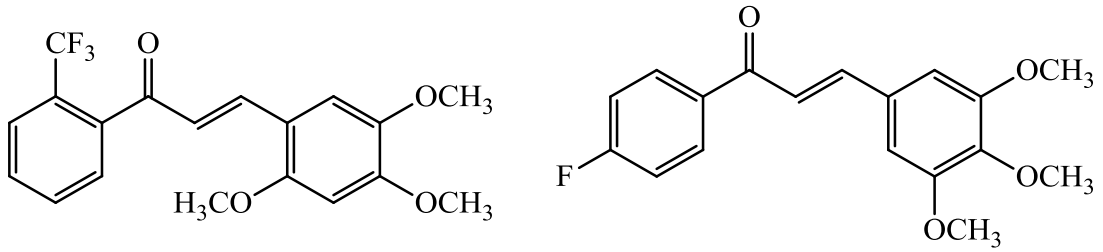

23 **24**

Figure 2.22 Chalcone with strong inhibition activity against nitrite production
Source: Rojas (2002)

Chalcone compounds **23** and **24** in Figure 2.22 have exhibited remarkable inhibitory activity against nitrite production, measured in percentage, which value were 73.7 ± 3.1% and 94.1 ± 1.4%, respectively. The IC_{50} value for the inhibition of nitrite accumulation of compound **23** and **24** are 0.28 μM and 0.03 μM, respectively The extent of influence that trimethoxy moiety has on inhibitory activity strongly depends on the substitution pattern of fluorine/ trifluoromethyl (CF_3) in the benzoyl group of the compound. The presence of fluoro substituent at position 4 in ring A and trifluoromethyl substituent at position 2 in ring A has rendered improved inhibitory activity of chalcones against nitrite production (Rojas et al., 2002).

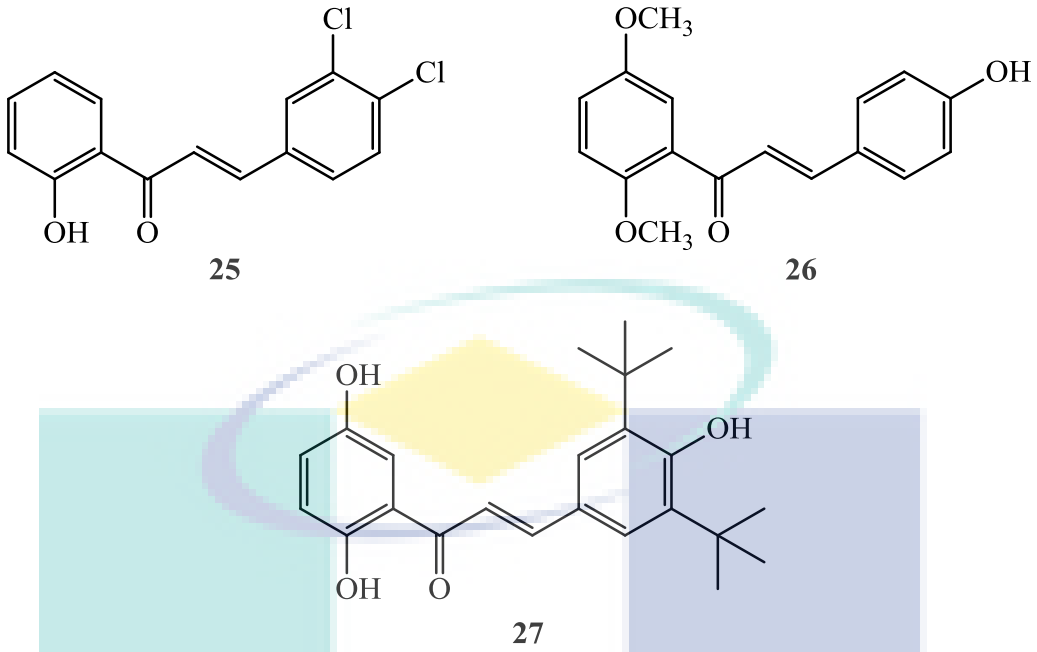

Figure 2.23 Chalcone derivatives with inhibitory activity against NO accumulation in RAW 264.7 cells

Source: Won (2005)

Other chalcone derivatives, labeled as **25**, **26** and **27**, represent 2′-hydroxy-3,4-dichlorochalcone,2′,5′-dimethoxy-4-hydroxychalcone and 3,5-di-tert-butyl-2′,4,5′ trihydroxychalcone, respectively (Won et al., 2005) shown in Figure 2.23 exhibited potent and concentration-dependent inhibitory activity against NO accumulation in RAW 264.7 cells with MIC values of 23.8 ± 1.0 µM, 23.3 ± 2.6 µM and 14.6 ± 0.1 µM, respectively.

Compounds with electron donating groups such as methoxy and hydroxy exhibited good anti-inflammatory activity than that of which without such groups. Compounds containing halogen substituents such as chloro, fluoro and bromo groups have also exhibited significant anti-inflammatory activity (Avupati et al., 2014).

2.3.4 Anti-bacterial Properties

Chalcone, an important intermediate in flavonoid synthetic pathway, has exhibited diverse pharmacological activities, whereof anti-bacterial is one of them (Doan et al., 2011). The presence of a reactive α,β-unsaturated keto function in chalcones has resulted in improved antimicrobial activity of chalcones (Choudhary et al., 2011; Prasad et al., 2008a). Anti-bacterial drug refers to the compound that will kill

bacteria and cure bacterial infections on various parts of the body by penetrating the cell wall of the associated microorganisms and disrupting the main functions of cells, which leads to suppressed microbial growth and reproduction.

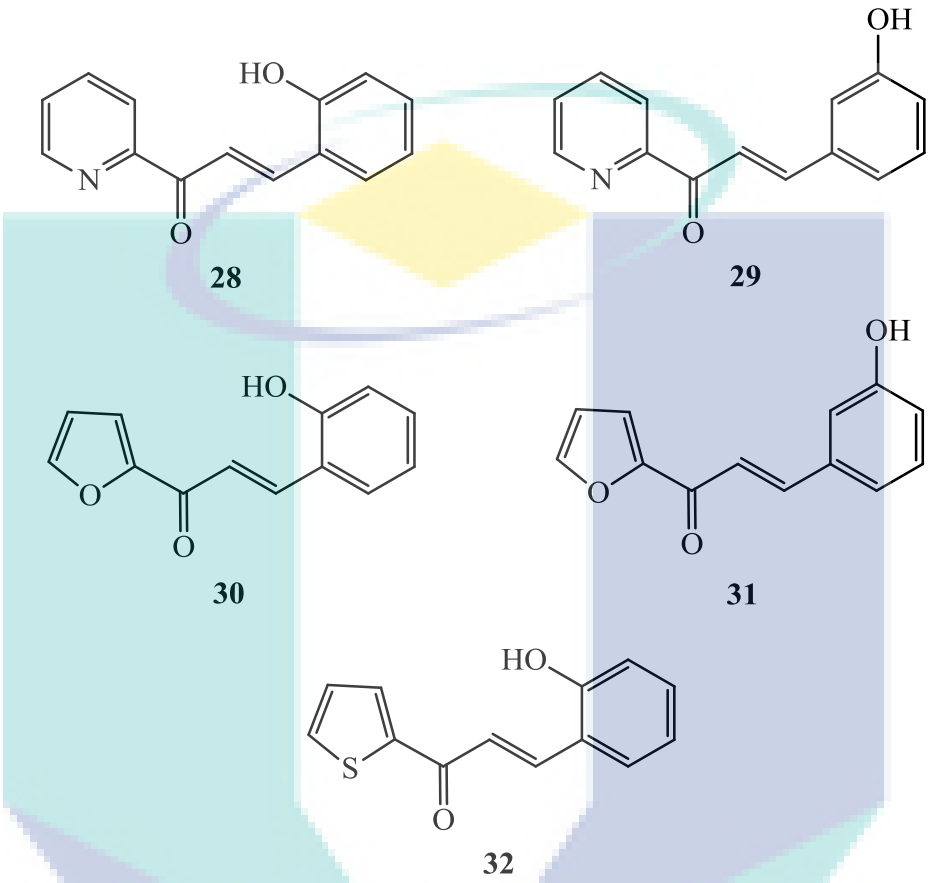

Figure 2.24 Chalcone with anti-*Staphyloccus aureus* activity
Source: Tran (2012)

Heterocyclic chalcone analogs **28-32** in Figure 2.24 have demonstrated anti-*Staphyloccus aureus* activity. The positions of phenolic hydroxy groups in the ring B of active chalcone skeleton play important role in the anti-bacterial activity (Tran et al., 2012). The synthesized chalcones **33-37** with fluoro and nitro substituted in ring A shown in Figure. 2.25 have showed good anti-bacterial activity when screened against *Eschericia coli* and *Pseudomonas aeruginosa*. In vitro anti-bacterial activity against *Eschericia coli* in term of zone of inhibition in mm for compound **33**, **34**, **35, 36** and **37** were 15 mm, 12 mm, 10 mm, 12 mm and 14 mm, respectively in comparison with streptomycin, with value of 18 mm. Compound **33**, **34**, **35**, **36** and **37** exhibited anti-bacterial properties on *Pseudomonas aeruginosa* with value of 14 mm, 9 mm, 10 mm, 9 mm and 8 mm, respectively in comparison with 18 mm of zone of inhibition for

standard streptomycin (Tiwari et al., 2010). Compound **38** in Figure 2.26 has been reported for its potent anti-microbial activity than norfloxacin, when tested against *Staphylococcus aureus* with minimum inhibitory concentration (MIC) of 2 µg/mL (Chen et al., 2010). Derivative **38** has showed strong inhibitory capability which suggests that the addition of two halogen atoms to the hybrid compound may improve associated anti-bacterial properties. Chalcones **39-43** in Figure 2.27 have showed good anti-bacterial activity against various bacterial strains such as *Bacillus subtilis, Pseudomonas species, Escherichia coli* and *Staphylococcus aureus*. Compound **39**, **40**, **41**, **42**, **43** along with standard amphicilin with minimum inhibitory concentration (MIC) used at 50 µg/mL have exhibited anti-bacterial activity against strain *Bacillus subtilis* (BS) with zone of inhibition value of 17 mm, 20 mm, 15 mm, 14 mm, 17 mm and 19 mm, respectively. Compound **39-43** against *Pseudomonas species* (PS) have 13 mm, 10 mm, 12 mm, 14 mm and 13 mm of inhibition zone in comparison with amphicilin with value of 23 mm. Compound **39-43** in comparison with amphicilin had exhibited anti-bacterial properties against *Escherichia coli* (EC) with zone of inhibition value of 11 mm, 16 mm, 12 mm, 15 mm, 16 mm and 15 mm, respectively, while for activity against *Staphylococcus aureus* (SA), the value of inhibition zone are 13 mm, 12 mm, 13 mm, 14 mm, 13 mm and 17 mm, respectively (Jadhav et al., 2013).

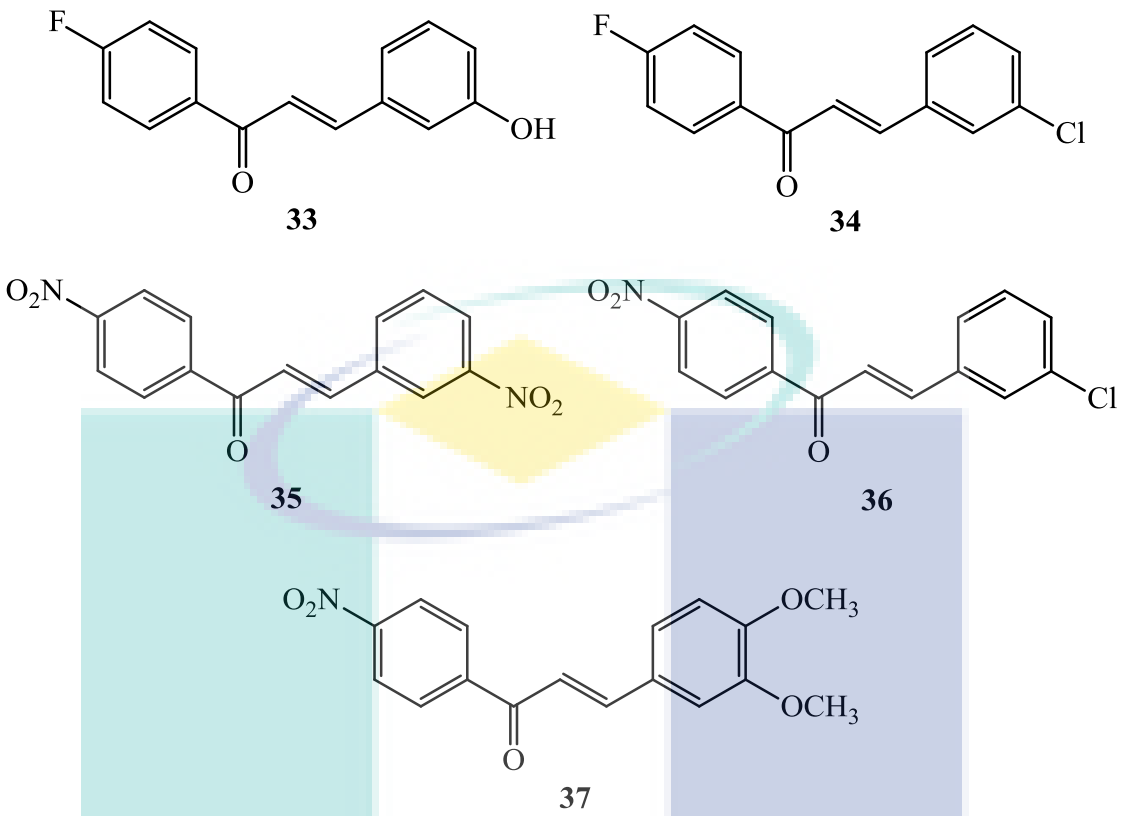

Figure 2.25 Chalcone with potent anti-bacterial activity screened against *Eschericia coli* and *Pseudomonas aeruginosa*

Source: Tiwari (2010)

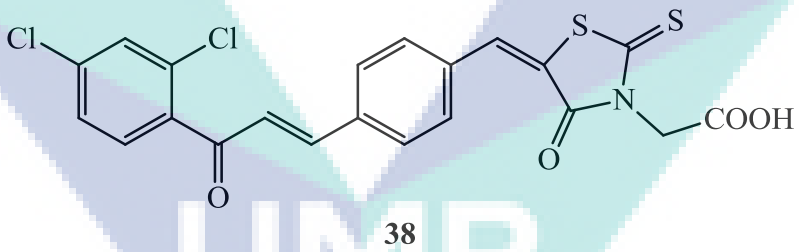

Figure 2.26 Hybrid chalcone with potent anti-bacteria properties than standard norfloxacin against *Staphylococcus aureus* with minimum inhibitory concentration value of 2 μg/mL

Source: Chen (2010)

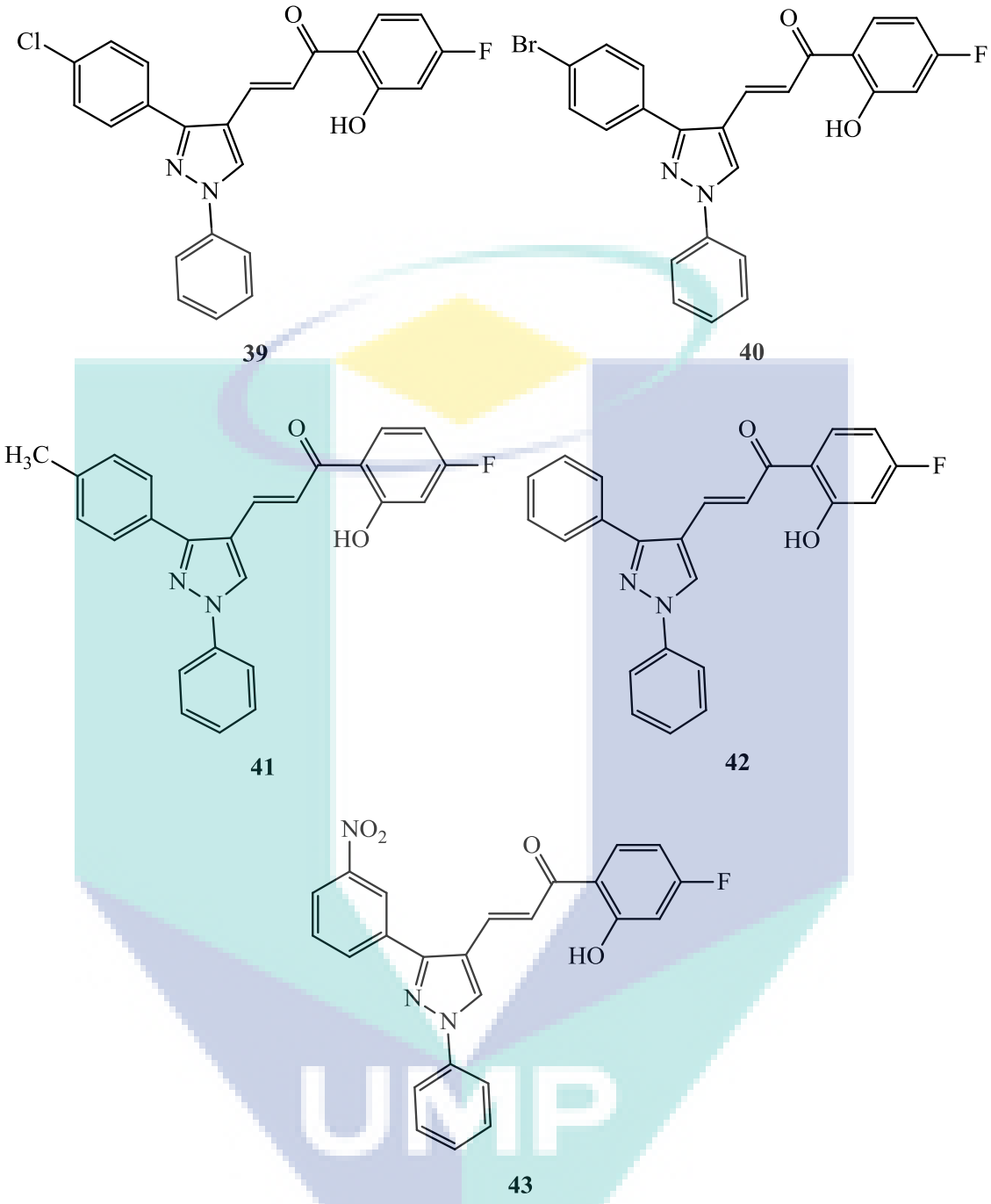

Figure 2.27 Compound with potent anti-bacterial activity against *Bacillus subtilis, Pseudomonas species, Escherichia coli* and *Staphylococcus aureus* compared to amphicilin

Source: Jadhav (2013)

2.3.5 Anti-leishmanial Properties

Chalcone exhibiting anti-leishmanial activity has been used in the treatment of leishmaniasis to destroy the associated parasitic protozoa of genus *Leishmania*. Research have been conducted to determine the effects of different substitutions on ring

A and B in chalcones on the associated anti-leishmanial and cytotoxic activities. Such study is important for development of various synthetic chalcones with enhanced anti-leishmanial and cytotoxic activities. Synthesized chalcones **44-46** in Figure 2.28 have exhibited highly potent anti-leishmanial activity against promastigotes of *Leishmanial amazonensis* with IC_{50} value of 0.7 ± 0.1 μM, 0.8 ± 0.0 μM and 0.5 ± 0.4 μM, respectively in comparison with pentamidine with IC_{50} value of 6.0 ± 0.5; and against intracellular amastigotes of *Leishmanial amazonensis* with IC_{50} value of 15.8 ± 0.4 μM, 4.3 ± 0.8 μM and 6.3 ± 0.5 μM, respectively compared to pentostan with IC_{50} value of 4.4 ± 0.2 μM due to substitutions of fluorine or a nitro group at *para* and *meta* positions in ring B and insertion of bromine substituent in ring A (Boeck et al., 2006).

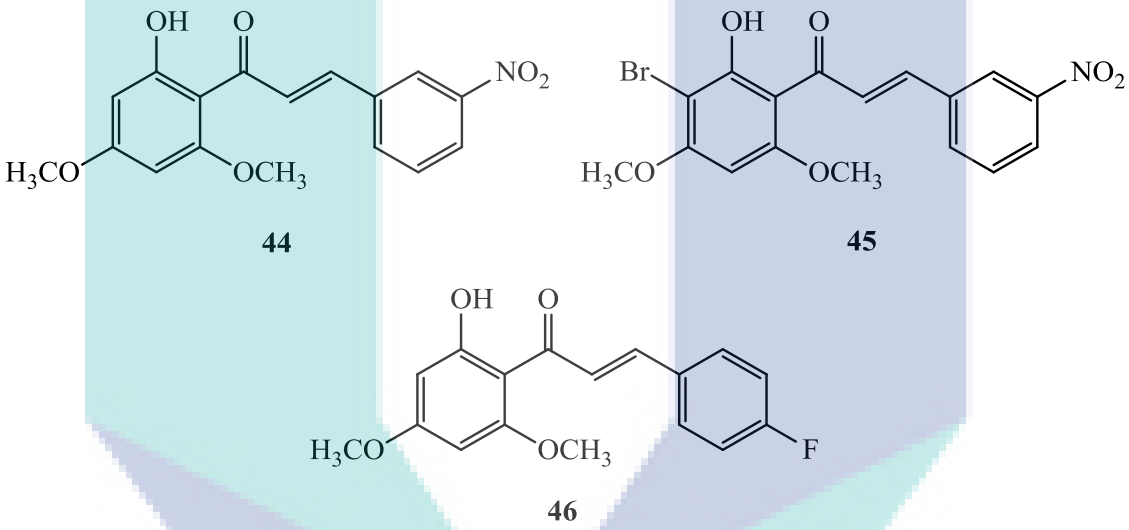

Figure 2.28 Chalcone with anti-leishmanial activity against promastigotes and intracellular amastigotes of *Leishmanial amazonensis*

Source: Boeck (2006)

Ten compounds as shown in Figure 2.29 have been found to be significantly more active than the standard anti-leishmanial drugs such as miltefosine and sodium stibogluconate (SSG) in an *in vitro* evaluation against leishmania promastigote and amastigotes. Compound **47-56** have exhibited inhibition percentage (%) at 25 μM with value of 88.9, 98.7, 97.4, 99.9, 99.8, 84.2, 100, 93.0, 99.9 and 100, respectively against extracellular promastigote and also exhibited IC_{50} value (μM) of 5.1, 6.1, 5.2, 2.0, 5.3, 4.1, 2.0, 3.1, 2.5 and 2.8, respectively against intracellular amastigote of *Leishmanial donovani*. (Gupta et al., 2014).

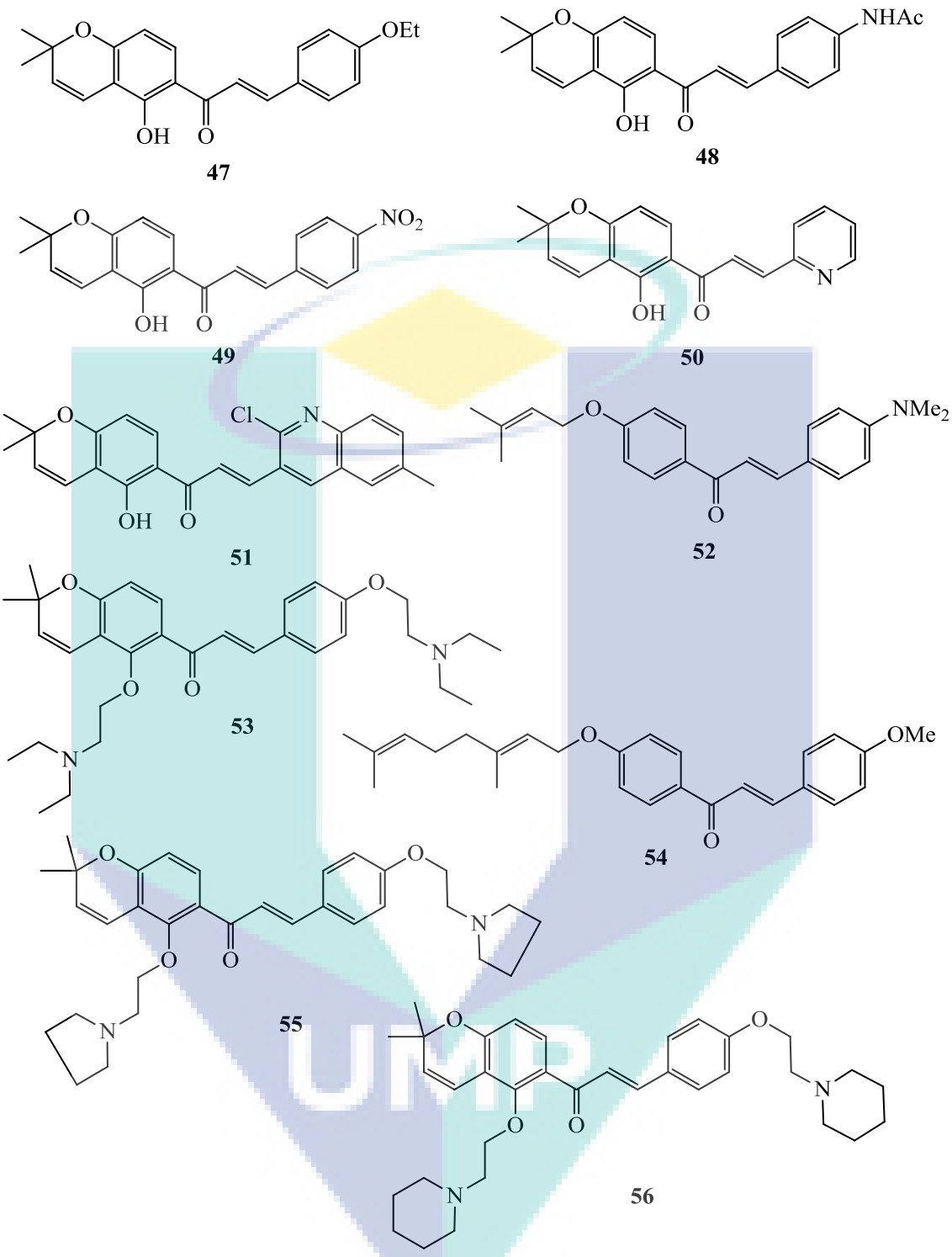

Figure 2.29 Chalcone **47-56** with potent *in vitro* anti-leishmanial activity against extracellular promastigote and intracellular amastigote of *Leishmania donovani*

Source: Gupta (2014)

2.3.6 Anti-malarial Properties

Anti-malarial drug is designed to prevent or cure malaria. It defeat the symptoms of the infection by killing the parasites in the liver or bloodstream. Most of the malaria cases have been caused by *Plasmodium falciparum*. Chalcone is known for its biological potential that includes anti-malarial activity. Chalcone **57** in Figure 2.30 is the most active, exhibiting IC_{50} value of 3.4 µM and 3.8 µM when tested against D10 (chloroquine-sensitive) and W2 (chloroquine-resistant) strains of *P. falciparum*, respectively (Hans et al., 2010). Another article has reported that some analogs of oxygenated chalcones, bischalcones and quinolinyl chalcones have showed anti-malarial activity against *P. falciparum* K1 (Mei Liu et al., 2003b; Reddy et al., 2008).

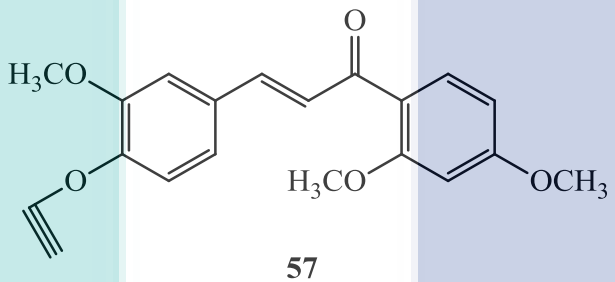

57

Figure 2.30 Chalcone with anti-malarial activity against D10 and W2 strains of *P. falciparum*

Source: Hans (2010)

Electron-deficient in ring A and methoxylated group in ring B of chalcones **58-63** shown in Figure 2.31 have resulted in improved anti-malarial activity against *P. falciparum* 3D7 strain, rendering IC_{50} value of 1.8 µM, 2 µM, 4 µM, 4.6 µM, 6 µM and 8 µM, respectively. It has also been found that 2,4,5-trimethoxy substitution in ring B is vital for anti-malarial activity (Kumar et al., 2010).

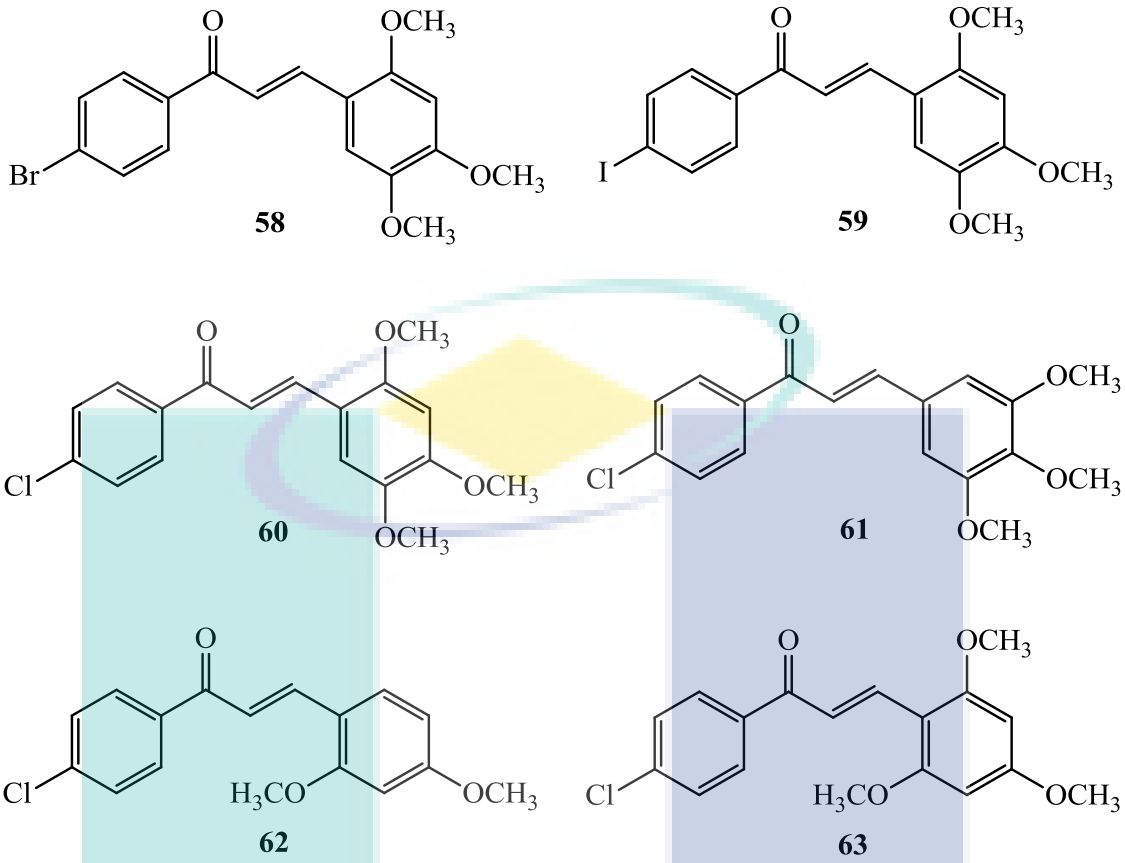

Figure 2.31 Chalcone derivatives with anti-malarial activity against *P. falciparum* 3D7 strain

Source: Kumar (2010)

2.3.7 Immunosuppressive Activity of Chalcone

Immunosuppressive drug prevents the activity of the immune system and lower the body's ability to reject a transplanted organ. Chalcone derivative **64** shown in Figure 2.32 has showed potent immunosuppressive activity which has been achieved through an increase in cleavage of caspase-3 and poly (ADP ribose) polymerase (PARP), resulting in apoptosis of lymph node cells stimulated with anti-CD3/anti-CD28. In general, the presence of electron donating substituent in both rings has contributed to immunosuppressive activities of the synthesized oximes (Luo et al., 2012).

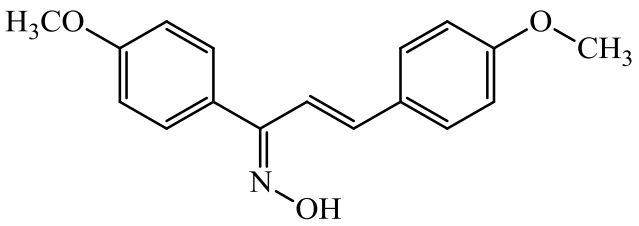

64

Figure 2.32 Chalcone with potent immunosuppressive activity

Source: Luo (2012)

2.3.8 Anti-proliferative Properties

Chalcone with anti-proliferative activity has the ability to inhibit the cell growth, especially that of malignant cells invading surrounding tissues. Figure 2.33 shows compounds **65-67** containing conjugated azazerumbone and chalcone with 1-ethylene-4-methylene-1,2,3-triazole linker. Anti-proliferative activity of the synthesized chalcones have been significantly improved due to the presence of methoxy group at position 3 of phenyl moiety in chalcone (Truong et al., 2015). Compound **65** has showed the best activity against lung adenocarcinoma (LU) cell lines with IC_{50} value of 0.61 μg/mL whereas compound **67** has increased and exhibited good activity against breast cancer (MCF-7), colon adenocarcinoma (SW480), leukemia (P338), liver hepatocellular (Hep-G2) and lung adenocarcinoma (LU) cancer cell lines with IC_{50} values of 0.58, 0.71, 0.77, 0.99, and 1.01 μg/mL, respectively where according to the rule established by the American National Cancer Institute (NCI) is in IC_{50} less than 30 μg/mL, and for all standard anti-cancer agents the IC_{50} value was less than 25 μg/mL (Zheng et al., 2000) . Conjugated derivatives **65**, **66** and **67** have demonstrated anti-proliferative activities that are nearly comparable to that of ellipticine (Truong et al., 2015).

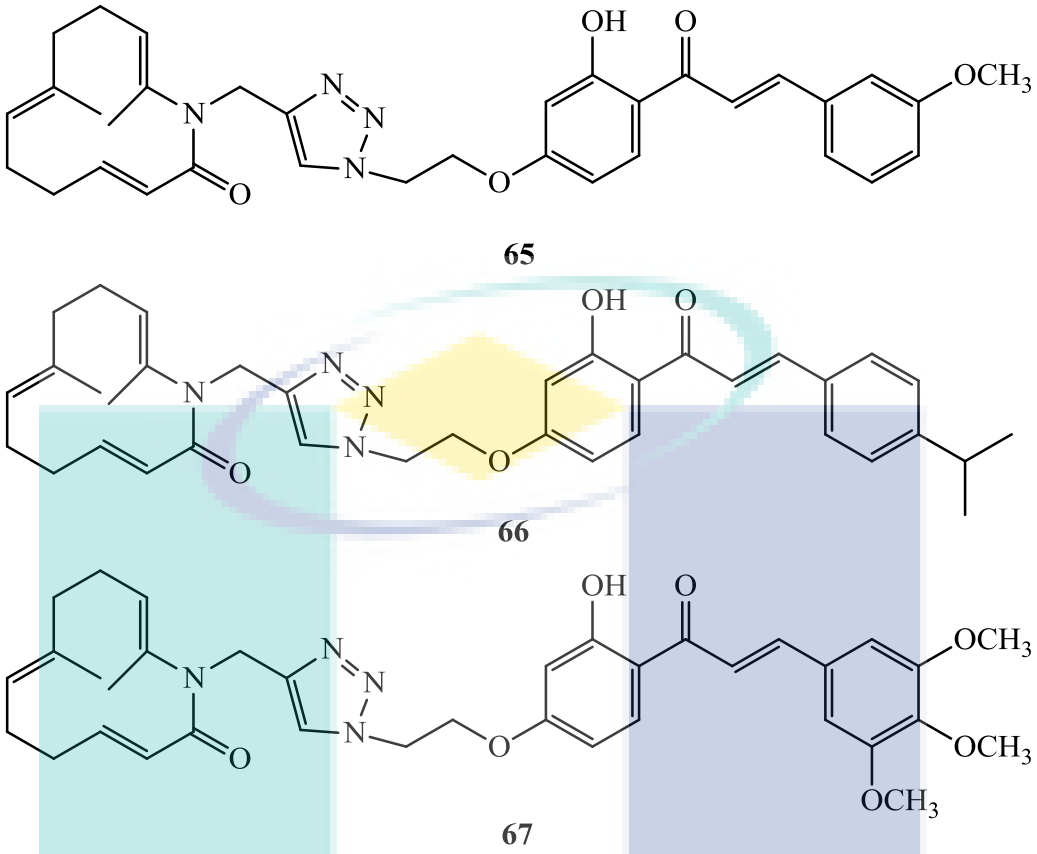

Figure 2.33 Conjugated chalcone and azazerumbone derivatives with 1-ethylene-4-methylene-1,2,3-triazole linker with potent anti-proliferative activity

Source: Truong (2015)

Compound **68** in Figure 2.34 has showed strong cytotoxicity and promoted apoptosis in human hepatoma Hep-G2 cells. The IC_{50} value of compound **68** is 26 μM and less toxic when screened against normal porcine kidney proximal tubular ephitelial LLC-PK1 cells with IC_{50} value of 83 μM. The percentage inhibition of Hep-G2 cell growth are up to 91% and 98% of the control growth at 50 μM and 100 μM, respectively The exposure to compound **68** for 24 hr has induced the cleavage of caspase-8, caspase-3 and poly (ADP-ribose) polymerase (PARP). The percentage of apoptotic cells was significantly higher in cells treated with compound **68** than that of control. Compound **68** have exhibited 8.5 ± 2.2% and 31.2 ± 2.9% early apoptotic cell populations at 25 μM and 50 μM, respectively in comparison with 1.9 ± 0.5% of control (Park. et al., 2015).

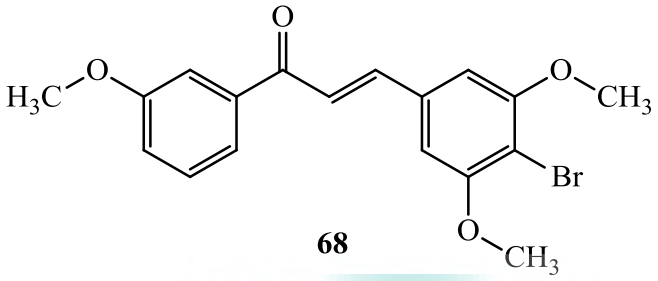

68

Figure 2.34 Chemical compound that promote apoptotic cell death in human hepatoma cells

Source: Park (2015)

Combination of quinazolines structural features such as 2-phenyl ring bearing two methoxy groups and chalcone has led to an increase in inhibitory activity. Compounds **69** in Figure 2.35 has showed low cytotoxicity but proved to be the most effective inhibitor of ATP-binding cassette sub-family G member 2 (ABCG2) with GI_{50} (median growth inhibition) value of about 93 μM. The compound was able to reverse MDR for the ABCG2 substrate SN-38 in the same concentration range as Ko143, the most potent ABCG2 inhibitor (Kraege et al., 2016).

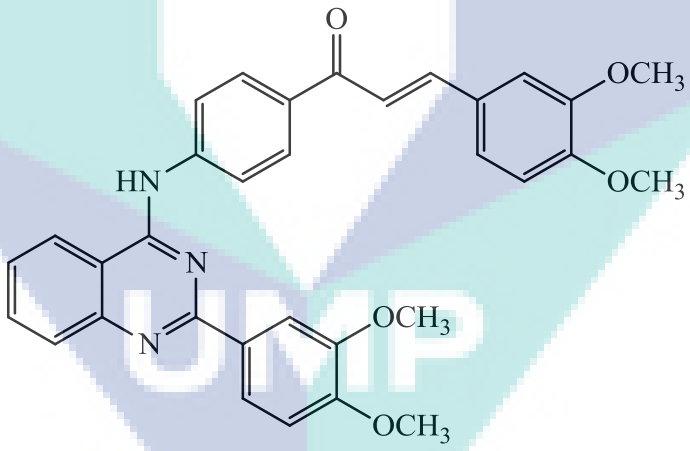

69

Figure 2.35 Compound with effective inhibitory activity against ABCG2

Source: Kraege (2016)

2.4 Structure-Activity Relationship of Chalcone

The structure-activity analysis has showed that the presence of various functional groups in substituted chalcone plays important role in the pharmacological activities of chalcone. Hydroxy and methoxy group in phenyl rings of chalcone at

specific position have been found to favor anti-cancer activity (Karthikeyan et al., 2015). Hydroxychalcone derivatives **70**, **71** and **72** shown in Figure 2.36 have played important role in anti-cancer activity through their ability to uncouple mitochondria (Sabzevari et al., 2004). Compound **4**, **5** and **6** in Figure 2.13 are natural chalcones that have exhibited potential cytotoxicity against breast cancer cell lines, indicating the role of methoxy and hydroxy moiety at position 4 in ring B contribute to anti-cancer activity (Abu et al., 2013).

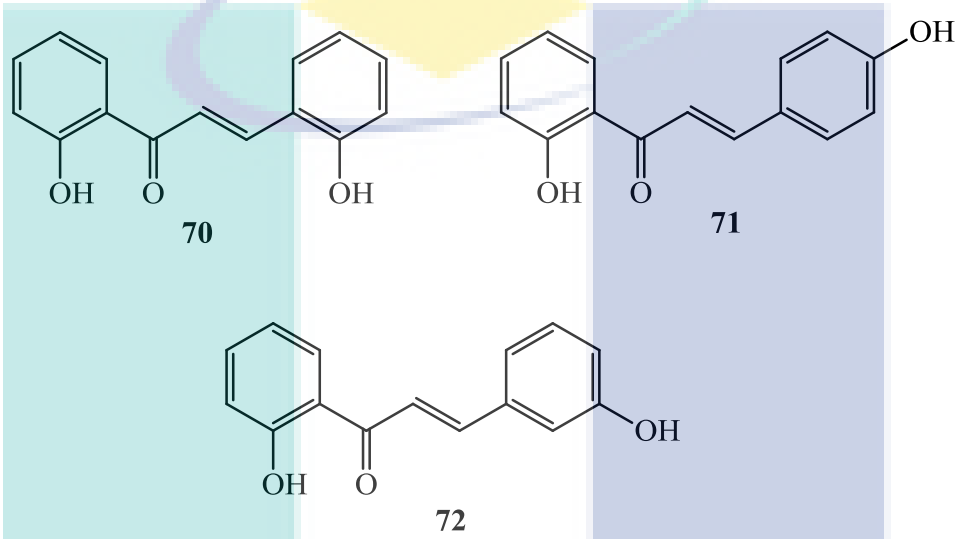

Figure 2.36 Hydroxychalcone derivatives with potential to uncouple mitochondria
Source: Sabzevari (2004)

Heteroatom substituted chalcone has also contributed to anti-cancer properties of chalcone. Dihalogenated chalcone **8**-**13** shown in Figure 2.15 have exhibited cytotoxic activity on lung cancer cell and inhibited tubulin polymerization (Dyrager et al., 2011). Chalcone **73** and **74** with chloro group at position *ortho* and *meta* in ring B of chalcone shown in Figure 2.37 have exhibited potent anti-cancer activity against breast cancer cells by inducing apoptosis in MCF-7 cells (Syam. et al., 2012).

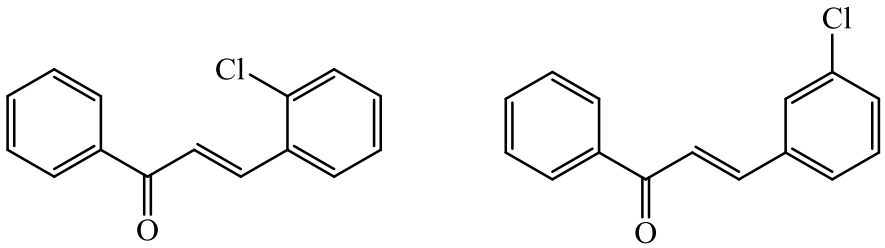

73 74

Figure 2.37 Halogenated chalcone with potent anti-cancer activity

Source: Syam (2012)

2.5 Breast Cancer

Breast cancer is the most frequently diagnosed invasive cancer and the leading cause of cancer death after lung cancer in women aged 20 to 59 years (Li et al., 2016) worldwide (Siegel et al., 2016). The most common early sign of breast cancer is formation of breast lump, which is often painless and less common symptoms include the change in breast shape, dimpling of the skin and discharged of fluid from the nipple. Patient with distant cancer, may experience bone pain, swollen lymph nodes, shortness of breath, or yellow skin. Breast cancer occurs in stages: early, curable breast cancer and metastatic breast cancer.

Figure 2.38 Mammograms image of breast cancer

Source: Singh (2015)

Breast cancer is a cancer that develops from breast tissue. It most commonly developed in cells from the lining of milk ducts and the lobules that supply the ducts with milk (Sharma et al., 2010). Figure 2.38 shows the mammogram image of breast

cancer (Singh et al., 2015). In recent years, breast cancer does not only represent a single disease but rather a number of molecularly-distinct tumors arising from the epthilial cell of the breast (Comşa et al., 2015). Breast cancer can be divided into some types where patients of breast cancer have the expression of estrogen receptor (ER), progesterone receptor (PR), and amplification of HER-2/Neu analyzed. Two type of breast cancer that are mostly used by the researcher are MCF-7 and MDA-MB-231 (Moses et al., 2016).

MCF-7, abbreviated from Michigan Cancer Foundation 7, is a breast cancer cell line (Ghasemi et al., 2016) which its name was derived from Michigan Cancer Foundation originally isolated from pleural effusion of a 69 year old Caucasian women in 1970, named Frances Mallon which was a nun that attended the Immaculate Heart of Mary Convent in Monroe, Michigan (Lee et al., 2015). It is estrogen receptor (ER) positive, progesterone receptor (PR) positive, epidermal growth factor receptor (EGFR) positive and human epidermal growth factor receptor-2 (HER-2) positive which are one of factors that controlled the growth of MCF-7 cancer cell line. It also fit in luminal A molecular subtype, non-invasive cell line and being considered to have low metastatic potential. Estradiol has significant role in promoting the breast cancer cell growth. (Comşa et al., 2015).

MDA-MB-231, known as triple negative breast cancer cell line, is an epithelial cell that was formed from a pleural effusion of a 51 year-old Caucasian female with the metastatic mammary adenocarcinoma (Cailleau et al., 1978). It is aggressive, invasive and in the group of triple negative breast cancer (TNBC) cell line because of its lack of estrogen receptor (ER) and progesterone receptor (PR) expression along with HER-2 (Human epidermal growth receptor 2) amplification (Chavez et al., 2010; H. Liu et al., 2003a).

There are many commercialized drugs that are used to treat cancer such as doxorubicin, tamoxifen, paclitaxel, fluorouracil and cisplatin (Bassiouni et al., 2012). Breast cancer were prevented and treated with tamoxifen that are commonly used as anti-cancer drug (Jordan, 1993). Tamoxifen generally acts via estrogen receptors and displays anti-cancer properties in breast cancer negative to ERs but this drug also produces some non-desirable side effects by acting on another different targets (Rivera-Guevara et al., 2011).

Chalcone exhibited anti-cancer properties toward breast cancer cell line. In recent studies, flavokawain A from chalcone family inhibits the proliferation and induce apoptosis in breast cancer cell line, MCF-7 and MDA-MB-231 as the selectivity index of this compound is noticeably higher that tamoxifen (Abu et al., 2014). Besides, chalcone based with newly β-carboline also have demonstrated strong inhibition of the cellular proliferation and highly effective in inducing apoptosis in MCF-7 cancer cell (Chauhan et al., 2014).

CHAPTER 3

RESEARCH METHODOLOGY

3.1 Synthesis of Flavokawain B Derivative (2, 4, 5, 44, 46, 75-91) by Claisen-Schmidt Condensation

Flavokawain B derivative were synthesized by using Claisen-Schmidt condensation. The 2′-hydroxy-4′,6′-dimethoxyacetophenone (ring A) (1.00 mmol) was dissolved in methanol (10 mL) and stirred. After that, aqueous potassium hydroxide (KOH) (40%, 4 mL) was added dropwise while stirring. After 15 min, the appropriate amount of substituted benzaldehyde (ring B) (1.00 mmol) was added gradually to the reaction and stirred at room temperature for 48-72 hr as shown in Figure 3.1 for the scheme of reaction. The completion of reaction was monitored by using Thin Layer Chromatography (TLC). After the reaction was completed, it was neutralized by using hydrochloric acid until the desired pH range was achieved. The crude product was extracted by solvent-solvent extraction using water and organic solvent such as ethyl acetate. The crude product was filtered with anhydrous sodium sulphate to remove moisture, followed by crystallization to get the corresponding product. The reactions gave out 75-95% yield.

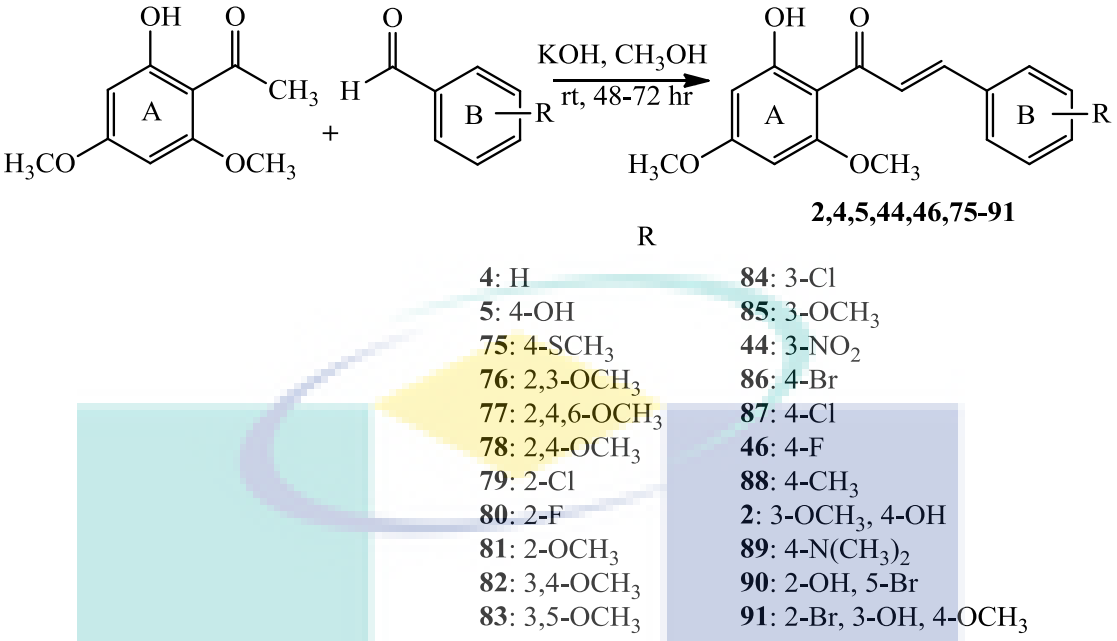

Figure 3.1 Scheme 1: Synthesis of flavokawain B derivative (**2, 4, 5, 44, 46, 75-91**) by Claisen-Schmidt Condensation method

3.2 Acetylation of 4-hydroxy-3-methoxybenzaldehyde

Acetylation was conducted by dissolving the 4-hydroxy-3-methoxybenzaldehyde (100 mg) with acetic anhydride (3 mL) in the presence of pyridine (5 mL) following the scheme 2 shown in Figure 3.2. The reaction was stirred at room temperature for 18 hr. The completion of reaction is monitored by using TLC. The product was collected and extracted by solvent-solvent extraction using water and chloroform. The pyridine from the product is removed by drying. The product of acetylation was later dissolved in chloroform and is passed through anhydrous sodium sulphate to eliminate the moisture.

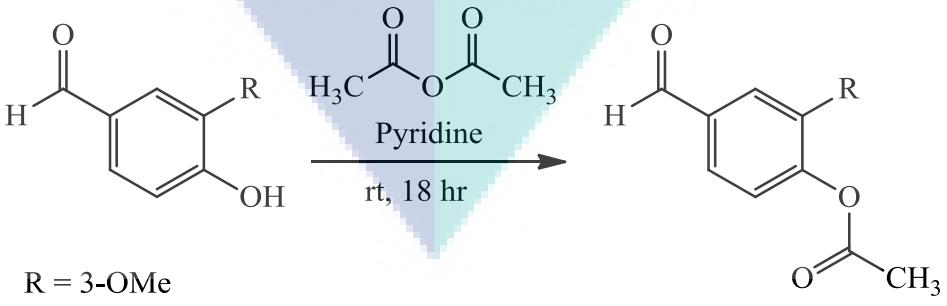

Figure 3.2 Scheme 2: General scheme for acetylation of 4-hydroxy-3-methoxybenzaldehyde

3.3 Purification of Flavokawain B Derivative

Flavokawain B derivative were purified by three techniques such as column chromatography, thin layer chromatography (TLC) and crystallization.

3.3.1 Column Chromatography

Purification of flavokawain B derivative was carried out by using silica gel column chromatography. Stationary phase used in this column chromatography was silica gel within size 100-200 mesh (Merck) and L230-400 mesh (Bendosen), while the mobile phase used was the mixture of hexane and ethyl acetate. Purification of the compound was done through slow and repetitive separation by column chromatography. The purity of each fraction collected in small vial was monitored by using Thin Layer Chromatography (TLC) plate.

3.3.2 Thin Layer Chromatography Analysis

Purity of compound isolated from column chromatography was checked on Thin Layer Chromatography (TLC) plate by using TLC silica gel 60 F_{254} (Merck). TLC analysis was done by spotting a small amount of samples on TLC plate using capillary tube. The size of TLC plate was cut according to the number of samples to be tested. TLC plate was put in TLC tank containing 10 ml of hexane:ethyl acetate. The developed and dried plates of TLC was observed under ultra-violet (UV) light at both long and short wavelengths for detection of UV-active compound. UV-inactive compound was observed on TLC plate after being sprayed with spraying reagent and heated. Pure compound appeared as a single spot on the TLC plate while impure compound appeared as multiple spots. The compounds were subjected to further purification process.

3.3.3 Crystallization

The synthesized flavokawain B derivative was purified by crystallization technique. The compound was dissolved in solvents such as ethyl acetate and methanol. It was then heated until supersaturated solution was formed. Next, the supersaturated solution was filtered on anhydrous sodium sulphate. Lastly, the solution was dried through slow evaporation until the crystal was formed.

3.4 Percentage Yield

Percentage yield refers to the efficiency of chemical reaction. Firstly, in order to calculate the percentage yield, the chemical equation of the reaction was balanced. The limiting reagent was determined by calculating the number of moles of each reactant; each of the calculated value was then divided by the equation coefficient. The reactant with the least value was identified as the limiting reagent. Next, the theoretical yield is calculated by multiplying the number of mole of limiting reagent; the experimental ratio of the mole of desired product in equation coefficient to mole of limiting reagent in equation coefficient; and the molar mass of desired product. The actual yield was calculated in gram. The actual yield was divided by the theoretical yield and multiplied by 100% to calculate the percentage yield.

$$yield = actual / theoretical \times 100\% \quad 3.1$$

3.5 Characterization of Flavokawain B Derivative

Pure flavokawain B derivative were characterized and identified using Ultraviolet-Visible (UV-Vis), Fourier Transform Infrared (FTIR), Gas Chromatography-Mass Spectroscopy (GC-MS) and Nuclear Magnetic Resonance (NMR) spectroscopic techniques.

3.5.1 Ultraviolet-Visible Spectroscopic Analysis

Ultraviolet-Visible (UV-Vis) spectroscopy was carried out by using UV-VIS spectrophotometer of Genesys 10s Thermo Scientific model. 1 mg of the isolated pure flavokawain B derivative was first diluted in 2 mL of chloroform or methanol and transferred into 1 cm path length glass cuvettes. Plastic cuvettes should not be used due to corrosive effects of chloroform on plastic. The cuvette walls were carefully cleaned. The solutions were scanned by light transmission of wavelength ranged from 200 nm to 600 nm. UV-Vis spectrum of the unknown compound was elucidated and used to identify the wavelength of maximum absorbance of the isolated pure compound.

3.5.2 Fourier Transform Infrared Spectroscopy Analysis

The pure unknown synthesized compound in the crystal form was scanned by using Fourier Transform Infrared Spectroscopy (FTIR) of Perkin Elmer Spectrum 1000 model at room temperature with the spectral range of 4000 cm^{-1} to 400 cm^{-1}. Potassum bromide (KBr) disk sample preparation method was used for FTIR scanning. As a precaution, KBr powder was dried overnight in an oven at temperature ranged from 100 to 120°C to eliminate the moisture. Certain amount of dry solid compound was mixed with KBr powder at a ratio of one to ten by grinding the mixture using mortar and the pestle until the KBr was finely and equally mixed with the compound. The mixture of KBr powder was then equally spread on the KBr pellet dies and sandwiched between stainless steel die sets before it was pressed in a pelletizer under high pressure condition (5,000 ton) to form a thin, transparent sample disk. The sample disk was transferred onto FTIR sample holder and was placed inside FTIR spectrophotometer for transmission analysis. The background spectrum generated by FTIR spectrophotometer was collected prior to running FTIR analysis on the sample. This was done to subtract the background noise from the generated sample's spectrum. Then, the sample was scanned and the single-beam spectrum displaying the absorption band of the sample was collected. Each band in the spectrum was labelled with respective name and value.

3.5.3 Gas Chromatography-Mass Spectroscopy Analysis

Characterization of compounds was carried out by using Agilent 19091s-433 Gas Chromatography. The sample for analysis using Gas Chromatography-Mass Spectroscopy (GC-MS) was prepared by diluting 1 mg of pure compound in 1 mL of acetone or chloroform solvent. Sample injection volume of 1 µL was required to conduct the analysis on the column of gas chromatography. Separation was carried out on HP-5 MS column with 0.25 µM film thickness for 32 min. The sample was injected into the gas chromatography using splitless injector with helium as the carrier gas, flowed at the rate of 1 mL/min. The temperatures of injector and detector were set at 250°C and the solvent delay time was set to 2 min.

3.5.4 Nuclear Magnetic Resonance Spectroscopy Analysis

The structure of unknown synthesized compound was confirmed through interpretation of spectra obtained from analysis using Proton Nuclear Magnetic Resonance (^{1}H-NMR) and Carbon Nuclear Magnetic Resonance (^{13}C-NMR) spectroscopy, conducted at Central Laboratory of Universiti Malaysia Pahang. The compound was dissolved in deuterochloroform ($CDCl_3$) and transferred into 5 mm thin-walled glass tube for NMR analysis. The glass tube was then placed between the poles of a powerful magnet and spun inside NMR tank. The analysis of ^{1}H-NMR and ^{13}C-NMR were conducted using Ultra Bruker DPX-400 spectrometer at frequency of 500 MHz, 600 MHz and 150 MHz, with tetramethylsilane as an internal standard. After complete set-up, the structure of unknown compound was projected on the screen following NMR data interpretation according to the H-NMR spectrum obtained.

3.6 Cytotoxic Effects of Synthetic Flavokawain B Derivative

Study on cytotoxic effects of twenty-two synthesized flavokawain B derivative was carried out in collaboration with Faculty of Biotechnology and Biomolecular Science, Universiti Putra (UPM). UPM provided the cultured cancer cell lines of MCF-7 and MDA-MB-231 for the purpose of this study. The steps occurred in completing this biological analysis were preparation of cell line, preparation of stock solution bg, and determination of cell viability by 3-(4,5-dimethylthiazol-2-yl)-2,5-diphenyltetrazolium bromide (MTT) assay.

3.6.1 Preparation of Cell Line

Roswell Park Medium Institute (RPMI) medium supplemented with fetal bovine serum, penicillin (100 U/mL) and streptomycin (100 µg/mL) was used to grow MCF7-(Human breast adenocarcinoma cell line) obtained from American Type Culture Collection (ATCC) in a 5% carbon dioxide (CO_2) incubator at 37°C (Abu et al., 2014). Dulbecco's Modified Eagle Medium (DMEM) supplemented with fetal bovine serum, penicillin (100 U/mL) and streptomycin (100 µg/mL) was used to grow MDA-MB231-(Human breast adenocarcinoma cell line) obtained from American Type Culture Collection (ATCC) in a 5% CO_2 incubator at 37°C (Abu et al., 2014).

3.6.2 Preparation of Stock Solution of Flavokawain B Derivative

Stock solution of 1 mg/mL was prepared by dissolving the derivatives of flavokawain B derivative chalcone (1 mg) in 1 mL dimethyl sulphoxide (DMSO) (Sigma, USA) and stored in a chiller at 4^{o}C.

3.6.3 Determination of Cell Viability by 3-(4,5-dimethylthiazol-2-yl)-2,5-diphenyltetrazolium bromide (MTT) Assay

Anti-cancer effects of flavokawain B derivative against different cancer cell lines, namely MCF-7 and MDA-MB-231 were evaluated via 3-(4,5-dimethylthiazol-2-yl)-2,5-diphenyltetrazolium bromide (MTT) assay (Merck). MTT assay is a colorimetric assay used to evaluate cellular metabolic activity. MTT assay was performed to evaluate the viability of cells and determine the toxicity effects of the synthesized flavokawain B derivative and doxorubicin (positive control) on the breast cancer cell lines. The MTT assay was conducted according to (Mosmann, 1983) with slight modification in cell type, volume of MTT solution and type of solvent used. The cells were seeded in a 96-well plates at a concentration of 0.8×10^5 cells/well. The cells were then incubated overnight in a CO_2 incubator at 37°C. The synthesized flavokawain B derivative with seven different concentrations was added to the wells in the following day. The cell viability was measured at 72 hr after the treatment. MTT solution (5 mg/mL) with a volume of 20 µL was added to each well and incubated for 4 hr. The solution was discarded afterwards and 100 µL of dimethyl sulphoxide (DMSO) instead of acid-isopropanol was added to each well to solubilize the formazan crystals. Finally, the plates was read by using µ Quant ELISA Reader (Bio-tech Instruments, USA) at a wavelength of 570 nm and 630 nm as the reference wavelength. The results obtained from analysis of the compound-treated cells were compared to standard, doxorubicin as the positive control. Each cell line was assayed in triplicate in three independent experiments (Abu et al., 2014).

3.7 Flow Chart of Research Activities

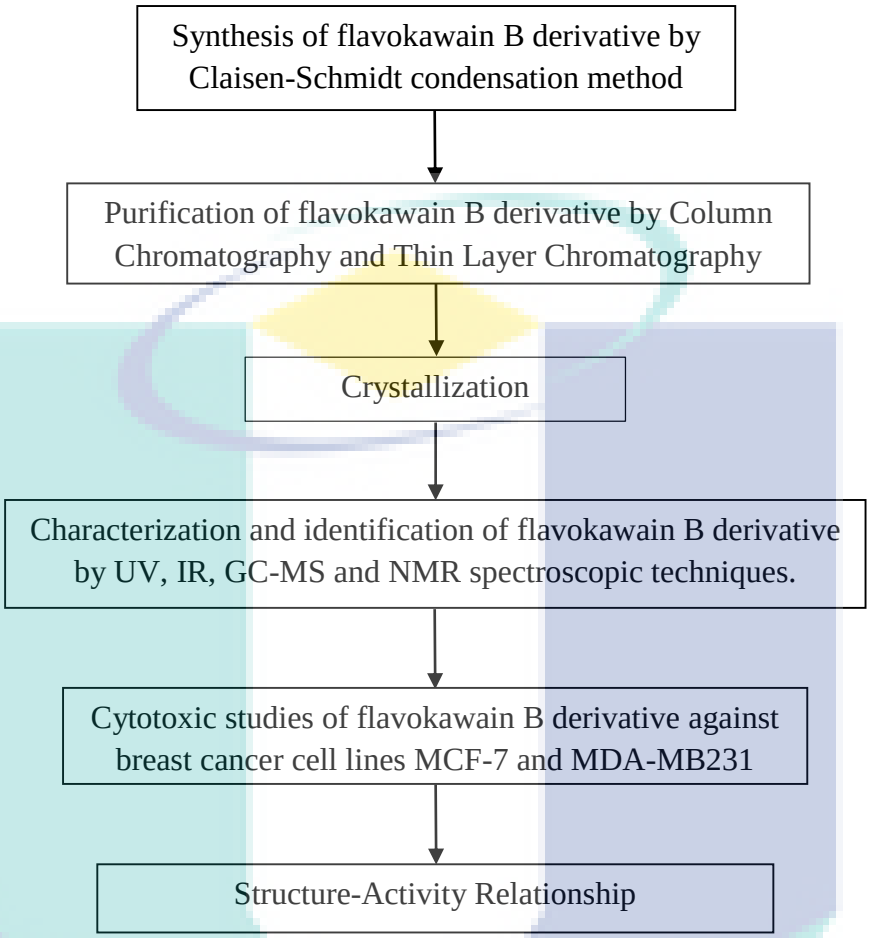

CHAPTER 4

RESULTS & DISCUSSION

4.1 Characterization of Synthesized Flavokawain B Derivative (2, 4, 5, 44, 46, 75-91)

Flavokawain B derivative were synthesized via Claisen-Schmidt condensation method performed under basic condition as described in page 38. These synthesized compounds were characterized by using UV-visible, FTIR spectrophotometry, GC-MS, ^{1}H-NMR and ^{13}C-NMR spectroscopy techniques. The percentage yield obtained from the reactions was in a range of 75-95%.

4.1.1 (*E*)-1-(2′-hydroxy-4′,6′-dimethoxyphenyl)-3-phenylprop-2-en-1-one (4)

Flavokawain B derivative, (*E*)-1-(2′-hydroxy-4′,6′-dimethoxyphenyl)-3-phenylprop-2-en-1-one (**4**) was synthesized via Claisen-Schmidt condensation method as described in page 38, involving 2′-hydroxy-4′,6′-dimethoxyacetophenone (1.00 mmol) and benzaldehyde (1.00 mmol) diluted in 5 mL MeOH, catalyzed by 40% KOH and stirred at room temperature for 48 hr. The product was purified by column chromatography and obtained in yellow needle-shaped crystal with a yield 82.3% and melting point of 96-98°C (Abu et al., 2013).

Compound **4** absorbed UV light in the wavelength range of 290-380 nm, which corresponded to the conjugated α,β-unsaturated carbonyl (C=O) chromophore (Hufford et al., 1982). Figure 4.1 shows the UV-Visible spectrum of compound **4** with maximum absorption at wavelength, λ_{max} of 340 nm.

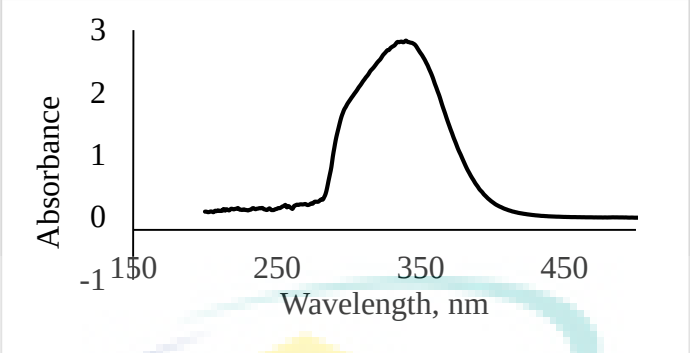

Figure 4.1 UV spectrum of (*E*)-1-(2′-hydroxy-4′,6′-dimethoxyphenyl)-3-phenylprop-2-en-1-one (**4**)

IR spectrum of compound **4** in Figure 4.2 shows absorption band at 3456 cm^{-1}, which corresponded to hydroxy (O-H) and between 2940-3092 cm^{-1}, which corresponded to aromatic C-H stretch Absorption band at 1623 cm^{-1} and between 1416-1439 cm^{-1} was indicated the presence of carbonyl (C=O) and aromatic ring C=C, respectively. Absorption band appeared in the range of 1158-1219 cm^{-1} corresponded to (C-O) moiety (Akhtar et al., 2015).

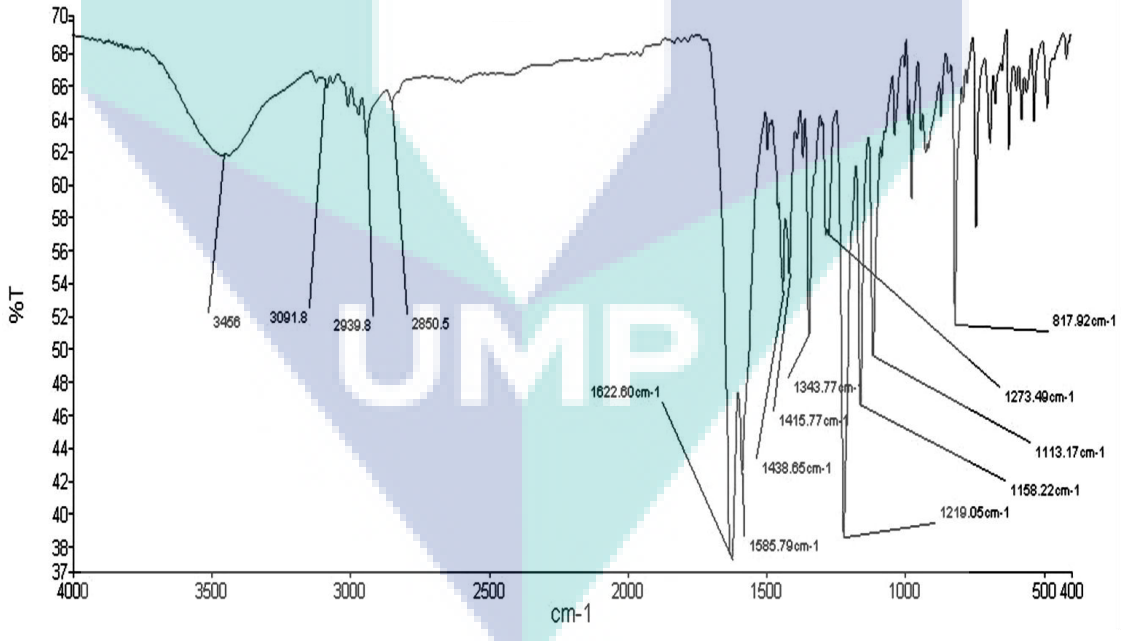

Figure 4.2 IR spectrum of (*E*)-1-(2′-hydroxy-4′,6′-dimethoxyphenyl)-3-phenylprop-2-en-1-one (**4**)

The ^{1}H-NMR spectrum (600 MHz, $CDCl_3$) of compound **4** in Figure 4.3 (Appendix A1) shows two singlet at δ 3.84 and 3.92 which were assigned to the methoxy protons at C-4′ and C-6′, respectively. Two doublet that appeared at 5.96 (d, *J*

= 2.46 Hz) and 6.11 (d, *J* = 2.40 Hz) were assigned to C-5′ and C-3′ protons, respectively. A broad multiplet that appeared in the range of 7.38-7.42 was assigned to C-3, C-4 and C-5 protons. Two doublets observed at 7.62 (d, *J* = 8.04 Hz) and 7.60 (d, *J* = 8.04 Hz) were assigned to C-2 and C-6 protons, respectively. A downfield doublet at 7.78 (d, *J* = 15.55 Hz) was assigned to proton at α-carbon and another doublet observed at 7.90 (d, *J* = 15.55 Hz) was assigned to proton at β-carbon, which data is supported by previous publication (Abu et al., 2016; Seo et al., 2013). A downfield singlet that appeared at 14.30 was assigned to C-2′ hydroxyl proton chelated to carbonyl group. Further details of ^{1}H-NMR and ^{13}C-NMR spectra are shown in Table 4.1.

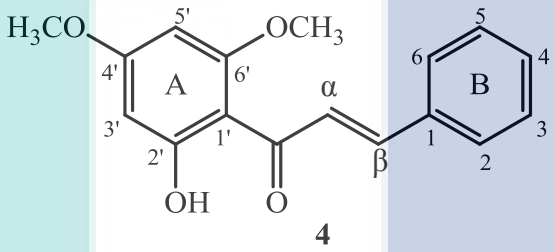

4

Figure 4.3 Structure of (*E*)-1-(2′-hydroxy-4′,6′-dimethoxyphenyl)-3-phenylprop-2-en-1-one (**4**)

Table 4.1 NMR data of (*E*)-1-(2′-hydroxy-4′,6′-dimethoxyphenyl)-3-phenylprop-2-en-1-one (**4**)

Carbon	**^{13}C (δ)**	**^{1}H (δ)**	**Multiplicity**	**Designation**
1′	108.14	-	-	-
2′	168.90	-	-	-
3′	93.60	6.11	(d, *J* = 2.40 Hz, 1H)	C3′-H
4′	166.70	-	-	-
5′	90.94	5.96	(d, *J* = 2.46 Hz, 1H)	C5′-H
6′	162.50	-	-	-
1	132.90	-	-	-
2	130.20	7.62	(d, *J* = 8.04 Hz, 1H)	C2-H
3	128.10	7.38-7.42	(m, 3H)	C3-H
4	141.00	7.38-7.42	(m, 3H)	C4-H
5	128.10	7.38-7.42	(m, 3H)	C5-H
6	130.20	7.60	(d, *J* = 8.04 Hz, 1H)	C6-H
α	126.60	7.78	(d, *J* = 15.55 Hz, 1H, H-α)	Cα-H
β	142.51	7.90	(d, *J* = 15.55 Hz, 1H, H-β)	Cβ-H
OCH_3 (C4′)	55.70	3.84	(s, 3H)	OCH_3 (C4′)
OCH_3 (C6′)	55.53	3.92	(s, 3H)	OCH_3 (C6′)
OH (C2′)	-	14.30	(s, 1H)	OH (C2′)
C=O	193.20	-	-	-

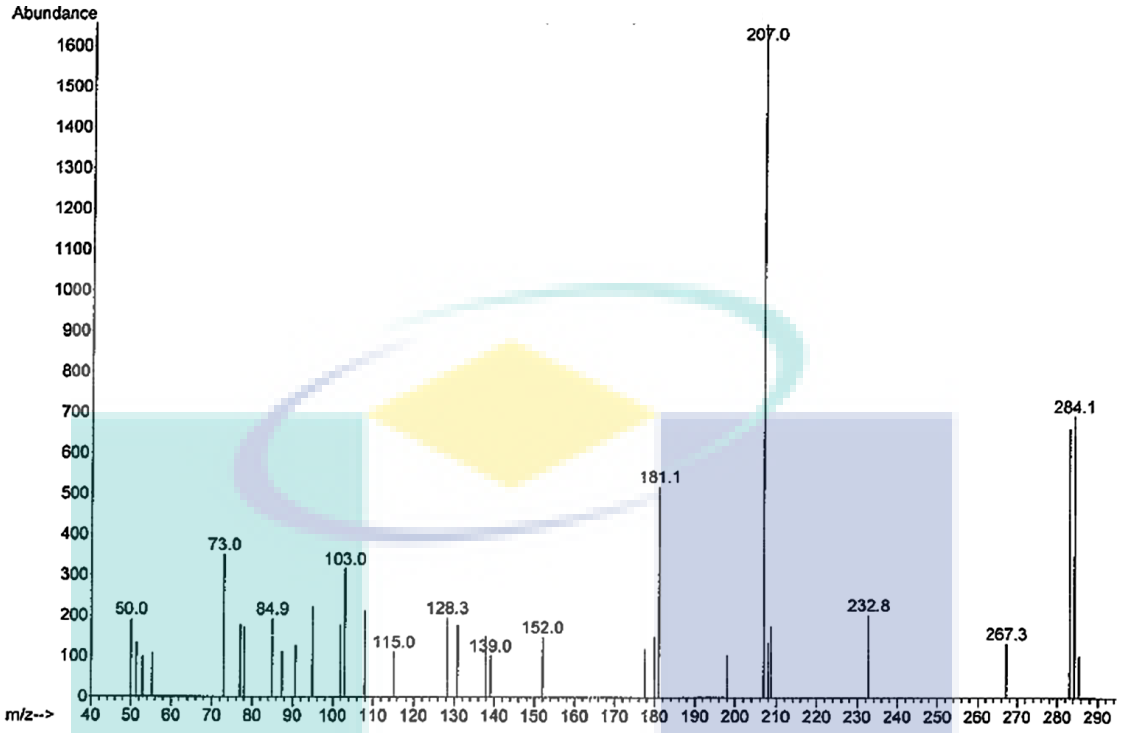

Figure 4.4 GC-MS spectrum of (*E*)-1-(2′-hydroxy-4′,6′-dimethoxyphenyl)-3-phenylprop-2-en-1-one (**4**)

GC-MS spectrum of compound **4** shown in Figure 4.4 displays the main fragment ion at *m/z* = 284, 267, 207, 181, 152, 131, 103 and 77. The abundance of molecular peak at *m/z* = 284 was about 50%. Loss of ·OH radical from the molecular ion produced fragment ion at *m/z* = 267. The base peak at *m/z* = 207 was produced due to loss of phenyl group while another fragment formed at *m/z* = 77 due to β-cleavage. The fragment ion at *m/z* = 181 could be the radical ketone moiety formed due to α-cleavage. Formation of fragment ion at *m/z* = 152 could be due to the cleavage of bond next to C=O and subsequent rearrangement; the other part formed a fragment ion at *m/z* = 131. The fragment ion at *m/z* = 103 was probably the $C_8H_7^+$ ion, formed after cleavage of bond next to C=O in structure of fragment ion observed at *m/z* = 131. The proposed mechanism of mass fragmentation is shown in Figure 4.5.

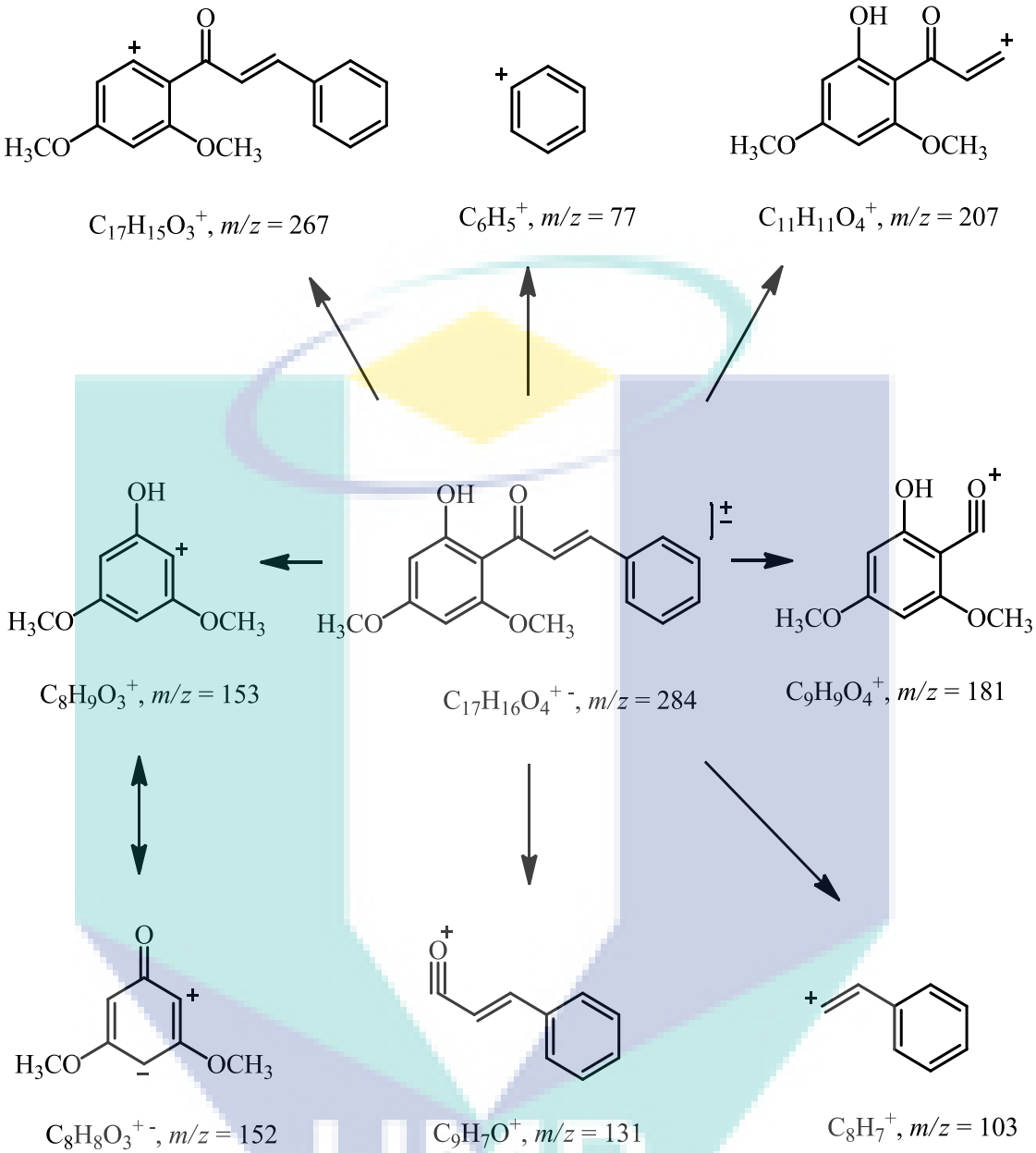

Figure 4.5 Mass fragmentation of (*E*)-1-(2′-hydroxy-4′,6′-dimethoxyphenyl)-3-phenylprop-2-en-1-one (**4**)

4.1.2 (*E*)-1-(2′-hydroxyl-4′,6′-dimethoxyphenyl)-3-(4-methoxyphenyl)prop-2-en-1-one (5)

Using the procedure described in page 38, 2′-hydroxy-4′,6′-dimethoxyacetophenone (1.00 mmol) and 4-hydroxybenzaldehyde (1.00 mmol) diluted in 5 mL MeOH, catalyzed by 40% KOH and stirred at room temperature for 48 hr, gave product after purification by column chromatography, (*E*)-1-(2′-hydroxyl-4′,6′-dimethoxyphenyl)-3-(4-methoxyphenyl)prop-2-en-1-one (**5**) with yield of 72.5%, melting point of 109-110°C (Boeck et al., 2006) as yellow flat crystal shaped.

Compound **5** absorbed UV light in the wavelength range of 290-405 nm, which corresponded to the conjugated α,β-unsaturated carbonyl (C=O) chromophore (Rapado. et al., 2014). Figure 4.6 shows the UV-Visible spectrum of compound **5** with maximum absorption observed at wavelength, λ_{max} of 364-365 nm.

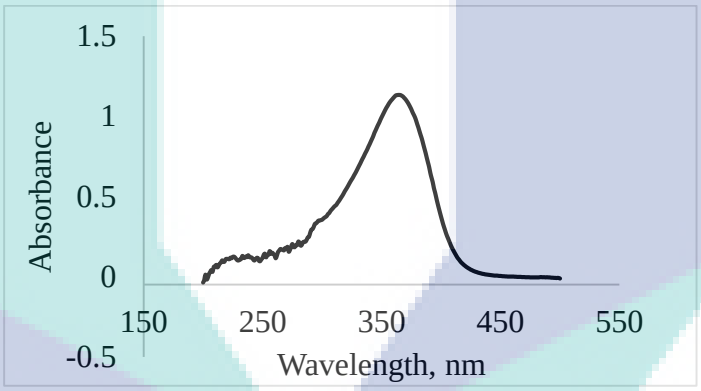

Figure 4.6 UV spectrum of (*E*)-1-(2′-hydroxyl-4′,6′-dimethoxyphenyl)-3-(4-methoxyphenyl)prop-2-en-1-one (**5**)

IR spectrum of compound **5** shown in Figure 4.7 shows the absorption bands at 3389 cm^{-1} and between 2860-3006 cm^{-1}, which corresponded to hydroxyl (O-H) group and aromatic C-H stretch, respectively. The absorption bands at 1603 cm^{-1} and 1426-1513 cm^{-1} corresponded to carbonyl (C=O) group and aromatic ring C=C, respectively.

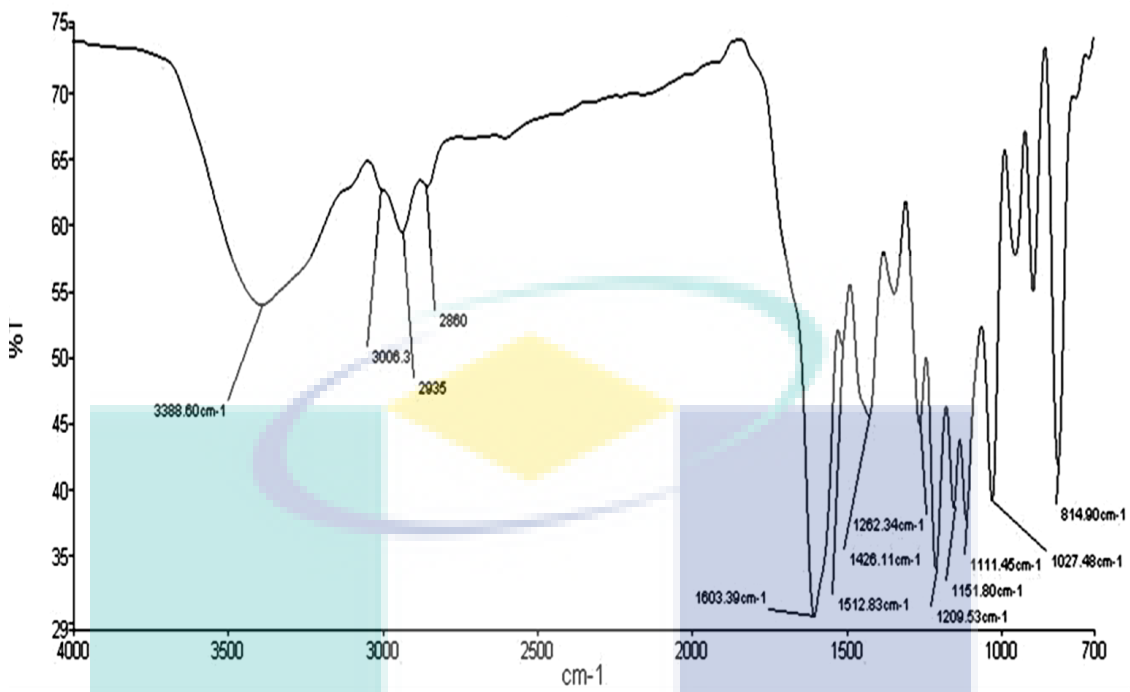

Figure 4.7 IR spectrum of (*E*)-1-(2′-hydroxyl-4′,6′-dimethoxyphenyl)-3-(4-methoxyphenyl)prop-2-en-1-one (**5**)

The ^{1}H-NMR spectrum (600 MHz, $CDCl_3$) of compound **5** in Figure 4.8 (Appendix A1) shows that a signal appeared as doublet at δ 6.09 (d, *J* = 2.40 Hz), and assigned to the C-3′ proton. A doublet appeared at 5.94 (d, *J* = 2.40 Hz) and was assigned to the C-5′ proton. Two doublets appeared at 7.56 (d, *J* = 8.76 Hz) and 7.54 (d, *J* = 8.76 Hz) were assigned to the C-2 and C-6 proton, respectively. Another doublet appeared at 6.92 (d, *J* = 8.70 Hz) and 6.91 (d, *J* = 8.70 Hz) were assigned to the C-3 and C-5 proton, respectively. Three signals of singlet that appeared at 3.82 (s, 3H), 3.84 (s, 3H) and 3.90 (s, 3H) were assigned to the methoxy protons at C-4, C-4′ and C-6′, respectively. A signal of doublet which appeared at 7.78 (d, *J* = 15.48 Hz) was assigned to proton α-carbon and a doublet at 7.79 (d, *J* = 15.48 Hz) was assigned to proton β-carbon. A downfield singlet that appeared at 14.45 was assigned to the C-2′ hydroxyl proton chelated to carbonyl group, which data is supported by previous journal (Abu et al., 2014). The details of ^{1}H-NMR and ^{13}C-NMR spectra are shown in Table 4.2.

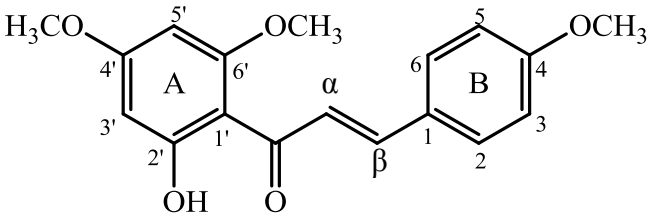

5

Figure 4.8 Structure of (*E*)-1-(2′-hydroxyl-4′,6′-dimethoxyphenyl)-3-(4-methoxyphenyl)prop-2-en-1-one (**5**)

Table 4.2 NMR data of (*E*)-1-(2′-hydroxyl-4′,6′-dimethoxyphenyl)-3-(4-methoxyphenyl)prop-2-en-1-one (**5**)

Carbon	**^{13}C (δ)**	**^{1}H (δ)**	**Multiplicity**	**Designation**
1′	130.10	-	-	-
2′	168.70	-	-	-
3′	93.56	6.09	(d, *J* = 2.40 Hz, 1H)	C3′-H
4′	166.20	-	-	-
5′	91.40	5.94	(d, *J* = 2.40 Hz, 1H)	C5′-H
6′	163.10	-	-	-
1	127.50	-	-	-
2	130.10	7.56	(d, *J* = 8.76 Hz, 1H)	C2-H
3	114.30	6.92	(d, *J* = 8.70 Hz, 1H)	C3-H
4	160.90	-	-	-
5	114.30	6.91	(d, *J* = 8.70 Hz, 1H)	C5-H
6	130.10	7.54	(d, *J* = 8.76 Hz, 1H)	C6-H
α	125.40	7.78	(d, *J* = 15.48 Hz, 1H, H-α)	Cα-H
β	141.60	7.79	(d, *J* = 15.48 Hz, 1H, H-β)	Cβ-H
OCH_3 (C4′)	55.79	3.84	(s, 3H)	OCH_3 (C4′)
OCH_3 (C6′)	55.53	3.90	(s, 3H)	OCH_3 (C6′)
OCH_3 (C4)	55.35	3.82	(s, 3H)	OCH_3 (C4)
OH (C2′)	-	14.45	(s, 1H)	OH (C2′)
C=O	192.60	-	-	-

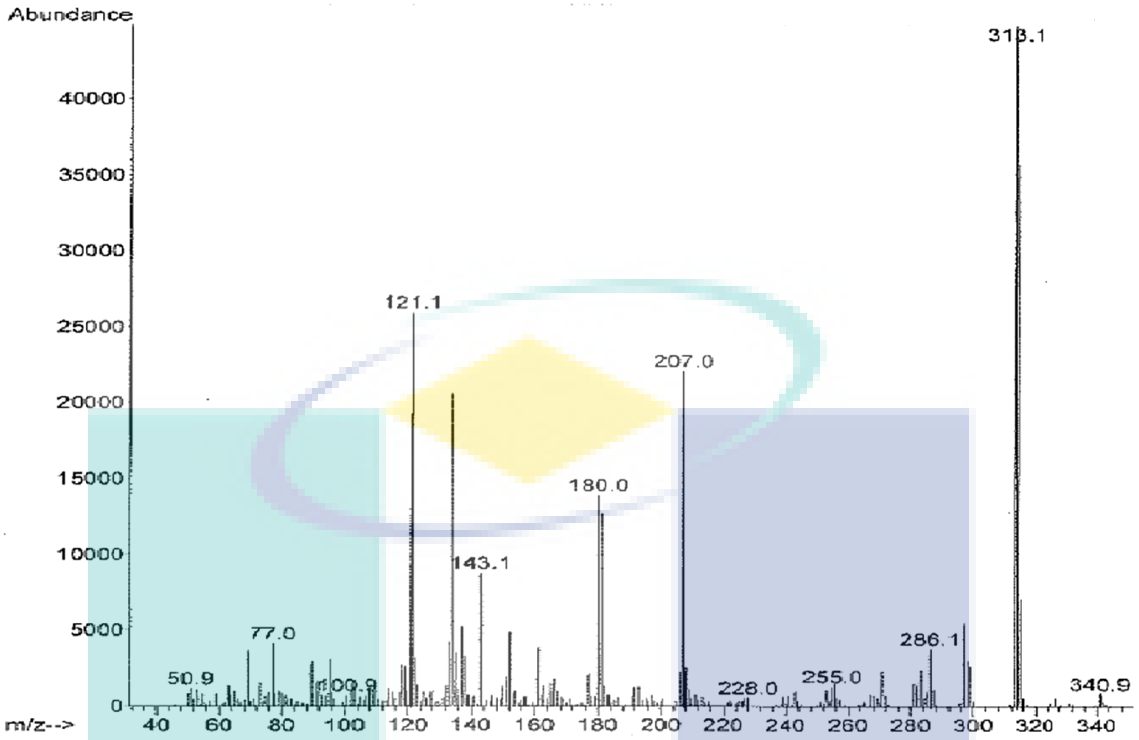

Figure 4.9 GC-MS spectrum of (*E*)-1-(2′-hydroxyl-4′,6′-dimethoxyphenyl)-3-(4-methoxyphenyl)prop-2-en-1-one (**5**)

GC-MS spectrum of compound **5** is shown in Figure 4.9, which displays the main fragment ions at *m/z* = 314, 313, 297, 207, 181, 161, 152, 133 and 107. The abundance of molecular peak at *m/z* = 314 was about 80% and the base peak was produced at *m/z* = 313. Formation of fragment ion at *m/z* = 297 was due to loss of ·OH radical from the molecular ion. β-cleavage of carbon bond next to β-carbon gave out a fragment ion at *m/z* = 207, whereas the fragment ion observed at *m/z* = 107 was formed due to $C_7H_7O^+$ radical. Fragment at *m/z* = 181 represented ketone moiety cation. Formation of fragment ions at *m/z* = 152 and *m/z* = 161 could be due to the cleavage of bond next to C=O and rearrangement. The fragment ion at *m/z* = 133 probably representing C_9H_9O· ion which formed following the α-cleavage of bond next to carbonyl group in a fragment observed at *m/z* = 161. The possible mechanisms of main fragmentation was proposed and is shown in Figure 4.10.

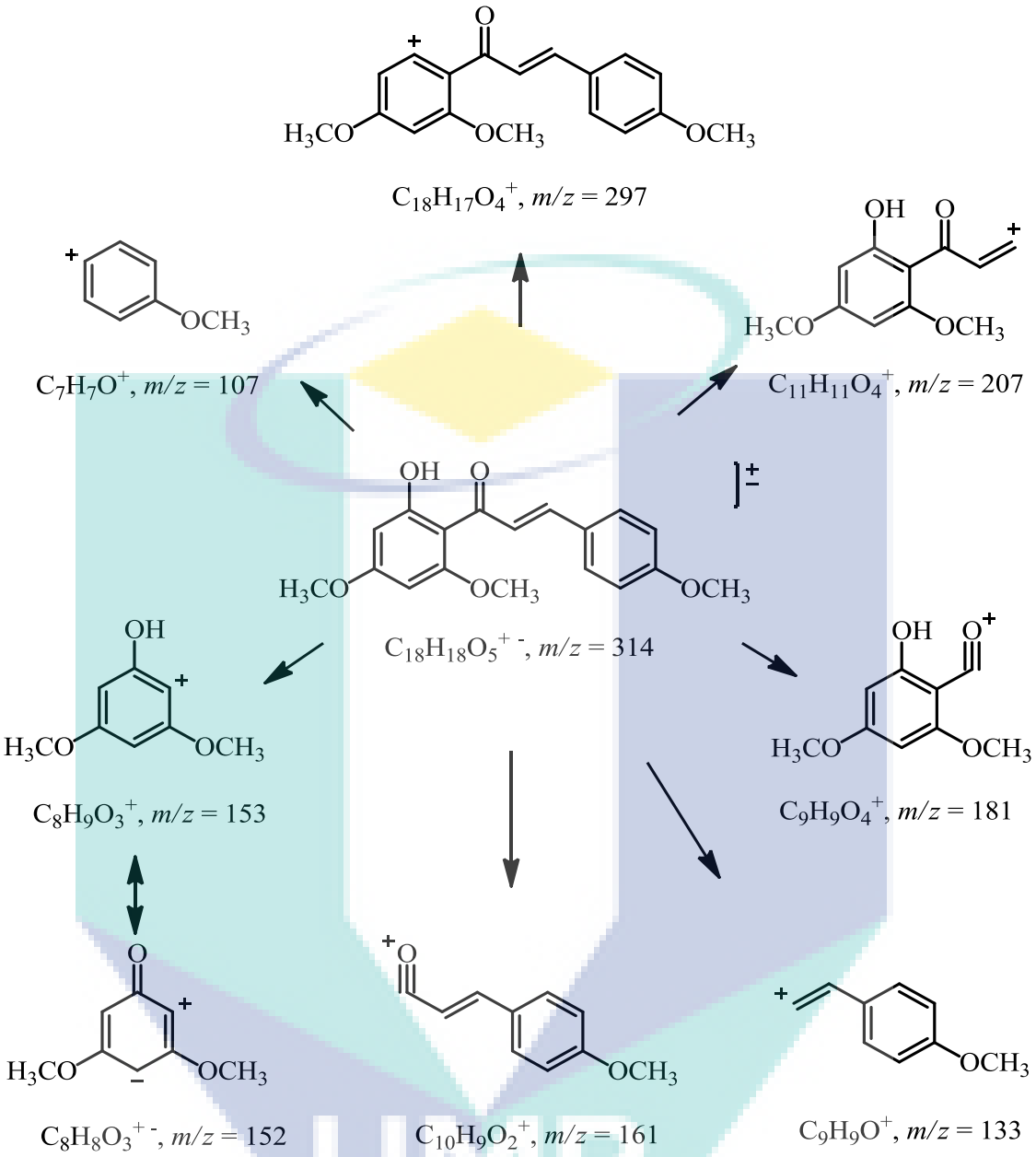

Figure 4.10 Mass fragmentation of (*E*)-1-(2′-hydroxyl-4′,6′-dimethoxyphenyl)-3-(4-methoxyphenyl)prop-2-en-1-one (**5**)

4.1.3 (*E*)-1-(2′-hydroxy-4′,6′-dimethoxyphenyl)-3-(4-(methylthio)phenyl)prop-2-en-1-one (75)

Flavokawain B derivative, (*E*)-1-(2′-hydroxy-4′,6′-dimethoxyphenyl)-3-(4-(methylthio)phenyl)prop-2-en-1-one (**75**) was synthesized via Claisen-Schmidt condensation method between 2′-hydroxy-4′,6′-dimethoxyacetophenone (1.00 mmol) and 4-(methylthio)benzaldehyde (1.00 mmol) diluted in 4 mL MeOH, catalyzed by 40% KOH and stirred at room temperature for 50 hr as described in page 38. The product was obtained in a form of orange flat crystal with a yield of 78.3% and melting point of 129-131°C.

Compound **75** absorbed UV-Visible light in a wavelength range of 300-420 nm, which corresponded to the conjugated α,β-unsaturated carbonyl (C=O) chromophore. Figure 4.11 shows the UV-Visible spectrum of compound **75** with maximum absorption observed at the wavelength, λ_{max} of 371-372 nm.

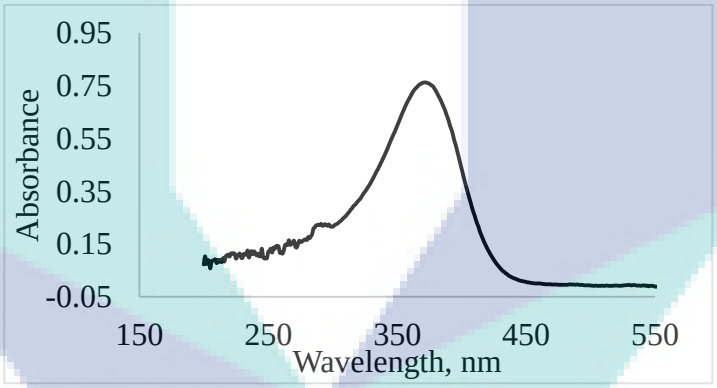

Figure 4.11 UV spectrum of (*E*)-1-(2′-hydroxy-4′,6′-dimethoxyphenyl)-3-(4-(methylthio)phenyl)prop-2-en-1-one (**75**)

IR spectrum of compound **75** shown in Figure 4.12 displays the absorption bands at 3469 cm^{-1} and 1619 cm^{-1}, which representing the hydroxyl (O-H) and carbonyl (C=O) groups, respectively. Absorption band observed in a range of 1431-1432 cm^{-1} and 2981-3014 cm^{-1} were assigned to aromatic ring (C=C) and aromatic carbon-proton (Ar C-H), respectively. Absorption bands that appeared in a range of 1155-1218 cm^{-1} and 1548-1584 cm^{-1} corresponded to (C-O) and (C=C-C=O), respectively (Ali et al., 2016).

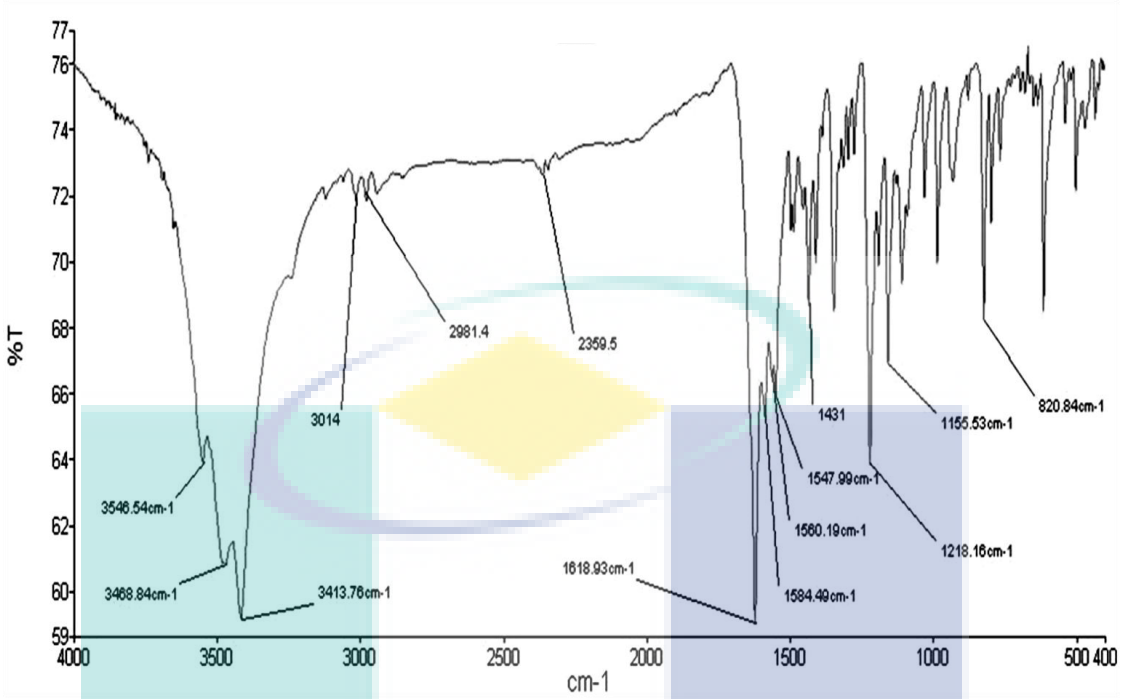

Figure 4.12 IR spectrum of (*E*)-1-(2′-hydroxy-4′,6′-dimethoxyphenyl)-3-(4-(methylthio)phenyl)prop-2-en-1-one (**75**)

^{1}H-NMR spectrum (500 MHz, $CDCl_3$) of compound **75** in Figure 4.13 (Appendix A2) shows that a singlet appeared at δ 2.51 and was assigned to the thio-methyl protons at C-4. Two singlets that appeared at 3.83 and 3.91 were assigned to the methoxy proton at C-4′ and C-6′, respectively. Two doublets that appeared at 5.95 (d, *J* = 2.50 Hz) and 6.10 (d, *J* = 2.50 Hz) were assigned to the C-5′ and C-3′ protons, respectively. Two doublets that appeared at 7.25 (d, *J* = 8.50 Hz) and 7.23 (d, *J* = 8.50 Hz) were assigned to the C-3 and C-5 protons, respectively. Two doublets observed at 7.52 (d, *J* = 8.50 Hz) and 7.50 (d, *J* = 8.50 Hz) were assigned to the C-2 and C-6 protons, respectively. A doublet that appeared at 7.76 (d, *J* = 15.50 Hz) was assigned to the proton at α-carbon while another doublet at 7.84 (d, *J* = 15.50 Hz) was assigned to the proton at β-carbon. A downfield singlet observed at 14.34 was assigned to the C-2′ hydroxyl proton (O-H) chelated to carbonyl which data is partially supported by previous research (Ali et al., 2016). The details of ^{1}H-NMR spectra is shown in Table 4.3.

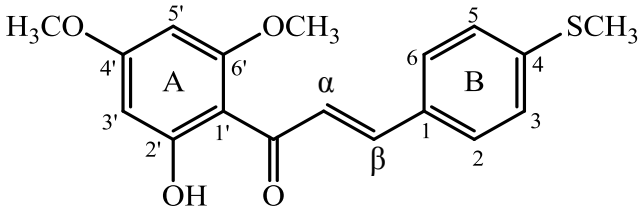

75

Figure 4.13 Structure of (*E*)-1-(2′-hydroxy-4′,6′-dimethoxyphenyl)-3-(4-(methylthio)phenyl)prop-2-en-1-one (**75**)

Table 4.3 NMR data of (*E*)-1-(2′-hydroxy-4′,6′-dimethoxyphenyl)-3-(4-(methylthio)phenyl)prop-2-en-1-one (**75**)

Carbon	^{1}H (δ)	Multiplicity	Designation
1′	-	-	-
2′	-	-	-
3′	6.10	(d, *J* = 2.50 Hz, 1H)	C3′-H
4′	-	-	-
5′	5.95	(d, *J* = 2.50 Hz, 1H)	C5′-H
6′	-	-	-
1	-	-	-
2	7.52	(d, *J* = 8.50 Hz, 1H)	C2-H & C6-H
3	7.25	(d, *J* = 8.50 Hz, 1H)	C3-H & C5-H
4	-	-	-
5	7.23	(d, *J* = 8.50 Hz, 1H)	C5-H & C3-H
6	7.50	(d, *J* = 8.50 Hz, 1H)	C6-H & C2-H
α	7.76	(d, *J* = 15.50 Hz, 1H, H-α)	Cα-H
β	7.84	(d, *J* = 15.50 Hz, 1H, H-β)	Cβ-H
OCH_3 (C4′)	3.83	(s, 3H)	OCH_3 (C4′)
OCH_3 (C6′)	3.91	(s, 3H)	OCH_3 (C6′)
S-CH_3 (C4)	2.51	(s, 3H)	S-CH_3 (C4)
OH (C2′)	14.34	(s, 1H)	OH (C2′)

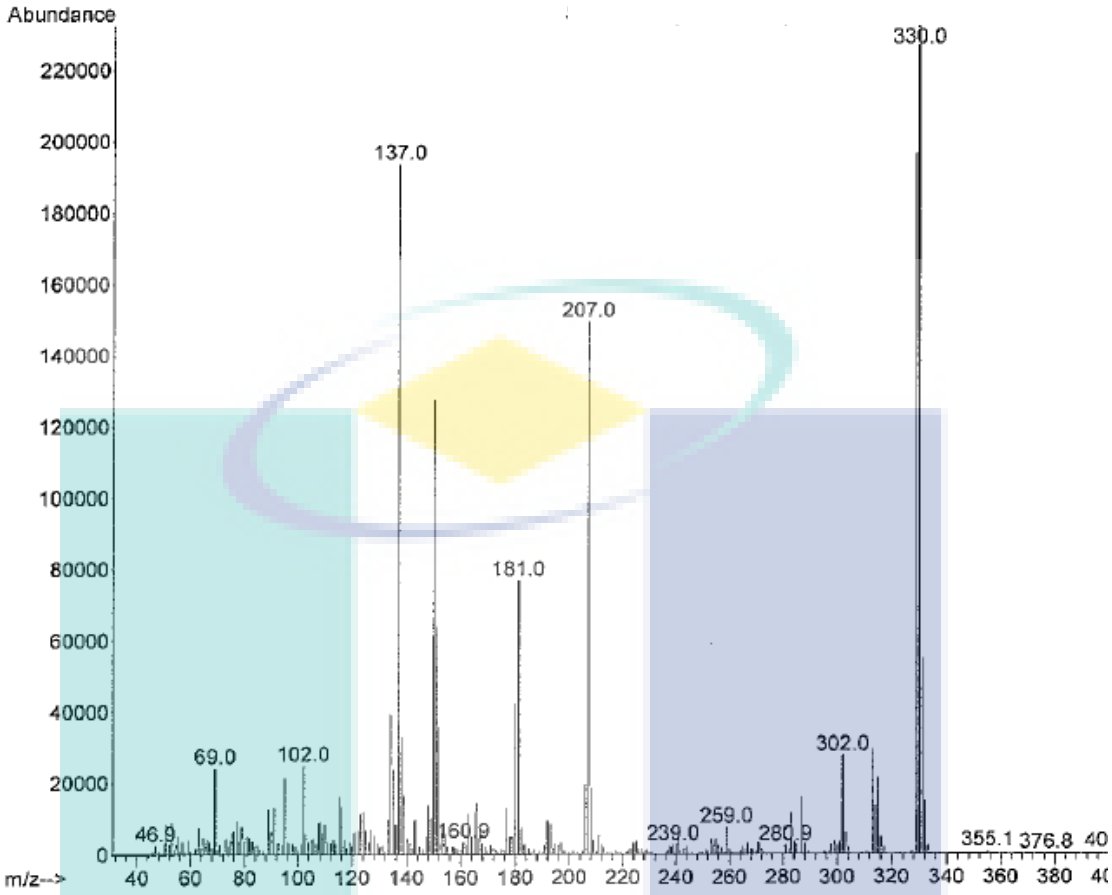

Figure 4.14 GC-MS spectrum of (*E*)-1-(2′-hydroxy-4′,6′-dimethoxyphenyl)-3-(4-(methylthio)phenyl)prop-2-en-1-one (**75**)

GC-MS spectrum of compound **75** is shown in Figure 4.14, which displays the presence of the main fragment ion of a molecular structure at *m/z* = 330, 302, 207, 181, 151, 137 and 102. This finding may support the proposed structure of the synthesized compound **75**.

4.1.4 (*E*)-3-(2,3-dimethoxyphenyl)-1-(2′-hydroxy-4′,6′-dimethoxyphenyl)prop-2-en-1-one (76)

Flavokawain B derivative, (*E*)-3-(2,3-dimethoxyphenyl)-1-(2′-hydroxy-4′,6′-dimethoxyphenyl)prop-2-en-1-one (**76**) was synthesized via Claisen-Schmidt condensation method between 2′-hydroxy-4′,6′-dimethoxyacetophenone (1.00 mmol) and 2,3-dimethoxybenzaldehyde (1.00 mmol) diluted in 5 mL MeOH, catalyzed by 40% KOH and stirred at room temperature for 48 hr as described in page 38. The product was obtained in a form of yellowish orange crystal with a yield of 83.4% and melting point of 121-123°C (Srinivas et al., 2003).

Compound **76** absorbed UV light in a wavelength range of 280-400 nm, which corresponded to the conjugated α,β-unsaturated carbonyl (C=O) chromophore. The UV-Visible spectrum of compound **76** shown in Figure 4.15 displays the absorption peak at wavelength, λ_{max} between 335-337 nm.

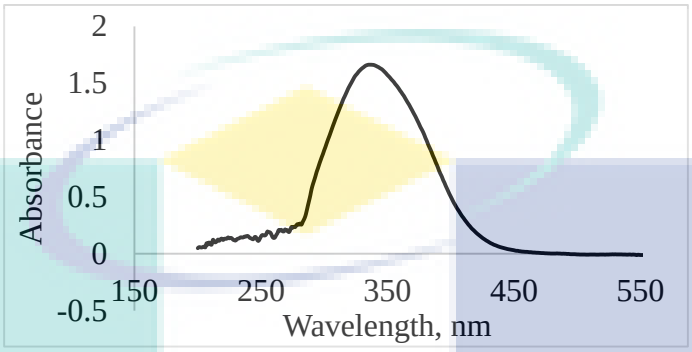

Figure 4.15 UV spectrum of (*E*)-3-(2,3-dimethoxyphenyl)-1-(2′-hydroxy-4′,6′-dimethoxyphenyl)prop-2-en-1-one (**76**)

IR spectrum of compound **76** shown in Figure 4.16 displays the absorption bands at 3458 cm^{-1} and between 2839-2985 cm^{-1}, which corresponded to the hydroxyl (O-H) group and aromatic C-H stretch, respectively. Formation of absorption bands at 1627 cm^{-1} and between 1350-1442 cm^{-1} were due to the presence of carbonyl (C=O) group and aromatic ring C=C, respectively. The absorption bands observed in a range of 1556-1581 cm^{-1} and 1213-1268 cm^{-1} corresponded to (C=C-C=O) and (C-O) groups, respectively.

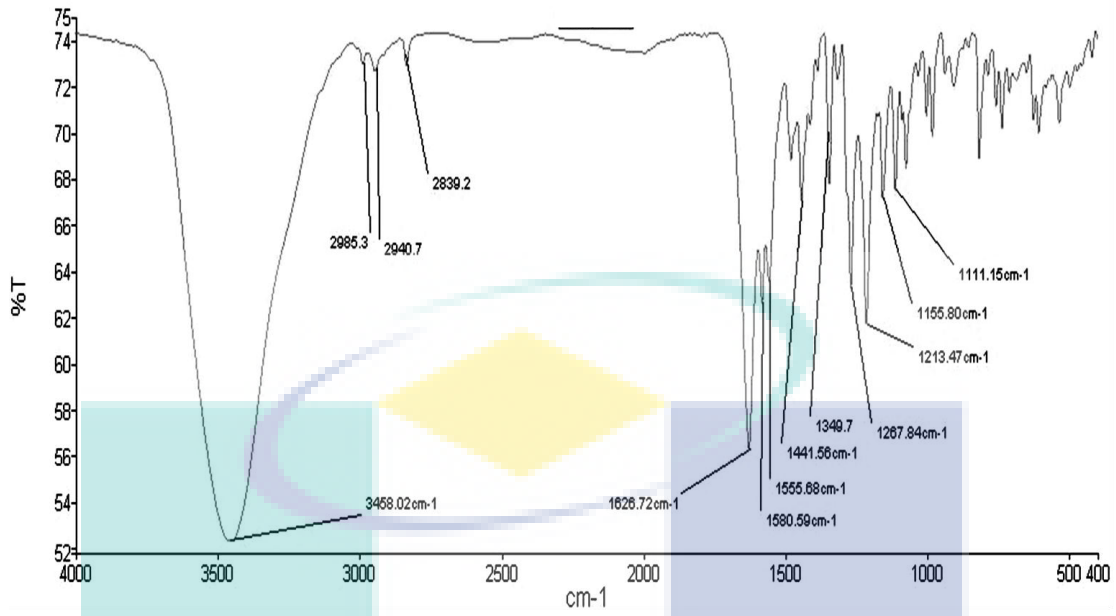

Figure 4.16 IR spectrum of (*E*)-3-(2,3-dimethoxyphenyl)-1-(2′-hydroxy-4′,6′-dimethoxyphenyl)prop-2-en-1-one (**76**)

The ^{1}H-NMR spectrum (600 MHz, $CDCl_3$) of compound **76** shown in Figure 4.17 (Appendix A2) displays four signals of singlet at δ 3.84, 3.89, 3.90 and 3.91, which were assigned to the methoxy protons at C-4′, C-3, C-2 and C-6′, respectively. The doublet observed at 5.96 (d, *J* = 2.10 Hz) was assigned to the C-5′ proton and another doublet at 6.11 (d, *J* = 2.10 Hz) was assigned to the C-3′ proton. The doublet appeared at 6.95 (d, *J* = 8.04 Hz) was assigned to the C-4 proton and another doublet at 7.24 (d, *J* = 7.74 Hz) was assigned to the C-6 proton. A triplet that appeared at 7.08 (t, *J* = 8.04 Hz, 7.98 Hz) was assigned to the C-5 proton. A doublet observed at 7.96 (d, *J* = 15.78 Hz) was assigned to the proton at α-carbon and a doublet at 8.08 (d, *J* = 15.78 Hz) was assigned to the proton at β-carbon. A downfield singlet that appeared at 14.34 represented the C-2′ hydroxyl proton, formed by chelation with carbonyl group. The details of ^{1}H-NMR spectra is shown in Table 4.4.

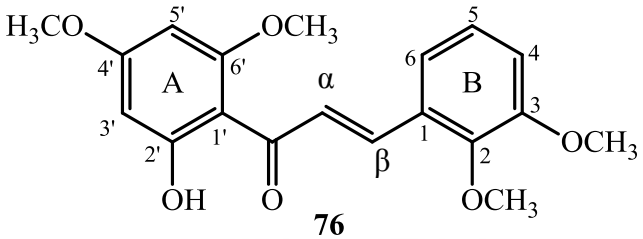

Figure 4.17 Structure of (*E*)-3-(2,3-dimethoxyphenyl)-1-(2′-hydroxy-4′,6′-dimethoxyphenyl)prop-2-en-1-one (**76**)

Table 4.4 NMR data of (*E*)-3-(2,3-dimethoxyphenyl)-1-(2′-hydroxy-4′,6′-dimethoxyphenyl)prop-2-en-1-one (**76**)

Carbon	**^{13}C (δ)**	**^{1}H (δ)**	**Multiplicity**	**Designation**
1′	106.47	-	-	-
2′	137.19	-	-	-
3′	113.76	6.11	(d, *J* = 2.10 Hz, 1H)	C3′-H
4′	162.55	-	-	-
5′	119.80	5.96	(d, *J* = 2.10 Hz, 1H)	C5′-H
6′	166.18	-	-	-
1	148.88	-	-	-
2	168.40	-	-	-
3	153.24	-	-	-
4	124.12	6.95	(d, *J* = 8.04 Hz, 1H)	C4-H
5	129.79	7.08	(t, *J* = 8.04 Hz, 7.98 Hz, 1H)	C5-H
6	128.95	7.24	(d, *J* = 7.74 Hz, 1H)	C6-H
α	91.2	7.96	(d, *J* = 15.78 Hz, 1H, H-α)	Cα-H
β	93.7	8.08	(d, *J* = 15.78 Hz, 1H, H-β)	Cβ-H
OCH_3 (C4′)	55.84	3.84	(s, 3H)	OCH_3 (C4′)
OCH_3 (C6′)	55.58	3.91	(s, 3H)	OCH_3 (C6′)
OCH_3 (C2)	61.31	3.90	(s, 3H)	OCH_3 (C2)
OCH_3 (C3)	55.92	3.89	(s, 3H)	OCH_3 (C3)
OH (C2′)	-	14.34	(s, 1H)	OH (C2′)
C=O	192.93	-	-	-

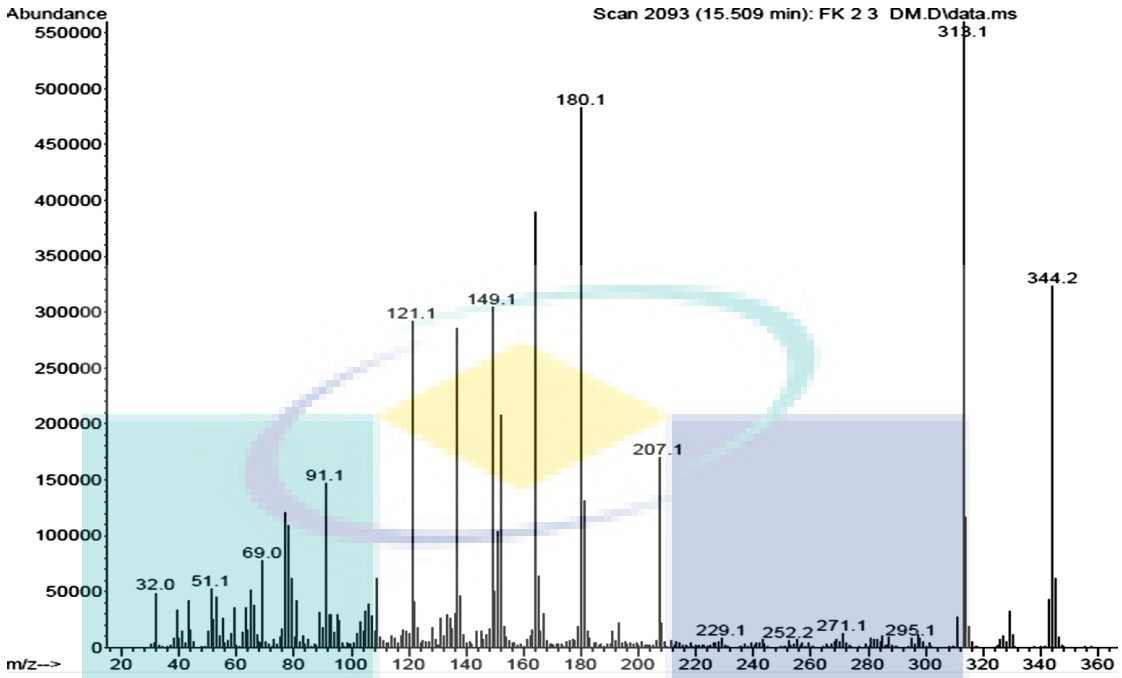

Figure 4.18 GC-MS spectrum of (*E*)-3-(2,3-dimethoxyphenyl)-1-(2′-hydroxy-4′,6′-dimethoxyphenyl)prop-2-en-1-one (**76**)

The GC-MS spectrum of compound **76** shown in Figure 4.18 displays the presence of the main fragment ions of a molecular structure at *m/z* = 344, 329, 313, 207, 181, 164, 152, 149, 137 and 121. The result could support the tentative of synthesized compound **76**.

4.1.5 (*E*)-1-(2′-hydroxy-4′,6′-dimethoxyphenyl)-3-(2,4,6-trimethoxyphenyl)prop-2-en-1-one (77)

Flavokawain B derivative, (*E*)-1-(2′-hydroxy-4′,6′-dimethoxyphenyl)-3-(2,4,6-trimethoxyphenyl)prop-2-en-1-one (**77**) was synthesized via Claisen-Schmidt condensation method between 2′-hydroxy-4′,6′-dimethoxyacetophenone (1.00 mmol) and 2,4,6-trimethoxybenzaldehyde (1.00 mmol) diluted in 5 mL MeOH, catalyzed by 40% KOH and stirred at room temperature for 48 hr as described in page 38. The product was obtained in a form of orange crystal with a yield of 82.8% and melting point of 158-159°C (Rao et al., 2004)).

Compound **77** absorbed the UV light in the wavelength range of 310-435 nm, which corresponded to the conjugated α,β-unsaturated carbonyl (C=O) chromophore. The UV-Visible spectrum of compound **77** shown in Figure 4.19 shows that the maximum absorption occurred at a wavelength, λ_{max} of 386 nm.

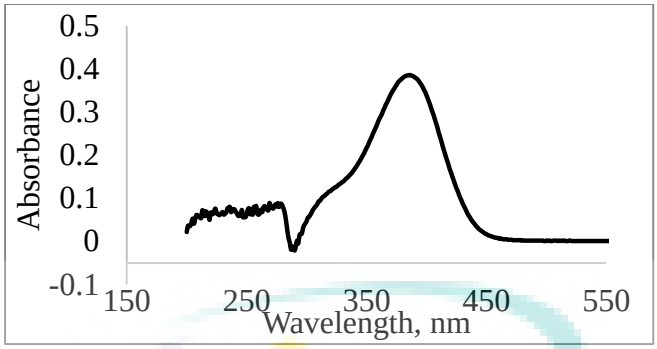

Figure 4.19 UV spectrum of (*E*)-1-(2′-hydroxy-4′,6′-dimethoxyphenyl)-3-(2,4,6-trimethoxyphenyl)prop-2-en-1-one (**77**)

IR spectrum of compound **77** shown in Figure 4.20 displays the absorption bands at 3464 cm^{-1} and 1618 cm^{-1}, representing the hydroxyl (O-H) and carbonyl (C=O) groups, respectively. Absorption bands that appeared in a range of 1414-1545 cm^{-1} and 2941-3010 cm^{-1} represented the aromatic ring (C=C) and aromatic proton (Ar C-H), respectively. Absorption band appeared in a range of 1122-1217 cm^{-1} indicated the presence of (C-O).

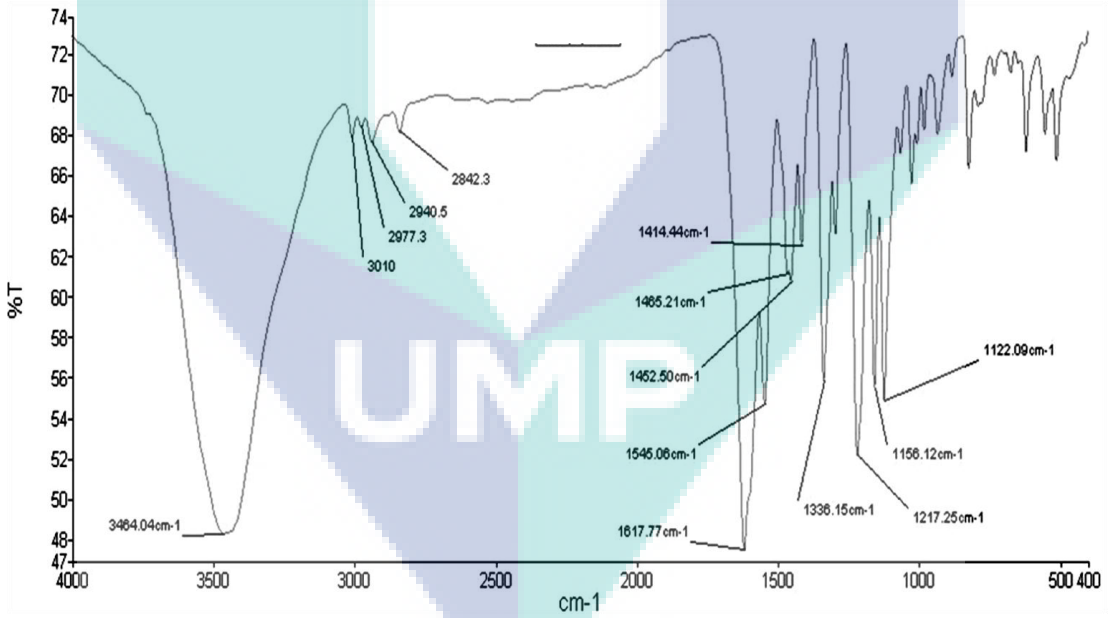

Figure 4.20 IR spectrum of (*E*)-1-(2′-hydroxy-4′,6′-dimethoxyphenyl)-3-(2,4,6-trimethoxyphenyl)prop-2-en-1-one (**76**)

The ^{1}H-NMR spectrum (600 MHz, $CDCl_3$) of compound **76** shown in Figure 4.21 (Appendix A3) displays five singlets at δ 3.82, 3.85, 3.89, 3.90 and 3.90, which were assigned to the methoxy proton at C-4, C-4′, C-2, C-6 and C-6′, respectively. The doublet that appeared at 5.94 (d, J = 2.40 Hz) was assigned to the C-5′ proton and

another doublet at 6.09 (d, *J* = 2.40 Hz) was assigned to the C-3′ proton. The singlet appeared at 6.13 (s, 2H) was assigned to the C-3 and C-5 proton. A doublet appeared at 8.25 (d, *J* = 15.78 Hz) was assigned to the α-carbon and another doublet at 8.32 (d, *J* = 15.78 Hz) was assigned to the β-carbon. A downfield singlet observed at 14.76 was assigned to the C-2′ hydroxyl proton due to chelation with carbonyl group. The details of ^{1}H-NMR spectra is shown in Table 4.5.

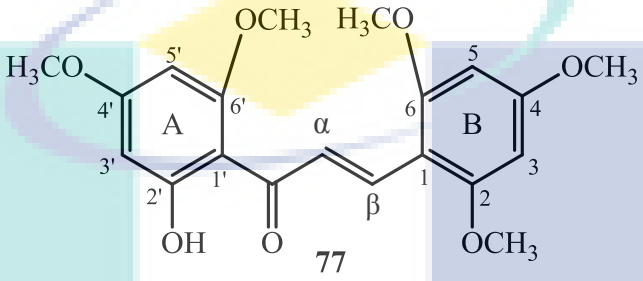

77

Figure 4.21 Structure of (*E*)-1-(2′-hydroxy-4′,6′-dimethoxyphenyl)-3-(2,4,6-trimethoxyphenyl)prop-2-en-1-one (**77**)

Table 4.5 NMR data of (*E*)-1-(2′-hydroxy-4′,6′-dimethoxyphenyl)-3-(2,4,6-trimethoxyphenyl)prop-2-en-1-one (**77**)

Carbon	^{1}H (δ)	Multiplicity	Designation
1′	-	-	-
2′	-	-	-
3′	6.09	(d, *J* = 2.40 Hz, 1H)	C3′-H
4′	-	-	-
5′	5.94	(d, *J* = 2.40 Hz, 1H)	C5′-H
6′	-	-	-
1	-	-	-
2	-	-	-
3	6.13	(s, 2H)	C3-H
4	-	-	-
5	6.13	(s, 2H)	C5-H
6	-	-	-
α	8.25	(d, *J* = 15.78 Hz, 1H, H-α)	Cα-H
β	8.32	(d, *J* = 15.78 Hz, 1H, H-β)	Cβ-H
OCH_3 (C4′)	3.85	(s, 3H)	OCH_3 (C4′)
OCH_3 (C6′)	3.90	(s, 3H)	OCH_3 (C6′)
OCH_3 (C2)	3.89	(s, 3H)	OCH_3 (C2)
OCH_3 (C4)	3.82	(s, 3H)	OCH_3 (C4)
OCH_3 (C6)	3.90	(s, 3H)	OCH_3 (C6)
OH (C2′)	14.76	(s, 1H)	OH (C2′)

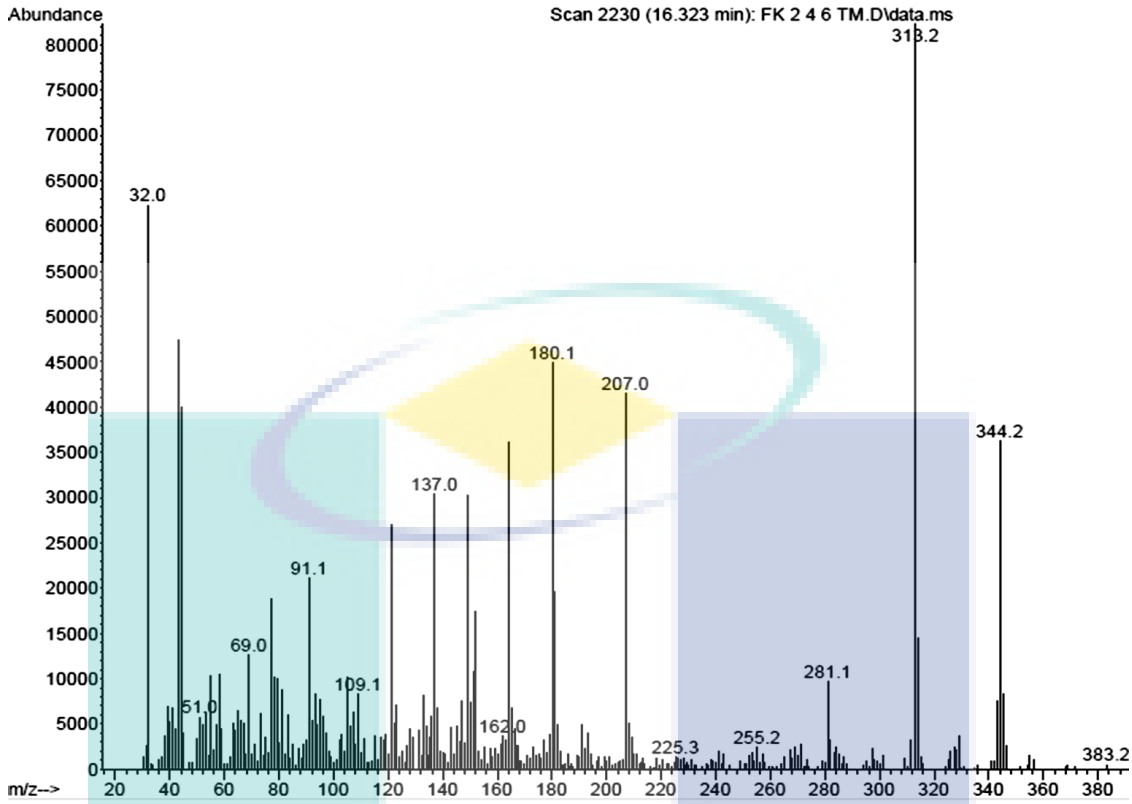

Figure 4.22 GC-MS spectrum of (*E*)-1-(2′-hydroxy-4′,6′-dimethoxyphenyl)-3-(2,4,6-trimethoxyphenyl)prop-2-en-1-one (**77**)

GC-MS spectrum of compound **77** shown in Figure 4.22 displays the main fragment ions of a molecular structure at *m/z* = 374, 344, 329, 313, 281, 207, 181, 164, 152, 149, 137 and 121. The result from this analysis could support the tentative of synthesized of compound **77**.

4.1.6 (*E*)-3-(2,4-dimethoxyphenyl)-1-(2′-hydroxy-4′,6′-dimethoxyphenyl)prop-2-en-1-one (78)

Flavokawain B derivative, (*E*)-3-(2,4-dimethoxyphenyl)-1-(2′-hydroxy-4′,6′-dimethoxyphenyl)prop-2-en-1-one (**78**) was synthesized via Claisen-Schmidt condensation of 2′-hydroxy-4′,6′-dimethoxyacetophenone (1.00 mmol) and 2,4-dimethoxybenzaldehyde (1.00 mmol) diluted in 5 mL MeOH. The reaction was catalyzed by 40% KOH and stirred at room temperature for 52 hr as described in page 38. The product was obtained in a form of yellow crystal with a yield of 80.6% and melting point of 127-129°C (171-173°C, (Sekizaki, 1988)). The compound was characterized by using UV-visible, FTIR, GC-MS and ^{1}H-NMR spectroscopy techniques.

Compound **78** absorbed UV light in the wavelength range of 290-420 nm, corresponded to the conjugated α,β-unsaturated carbonyl (C=O) chromophore. The maximum absorption of compound **77** was observed at wavelength, λ_{max}, ranged from 380-381 nm as elucidated on UV-Visible spectrum in Figure 4.23.

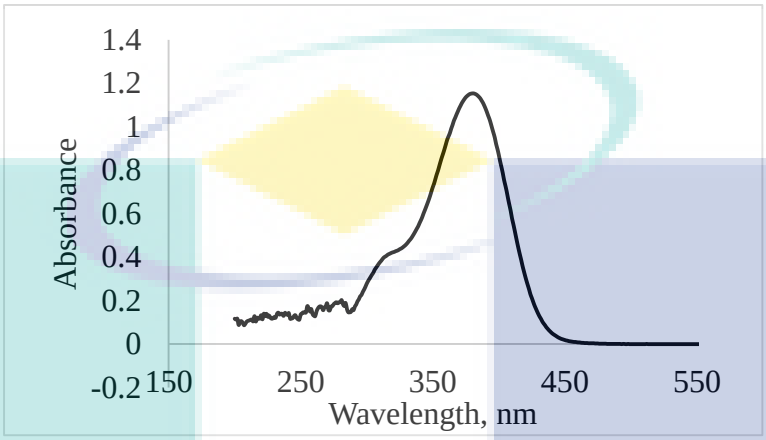

Figure 4.23 UV spectrum of (*E*)-3-(2,4-dimethoxyphenyl)-1-(2′-hydroxy-4′,6′-dimethoxyphenyl)prop-2-en-1-one (**78**)

IR spectrum of compound **78** shown in Figure 4.24 displays the absorption bands at 3465 cm^{-1} and 1625 cm^{-1}, which represented the hydroxyl (O-H) and carbonyl (C=O) groups, respectively. Absorption bands produced in a range of 1447-1551 cm^{-1} and 2842-3002 cm^{-1} were assigned to aromatic ring (C=C) and aromatic proton (Ar C-H), respectively. Absorption band that appeared in a range of 1162-1215 cm^{-1} was assigned to (C-O) group.

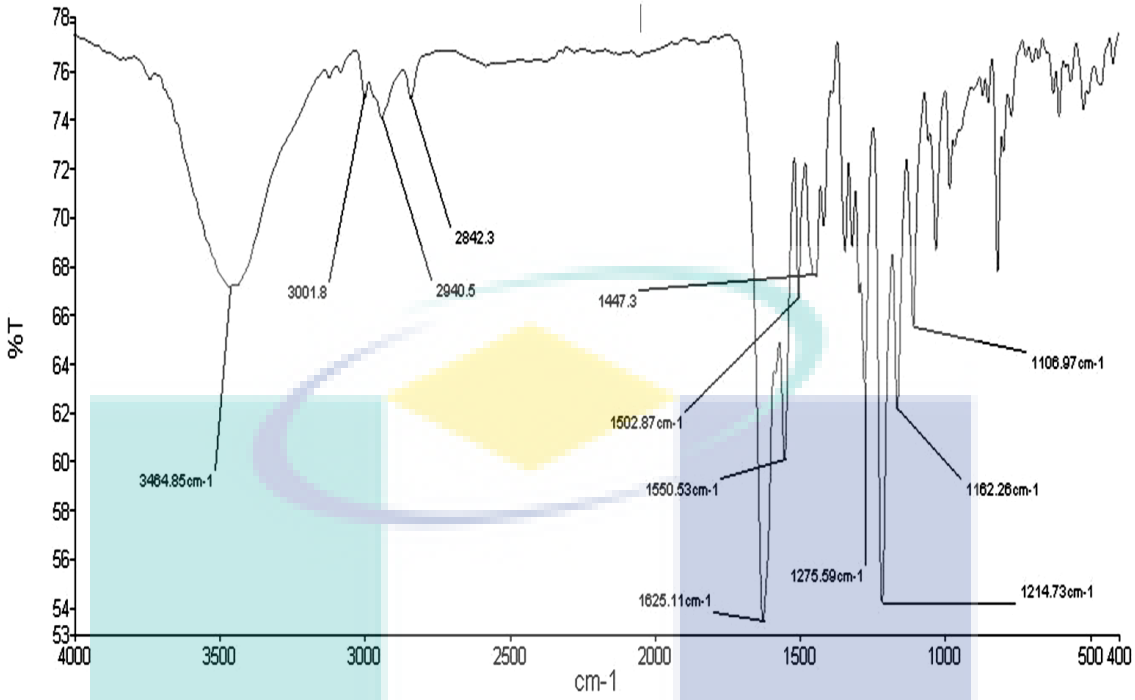

Figure 4.24 IR spectrum of (*E*)-3-(2,4-dimethoxyphenyl)-1-(2′-hydroxy-4′,6′-dimethoxyphenyl)prop-2-en-1-one (**78**)

The ^{1}H-NMR spectrum (600 MHz, $CDCl_3$) of compound **78** is shown in Figure 4.25 (Appendix A3). Four singlets elucidated at δ 3.83, 3.86, 3.89 and 3.91 were assigned to the methoxy protons at C-4, C-4′, C-2 and C-6′, respectively. A doublet at 6.10 (d, J = 2.40 Hz) was assigned to the C-3′ proton and doublet observed at 5.95 (d, J = 2.34 Hz) was assigned to the C-5′ proton. A doublet appeared at 6.47 (d, J = 2.34 Hz) was assigned to the C-3 proton. A doublet of doublet elucidated at 6.53 (d, J = 2.34 Hz, 8.58 Hz) was assigned to the C-5 proton. A doublet observed at 7.55 (d, J = 8.58 Hz) was assigned to the C-6 proton. A doublet that appeared at 7.90 (d, J = 15.72 Hz) was assigned to the proton at α-carbon and doublet at 8.11 (d, J = 15.72 Hz) was assigned to the proton at β-carbon. A downfield singlet observed at 14.56 was assigned to the C-2′ hydroxyl proton. The details of ^{1}H-NMR spectra is shown in Table 4.6.

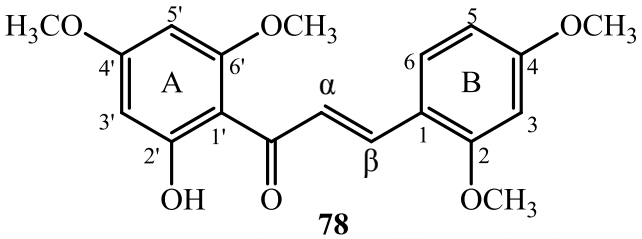

78

Figure 4.25 Structure of (*E*)-3-(2,4-dimethoxyphenyl)-1-(2′-hydroxy-4′,6′-dimethoxyphenyl)prop-2-en-1-one (**78**)

Table 4.6 NMR data of (*E*)-3-(2,4-dimethoxyphenyl)-1-(2′-hydroxy-4′,6′-dimethoxyphenyl)prop-2-en-1-one (**78**)

Carbon	**^{1}H (δ)**	**Multiplicity**	**Designation**
1′	-	-	-
2′	-	-	-
3′	6.10	(d, *J* = 2.40 Hz, 1H)	C3′-H
4′	-	-	-
5′	5.95	(d, *J* = 2.34 Hz, 1H)	C5′-H
6′	-	-	-
1	-	-	-
2	-	-	-
3	6.47	(d, *J* = 2.34 Hz, 1H)	C3-H
4	-	-	-
5	6.53	(dd, *J* = 2.34 Hz, 8.58 Hz, 1H)	C5-H
6	7.55	(d, *J* = 8.58 Hz, 1H)	C6-H
α	7.90	(d, *J* = 15.72 Hz, 1H, H-α)	Cα-H
β	8.11	(d, *J* = 15.72 Hz, 1H, H-β)	Cβ-H
OCH_3 (C4′)	3.86	(s, 3H)	OCH_3 (C4′)
OCH_3 (C6′)	3.91	(s, 3H)	OCH_3 (C6′)
OCH_3 (C2)	3.89	(s, 3H)	OCH_3 (C2)
OCH_3 (C4)	3.83	(s, 3H)	OCH_3 (C4)
OH (C2′)	14.56	(s, 1H)	OH (C2′)

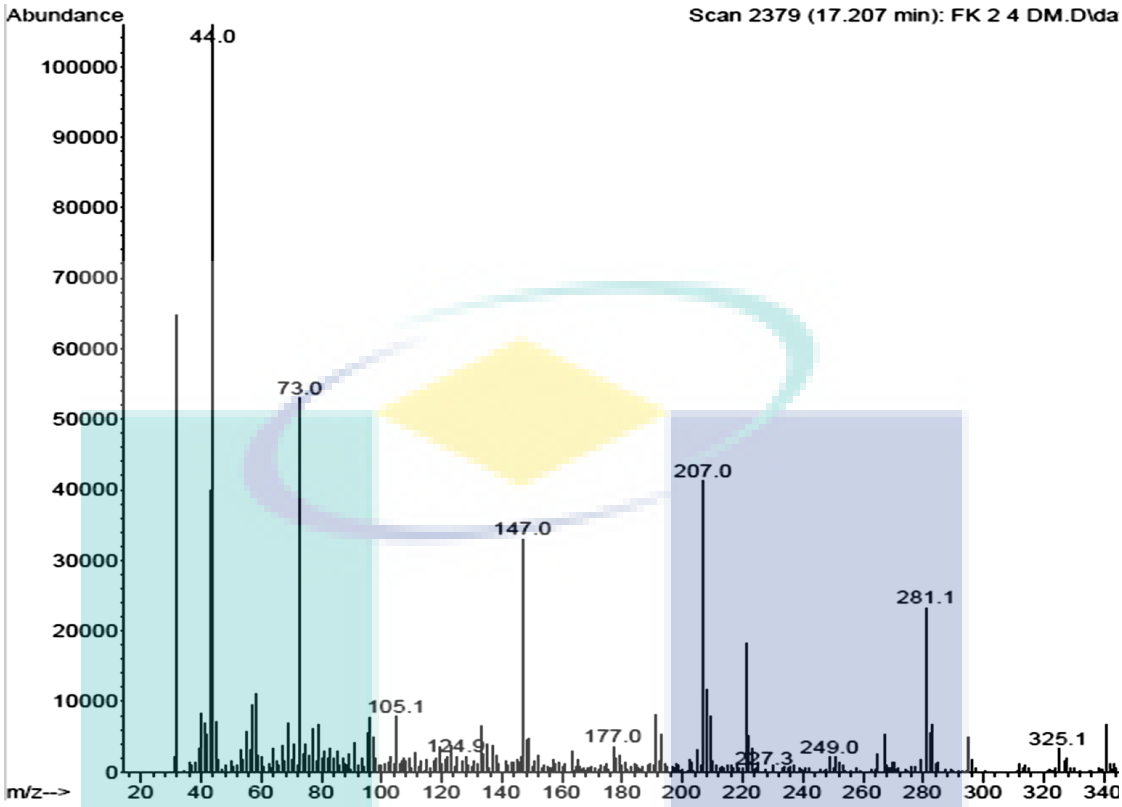

Figure 4.26 GC-MS spectrum of (*E*)-3-(2,4-dimethoxyphenyl)-1-(2′-hydroxy-4′,6′-dimethoxyphenyl)prop-2-en-1-one (**78**)

GC-MS spectrum of compound **78** shown in Figure 4.26 displays the main fragment ions of a molecular structure at *m/z* = 344, 325, 313, 297, 281, 207, 181, 164, 152, 147, 137 and 121. The result from this analysis could support the tentative of the synthesized compound **78**.

4.1.7 (*E*)-3-(2-chlorophenyl)-1-(2′-hydroxy-4′,6′-dimethoxyphenyl)prop-2-en-1-one (79)

Flavokawain B derivative, (*E*)-3-(2-chlorophenyl)-1-(2′-hydroxy-4′,6′-dimethoxyphenyl)prop-2-en-1-one (**79**) was synthesized via Claisen-Schmidt condensation of 2′-hydroxy-4′,6′-dimethoxyacetophenone (1.00 mmol) and 2-chlorobenzaldehyde (1.00 mmol) diluted in 5 mL MeOH, catalyzed by 40% KOH and stirred at room temperature for 64 hr as described in page 38. The product was obtained in a form of yellow crystal with a yield of 80.7% and melting point between 132-134°C (Roussaki et al., 2012).

Compound **79** absorbed UV light in the wavelength range of 290-385 nm, which corresponded to the conjugated α,β-unsaturated carbonyl (C=O) chromophore. The UV-Visible spectrum of compound **79** shown in Figure 4.27 shows that the maximum absorption occurred at wavelength, λ_{max} in a range of 341-342 nm (Boeck et al., 2006).

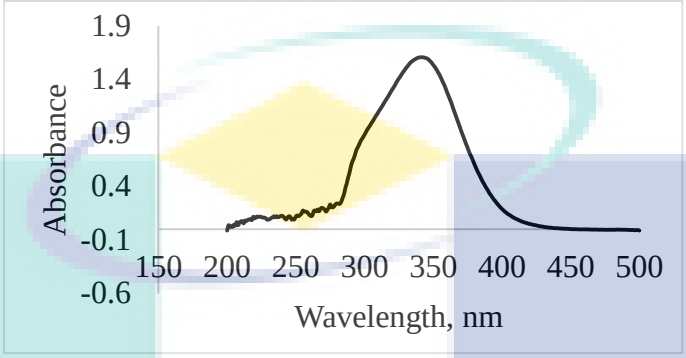

Figure 4.27 UV spectrum of (*E*)-3-(2-chlorophenyl)-1-(2′-hydroxy-4′,6′-dimethoxyphenyl)prop-2-en-1-one (**79**)

IR spectrum of compound **79** is shown in Figure 4.28. The absorption bands observed at 3448 cm^{-1} and 2957-3132 cm^{-1} corresponded to the hydroxyl (O-H) group and aromatic C-H stretch, respectively. The absorption bands that appeared at 1632 cm^{-1} and between 1338-1435 cm^{-1} represented to the carbonyl (C=O) group and aromatic ring (C=C), respectively. The absorption bands observed in a range of 1110-1219 cm^{-1} and 1556-1585 cm^{-1} corresponded to the (C-O) and (C=C-C=O), respectively. The absorption band appeared in a range of 745-748 cm^{-1} was assigned to (C-Cl) (Boeck et al., 2006).

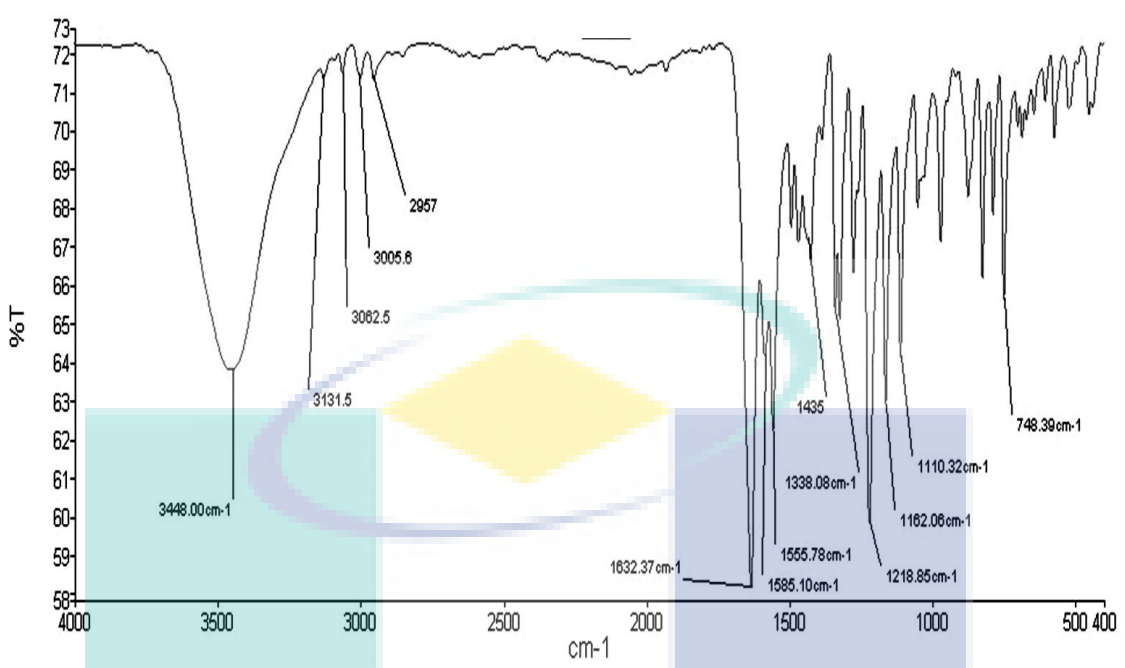

Figure 4.28 IR spectrum of (*E*)-3-(2-chlorophenyl)-1-(2′-hydroxy-4′,6′-dimethoxyphenyl)prop-2-en-1-one (**79)**

The ^{1}H-NMR spectrum (600 MHz, $CDCl_3$) of compound **79** is shown in Figure 4.29 (Appendix A4). Two singlets elucidated at δ 3.81 and 3.88 were assigned to the methoxy proton at C-4′ and C-6′, respectively. A doublet observed at 6.08 (d, *J* = 2.34 Hz) was assigned to the C-3′ proton and a doublet at 5.93 (d, *J* = 2.40 Hz) was assigned to the C-5′ proton. Two broad multiplet were observed at 7.40 (m, 1H) and 7.67 (m, 1H) and assigned to the C-3 proton and C-6 proton, respectively. A broad multiplet that appeared at 7.28 (m, 1H) was assigned to the C-4 and C-5 proton. A doublet appeared at 7.85 (d, *J* = 15.60 Hz) was assigned to the proton at α-carbon and another doublet at 8.12 (d, *J* = 15.60 Hz) was assigned to the proton at β-carbon. A singlet that appeared at 14.24 represent the C-2′ hydroxyl proton (Boeck et al., 2006). The details of ^{1}H-NMR spectra is shown in Table 4.7.

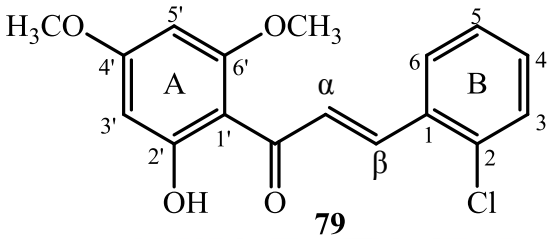

Figure 4.29 Structure of (*E*)-3-(2-chlorophenyl)-1-(2′-hydroxy-4′,6′-dimethoxyphenyl)prop-2-en-1-one (**79**)

Table 4.7 NMR data of (*E*)-3-(2-chlorophenyl)-1-(2′-hydroxy-4′,6′-dimethoxyphenyl)prop-2-en-1-one (**79**)

Carbon	^{1}H (δ)	Multiplicity	Designation
1′	-	-	-
2′	-	-	-
3′	6.08	(d, *J* = 2.34 Hz, 1H)	C3′-H
4′	-	-	-
5′	5.93	(d, *J* = 2.40 Hz, 1H)	C5′-H
6′	-	-	-
1	-	-	-
2	-	-	-
3	7.40	(m, 1H)	C3-H
4	7.28	(m, 1H)	C4-H
5	7.28	(m, 1H)	C5-H
6	7.67	(m, 1H)	C6-H
α	7.85	(d, *J* = 15.60 Hz, 1H, H-α)	Cα-H
β	8.12	(d, *J* = 15.60 Hz, 1H, H-β)	Cβ-H
OCH_3 (C4′)	3.81	(s, 3H)	OCH_3 (C4′)
OCH_3 (C6′)	3.88	(s, 3H)	OCH_3 (C6′)
OH (C2′)	14.24	(s, 1H)	OH (C2′)

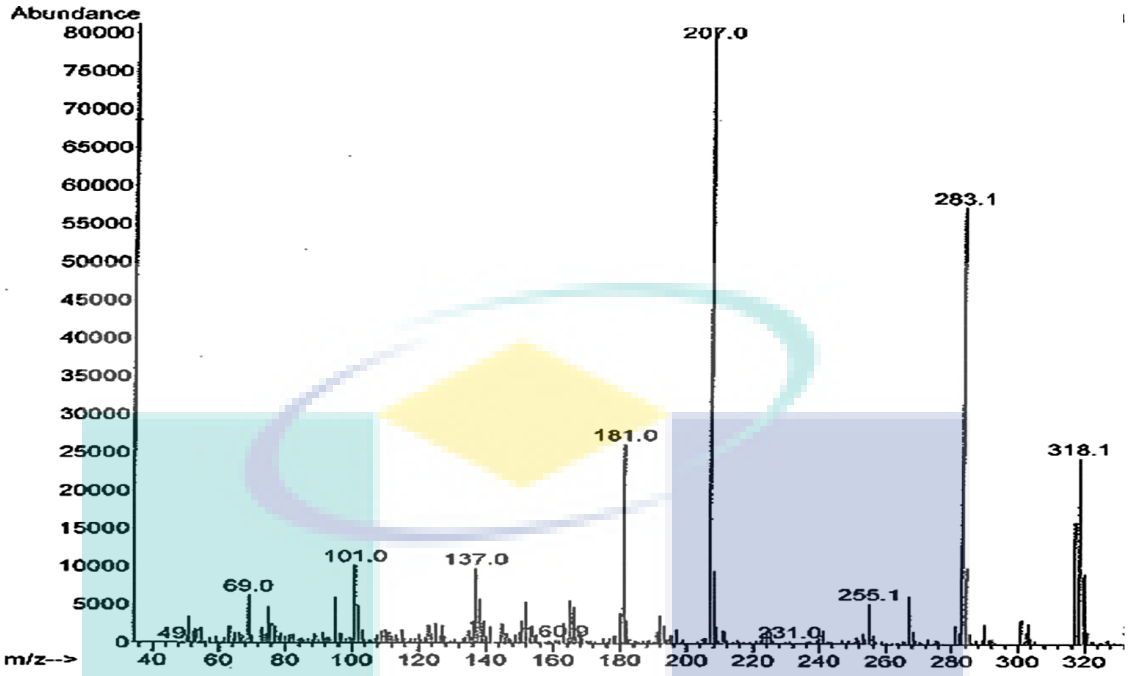

Figure 4.30 GC-MS spectrum of (*E*)-3-(2-chlorophenyl)-1-(2′-hydroxy-4′,6′-dimethoxyphenyl)prop-2-en-1-one (**79**)

GC-MS spectrum of compound **79** shown in Figure 4.30 displays the main fragment ions of a molecular structure at *m/z* = 318, 301, 283, 267, 207, 181, 165, 152, 137 and 101. The result from this analysis could support the tentative of synthesized compound **79**.

4.1.8 (*E*)-3-(2-fluorophenyl)-1-(2′-hydroxy-4′,6′-dimethoxyphenyl)prop-2-en-1-one (80)

Flavokawain B derivative, (*E*)-3-(2-fluorophenyl)-1-(2′-hydroxy-4′,6′-dimethoxyphenyl)prop-2-en-1-one (**80**) was synthesized via Claisen-Schmidt condensation of 2′-hydroxy-4′,6′-dimethoxyacetophenone (1.00 mmol) and 2-fluorobenzaldehyde (1.00 mmol) diluted in 5 mL MeOH. The reaction was catalyzed by 40% KOH and stirred at room temperature for 72 hr as described in page 38. The product was obtained in a form of yellow crystal with a yield of 79.2% and melting point between 101-103°C.

Compound **80** absorbed UV light in a wavelength range of 290-390 nm, which corresponded to the conjugated α,β-unsaturated carbonyl (C=O) chromophore. The UV-Visible spectrum of compound **80** shown in Figure 4.31 shows that the maximum absorption occurred at a wavelength, λ_{max} of 344 nm.

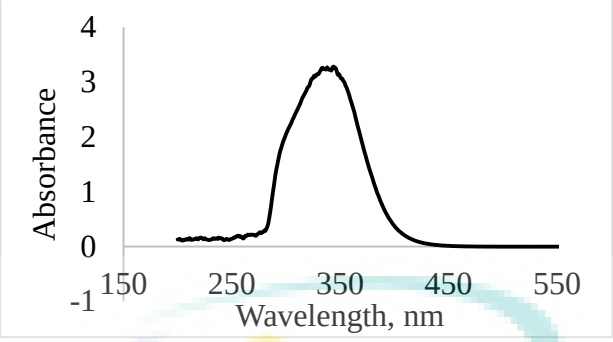

Figure 4.31 UV spectrum of (*E*)-3-(2-fluorophenyl)-1-(2′-hydroxy-4′,6′-dimethoxyphenyl)prop-2-en-1-one (**80**)

IR spectrum of compound **80** is shown in Figure 4.32. The absorption bands observed at 3445 cm^{-1} and 1632 cm^{-1} represented the hydroxyl (O-H) and carbonyl (C=O) groups, respectively. Absorption bands in a range of 1344-1488 cm^{-1} and 2941-3088 cm^{-1} represented the aromatic ring (C=C) and aromatic proton (Ar C-H), respectively. Absorption band produced in a range of 1219-1220 cm^{-1} and 1568-1594 cm^{-1} represented (C-O) and (C=C-C=O), respectively.

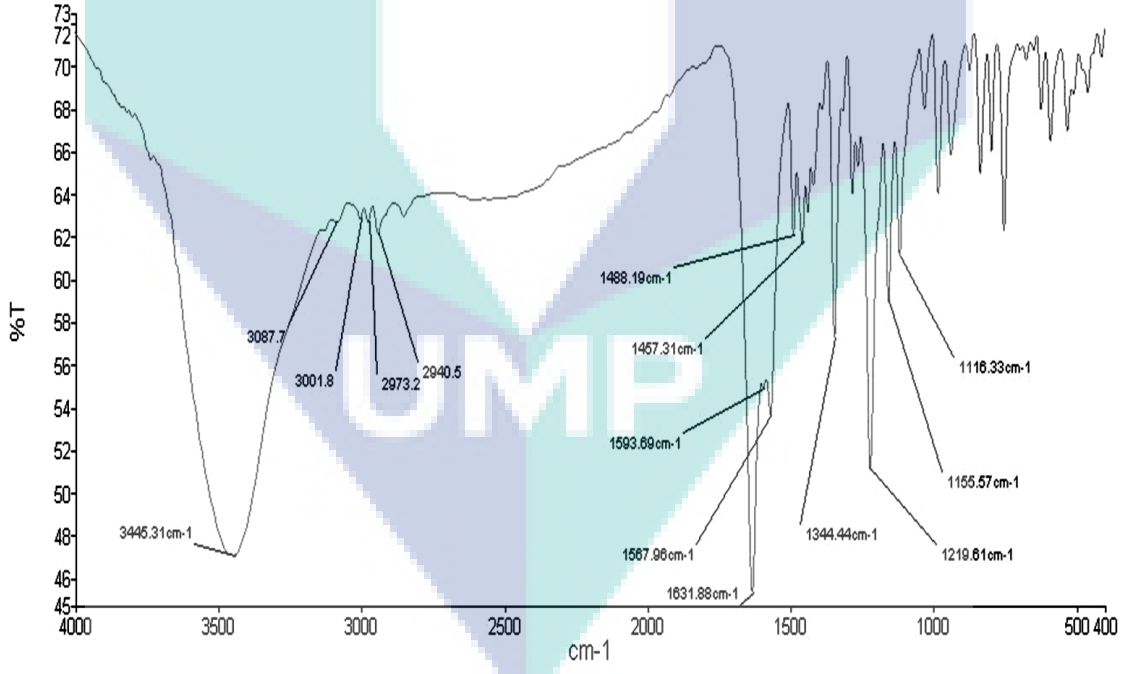

Figure 4.32 IR spectrum of (*E*)-3-(2-fluorophenyl)-1-(2′-hydroxy-4′,6′-dimethoxyphenyl)prop-2-en-1-one (**80**)

The ^{1}H-NMR spectrum (600 MHz, $CDCl_3$) of compound **80** is shown in Figure 4.33 (Appendix A4). A doublet at δ 6.11 (d, *J* = 2.40 Hz) was assigned to the C-3′ proton and doublet at 5.96 (d, *J* = 2.34 Hz) was assigned to the C-5′ proton. A multiplet

that appeared at 7.11 (m, 1H) was assigned to the C-3 proton. Another multiplet that appeared at 7.35 (m, 1H) was assigned to the C-6 proton. The signals of triplet of doublet observed at 7.18 (td, *J* = 7.56 Hz, 7.50 Hz) was assigned to the C-4 proton and another triplet of doublet at 7.59 (td, *J* = 7.56 Hz, 7.68 Hz) was assigned to the C-5 proton. The signal of doublet that appeared at 7.86 (d, *J* = 15.78 Hz) was assigned to the proton at α-carbon and doublet at 8.00 (d, *J* = 15.78 Hz) was assigned to the proton at β-carbon. Two singlets elucidated at 3.91 (s, 3H) and 3.84 (s, 3H) were assigned to the methoxy proton at C-6′ and C-4′, respectively. A singlet that appeared at 14.25 (s, 1H) represented the C-2′ hydroxyl proton. The details of ^{1}H-NMR spectra is shown in Table 4.8.

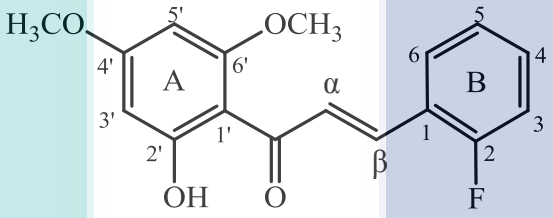

80

Figure 4.33 Structure of (*E*)-3-(2-fluorophenyl)-1-(2′-hydroxy-4′,6′-dimethoxyphenyl)prop-2-en-1-one (**80**)

Table 4.8 NMR data of (*E*)-3-(2-fluorophenyl)-1-(2′-hydroxy-4′,6′-dimethoxyphenyl)prop-2-en-1-one (**80**)

Carbon	^{1}H (δ)	Multiplicity	Designation
1′	-	-	-
2′	-	-	-
3′	6.11	(d, *J* = 2.40 Hz, 1H)	C3′-H
4′	-	-	-
5′	5.96	(d, *J* = 2.34 Hz, 1H)	C5′-H
6′	-	-	-
1	-	-	-
2	-	-	-
3	7.11	(m, 1H)	C3-H
4	7.18	(td, *J* = 7.56 Hz, 7.50 Hz, 1H)	C4-H
5	7.59	(td, *J* = 7.56 Hz, 7.68 Hz, 1H)	C5-H
6	7.35	(m, 1H)	C6-H
α	7.86	(d, *J* = 15.78 Hz, 1H, H-α)	Cα-H
β	8.0	(d, *J* = 15.78 Hz, 1H, H-β)	Cβ-H
OCH_3 (C4′)	3.84	(s, 3H)	OCH_3 (C4′)
OCH_3 (C6′)	3.91	(s, 3H)	OCH_3 (C6′)
OH (C2′)	14.25	(s, 1H)	OH (C2′)

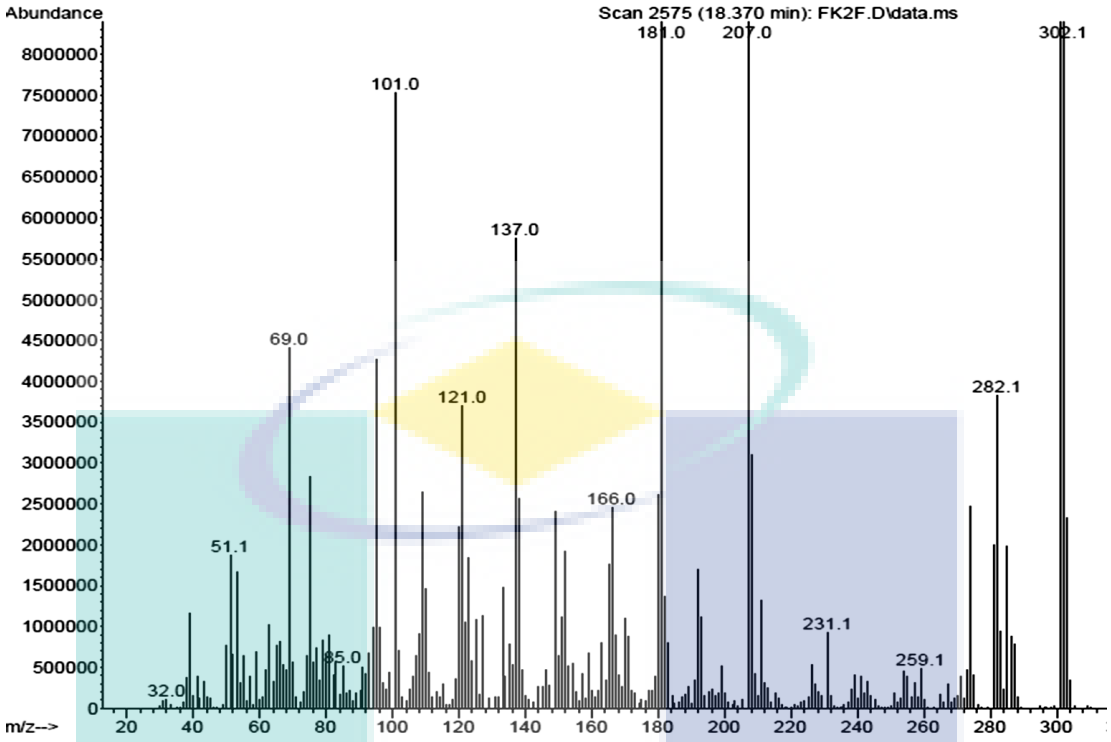

Figure 4.34 GC-MS spectrum of (*E*)-3-(2-fluorophenyl)-1-(2′-hydroxy-4′,6′-dimethoxyphenyl)prop-2-en-1-one (**80**)

GC-MS spectrum of compound **80** shown in Figure 4.34 displays the main fragment ions of a molecular structure at *m/z* = 302, 301, 285, 282, 207, 181, 166, 152, 149, 137, 121, 101, 95 and 69. The result from this analysis could support the tentative of synthesized compound **80**.

4.1.9 (*E*)-1-(2′-hydroxy-4′,6′-dimethoxyphenyl)-3-(2-methoxyphenyl)prop-2-en-1-one (81)

Flavokawain B derivative, (*E*)-1-(2′-hydroxy-4′,6′-dimethoxyphenyl)-3-(2-methoxyphenyl)prop-2-en-1-one (**81**) was synthesized via Claisen-Schmidt condensation of 2′-hydroxy-4′,6′-dimethoxyacetophenone (1.00 mmol) and 2-methoxybenzaldehyde (1.00 mmol) diluted in 5 mL MeOH, catalyzed by 40% KOH and stirred at room temperature for 48 hr as described in page 38. The product was obtained in a form of yellow crystal form with a yield of 85.2% and melting point in a range of 113-114°C (Sekizaki, 1988).

Compound **81** absorbed UV light in the wavelength range of 294-400 nm, which corresponded to the conjugated α,β-unsaturated carbonyl (C=O) chromophore. The UV-Visible spectrum of compound **81** shown in Figure 4.35 shows that the maximum absorption occurred at wavelength, λ_{max} in a range of 360-362 nm.

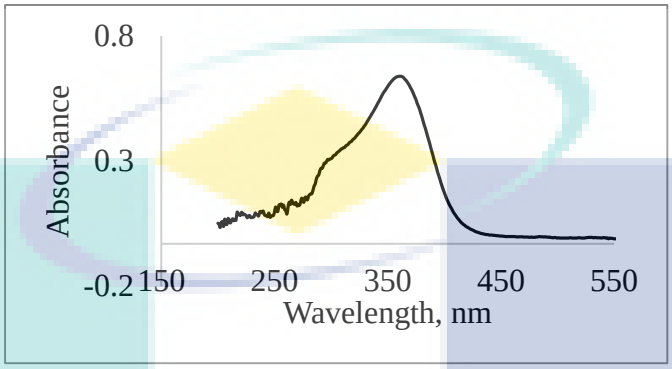

Figure 4.35 UV spectrum of (*E*)-1-(2′-hydroxy-4′,6′-dimethoxyphenyl)-3-(2-methoxyphenyl)prop-2-en-1-one (**81**)

IR spectrum of compound **81** is shown in Figure 4.36. The absorption bands at 3448 cm^{-1} and 1626 cm^{-1} corresponded to the hydroxyl (O-H) and carbonyl (C=O) groups, respectively. Absorption bands produced in a range of 1421-1487 cm^{-1} and 2944-2997 cm^{-1} were assigned to the aromatic ring (C=C) and aromatic proton (Ar C-H), respectively. Absorption band that appeared in a range of 1107-1250 cm^{-1} was assigned to (C-O).

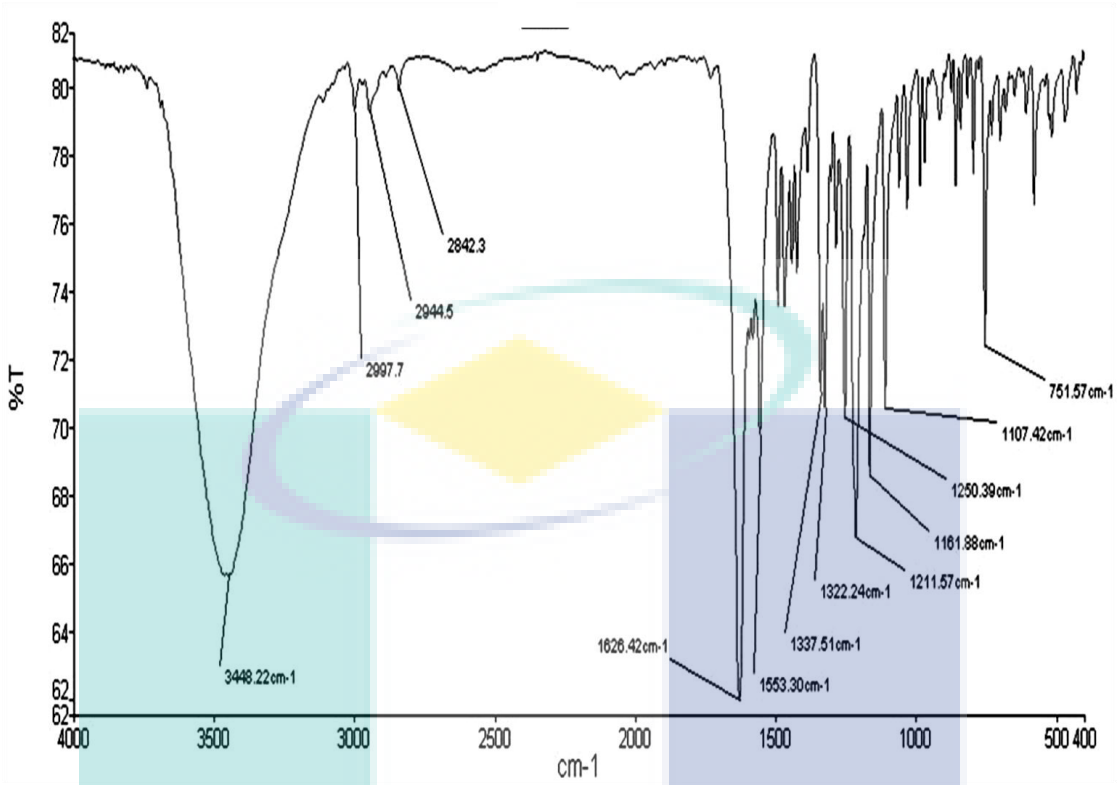

Figure 4.36 IR spectrum of (*E*)-1-(2′-hydroxy-4′,6′-dimethoxyphenyl)-3-(2-methoxyphenyl)prop-2-en-1-one (**81**)

The ^{1}H-NMR spectrum (600 MHz, $CDCl_3$) of compound **81** is shown in Figure 4.37 (Appendix A5). A singlet that appeared at δ 3.82 was assigned to the C-4′ methoxy proton. A singlet observed at 3.89 was assigned to the C-2 methoxy proton and another singlet at 3.90 was assigned to the C-6′ methoxy proton. A doublet appeared at 5.95 (d, *J* = 2.40 Hz) was assigned to the C-5′ proton and another doublet at 6.10 (d, *J* = 2.40 Hz) was assigned to the C-3′ proton. A doublet observed at 6.92 (d, *J* = 7.32 Hz) was assigned to the C-3 proton. A multiplet that appeared at 7.35 was assigned to the C-4 proton and another multiplet at 6.98 was assigned to the C-5 proton. The doublet of doublet that appeared at 7.60 (dd, *J* = 1.68 Hz, 7.68 Hz) was assigned to the C-6 proton. A doublet that appeared at 7.96 (d, *J* = 15.78 Hz) was assigned to the proton at α-carbon and a doublet at 8.14 δ (d, *J* = 15.78 Hz) was assigned to the proton at β-carbon. A singlet that appeared at 14.44 represented the C-2′ hydroxyl proton. The details of ^{1}H-NMR spectra is shown in Table 4.9.

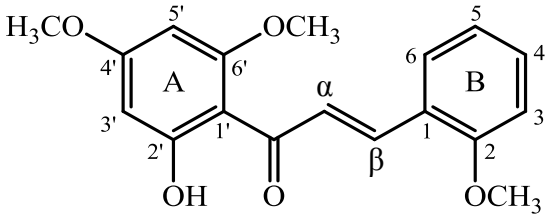

81

Figure 4.37 Structure of (*E*)-1-(2′-hydroxy-4′,6′-dimethoxyphenyl)-3-(2-methoxyphenyl)prop-2-en-1-one (**81**)

Table 4.9 NMR data of (*E*)-1-(2′-hydroxy-4′,6′-dimethoxyphenyl)-3-(2-methoxyphenyl)prop-2-en-1-one (**81**)

Carbon	^{13}C (δ)	^{1}H (δ)	Multiplicity	Designation
1′	106.45	-	-	-
2′	162.52	-	-	-
3′	93.80	6.10	(d, *J* = 2.40 Hz, 1H)	C3′-H
4′	168.36	-	-	-
5′	91.18	5.95	(d, *J* = 2.40 Hz, 1H)	C5′-H
6′	166.05	-	-	-
1	137.84	-	-	-
2	131.20	-	-	-
3	124.57	6.92	(d, *J* = 7.32 Hz, 1H)	C3-H
4	127.88	7.35	(m, 1H)	C4-H
5	111.20	6.98	(m, 1H)	C5-H
6	120.70	7.60	(dd, *J* = 1.68 Hz, 7.68 Hz, 1H)	C6-H
α	128.77	7.96	(d, *J* = 15.78 Hz, 1H, H-α)	Cα-H
β	158.65	8.14	(d, *J* = 15.78 Hz, 1H, H-β)	Cβ-H
OCH_3 (C4′)	55.76	3.82	(s, 3H)	OCH_3 (C4′)
OCH_3 (C6′)	55.55	3.90	(s, 3H)	OCH_3 (C6′)
OCH_3 (C2)	55.50	3.89	(s, 3H)	OCH_3 (C2)
OH (C2′)	-	14.44	(s, 1H)	OH (C2′)
C=O	193.06	-	-	-

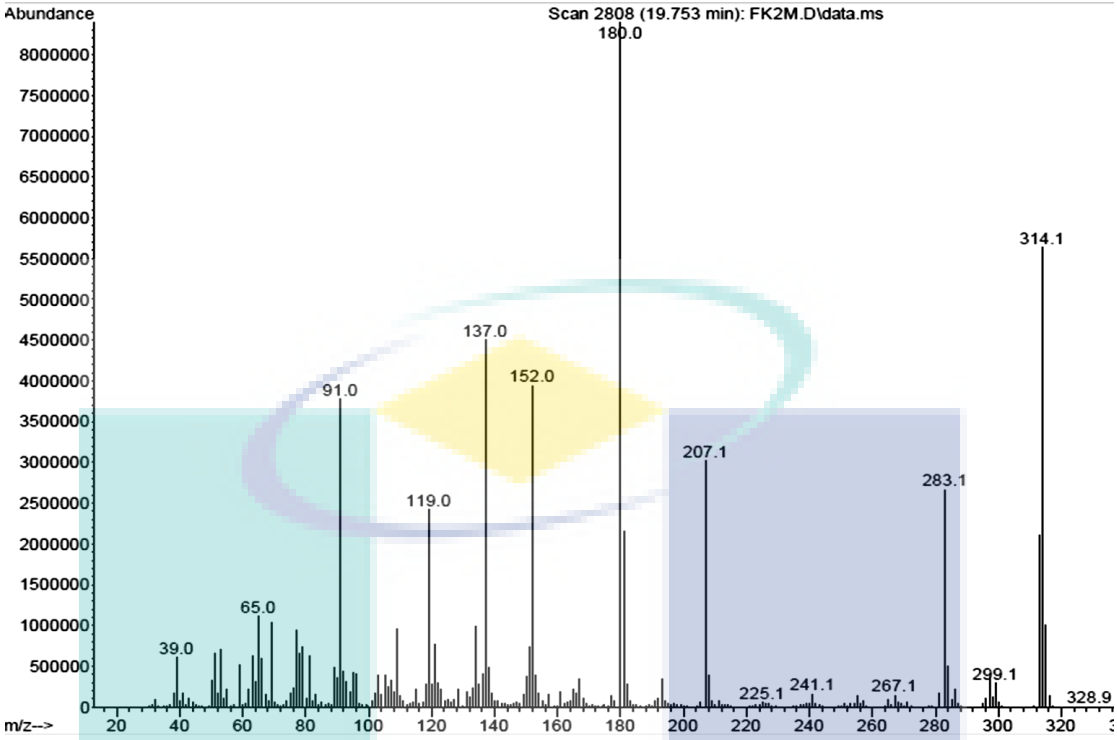

Figure 4.38 GC-MS spectrum of (*E*)-1-(2′-hydroxy-4′,6′-dimethoxyphenyl)-3-(2-methoxyphenyl)prop-2-en-1-one (**81**)

GC-MS spectrum of compound **81** shown in Figure 4.38 displays the main fragment ions of a molecular structure at *m/z* = 314, 299, 297, 283, 207, 180, 161, 152, 137, 134, 119 and 91. The result from this analysis could support the tentative of synthesized compound **81**.

4.1.10 (*E*)-3-(3,4-dimethoxyphenyl)-1-(2′-hydroxy-4′,6′-dimethoxyphenyl)prop-2-en-1-one (82)

Flavokawain B derivative, (*E*)-3-(3,4-dimethoxyphenyl)-1-(2′-hydroxy-4′,6′-dimethoxyphenyl)prop-2-en-1-one (**82**) was synthesized via Claisen-Schmidt condensation of 2′-hydroxy-4′,6′-dimethoxyacetophenone (1.00 mmol) and 3,4-dimethoxybenzaldehyde (1.00 mmol) diluted in 5 mL MeOH, was catalyzed by 40% KOH and stirred at room temperature for 54 hr as described in page 38. The product was obtained in a form of orange crystal form with a yield of 84.7% and melting point in a range of 151-153°C (Detsi et al., 2009)).

Compound **82** absorbed UV light in the wavelength range of 310-410 nm, which corresponded to the conjugated α,β-unsaturated carbonyl (C=O) chromophore. The UV-Visible spectrum of compound **82** shown in Figure 4.39 shows that the maximum absorption occurred at wavelength, λ_{max} in a range of 373-374 nm.

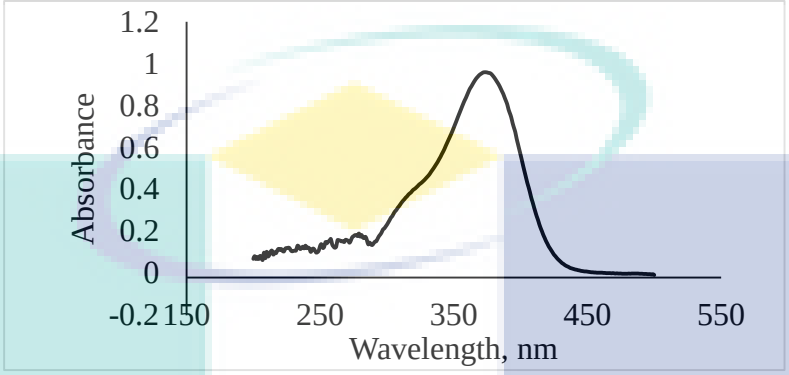

Figure 4.39 UV spectrum of (*E*)-3-(3,4-dimethoxyphenyl)-1-(2′-hydroxy-4′,6′-dimethoxyphenyl)prop-2-en-1-one (**82**)

IR spectrum of compound **82** is shown in Figure 4.40. The absorption bands at 3447 cm^{-1} and 1622 cm^{-1} represented the hydroxyl (O-H) and carbonyl (C=O) groups, respectively. Absorption bands observed in a range of 1443-1509 cm^{-1} and 2851-2994 cm^{-1} were assigned to the aromatic ring (C=C) and (Ar C-H), respectively. Absorption bands that appeared at 1220 cm^{-1} and between 1583-1584 cm^{-1} were corresponded to the (C-O) and (C=C-C=O) groups, respectively.

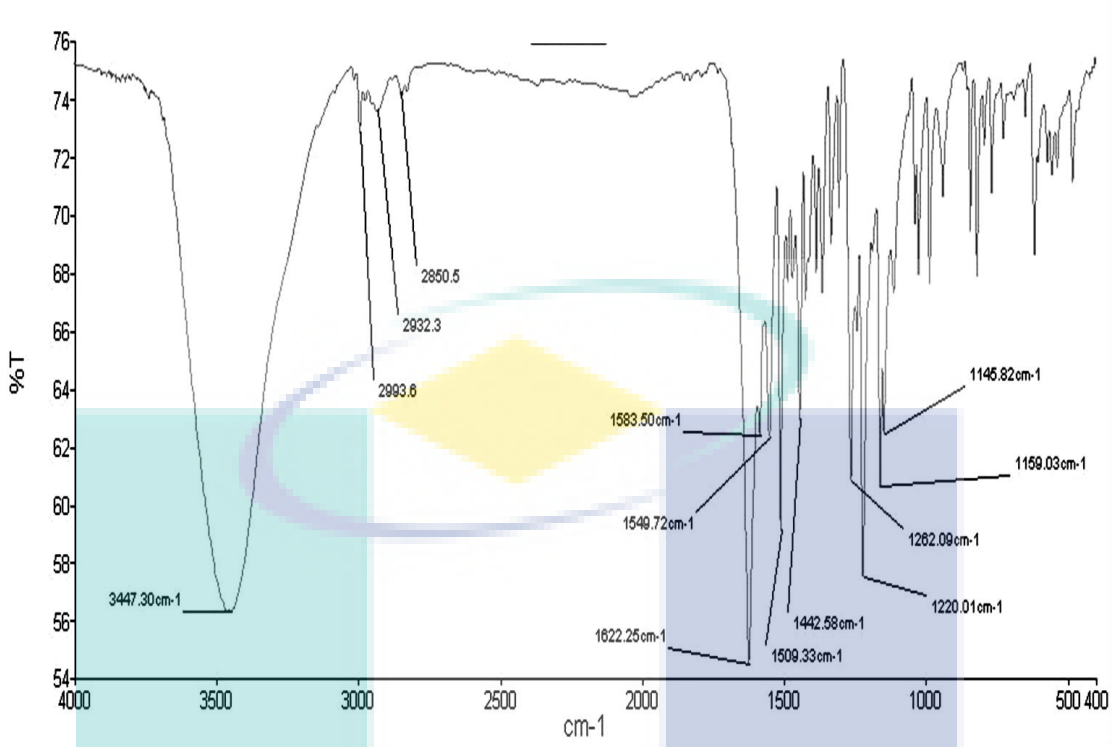

Figure 4.40 IR spectrum of (*E*)-3-(3,4-dimethoxyphenyl)-1-(2′-hydroxy-4′,6′-dimethoxyphenyl)prop-2-en-1-one (**82**)

^{1}H-NMR spectrum (600 MHz, $CDCl_3$) of compound **82** is shown in Figure 4.41 (Appendix A5). Two doublets at δ 6.11 (d, *J* = 2.40 Hz) and 5.96 (d, *J* = 2.40 Hz) were assigned to the C-3′ and C-5′ proton, respectively. A doublet that appeared at 7.12 (d, *J* = 1.98 Hz) was assigned to the C-2 proton and a doublet at 6.90 (d, *J* = 8.28 Hz) was assigned to the C-5 proton. A doublet of doublet observed at 7.22 (dd, *J* = 1.98 Hz, 8.28 Hz) was assigned to the C-6 proton. The signal of doublet elucidated at 7.75 (d, *J* = 15.48 Hz) was assigned to the proton at α-carbon and a doublet at 7.80 (d, *J* = 15.48 Hz) was assigned to the proton at β-carbon. The signals of singlet produced at 3.93 (s, 3H) was assigned to the methoxy proton at C-4′ and singlet appeared at 3.94 (s, 3H) was assigned to the methoxy proton at C-6′, A singlet that appeared at 3.91 (s, 3H) represented the methoxy proton at C-3 and a singlet at 3.84 (s, 3H) corresponded to the methoxy proton at C-4. A singlet appeared at 14.42 (s, 1H) due to the presence of C-2′ hydroxyl proton chelated to carbonyl group. The details of ^{1}H-NMR spectra was shown in Table 4.10. The ORTEP diagram and crystal parameters and data for structure refinement of compound **82** were shown in Figure 4.42 and Table 4.11, respectively.

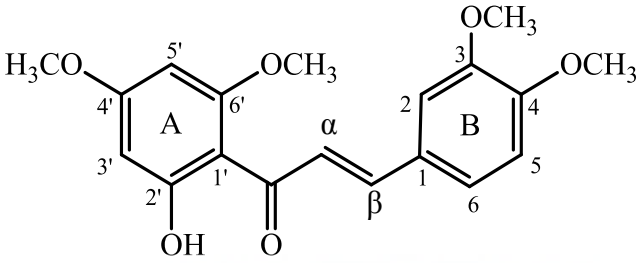

82

Figure 4.41 Structure of (*E*)-3-(3,4-dimethoxyphenyl)-1-(2′-hydroxy-4′,6′-dimethoxyphenyl)prop-2-en-1-one (**82**)

Table 4.10 NMR data of (*E*)-3-(3,4-dimethoxyphenyl)-1-(2′-hydroxy-4′,6′-dimethoxyphenyl)prop-2-en-1-one (**82**)

Carbon	**^{1}H (δ)**	**Multiplicity**	**Designation**
1′	-	-	-
2′	-	-	-
3′	6.11	(d, *J* = 2.40 Hz, 1H)	C3′-H
4′	-	-	-
5′	5.96	(d, *J* = 2.40 Hz, 1H)	C5′-H
6′	-	-	-
1	-	-	-
2	7.12	(d, *J* = 1.98 Hz, 1H)	C2-H
3	-	-	-
4	-	-	-
5	6.90	(d, *J* = 8.28 Hz, 1H)	C5-H
6	7.22	(dd, *J* = 1.98 Hz, 8.28 Hz, 1H)	C6-H
α	7.75	(d, *J* = 15.48 Hz, 1H, H-α)	Cα-H
β	7.80	(d, *J* = 15.48 Hz, 1H, H-β)	Cβ-H
OCH_3 (C4′)	3.93	(s, 3H)	OCH_3 (C4′)
OCH_3 (C6′)	3.94	(s, 3H)	OCH_3 (C6′)
OCH_3 (C3)	3.91	(s, 3H)	OCH_3 (C3)
OCH_3 (C4)	3.84	(s, 3H)	OCH_3 (C4)
OH (C2′)	14.42	(s, 1H)	OH (C2′)

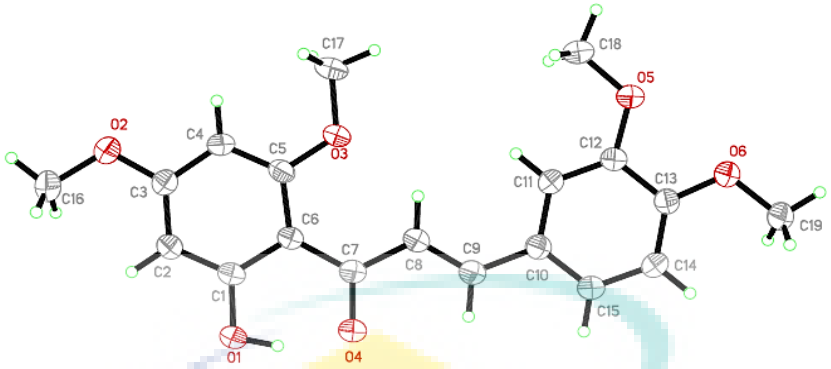

Figure 4.42 ORTEP diagram of (*E*)-3-(3,4-dimethoxyphenyl)-1-(2′-hydroxy-4′,6′-dimethoxyphenyl)prop-2-en-1-one (**82**)

Table 4.11 Crystal parameters and data for structure refinement of (*E*)-3-(3,4-dimethoxyphenyl)-1-(2′-hydroxy-4′,6′-dimethoxyphenyl)prop-2-en-1-one (**82**)

Parameter	**Data**
CCDC Number	1548734
Molecular Formula	$C_{19}H_{20}O_6$
Molecular Weight	344.35
Crystal System	Triclinic
Space Group	$P\bar{1}$
a (Å)	8.4560 (17)
b (Å)	8.4790 (17)
c (Å)	12.549 (3)
α (°)	104.166 (3)
β (°)	92.063 (3)
γ (°)	106.227 (3)
V (Å^3)	832.4 (3)
Z	2
*D*calc (g cm^{-3})	1.374
Crystal dimensions (mm)	0.58 × 0.18 × 0.11
μ (mm^{-1})	0.10
T_{min}/T_{max}	0.7665, 0.9584
Reflections measured	28367
Ranges/indices (*h*, *k*, *l*)	-11→11; -11→11; -17→17
θ limit (°)	1.7-29.2
Unique reflections	4491
Observed reflections ($I > 2\sigma(I)$)	2352
Parameters	234
Goodness of fit on F^2	1.02
R_1, wR_2 [$I \geq 2\sigma(I)$]	0.055, 0.176

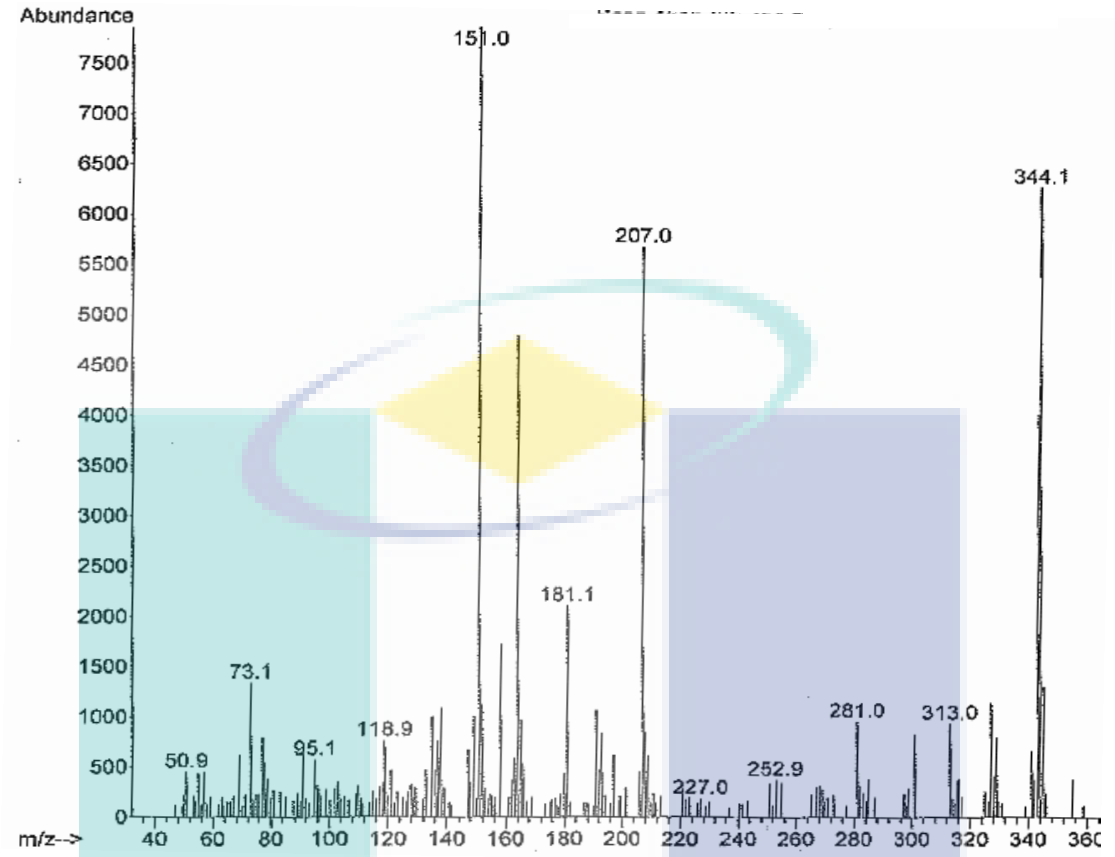

Figure 4.43 GC-MS spectrum of (*E*)-3-(3,4-dimethoxyphenyl)-1-(2′-hydroxy-4′,6′-dimethoxyphenyl)prop-2-en-1-one (**82**)

GC-MS spectrum of compound **82** shown in Figure 4.43 displays the main fragment ion of a molecular structure at *m/z* = 344, 327, 313, 282, 207, 191, 181, 164, 152 and 137. The abundance of a molecular peak at *m/z* = 344 was about 82%. Loss of ·OH radical from the molecular peak gave out a fragment ion at *m/z* = 327. Loss of one methoxy group (-OCH_3) at ring B resulted in formation of fragment ion at *m/z* = 313 and loss of one more methoxy group resulted in fragment ion observed at *m/z* = 282. The fragment ion at *m/z* = 207 was formed due to β-cleavage of bond in between the β-carbon and $C_8H_9O_2^+$ groups and resulted in the formation of fragment ion at *m/z* = 137. The fragment ion at *m/z* = 181 was formed due referred to α-cleavage of bond next to carbonyl group and another fragment ion was produced at *m/z* = 163. Formation of fragment ions at *m/z* = 152 and 191 could be due to cleavage of bond next to carbonyl and rearrangement afterwards. Loss of ·OH radical from the fragment ion observed at *m/z* = 181 probably resulted in formation of fragment ion at *m/z* = 164. The proposed cleavage mechanisms of compound **82** is shown in Figure 4.44.

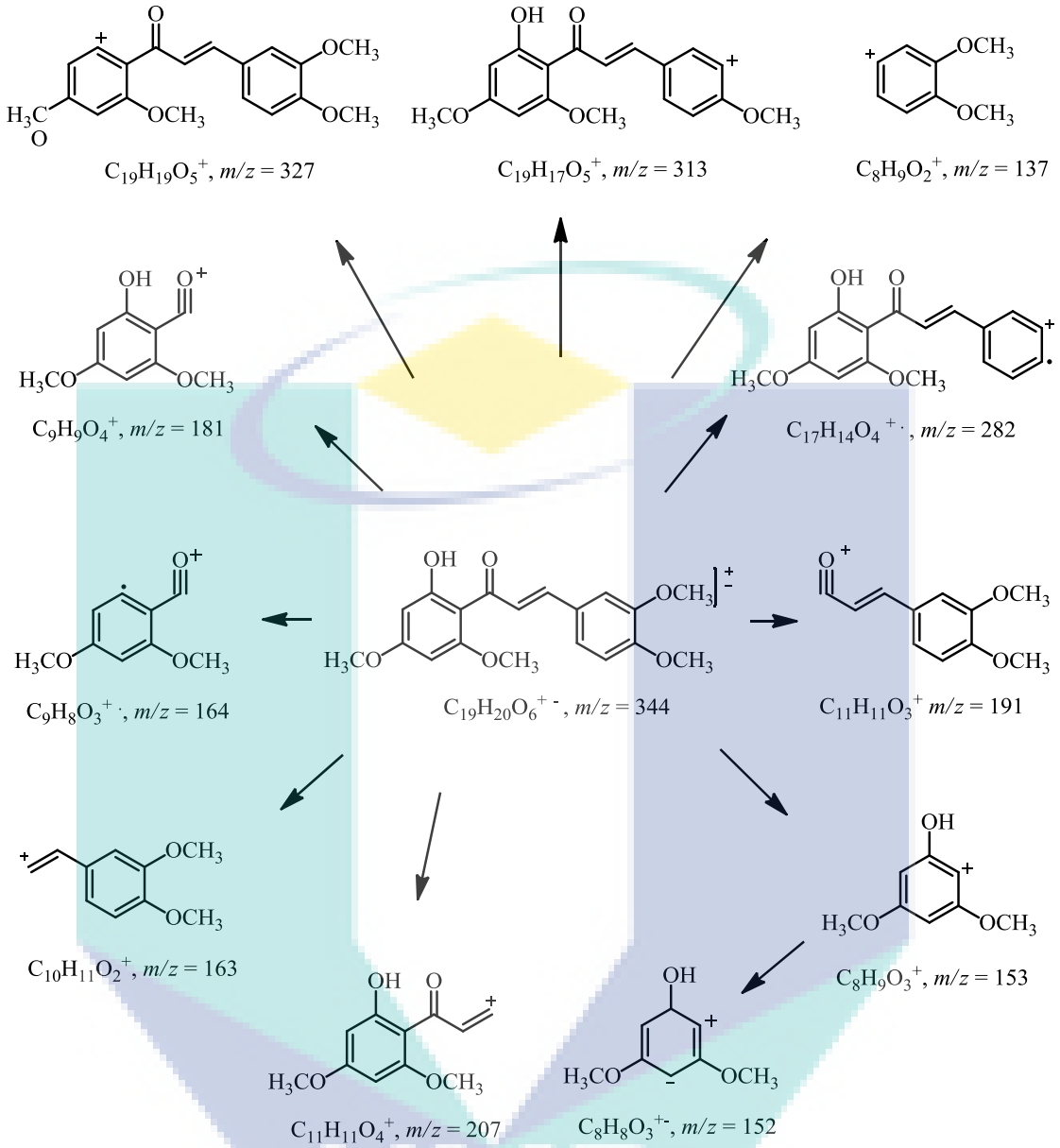

Figure 4.44 Mass fragmentation (*E*)-3-(3,4-dimethoxyphenyl)-1-(2′-hydroxy-4′,6′-dimethoxyphenyl)prop-2-en-1-one (**82**)

4.1.11 (*E*)-3-(3,5-dimethoxyphenyl)-1-(2′-hydroxy-4′,6′-dimethoxyphenyl)prop-2-en-1-one (83)

Flavokawain B derivative, (*E*)-3-(3,5-dimethoxyphenyl)-1-(2′-hydroxy-4′,6′-dimethoxyphenyl)prop-2-en-1-one (**83**) was synthesized via Claisen-Schmidt condensation of 2′-hydroxy-4′,6′-dimethoxyacetophenone (1.00 mmol) and 3,5-dimethoxybenzaldehyde (1.00 mmol) diluted in 5 mL MeOH, catalyzed by 40% KOH and stirred at room temperature for 47 hr as described in page 38. The product was obtained in a form of yellow crystal with a yield of 86.3% and melting point in a range of 155-158°C (Valdameri et al., 2012).

Compound **83** absorbed UV light in the wavelength range of 290-400 nm, which corresponded to the conjugated α,β-unsaturated carbonyl (C=O) chromophore. The UV-Visible spectrum of compound **83** shown in Figure 4.45 shows that the maximum absorption occurred at a wavelength, λ_{max} of 346 nm.

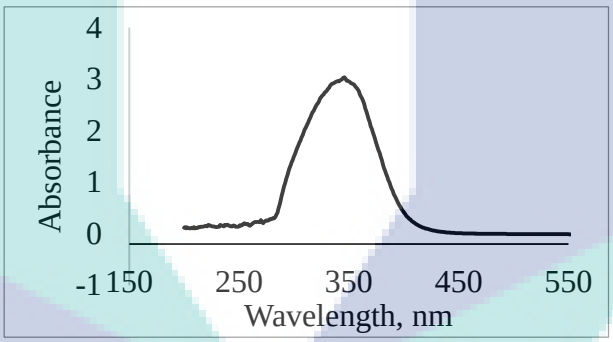

Figure 4.45 UV spectrum of (*E*)-3-(3,5-dimethoxyphenyl)-1-(2′-hydroxy-4′,6′-dimethoxyphenyl)prop-2-en-1-one (**83**)

IR spectrum of compound **83** is shown in Figure 4.46. The absorption bands at 3448 cm^{-1} and 1634 cm^{-1} represented the hydroxyl (O-H) and carbonyl (C=O) groups, respectively. Absorption bands observed in a range of 1279-1456 cm^{-1} and 2965-3010 cm^{-1} were represented the aromatic ring (C=C) and aromatic proton (Ar C-H), respectively. Absorption bands that appeared in a range of 1220-1221 cm^{-1} and 1567-1595 cm^{-1} represented to (C-O) [1] and (C=C-C=O), respectively.

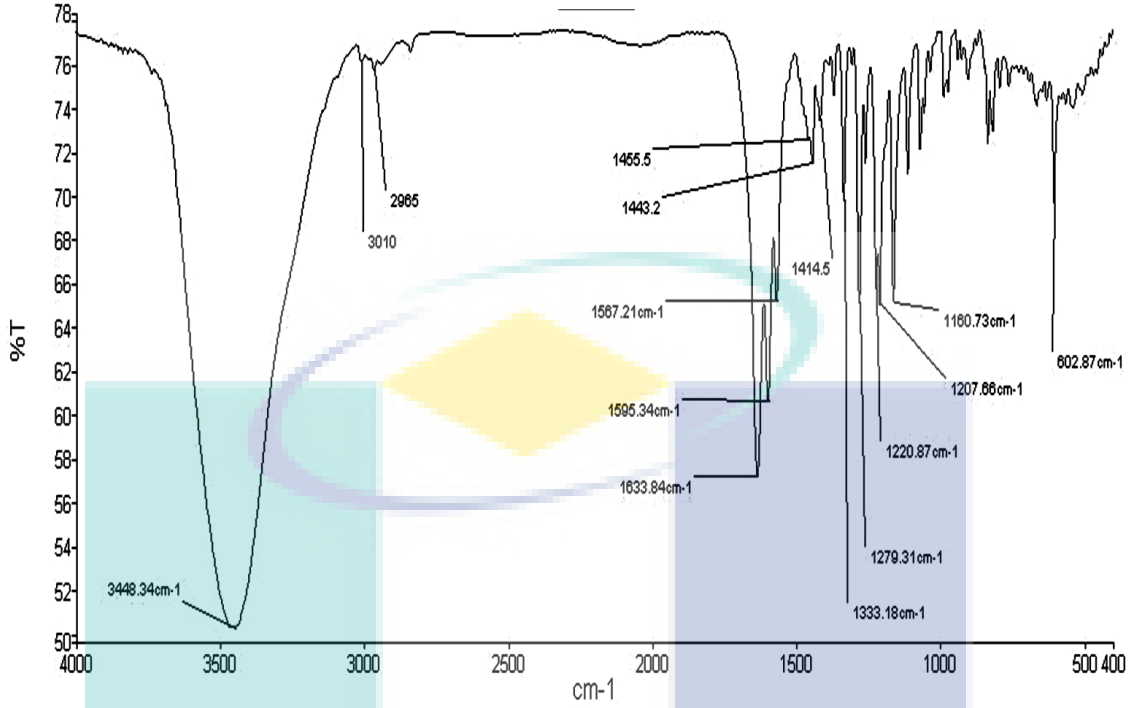

Figure 4.46 IR spectrum of (*E*)-3-(3,5-dimethoxyphenyl)-1-(2′-hydroxy-4′,6′-dimethoxyphenyl)prop-2-en-1-one (**83**)

^{1}H-NMR spectrum (600 MHz, $CDCl_3$) of compound **83** is shown in Figure 4.47 (Appendix A6). A doublet at δ 6.11 (d, *J* = 2.40 Hz) was assigned to the C-3′ proton and doublet at 5.96 (d, *J* = 2.34 Hz) was assigned to the C-5′ proton. Two doublets that appeared at 6.76 (d, *J* = 2.22 Hz) and 6.75 (d, *J* = 2.22 Hz) were assigned to the C-2 and C-6 proton, respectively. A triplet that appeared at 6.51 (t, *J* = 2.22 Hz, 2.28 Hz) was assigned to the C-4 proton. A doublet that appeared at 7.69 (d, *J* = 15.5 Hz) was assigned to the proton at α-carbon and doublet at 7.86 (d, *J* = 15.5 Hz) was assigned to the proton at β-carbon. The signals of singlet that appeared at 3.91 (s, 3H) was assigned to the methoxy proton at C-6′ and a singlet at 3.84 (s, 3H) corresponded to methoxy proton at C-4′. The signal of singlet that appeared at 3.837 (s, 3H) represented the methoxy proton at C-3 and singlet at 3.837 (s, 3H) was assigned to the methoxy proton at C-5. A singlet that appeared at 14.26 (s, 1H) represented the hydroxyl proton at C-2′ chelated to carbonyl group. The details of ^{1}H-NMR spectra shown in Table 4.12.

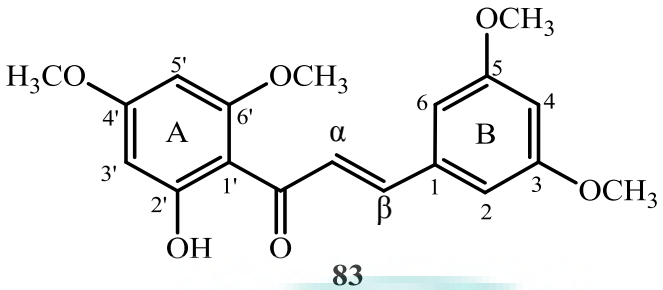

83

Figure 4.47 Structure of (*E*)-3-(3,5-dimethoxyphenyl)-1-(2′-hydroxy-4′,6′-dimethoxyphenyl)prop-2-en-1-one (**83**)

Table 4.12 NMR data of (*E*)-3-(3,5-dimethoxyphenyl)-1-(2′-hydroxy-4′,6′-dimethoxyphenyl)prop-2-en-1-one (**83**)

Carbon	^{1}H (δ)	Multiplicity	Designation
1′	-	-	-
2′	-	-	-
3′	6.11	(d, *J* = 2.40 Hz, 1H)	C3′-H
4′	-	-	-
5′	5.96	(d, *J* = 2.34 Hz, 1H)	C5′-H
6′	-	-	-
1	-	-	-
2	6.75	(d, *J* = 2.22 Hz, 1H)	C2-H
3	-	-	-
4	6.51	(t, *J* = 2.22 Hz, 2.28 Hz, 1H)	C4-H
5	-	-	-
6	6.75	(d, *J* = 2.22 Hz, 1H)	C6-H
α	7.69	(d, *J* = 15.50 Hz, 1H, H-α)	Cα-H
β	7.86	(d, *J* = 15.50 Hz, 1H, H-β)	Cβ-H
OCH_3 (C4′)	3.84	(s, 3H)	OCH_3 (C4′)
OCH_3 (C6′)	3.91	(s, 3H)	OCH_3 (C6′)
OCH_3 (C3)	3.837	(s, 3H)	OCH_3 (C3)
OCH_3 (C5)	3.837	(s, 3H)	OCH_3 (C5)
OH (C2′)	14.26	(s, 1H)	OH (C2′)

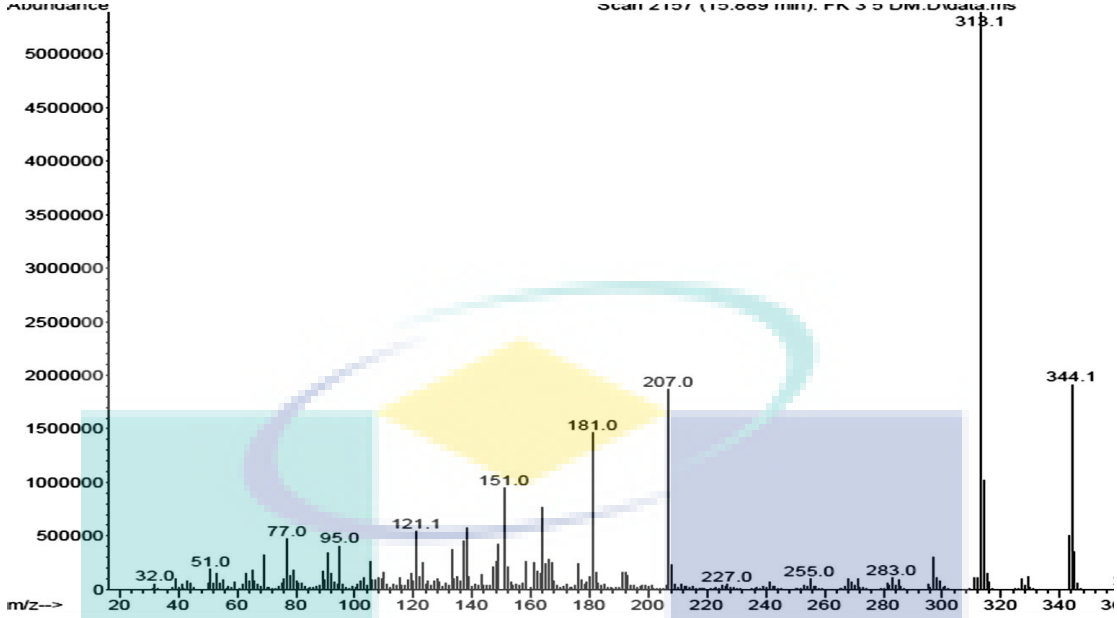

Figure 4.48 GC-MS spectrum of (*E*)-3-(3,5-dimethoxyphenyl)-1-(2′-hydroxy-4′,6′-dimethoxyphenyl)prop-2-en-1-one (**83**)

GC-MS spectrum of compound **83** shown in Figure 4.48 displays the main fragment ions of a molecular structure at *m/z* = 344, 329 313, 207, 181, 164, 151, 149, 137 and 121. The result from this analysis could support the tentative of synthesized compound **83**.

4.1.12 (*E*)-3-(3-chlorophenyl)-1-(2′-hydroxy-4′,6′-dimethoxyphenyl)prop-2-en-1-one (84)

Flavokawain B derivative, (*E*)-3-(3-chlorophenyl)-1-(2′-hydroxy-4′,6′-dimethoxyphenyl)prop-2-en-1-one (**84**) was synthesized by Claisen-Schmidt condensation of 2′-hydroxy-4′,6′-dimethoxyacetophenone (1.00 mmol) and 3-chlorobenzaldehyde (1.00 mmol) diluted in 5 mL MeOH, catalyzed by 40% KOH and stirred at room temperature for 58 hr as described in page 38. The product was obtained in a form of yellow crystal form with a yield of 83.1% and melting point in a range of 105-107°C (Chiaradia et al., 2008).

Compound **84** absorbed UV light in the wavelength range of 290-380 nm, which corresponded to the conjugated α,β-unsaturated carbonyl (C=O) chromophore. The UV-Visible spectrum of compound **84** shown in Figure 4.49 shows that the maximum absorption occurred at wavelength, λ_{max} in a range of 338-339 nm.

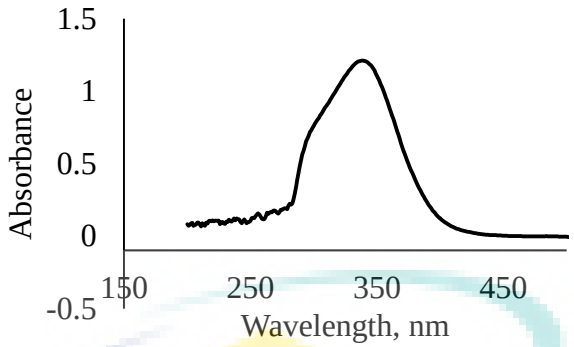

Figure 4.49 UV spectrum of (*E*)-3-(3-chlorophenyl)-1-(2′-hydroxy-4′,6′-dimethoxyphenyl)prop-2-en-1-one (**84**)

IR spectrum of compound **84** is shown in Figure 4.50. The absorption bands observed at 3460 cm^{-1} and 1634 cm^{-1} represented the hydroxyl (O-H) and carbonyl (C=O) group, respectively. Absorption bands in a range of 1342-1443 cm^{-1} and 2945-3014 cm^{-1} represented the aromatic ring (C=C) and aromatic proton (Ar C-H), respectively. Absorption bands observed in a range of 1213-1215 cm^{-1} and 1567-1585 cm^{-1} corresponded to (C-O) and (C=C-C=O), respectively.

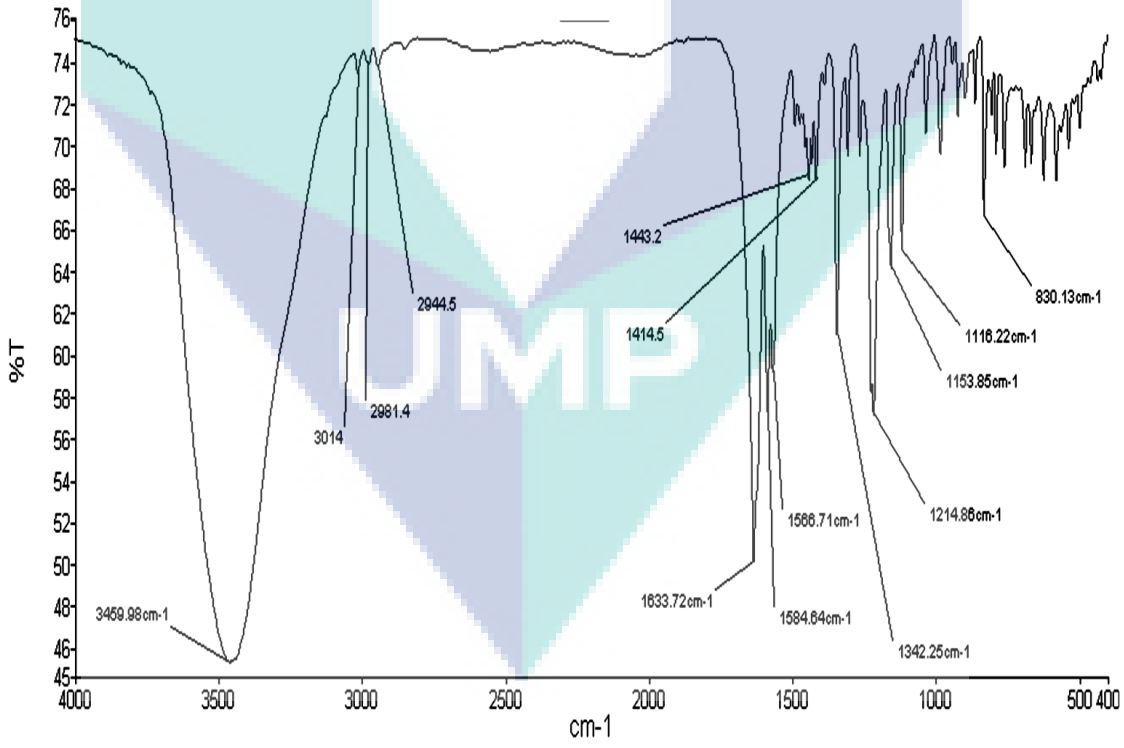

Figure 4.50 IR spectrum of (*E*)-3-(3-chlorophenyl)-1-(2′-hydroxy-4′,6′-dimethoxyphenyl)prop-2-en-1-one (**84**)

^{1}H-NMR spectrum (600 MHz, $CDCl_3$) of compound **84** is shown in Figure 4.51 (Appendix A6). A doublet at δ 6.11 (d, *J* = 2.34 Hz) was assigned to the C-3′ proton and a doublet at 5.97 (d, *J* = 2.34 Hz) was assigned to the C-5′ proton. One broad singlet that appeared at 7.57 (brs, 1H) was assigned to the C-2 proton. Two multiplets observed in a range of 7.35-7.46 were assigned to the C-4, C-5 and C-6 proton. The signal of doublet that appeared at 7.68 (d, *J* = 15.60 Hz) was assigned to the proton at α-carbon and a doublet observed at 7.86 (d, *J* = 15.60 Hz) was assigned to the proton at β-carbon. The signal of singlet elucidated at 3.93 (s, 3H) corresponded to the proton of methoxy at C-6′ and singlet observed at 3.85 (s, 3H) represented the methoxy proton at C-4′. A singlet appeared at 14.19 (s, 1H) due to the C-2′ hydroxyl proton chelated to carbonyl group. The details of ^{1}H-NMR spectra is shown in Table 4.13.

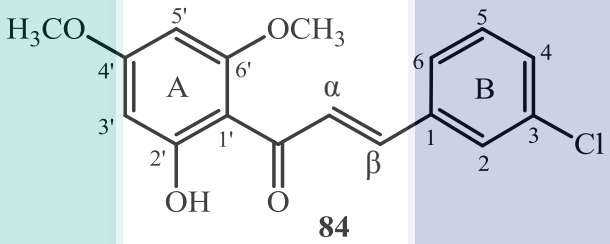

84

Figure 4.51 Structure of (*E*)-3-(3-chlorophenyl)-1-(2′-hydroxy-4′,6′-dimethoxyphenyl)prop-2-en-1-one (**84**)

Table 4.13 NMR data of (*E*)-3-(3-chlorophenyl)-1-(2′-hydroxy-4′,6′-dimethoxyphenyl)prop-2-en-1-one (**84**)

Carbon	^{1}H (δ)	Multiplicity	Designation
1′	-	-	-
2′	-	-	-
3′	6.11	(d, *J* = 2.34 Hz, 1H)	C3′-H
4′	-	-	-
5′	5.97	(d, *J* = 2.34 Hz, 1H)	C5′-H
6′	-	-	-
1	-	-	-
2	7.57	(brs, 1H)	C2-H
3	-	-	-
4	7.35	(m, 1H)	C4-H
5	7.46	(m, 1H)	C5-H
6	7.35	(m, 1H)	C6-H
α	7.68	(d, *J* = 15.60 Hz, 1H, H-α)	Cα-H
β	7.86	(d, *J* = 15.60 Hz, 1H, H-β)	Cβ-H
OCH_3 (C4′)	3.85	(s, 3H)	OCH_3 (C4′)
OCH_3 (C6′)	3.93	(s, 3H)	OCH_3 (C6′)
OH (C2′)	14.19	(s, 1H)	OH (C2′)

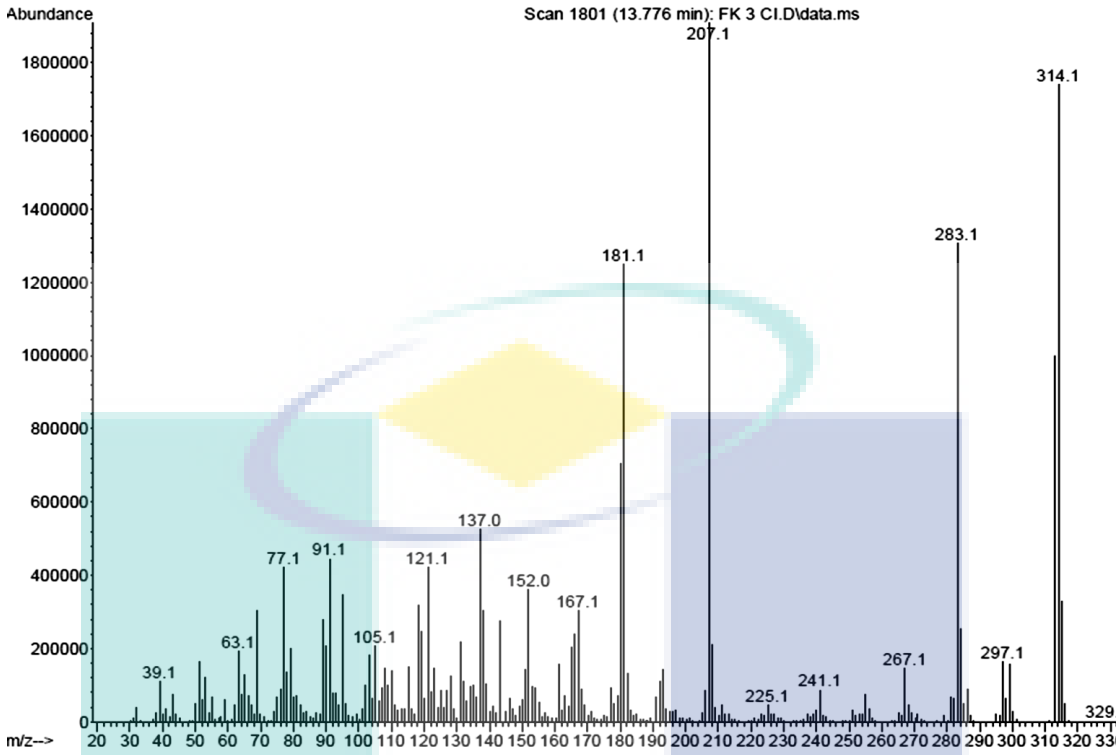

Figure 4.52 GC-MS spectrum of (*E*)-3-(3-chlorophenyl)-1-(2′-hydroxy-4′,6′-dimethoxyphenyl)prop-2-en-1-one (**84**)

GC-MS spectrum of compound **84** shown in Figure 4.52 displays the main fragment ions of a molecular structure at *m/z* = 317, 314, 297, 283, 267, 207, 181, 167, 152, 137 and 121. The result obtained from this analysis could support the tentative of synthesized compound **84**.

4.1.13 (*E*)-1-(2′-hydroxy-4′,6′-dimethoxyphenyl)-3-(3-methoxyphenyl)prop-2-en-1-one (85)

Flavokawain B derivative, (*E*)-1-(2′-hydroxy-4′,6′-dimethoxyphenyl)-3-(3-methoxyphenyl)prop-2-en-1-one (**85**) was synthesized via Claisen-Schmidt condensation of 2′-hydroxy-4′,6′-dimethoxyacetophenone (1.00 mmol) and 3-methoxybenzaldehyde (1.00 mmol) diluted in 5 mL MeOH, catalyzed by 40% KOH and stirred at room temperature for 49 hr as described in page 38. The product was obtained in a form of yellow crystal with a yield of 87.9% and melting point in a range of 111-112°C (Sekizaki, 1988).

Compound **85** absorbed UV light in the wavelength range of 290-390 nm, which corresponded to the conjugated α,β-unsaturated carbonyl (C=O) chromophore. The UV spectrum of compound **85** shown in Figure 4.53 shows that the maximum absorption occurred at a wavelength, λ_{max} of 345 nm (Sekizaki, 1988).

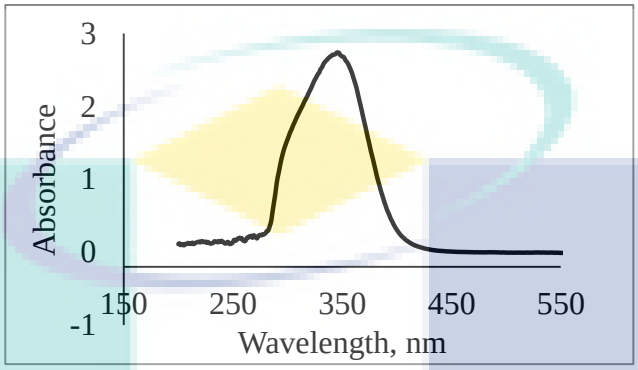

Figure 4.53 UV spectrum of (*E*)-1-(2′-hydroxy-4′,6′-dimethoxyphenyl)-3-(3-methoxyphenyl)prop-2-en-1-one (**85**)

IR spectrum of compound **85** is shown in Figure 4.54. The absorption bands at 3449 cm^{-1} and 1631 cm^{-1} represented the hydroxyl (O-H) and carbonyl (C=O) group, respectively (Sekizaki, 1988). Absorption bands elucidated in a range of 2949-3006 cm^{-1} and 1435-1484 cm^{-1} corresponded to the aromatic carbon-proton (Ar C-H str.) and aromatic ring (C=C), respectively. Absorption bands produced in a range of 1157-1247 cm^{-1} and 1575-1580 cm^{-1} represented (C-O) and (C=C-C=O), respectively.

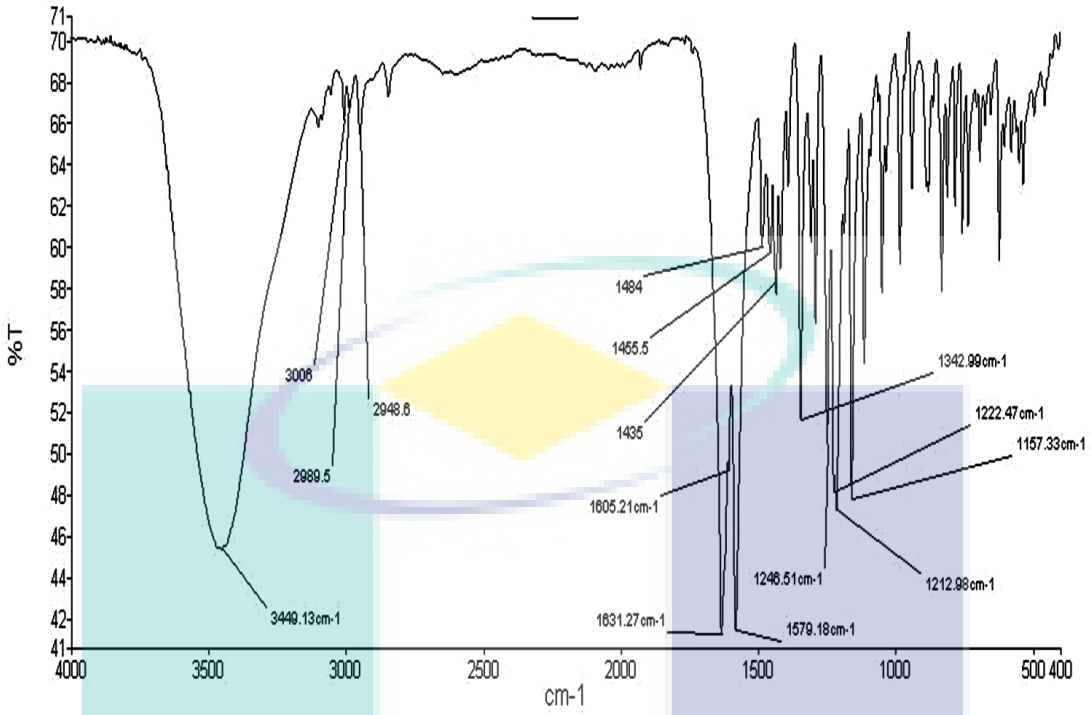

Figure 4.54 IR spectrum of (*E*)-1-(2′-hydroxy-4′,6′-dimethoxyphenyl)-3-(3-methoxyphenyl)prop-2-en-1-one (**85**)

^{1}H-NMR spectrum (600 MHz, $CDCl_3$) of compound **85** is shown in Figure 4.55 (Appendix A7). A singlet at δ 3.83 (s, 3H) represented the methoxy proton at C-3; a singlet at 3.84 (s, 3H) represented the methoxy proton at C-4′; a singlet at 3.91 (s, 3H) corresponded to the methoxy proton at C-6′. A broad singlet observed at 7.11 (brs, 1H) was assigned to the C-2′ proton. A doublet elucidated at 6.10 (d, *J* = 2.34 Hz, 1H) was assigned to the C-3′ proton and doublet at 5.95 (d, *J* = 2.40 Hz, 1H) was assigned to the C-5′ proton. A triplet produced at 7.32 (t, *J* = 7.92 Hz, 7.86 Hz, 1H) was assigned to the C-5 proton. A doublet that appeared at 6.94 (d, *J* = 8.22 Hz, 1H) was assigned to the C-4 proton and a doublet at 7.21 (d, *J* = 7.86 Hz, 1H) was assigned to the C-6 proton. A singlet that appeared at 14.29 (s, 1H) was assigned to the hydroxyl proton at C-2′ due to chelation with carbonyl group. A doublet observed at 7.73 (d, *J* = 15.54 Hz) was assigned to the proton at α-carbon and another doublet at 7.87 (d, *J* = 15.54 Hz) was assigned to the proton at β-carbon. The details of ^{1}H-NMR spectra is shown in Table 4.14. The ORTEP diagram and crystal parameters and data for structure refinement of compound **85** were shown in Figure 4.56 and Table 4.15, respectively.

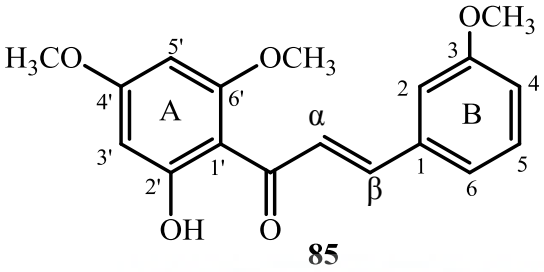

85

Figure 4.55 Structure of (*E*)-1-(2′-hydroxy-4′,6′-dimethoxyphenyl)-3-(3-methoxyphenyl)prop-2-en-1-one (**85**)

Table 4.14 NMR data of (*E*)-1-(2′-hydroxy-4′,6′-dimethoxyphenyl)-3-(3-methoxyphenyl)prop-2-en-1-one (**85**)

Carbon	^{1}H (δ)	Multiplicity	Designation
1′	-	-	-
2′	-	-	-
3′	6.10	(d, *J* = 2.34 Hz, 1H)	C3′-H
4′	-	-	-
5′	5.95	(d, *J* = 2.40 Hz, 1H)	C5′-H
6′	-	-	-
1	-	-	-
2	7.11	(brs, 1H)	C2-H
3	-	-	-
4	6.94	(d, *J* = 8.22 Hz, 1H)	C4-H
5	7.32	(t, *J* = 7.92 Hz, 7.86 Hz, 1H)	C5-H
6	7.21	(d, *J* = 7.86 Hz, 1H)	C6-H
α	7.73	(d, *J* = 15.54 Hz, 1H, H-α)	Cα-H
β	7.87	(d, *J* = 15.54 Hz, 1H, H-β)	Cβ-H
OCH_3 (C4′)	3.84	(s, 3H)	OCH_3 (C4′)
OCH_3 (C6′)	3.91	(s, 3H)	OCH_3 (C6′)
OCH_3 (C3)	3.83	(s, 3H)	OCH_3 (C3)
OH (C2′)	14.29	(s, 1H)	OH (C2′)

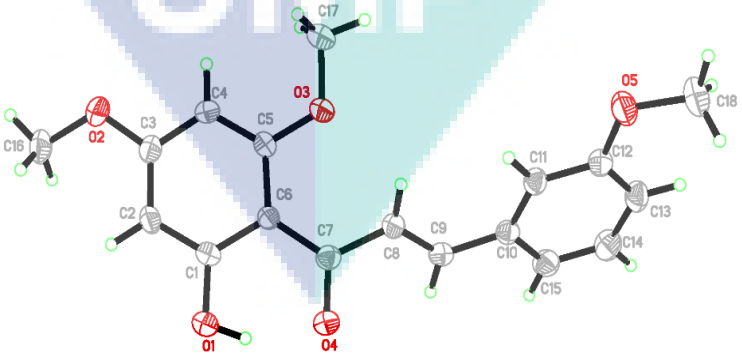

Figure 4.56 ORTEP diagram of (*E*)-1-(2′-hydroxy-4′,6′-dimethoxyphenyl)-3-(3-methoxyphenyl)prop-2-en-1-one (**85**)

Table 4.15 Crystal parameters and data for structure refinement of (*E*)-1-(2′-hydroxy-4′,6′-dimethoxyphenyl)-3-(3-methoxyphenyl)prop-2-en-1-one (**85**)

Parameter	Data
CCDC Number	1548733
Molecular Formula	$C_{18}H_{18}O_5$
Molecular Weight	314.32
Crystal System	Orthorhombic
Space Group	Pbca
a (Å)	14.447 (3)
b (Å)	7.9755 (15)
c (Å)	26.203 (5)
α (°)	90
β (°)	90
γ (°)	90
V (Å^3)	3019.0 (10)
Z	8
*D*calc (g cm^{-3})	1.383
Crystal dimensions (mm)	0.55 × 0.27 × 0.14
μ (mm^{-1})	0.10
T_{min}/T_{max}	0.8489, 0.9495
Reflections measured	14974
Ranges/indices (*h*, *k*, *l*)	-16→16; -9→9; -30→28
θ limit (°)	1.6-24.6
Unique reflections	2516
Observed reflections ($I > 2\sigma(I)$)	1594
Parameters	211
Goodness of fit on F^2	1.05
R_1, wR_2 [$I \geq 2\sigma(I)$]	0.056, 0.156

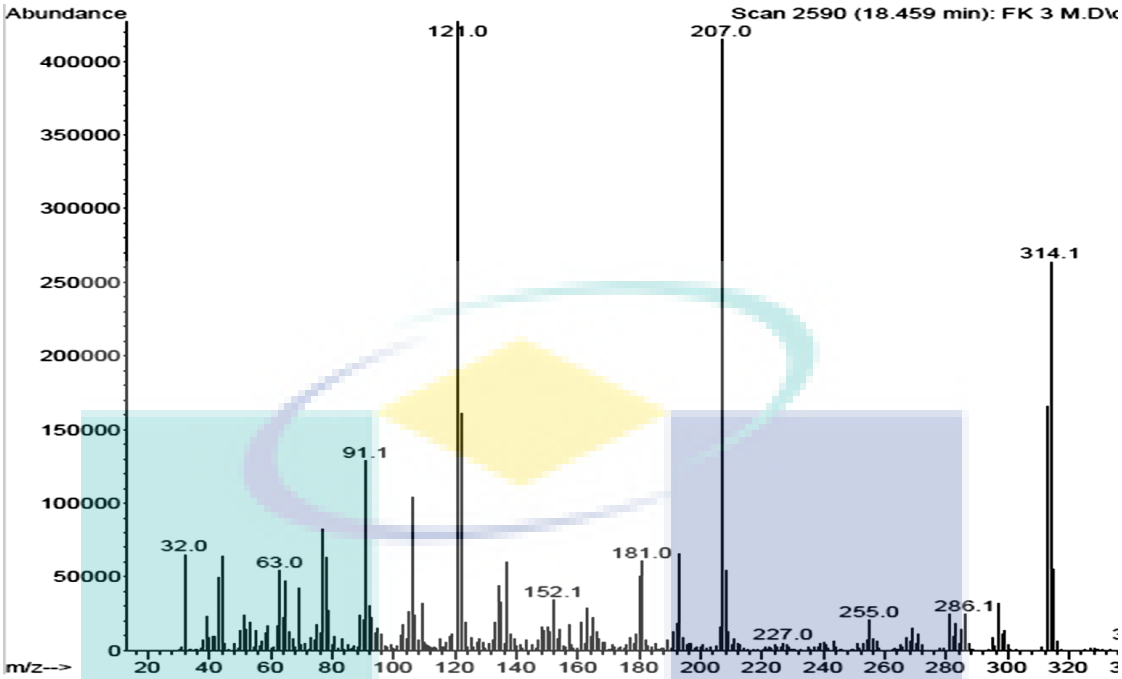

Figure 4.57 GC-MS spectrum of (*E*)-1-(2′-hydroxy-4′,6′-dimethoxyphenyl)-3-(3-methoxyphenyl)prop-2-en-1-one (**85**)

GC-MS spectrum of compound **85** shown in Figure 4.57 displays the main fragment ions of a molecular structure at *m/z* = 314, 297, 286, 207, 192, 181, 164, 152, 137 and 121. The result obtained from this analysis could support the tentative of synthesized compound **85**.

4.1.14 (*E*)-1-(2′-hydroxy-4′,6′-dimethoxyphenyl)-3-(3-nitrophenyl)prop-2-en-1-one (44)

Flavokawain B derivative, (*E*)-1-(2′-hydroxy-4′,6′-dimethoxyphenyl)-3-(3-nitrophenyl)prop-2-en-1-one (**44**) was synthesized via Claisen-Schmidt condensation of 2′-hydroxy-4′,6′-dimethoxyacetophenone (1.00 mmol) and 3-nitrobenzaldehyde (1.00 mmol) diluted in 5 mL MeOH, catalyzed by 40% KOH and stirred at room temperature for 48 hr as described in page 38. The product was obtained in a form of yellow cotton with a yield of 82.6% and melting point in a range of 169-171°C (Srinivasarao et al., 2013).

Compound **44** absorbed UV light in the wavelength range of 280-390 nm, which corresponded to the conjugated α,β-unsaturated carbonyl (C=O) chromophore. The UV-Visible spectrum of compound **44** shown in Figure 4.58 shows that the maximum absorption occurred at wavelength, λ_{max} of 336 nm (Boeck et al., 2006).

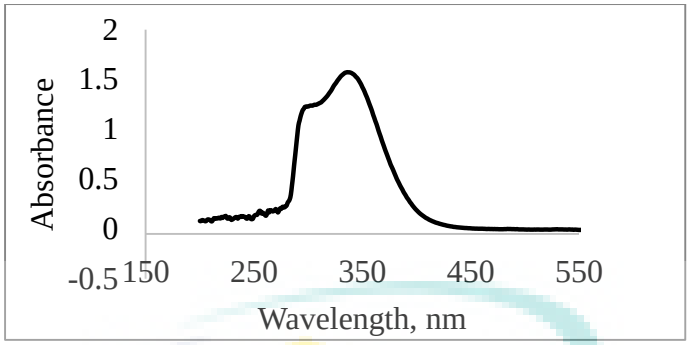

Figure 4.58 UV spectrum of (*E*)-1-(2′-hydroxy-4′,6′-dimethoxyphenyl)-3-(3-nitrophenyl)prop-2-en-1-one (**44**)

IR spectrum of compound **44** is shown in Figure 4.59. The absorption bands at 3460 cm^{-1} and 1638 cm^{-1} represented the hydroxyl (O-H) and carbonyl (C=O) group, respectively. Absorption bands at 1427-1525 cm^{-1} and 2851-3092 cm^{-1} corresponded to aromatic ring (C=C) and aromatic proton (Ar C-H), respectively. Absorption bands at 1223-1225 cm^{-1} and 1583 cm^{-1} represented the (C-O) and (C=C-C=O), respectively (Boeck et al., 2006).

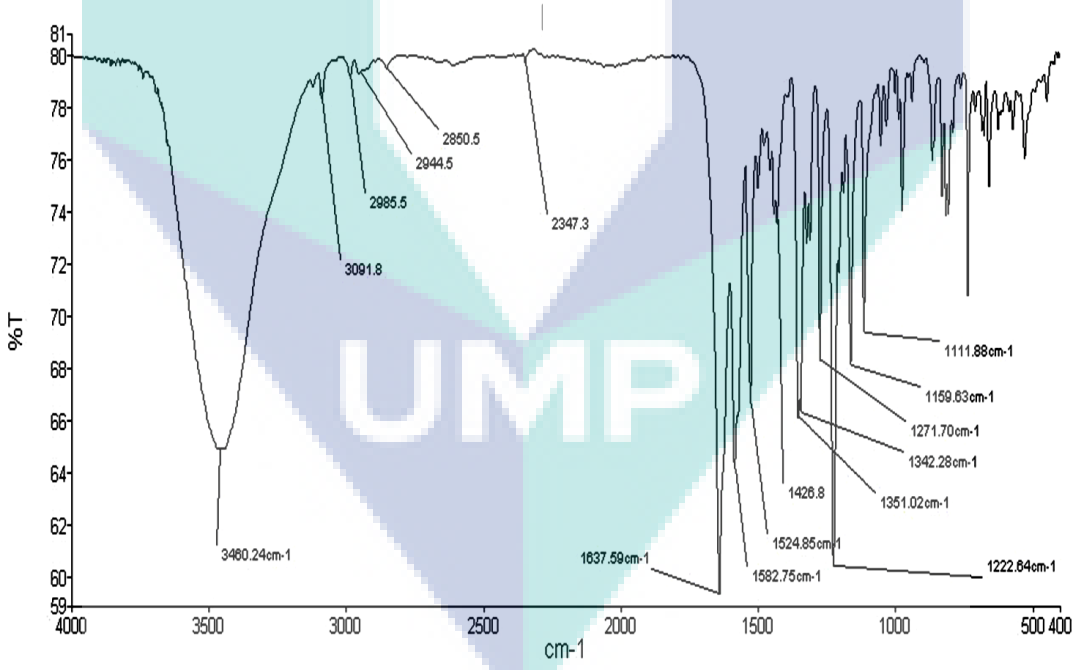

Figure 4.59 IR spectrum of (*E*)-1-(2′-hydroxy-4′,6′-dimethoxyphenyl)-3-(3-nitrophenyl)prop-2-en-1-one (**44**)

^{1}H-NMR spectrum (500 MHz, $CDCl_3$) of compound **44** is shown in Figure 4.60 (Appendix A7). Two singlet at δ 3.91 (s, 3H) and 4.04 (s, 3H) represented the methoxy proton at C-4′ and C-6′, respectively. A broad singlet that appeared at 8.56 (brs, 1H)

was assigned to the C-2 proton. Doublet observed at 6.17 (d, *J* = 2.35 Hz, 1H) and 6.14 (d, *J* = 2.35 Hz, 1H) were assigned to the C-3′ proton and C-5′ proton, respectively. A triplet that appeared at 7.78 (t, *J* = 7.95 Hz, 8.00 Hz, 1H) corresponded to the C-5 proton. A doublet elucidated at 8.30 (d, *J* = 8.00 Hz, 1H) was assigned to the C-4 proton and doublet at 8.22 (d, *J* = 7.75 Hz, 1H) was assigned to the C-6 proton. A doublet observed at 7.84 (d, *J* = 15.70 Hz) was assigned to the proton at α-carbon and a doublet at 8.15 (d, *J* = 15.70 Hz) was assigned to the proton at β-carbon (Boeck et al., 2006). The details of ^{1}H-NMR spectra is shown in Table 4.16.

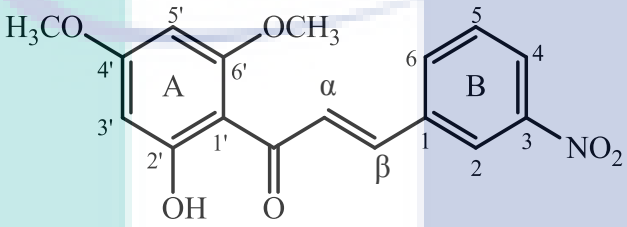

44

Figure 4.60 Structure of (*E*)-1-(2′-hydroxy-4′,6′-dimethoxyphenyl)-3-(3-nitrophenyl)prop-2-en-1-one (**44**)

Table 4.16 NMR data of (*E*)-1-(2′-hydroxy-4′,6′-dimethoxyphenyl)-3-(3-nitrophenyl)prop-2-en-1-one (**44**)

Carbon	^{1}H (δ)	Multiplicity	Designation
1′	-	-	-
2′	-	-	-
3′	6.17	(d, *J* = 2.35 Hz, 1H)	C3′-H
4′	-	-	-
5′	6.14	(d, *J* = 2.35 Hz, 1H)	C5′-H
6′	-	-	-
1	-	-	-
2	8.56	(brs, 1H)	C2-H
3	-	-	-
4	8.30	(d, *J* = 8.00 Hz, 1H)	C4-H
5	7.78	(t, *J* = 7.95 Hz, 8.00 Hz, 1H)	C5-H
6	8.22	(d, *J* = 7.75 Hz, 1H)	C6-H
α	7.84	(d, *J* = 15.70 Hz, 1H, H-α)	Cα-H
β	8.15	(d, *J* = 15.70 Hz, 1H, H-β)	Cβ-H
OCH_3 (C4′)	3.91	(s, 3H)	OCH_3 (C4′)
OCH_3 (C6′)	4.04	(s, 3H)	OCH_3 (C6′)
OH (C2′)	-	(s, 1H)	OH (C2′)

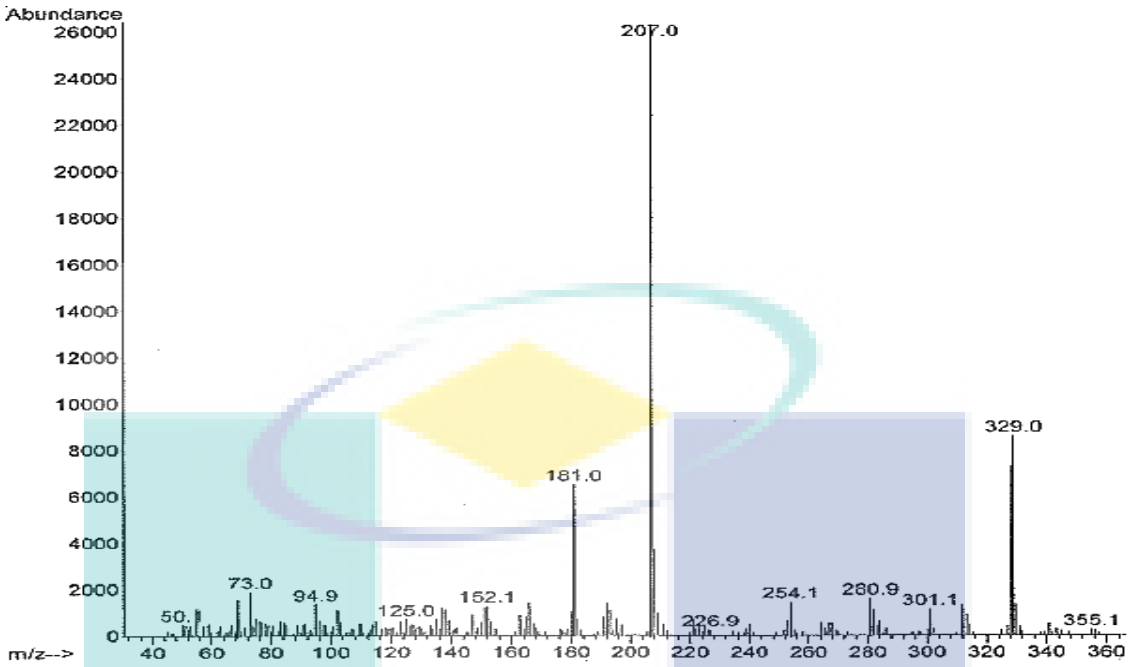

Figure 4.61 GC-MS spectrum of (*E*)-1-(2′-hydroxy-4′,6′-dimethoxyphenyl)-3-(3-nitrophenyl)prop-2-en-1-one (**44**)

GC-MS spectrum of compound **44** shown in Figure 4.61 displays the main fragment ions of a molecular structure at *m/z* = 329, 301, 281, 254, 207, 181, 152, 95 and 73. The result obtained from this analysis can support the tentative of synthesized compound **44**.

4.1.15 (*E*)-3-(4-bromophenyl)-1-(2′-hydroxy-4′,6′-dimethoxyphenyl)prop-2-en-1-one (86)

Flavokawain B derivative, (*E*)-3-(4-bromophenyl)-1-(2′-hydroxy-4′,6′-dimethoxyphenyl)prop-2-en-1-one (**86**) was synthesized via Claisen-Schmidt condensation of 2′-hydroxy-4′,6′-dimethoxyacetophenone (1.00 mmol) and 4-bromobenzaldehyde (1.00 mmol) diluted in 5 mL MeOH, catalyzed by 40% KOH and stirred at room temperature for 70 hr as described in page 38. The product was obtained in a form of orange crystal with a yield of 80.5% and melting point of 165.8-167.5°C (Boeck et al., 2006).

Compound **86** absorbed UV light in the wavelength range of 290-390 nm, which corresponded to the conjugated α,β-unsaturated carbonyl (C=O) chromophore. The UV-Visible spectrum of compound **86** shown in Figure 4.62 shows that the maximum absorption occurred at a wavelength, λ_{max} at 346 nm (Boeck et al., 2006).

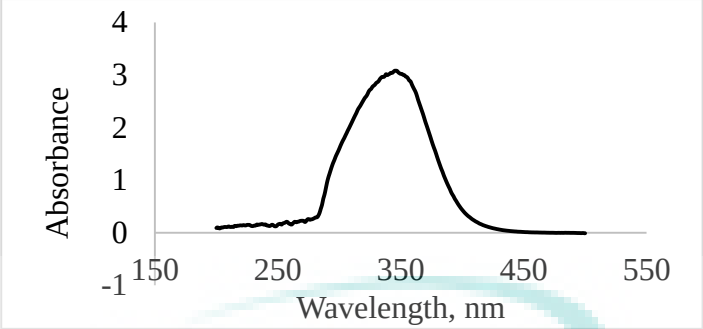

Figure 4.62 UV spectrum of (*E*)-3-(4-bromophenyl)-1-(2′-hydroxy-4′,6′-dimethoxyphenyl)prop-2-en-1-one (**86**)

IR spectrum of compound **86** is shown in Figure 4.63. The absorption bands at 3447 cm^{-1} and 1633 cm^{-1} corresponded to the hydroxyl (O-H) and carbonyl (C=O) group, respectively. Absorption band observed in a range of 1338-1488 cm^{-1} and 2949-3010 cm^{-1} represented the aromatic ring (C=C) and aromatic proton (Ar C-H), respectively. Absorption band elucidated in a range of 1215-1218 cm^{-1} and 1568-1590 cm^{-1} represented (C-O) and (C=C-C=O), respectively (Boeck et al., 2006).

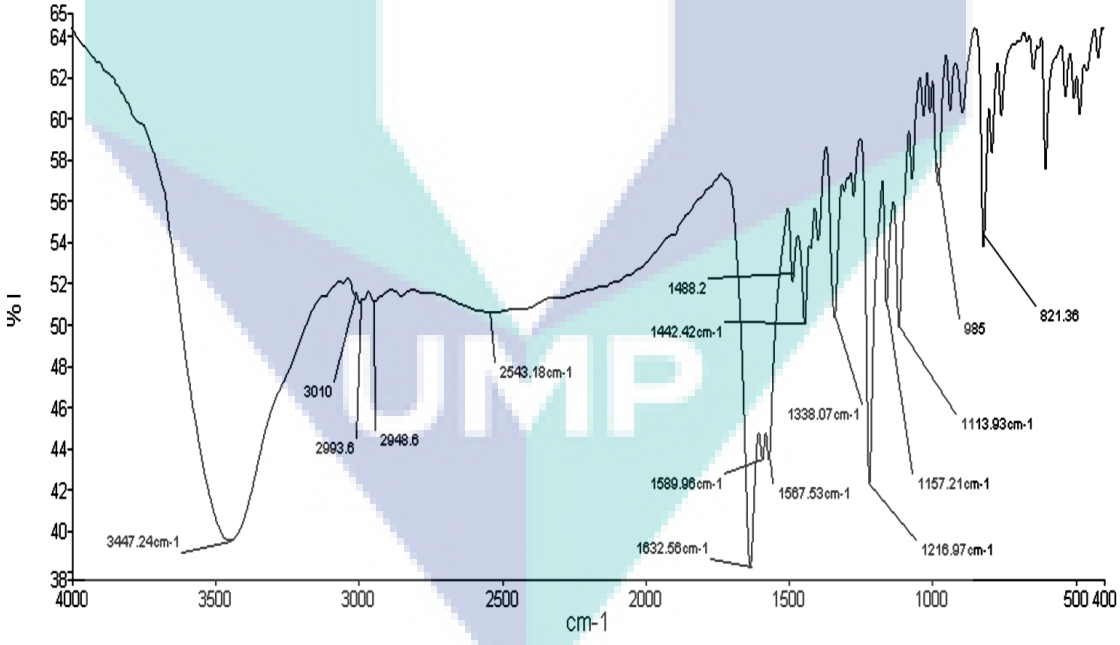

Figure 4.63 IR spectrum of (*E*)-3-(4-bromophenyl)-1-(2′-hydroxy-4′,6′-dimethoxyphenyl)prop-2-en-1-one (**86**)

^{1}H-NMR spectrum (500 MHz, $CDCl_3$) of compound **86** is shown in Figure 4.64 (Appendix A8). Two singlets at δ 3.83 (s, 3H) and 3.90 (s, 3H) represented the methoxy proton at C-6′ and C-4′, respectively. A doublet that appeared at 6.09 (d, J = 2.00 Hz)

was assigned to the C-3′ proton and doublet at 5.95 (d, *J* = 2.50 Hz) was assigned to the C-5′ proton. Two doublets that appeared at 7.53 (d, *J* = 8.50 Hz) and 7.51 (d, *J* = 8.50 Hz) were assigned to the C-2 and C-6 proton, respectively. Two doublets observed presented at 7.45 (d, *J* = 8.50 Hz) and 7.43 (d, *J* = 8.50 Hz) corresponded to the C-3 and C-5 proton, respectively. A doublet that appeared at 7.68 (d, *J* = 15.50 Hz) was assigned to the proton at α-carbon and a doublet at 7.85 (d, *J* = 15.50 Hz) was assigned to the proton at β-carbon (Boeck et al., 2006). The details of ^{1}H-NMR spectra is shown in Table 4.17.

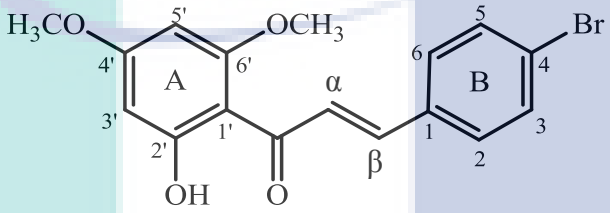

86

Figure 4.64 Structure of (*E*)-3-(4-bromophenyl)-1-(2′-hydroxy-4′,6′-dimethoxyphenyl)prop-2-en-1-one (**86**)

Table 4.17 NMR data of (*E*)-3-(4-bromophenyl)-1-(2′-hydroxy-4′,6′-dimethoxyphenyl)prop-2-en-1-one (**86**)

Carbon	^{13}C (δ)	^{1}H (δ)	Multiplicity	Designation
1′	106.29	-	-	-
2′	168.45	-	-	-
3′	93.85	6.09	(d, *J* = 2.00 Hz, 1H)	C3′-H
4′	166.40	-	-	-
5′	91.32	5.95	(d, *J* = 2.50 Hz, 1H)	C5′-H
6′	162.48	-	-	-
1	134.53	-	-	-
2	129.68	7.53	(d, *J* = 8.50 Hz, 1H)	C2-H
3	132.10	7.45	(d, *J* = 8.50 Hz, 1H)	C3-H
4	124.19	-	-	-
5	132.10	7.43	(d, *J* = 8.50 Hz, 1H)	C5-H
6	129.68	7.51	(d, *J* = 8.50 Hz, 1H)	C6-H
α	128.15	7.68	(d, *J* = 15.50 Hz, 1H, H-α)	Cα-H
β	140.78	7.85	(d, *J* = 15.50 Hz, 1H, H-β)	Cβ-H
OCH_3 (C4′)	55.89	3.83	(s, 3H)	OCH_3 (C4′)
OCH_3 (C6′)	55.61	3.90	(s, 3H)	OCH_3 (C6′)
OH (C2′)		-	(s, 1H)	OH (C2′)
C=O	192.31	-	-	-

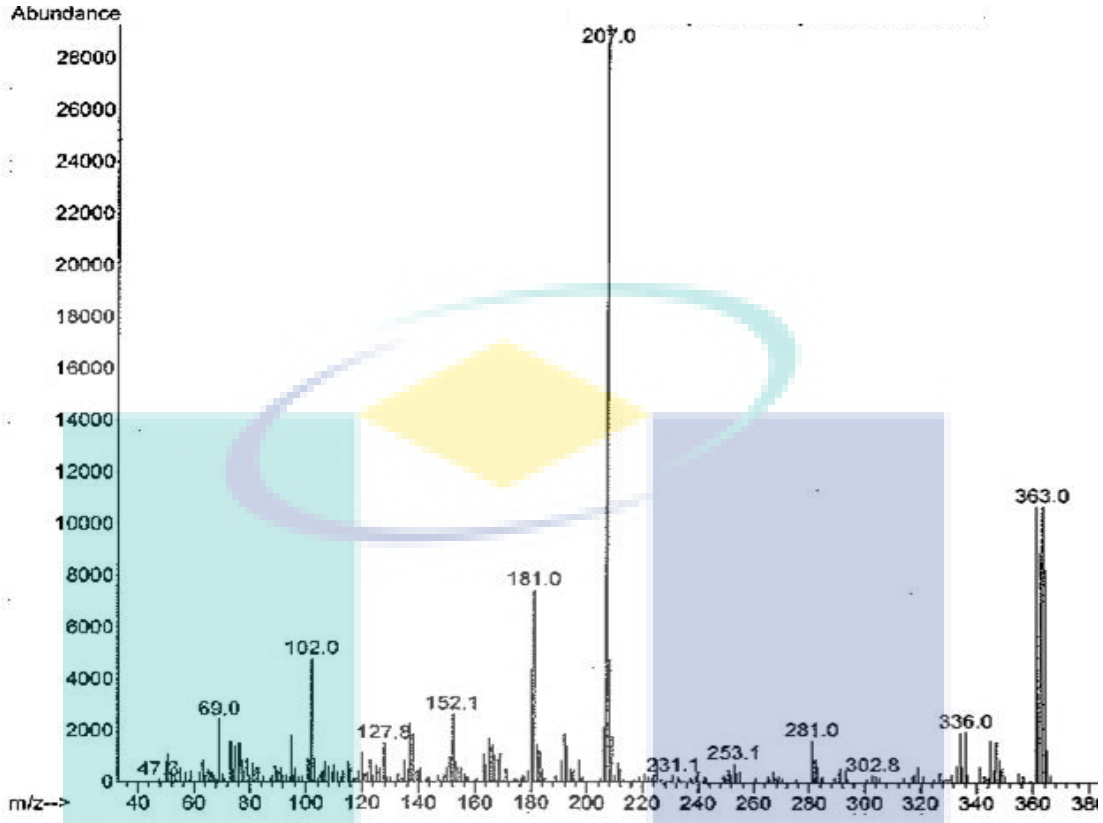

Figure 4.65 GC-MS spectrum of (*E*)-3-(4-bromophenyl)-1-(2′-hydroxy-4′,6′-dimethoxyphenyl)prop-2-en-1-one (**86**)

GC-MS spectrum of compound **86** shown in Figure 4.65 displays the main fragment ions of a molecular structure at *m/z* = 363, 362, 346, 281, 209, 207, 181 and 152. The result obtained from this analysis could support the tentative of synthesized compound **86**.

4.1.16 (*E*)-3-(4-chlorophenyl)-1-(2′-hydroxy-4′,6′-dimethoxyphenyl)prop-2-en-1-one (87)

Flavokawain B derivative, (*E*)-3-(4-chlorophenyl)-1-(2′-hydroxy-4',6'-dimethoxyphenyl)prop-2-en-1-one (**87**) was synthesized via Claisen-Schmidt condensation of 2'-hydroxy-4',6'-dimethoxyacetophenone (1.00 mmol) and 4-chlorobenzaldehyde (1.00 mmol) diluted in 5 mL MeOH, catalyzed by 40% KOH and stirred at room temperature for 50 hr as described in page 38. The product was obtained in a form of yellow crystal with a yield of 84.3% and melting point in a range of 171-173°C (Srinivasarao et al., 2013).

Compound **87** absorbed UV light in the wavelength range of 290-390 nm, which corresponded to the conjugated α,β-unsaturated carbonyl (C=O) chromophore. The UV spectrum of compound **87** shown in Figure 4.66 shows that the maximum absorption occurred at wavelength, λ_{max} in a range of 342-343 nm.

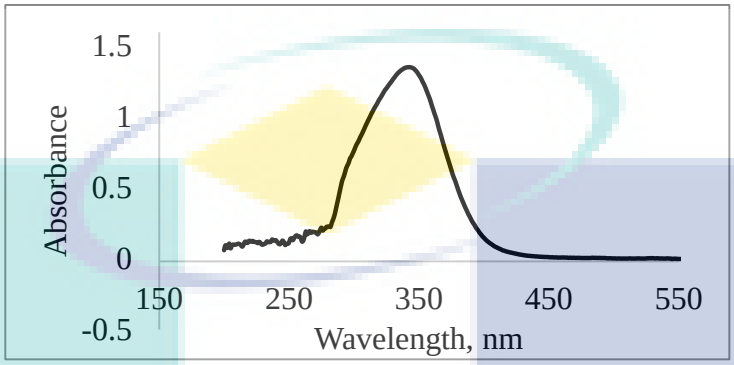

Figure 4.66 UV spectrum of (*E*)-3-(4-chlorophenyl)-1-(2'-hydroxy-4',6'-dimethoxyphenyl)prop-2-en-1-one (**87**)

IR spectrum of compound **87** is shown in Figure 4.67. The absorption bands at 3420 cm^{-1} and 1630 cm^{-1} represented the hydroxyl (O-H) and carbonyl (C=O) group, respectively. Absorption bands observed in a range 1488-1591 cm^{-1} and 2981-3018 cm^{1} corresponded to the aromatic ring (C=C) and aromatic proton (Ar C-H), respectively. Absorption bands observed in a range of 1217-1219 cm^{-1} and 820-822 cm^{-1} indicated the presence of (C-O) and aromatic carbon-chloro (Ar C-Cl) (Boeck et al., 2006).

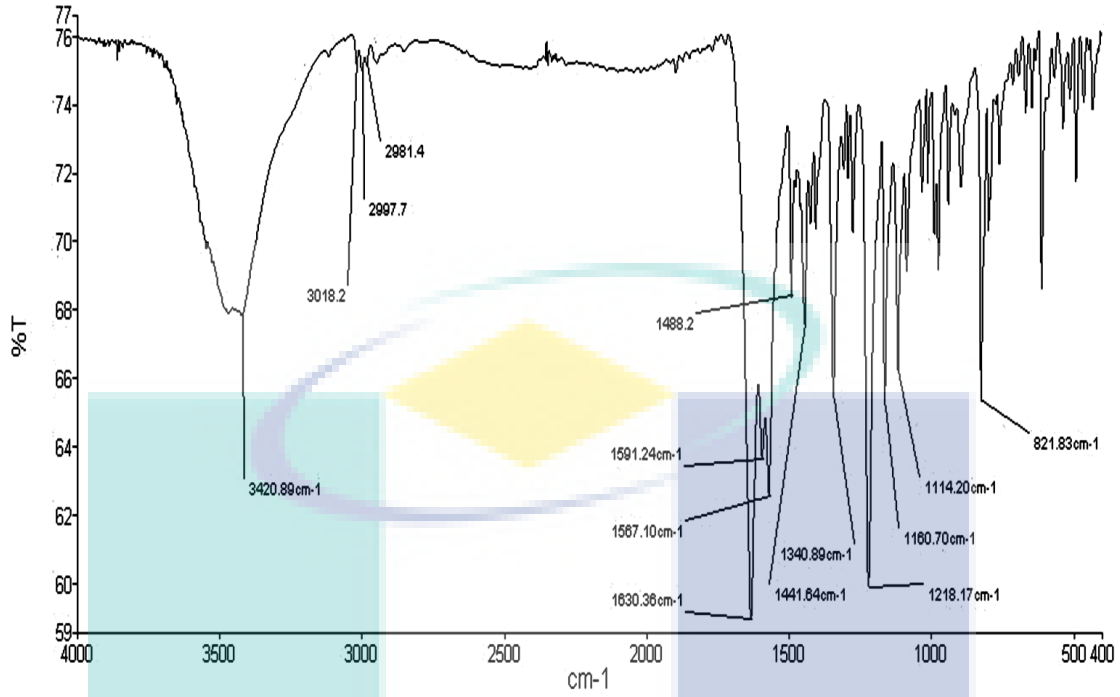

Figure 4.67 IR spectrum of (*E*)-3-(4-chlorophenyl)-1-(2'-hydroxy-4',6'-dimethoxyphenyl)prop-2-en-1-one (**87**)

^{1}H-NMR spectrum (600 MHz, $CDCl_3$) of compound **87** is shown in Figure 4.68 (Appendix A8). Two singlets at δ 3.84 and 3.92 were assigned to the methoxy proton at C-4' and C-6', respectively. Two doublets that appeared at 5.96 (d, *J* = 2.40 Hz) and 6.11 (d, *J* = 2.40 Hz) were assigned to the C-5' proton and C-3' proton, respectively. Two doublets elucidated at 7.38 (d, *J* = 8.46 Hz) and 7.37 (d, *J* = 8.46 Hz) were assigned to the C-3 and C-5 proton, respectively. Doublets produced at 7.53 (d, *J* = 8.46 Hz) and 7.52 (d, *J* = 8.46 Hz) were assigned to the C-2 and C-6 proton, respectively. A doublet that appeared at 7.72 (d, *J* = 15.60 Hz) was assigned to the proton at α-carbon and a doublet at 7.85 (d, *J* = 15.60 Hz) was assigned to the proton at β-carbon. A singlet observed at 14.24 represented the hydroxyl proton at C-2' chelated to carbonyl group (Boeck et al., 2006). The details of ^{1}H-NMR spectra is shown in Table 4.18.

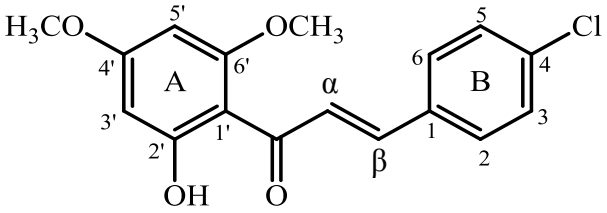

87

Figure 4.68 Structure of (*E*)-3-(4-chlorophenyl)-1-(2'-hydroxy-4',6'-dimethoxyphenyl)prop-2-en-1-one (**87**)

Table 4.18 NMR data of (*E*)-3-(4-chlorophenyl)-1-(2'-hydroxy-4',6'-dimethoxyphenyl)prop-2-en-1-one (**87**)

Carbon	^{1}H (δ)	Multiplicity	Designation
1'	-	-	-
2'	-	-	-
3'	6.11	(d, *J* = 2.40 Hz, 1H)	C3'-H
4'	-	-	-
5'	5.96	(d, *J* = 2.40 Hz, 1H)	C5'-H
6'	-	-	-
1	-	-	-
2	7.53	(d, *J* = 8.46 Hz, 1H)	C2-H
3	7.38	(d, *J* = 8.46 Hz, 1H)	C3-H
4	-	-	-
5	7.37	(d, *J* = 8.46 Hz, 1H)	C5-H
6	7.52	(d, *J* = 8.46 Hz, 1H)	C6-H
α	7.72	(d, *J* = 15.60 Hz, 1H, H-α)	Cα-H
β	7.85	(d, *J* = 15.60 Hz, 1H, H-β)	Cβ-H
OCH_3 (C4')	3.84	(s, 3H)	OCH_3 (C4')
OCH_3 (C6')	3.92	(s, 3H)	OCH_3 (C6')
OH (C2')	14.24	(s, 1H)	OH (C2')

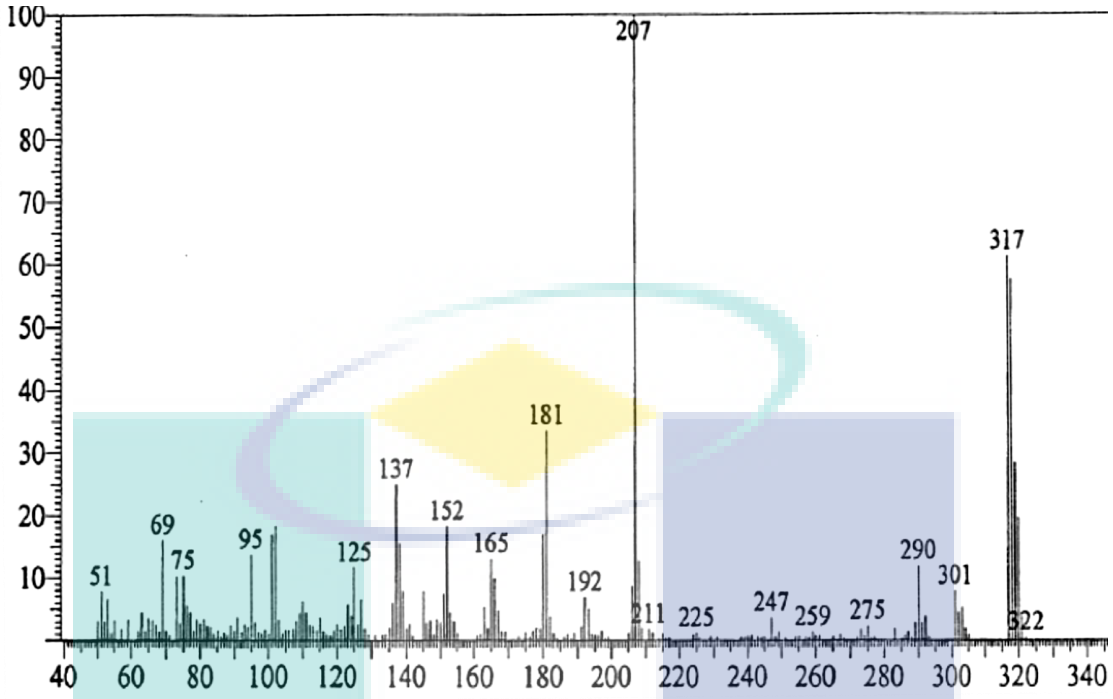

Figure 4.69 GC-MS spectrum of (*E*)-3-(4-chlorophenyl)-1-(2'-hydroxy-4',6'-dimethoxyphenyl)prop-2-en-1-one (**87**)

GC-MS spectrum of compound **87** shown in Figure 4.69 displays the main fragment ions of a molecular structure at *m/z* = 318, 301, 283, 207, 181, 165, 152, 137, 111 and 102. The abundance of molecular peak observed at *m/z* = 318 was about 57%. Fragment ion elucidated at *m/z* = 301 corresponded to the loss of radical ·OH from the molecular ion. Loss of radical ·Cl from the molecular ion led to formation of fragment ion at *m/z* = 283. The base peak was observed at *m/z* = 207 due to loss of phenyl chloride from molecule structure, which fragment was elucidated at *m/z* = 111. Fragment ion observed at *m/z* = 181 could potentially represented radical ketone moiety, formed due to α-cleavage with its counterpart observed at *m/z* = 137. Formation of fragment ion at *m/z* = 152 could be due to cleavage of bond next to C=O and further structural rearrangement, with its counterpart elucidated at *m/z* = 165. Fragment ion at *m/z* = 102 possibly represented $C_8H_6^{+\cdot}$ ion, formed as a result of the cleavage of Cl· radical from the fragment ion observed at *m/z* = 137. The proposed mechanisms of cleavage is shown in Figure 4.70.

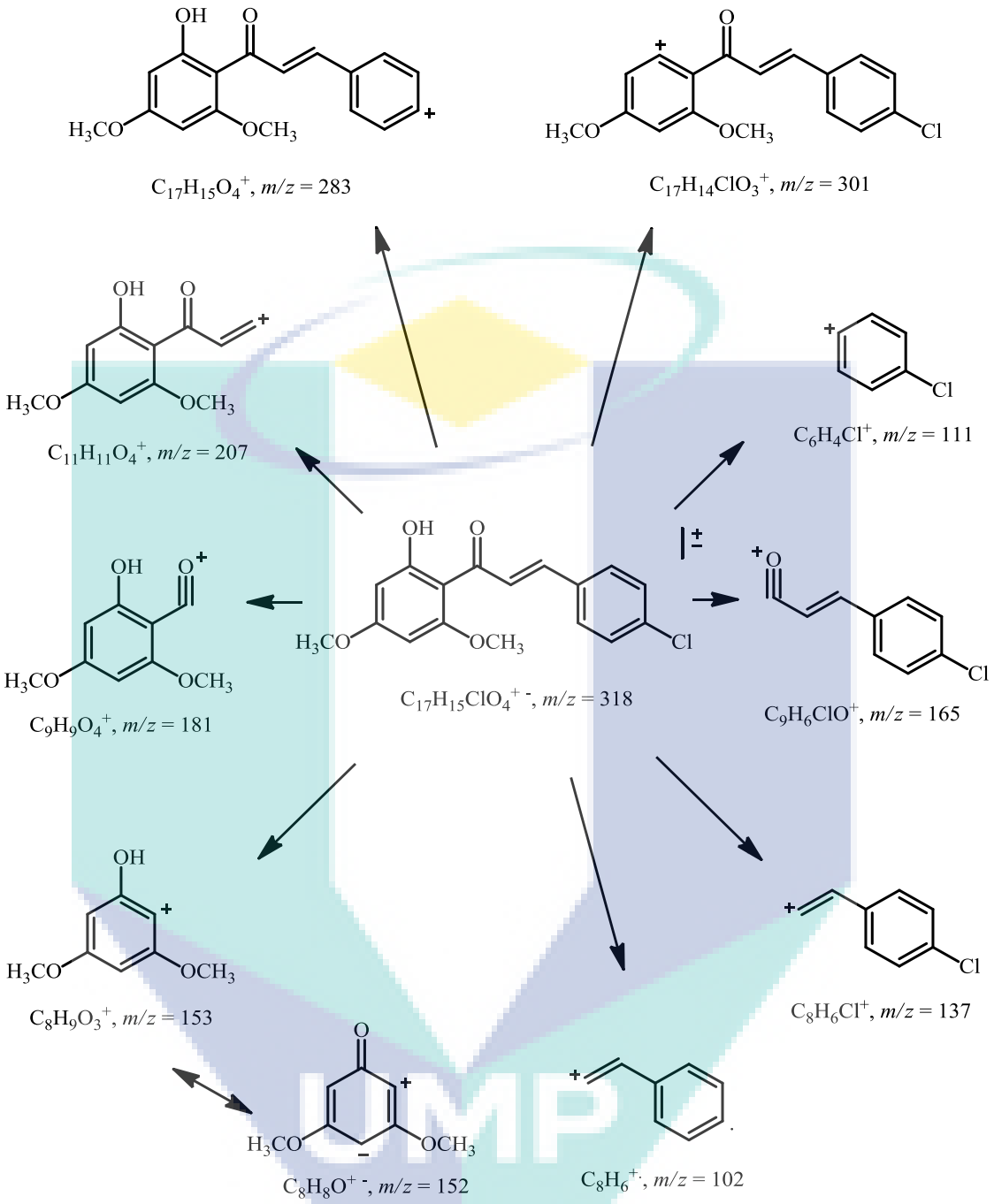

Figure 4.70 Mass fragmentation of (*E*)-3-(4-chlorophenyl)-1-(2'-hydroxy-4',6'-dimethoxyphenyl)prop-2-en-1-one (**87**)

4.1.17 (*E*)-3-(4-fluorophenyl)-1-(2'-hydroxy-4',6'-dimethoxyphenyl)prop-2-en-1-one (46)

Flavokawain B derivative, (*E*)-3-(4-fluorophenyl)-1-(2'-hydroxy-4',6'-dimethoxyphenyl)prop-2-en-1-one (**46**) was synthesized via Claisen-Schmidt condensation of 2'-hydroxy-4',6'-dimethoxyacetophenone (1.00 mmol) and 4-fluorobenzaldehyde (1.00 mmol) diluted in 5 mL MeOH, catalyzed by 40% KOH and stirred at room temperature for 48 hr as described in page 38. The product was obtained in a form of yellow crystal with a yield of 80.7% and melting point in a range of 144-145°C (Boeck et al., 2006).

Compound **46** absorbed UV light in the wavelength range of 290-390 nm, which corresponded to the conjugated α,β-unsaturated carbonyl (C=O) chromophore. The UV-Visible spectrum of compound **46** shown in Figure 4.71 shows that the maximum absorption occurred at wavelength, λ_{max}, in a range of 342-343 nm (Boeck et al., 2006).

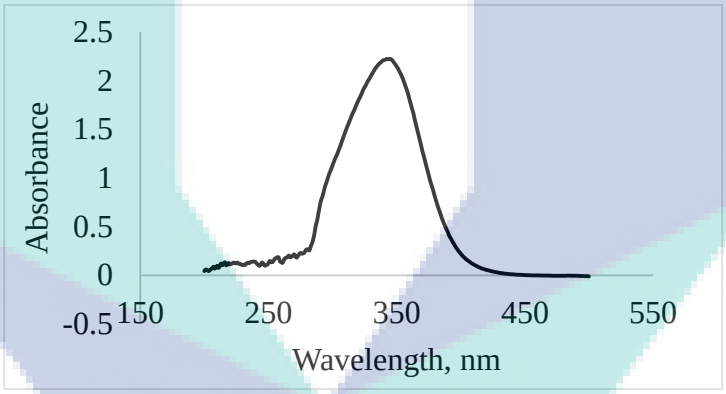

Figure 4.71 UV spectrum of (*E*)-3-(4-fluorophenyl)-1-(2'-hydroxy-4',6'-dimethoxyphenyl)prop-2-en-1-one (**46**)

IR spectrum of compound **46** is shown in Figure 4.72. The absorption bands at 3460 cm^{-1} and 1632 cm^{-1} represented the hydroxyl (O-H) and carbonyl (C=O) group, respectively. Absorption bands observed in a range of 2854-3118 cm^{-1} and 1345-1507 cm^{-1} corresponded to the aromatic carbon-proton (Ar C-H str.) and aromatic ring (C=C), respectively. Absorption bands produced in a range of 1115-1216 cm^{-1} and 1573-1592 cm^{-1} represented the (C-O) and (C=C-C=O) group, respectively (Boeck et al., 2006).

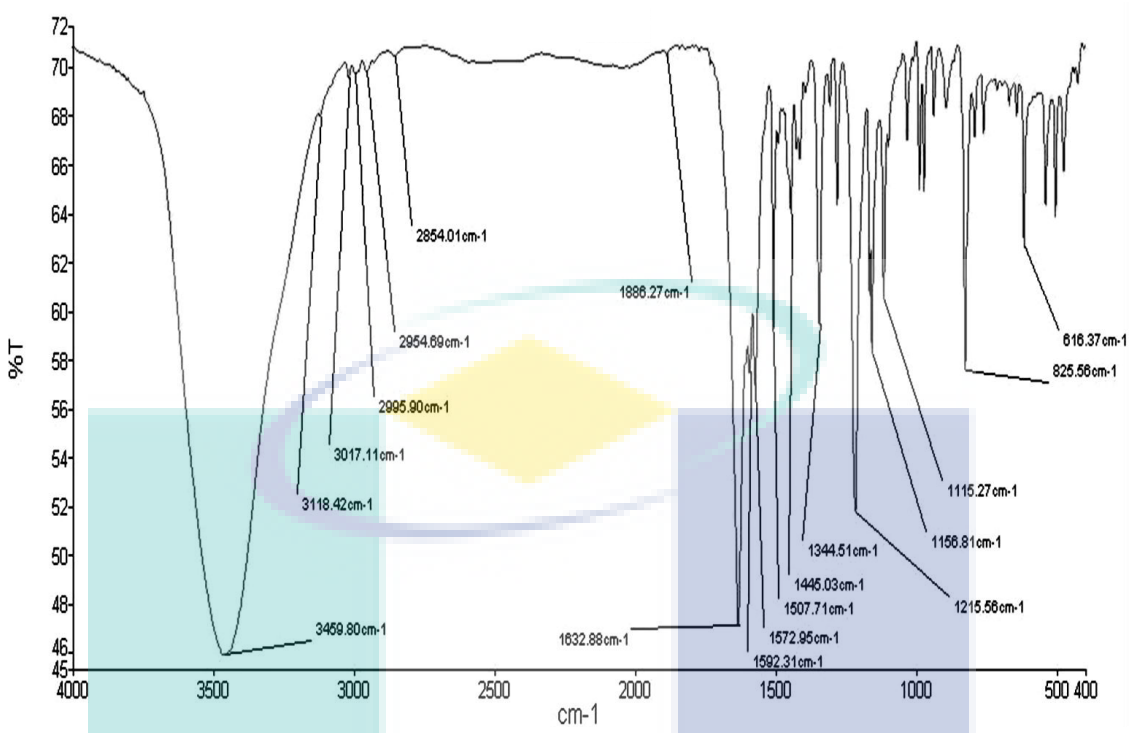

Figure 4.72 IR spectrum of (*E*)-3-(4-fluorophenyl)-1-(2'-hydroxy-4',6'-dimethoxyphenyl)prop-2-en-1-one (**46**)

^{1}H-NMR spectrum (600 MHz, $CDCl_3$) of compound **46** is shown in Figure 4.73 (Appendix A9). Doublets that appeared at δ 6.11 (d, *J* = 2.40 Hz) and 5.96 (d, *J* = 2.40 Hz) were assigned to the C-3' and C-5' proton, respectively. A multiplet elucidated at 7.09 was assigned to the C-3 and C-5 proton. A multiplet observed at 7.58 was assigned to the C-2 and C-6 proton. A doublet that appeared at 7.74 (d, *J* = 15.60 Hz) was assigned to the proton at α-carbon and doublet at 7.82 (d, *J* = 15.60 Hz) was assigned to the proton at β-carbon. A singlet produced at 3.84 (s, 3H) was assigned to the methoxy proton at C-4' and a singlet at 3.92 (s, 3H) was assigned to the methoxy proton at C-6'. A singlet that appeared at 14.28 represented the hydroxyl proton at C-2' due to chelation with carbonyl group (Boeck et al., 2006). The details of ^{1}H-NMR spectra is shown in Table 4.19.

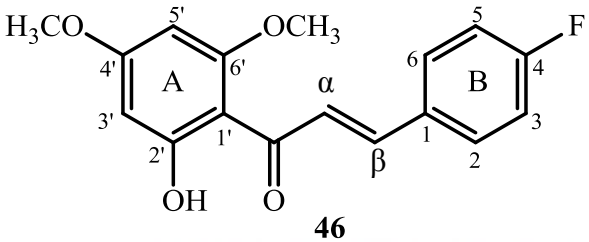

46

Figure 4.73 Structure of (*E*)-3-(4-fluorophenyl)-1-(2'-hydroxy-4',6'-dimethoxyphenyl)prop-2-en-1-one (**46**)

Table 4.19 NMR data of (*E*)-3-(4-fluorophenyl)-1-(2'-hydroxy-4',6'-dimethoxyphenyl)prop-2-en-1-one (**46**)

Carbon	^{1}H (δ)	Multiplicity	Designation
1'	-	-	-
2'	-	-	-
3'	6.11	(d, *J* = 2.40 Hz, 1H)	C3'-H
4'	-	-	-
5'	5.96	(d, *J* = 2.40 Hz, 1H)	C5'-H
6'	-	-	-
1	-	-	-
2	7.59	(m, 2H)	C2-H
3	7.10	(m, 2H)	C3-H
4	-	-	-
5	7.09	(m, 2H)	C5-H
6	7.58	(m, 2H)	C6-H
α	7.74	(d, *J* = 15.60 Hz, 1H, H-α)	Cα-H
β	7.82	(d, *J* = 15.60 Hz, 1H, H-β)	Cβ-H
OCH_3 (C4')	3.84	(s, 3H)	OCH_3 (C4')
OCH_3 (C6')	3.92	(s, 3H)	OCH_3 (C6')
OH (C2')	14.28	(s, 1H)	OH (C2')

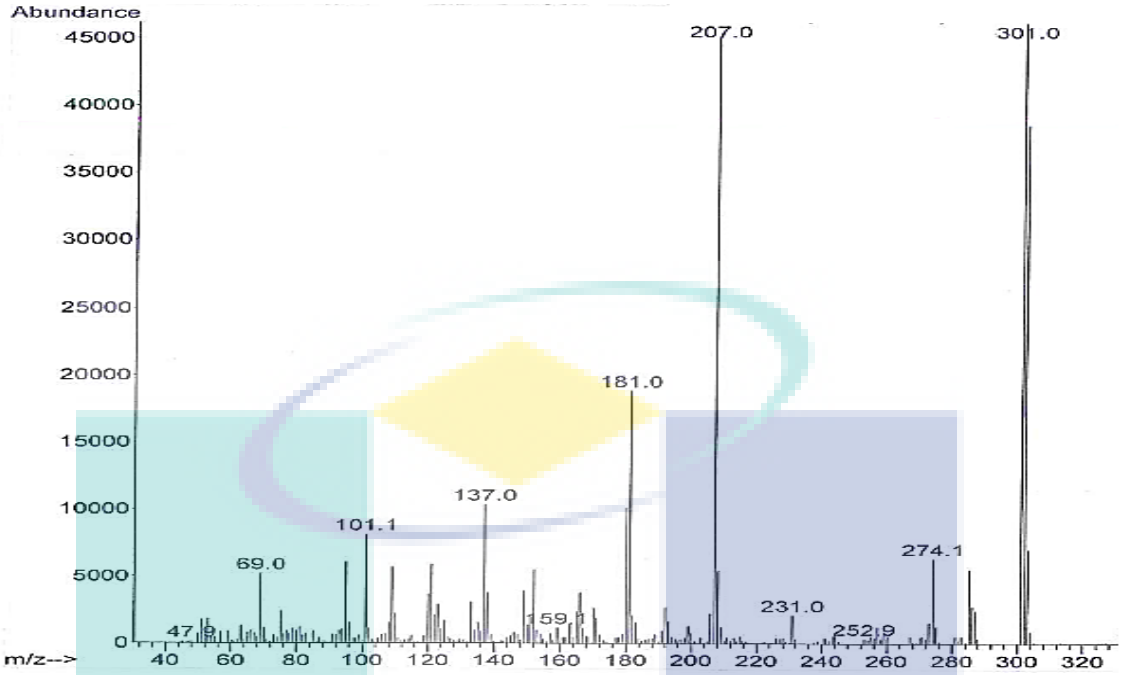

Figure 4.74 GC-MS spectra of (*E*)-3-(4-fluorophenyl)-1-(2'-hydroxy-4',6'-dimethoxyphenyl)prop-2-en-1-one (**46**)

GC-MS spectrum of compound **46** shown in Figure 4.74 displays the main fragment ions of a molecular structure at *m/z* = 302, 301, 285, 274, 207, 181, 153, 137, 121, 101 and 69. The result obtained from this analysis supports the tentative of synthesized compound **46**.

4.1.18 (*E*)-1-(2'-hydroxy-4',6'-dimethoxyphenyl)-3-(p-tolyl)prop-2-en-1-one (88)

Flavokawain B derivative, (*E*)-1-(2'-hydroxy-4',6'-dimethoxyphenyl)-3-(p-tolyl)prop-2-en-1-one (**88**) was synthesized via Claisen-Schmidt condensation of 2'-hydroxy-4',6'-dimethoxyacetophenone (1.00 mmol) and p-tolualdehyde (1.00 mmol) diluted in 5 mL MeOH, catalyzed by 40% KOH and stirred at room temperature for 55 hr as described in page 38. The product was obtained in a form of orange crystal with a yield of 84.6% and melting point in a range of 126-128°C (Boeck et al., 2006).

Compound **88** absorbed UV light in the wavelength range of 290-400 nm, which corresponded to the conjugated α,β-unsaturated carbonyl (C=O) chromophore. The UV-Visible spectrum of compound **88** shown in Figure 4.75 shows that the maximum absorption occurred at a wavelength, λ_{max}, of 349 nm.

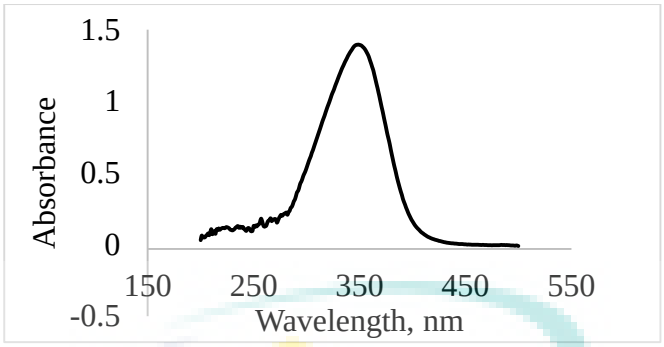

Figure 4.75 UV spectrum of (*E*)-1-(2'-hydroxy-4',6'-dimethoxyphenyl)-3-(p-tolyl)prop-2-en-1-one (**88**)

IR spectrum of compound **88** is shown in Figure 4.76. The absorption bands observed at 3453 cm^{-1} and 1624 cm^{-1} corresponded to the hydroxyl (O-H) and carbonyl (C=O) group, respectively. Absorption bands produced in a range of 1435-1437 cm^{-1} and 2916-2994 cm^{-1} represented the aromatic ring (C=C) and aromatic proton (Ar C-H), respectively. Absorption bands which appeared in a range of 1218-1220 cm^{-1} and 1558-1560 cm^{-1} were assigned to (C-O) and (C=C-C=O), respectively (Boeck et al., 2006).

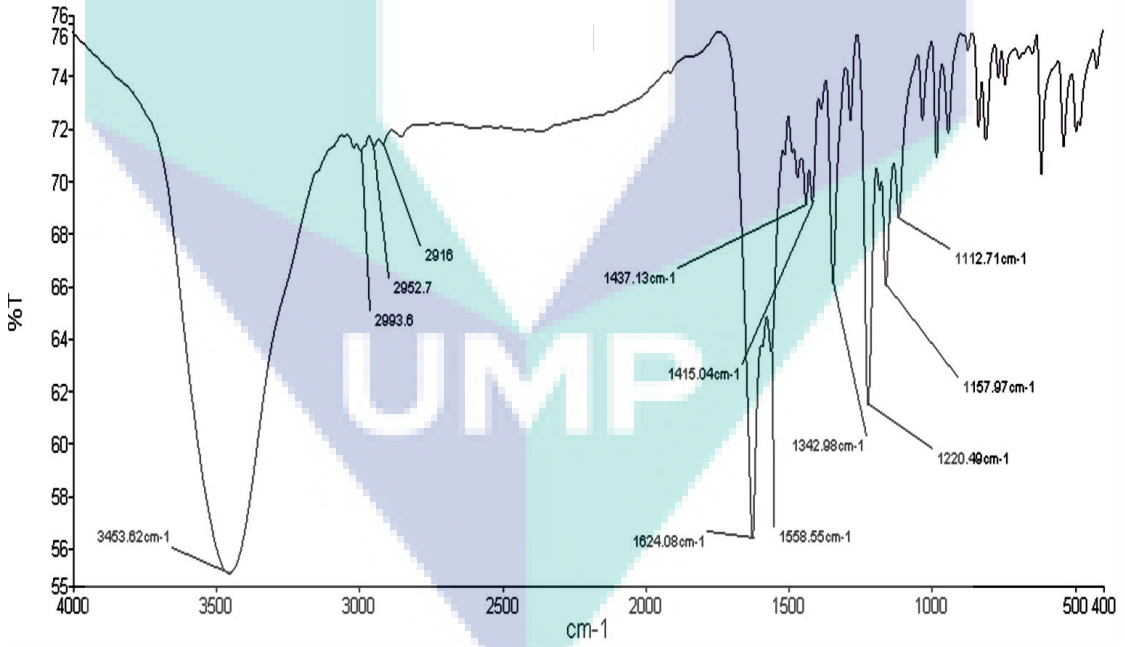

Figure 4.76 IR spectrum of (*E*)-1-(2'-hydroxy-4',6'-dimethoxyphenyl)-3-(p-tolyl)prop-2-en-1-one (**88**)

^{1}H-NMR spectrum (500 MHz, $CDCl_3$) of compound **88** is shown in Figure 4.77 (Appendix A9). Doublet at δ 6.11 (d, *J* = 2.35 Hz) was assigned to the C-3' proton and doublet at 5.96 (d, *J* = 2.40 Hz) was assigned to the C-5' proton. Two doublets

elucidated at 7.22 (d, *J* = 8.00 Hz) and 7.21 (d, *J* = 8.00 Hz) were assigned to the C-3 and C-5 proton, respectively. Two doublets observed at 7.52 (d, *J* = 8.10 Hz) and 7.50 (d, *J* = 8.10 Hz) were assigned to the C-2 and C-6 proton, respectively. A doublet that appeared at 7.77 (d, *J* = 15.60 Hz) was assigned to the proton at α-carbon and a doublet at 7.82 (d, *J* = 15.60 Hz) was assigned to the proton at β-carbon. A singlet at 3.84 (s, 3H) was assigned to the methoxy proton at C-4' and a singlet at 3.92 (s, 3H) was assigned to the methoxy proton at C-6'. A singlet elucidated at 2.39 (s, 3H) represented the methyl proton at C-4 (Boeck et al., 2006). The details of ^{1}H-NMR spectra is shown in Table 4.20.

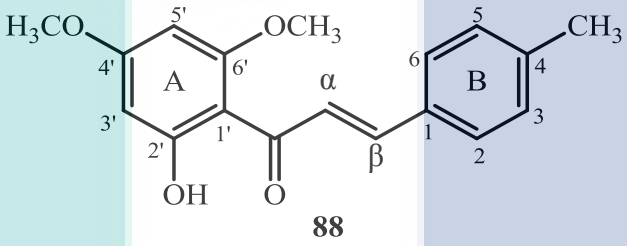

88

Figure 4.77 Structure of (*E*)-1-(2'-hydroxy-4',6'-dimethoxyphenyl)-3-(p-tolyl)prop-2-en-1-one (**88**)

Table 4.20 NMR data of (*E*)-1-(2'-hydroxy-4',6'-dimethoxyphenyl)-3-(p-tolyl)prop-2-en-1-one (**88**)

Carbon	^{13}C (δ)	^{1}H (δ)	Multiplicity	Designation
1'	106.35	-	-	-
2'	168.39	-	-	-
3'	93.77	6.11	(d, *J* = 2.35 Hz, 1H)	C3'-H
4'	166.14	-	-	-
5'	91.26	5.96	(d, *J* = 2.40 Hz, 1H)	C5'-H
6'	162.50	-	-	-
1	126.49	-	-	-
2	129.65	7.52	(d, *J* = 8.10 Hz, 1H)	C2-H
3	128.42	7.22	(d, *J* = 8.00 Hz, 1H)	C3-H
4	140.58	-	-	-
5	128.42	7.21	(d, *J* = 8.00 Hz, 1H)	C5-H
6	129.65	7.50	(d, *J* = 8.10 Hz, 1H)	C6-H
α	132.81	7.77	(d, *J* = 15.60 Hz, 1H, H-α)	Cα-H
β	142.58	7.86	(d, *J* = 15.60 Hz, 1H, H-β)	Cβ-H
OCH_3 (C4')	55.87	3.84	(s, 3H)	OCH_3 (C4')
OCH_3 (C6')	55.62	3.92	(s, 3H)	OCH_3 (C6')
OH (C2')	-	-	(s, 1H)	OH (C2')
CH_3 (C4)	21.56	2.39	(s, 3H)	CH_3 (C4)
C=O	192.73	-	-	-

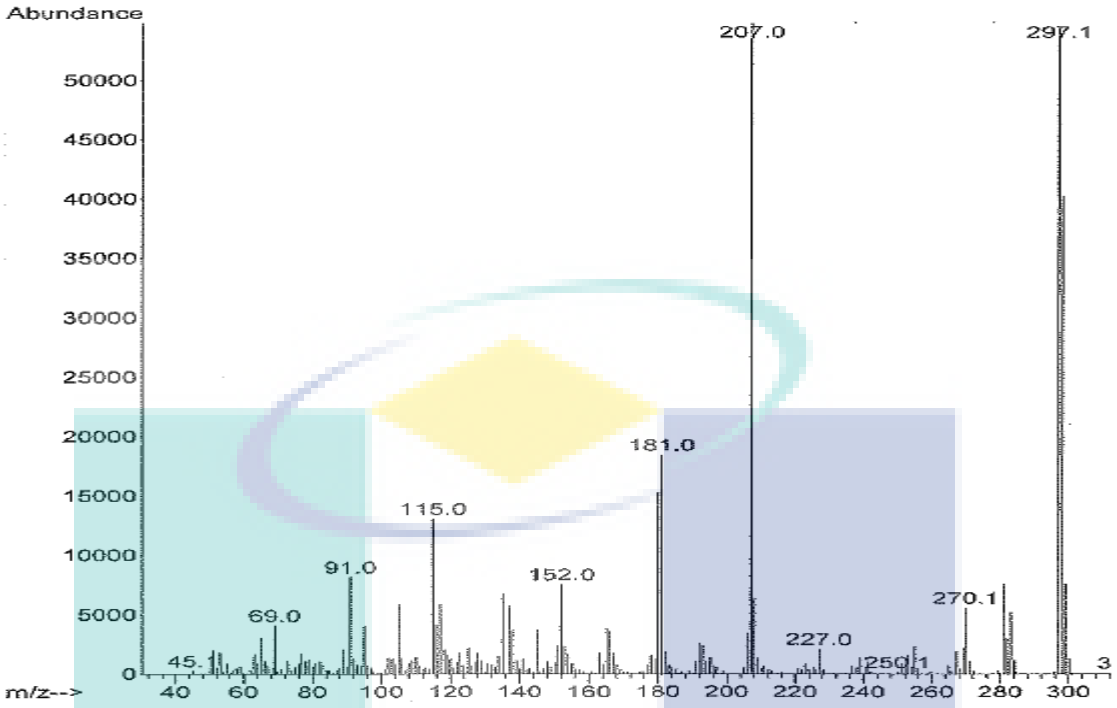

Figure 4.78 GC-MS spectrum of (*E*)-1-(2'-hydroxy-4',6'-dimethoxyphenyl)-3-(p-tolyl)prop-2-en-1-one (**88**)

GC-MS spectrum of compound **88** shown in Figure 4.78 displays the main fragment ions of a molecular structure at *m/z* = 298, 297, 282, 270, 207, 181, 152, 136, 115, 105, 91 and 69. The result obtained from this analysis support the tentative of synthesized compound **88**.

4.1.19 (*E*)-3-(4-hydroxy-3-methoxyphenyl)-1-(2'-hydroxy-4',6'-dimethoxyphenyl)prop-2-en-1-one (89)

Flavokawain B derivative, (*E*)-3-(4-hydroxy-3-methoxyphenyl)-1-(2'-hydroxy-4',6'-dimethoxyphenyl)prop-2-en-1-one (**89**) was synthesized by using method as described in page 39 and the product of acetylation (1.00 mmol) was then used in Claisen-Schmidt condensation method for a reaction with 2'-hydroxy-4',6'-dimethoxyacetophenone (1.00 mmol) after diluted in 5 mL MeOH, catalyzed by 40% KOH and stirred at room temperature for 48 hr as described in page 38. The product was obtained in a form of yellow solid particle with a yield of 72.2%.

Compound **89** absorbed UV light in the wavelength range of 300-420 nm, which corresponded to the conjugated α,β-unsaturated carbonyl (C=O) chromophore. The UV spectrum of compound **89** shown in Figure 4.79 shows that the maximum absorption occurred at wavelength, λ_{max}, in a range of 371-373 nm.

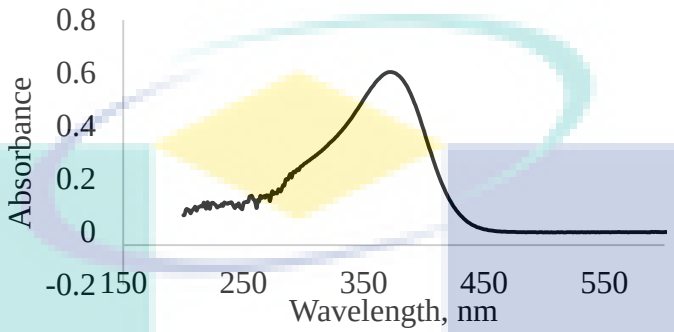

Figure 4.79 UV spectrum of (*E*)-3-(4-hydroxy-3-methoxyphenyl)-1-(2'-hydroxy-4',6'-dimethoxyphenyl)prop-2-en-1-one (**89**)

IR spectrum of compound **89** is shown in Figure 4.80. The absorption bands observed at 3415 cm^{-1} and 1624 cm^{-1} corresponded to the hydroxyl (O-H) and carbonyl (C=O) group, respectively. Absorption bands elucidated in a range of 1429-1554 cm^{-1} and 2925-2927 cm^{-1} represented the aromatic ring (C=C) and aromatic proton (Ar C-H), respectively. Absorption bands produced in a range of 2837-2838 cm^{-1} and 1162-1270 cm^{-1} corresponded to the alkane (C-H) and (C-O), respectively (Srinivasarao et al., 2013).

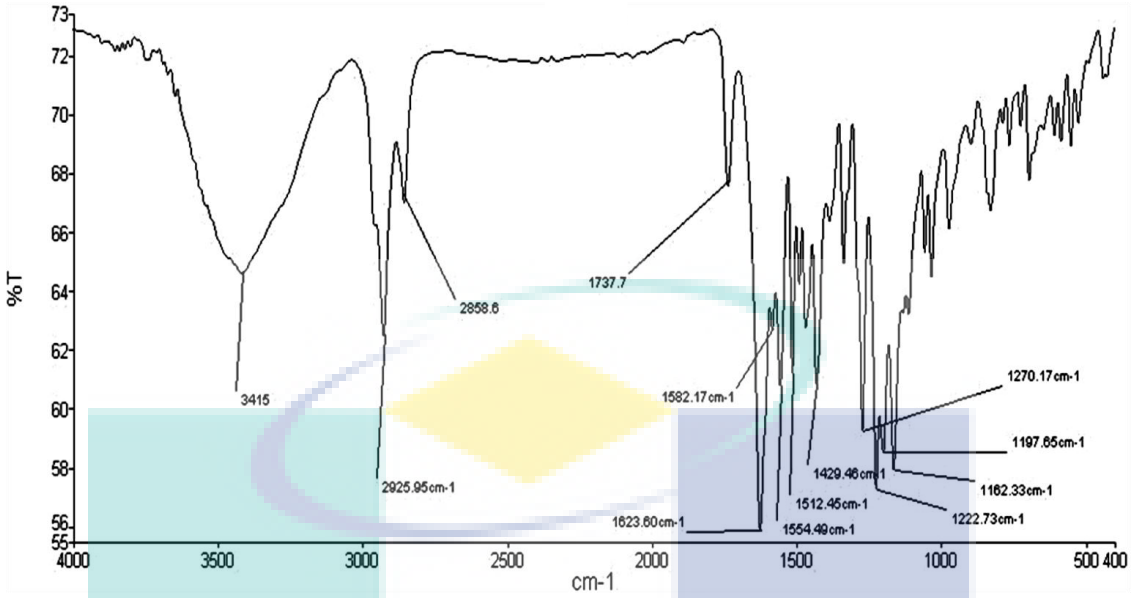

Figure 4.80 IR spectrum of (*E*)-3-(4-hydroxy-3-methoxyphenyl)-1-(2'-hydroxy-4',6'-dimethoxyphenyl)prop-2-en-1-one (**89**)

^{1}H-NMR spectrum (500 MHz, $CDCl_3$) of compound **89** is shown in Figure 4.81 (Appendix A10). Two doublets at δ 6.11 (d, *J* = 2.35 Hz) and 5.96 (d, *J* = 2.40 Hz) were assigned to the C-3' proton and C-5' proton, respectively. A doublet that appeared at 6.95 (d, *J* = 8.20 Hz) was assigned to the proton at C-5. A doublet elucidated at 7.08 (d, *J* = 1.80 Hz) represented the C-2 proton interacted with C-6 proton at meta-position. A doublet of doublet that appeared at 7.21 (dd, *J* = 1.85 Hz, 8.25 Hz) was assigned to the proton at C-6. A doublet observed at 7.75 (d *J* = 15.50 Hz) was assigned to the proton at α-carbon and a doublet at 7.8 (d, *J* = 15.50 Hz) was assigned to the proton at β-carbon. A singlet which appeared at 3.84 (s, 3H) was assigned to the methoxy proton at C-4'; a singlet at 3.95 (s, 3H) corresponded to the methoxy proton at C-3 and another singlet observed at 3.92 (s, 3H) was assigned to the methoxy proton at C-6' (Srinivasarao et al., 2013). The details of ^{1}H-NMR spectra is shown in Table 4.21.

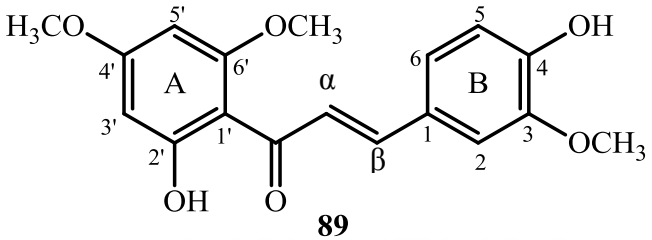

89

Figure 4.81 Structure of (*E*)-3-(4-hydroxy-3-methoxyphenyl)-1-(2'-hydroxy-4',6'-dimethoxyphenyl)prop-2-en-1-one (**89**)

Table 4.21 NMR data of (*E*)-3-(4-hydroxy-3-methoxyphenyl)-1-(2'-hydroxy-4',6'-dimethoxyphenyl)prop-2-en-1-one (**89**)

Carbon	^{1}H (δ)	Multiplicity	Designation
1'	-	-	-
2'	-	-	-
3'	6.11	(d, *J* = 2.35 Hz, 1H)	C3'-H
4'	-	-	-
5'	5.96	(d, *J* = 2.40 Hz, 1H)	C5'-H
6'	-	-	-
1	-	-	-
2	7.08	(d, *J* = 1.80 Hz, 1H)	C2-H
3	-	-	-
4	-	-	-
5	6.95	(d, *J* = 8.20 Hz, 1H)	C5-H
6	7.21	(dd, *J* = 1.85 Hz, 8.25 Hz, 1H)	C6-H
α	7.75	(d, *J* = 15.50 Hz, 1H, H-α)	Cα-H
β	7.80	(d, *J* = 15.50 Hz, 1H, H-β)	Cβ-H
OCH_3 (C4')	3.84	(s, 3H)	OCH_3 (C4')
OCH_3 (C6')	3.92	(s, 3H)	OCH_3 (C6')
OCH_3 (C3)	3.95	(s, 3H)	OCH_3 (C3)
OH (C2')	-	(s, 1H)	OH (C2')

4.1.20 (*E*)-3-(4-(dimethylamino)phenyl)-1-(2'-hydroxy-4',6'-dimethoxyphenyl)prop-2-en-1-one (2)

Flavokawain B derivative, (*E*)-3-(4-(dimethylamino)phenyl)-1-(2'-hydroxy-4',6'-dimethoxyphenyl)prop-2-en-1-one (**2**) was synthesized via Claisen-Schmidt condensation of 2'-hydroxy-4',6'-dimethoxyacetophenone (1.00 mmol) and 4-(dimethylamino)benzaldehyde (1.00 mmol) diluted in 5 mL MeOH, catalyzed by 40% KOH and stirred at room temperature for 48 hr as described in page 38. The product was obtained in a form of bluish-orange crystal with a yield of 89.7%.

Compound **2** absorbed UV light in the wavelength range of 370-480 nm, which corresponded to the conjugated α,β-unsaturated carbonyl (C=O) chromophore. The UV-Visible spectrum of compound **2** shown in Figure 4.82 shows that the maximum absorption occurred at wavelength, λ_{max}, in a range of 428-430 nm.

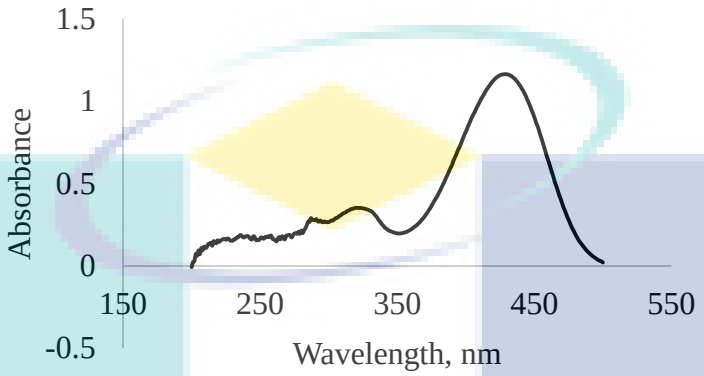

Figure 4.82 UV spectrum of (*E*)-3-(4-(dimethylamino)phenyl)-1-(2'-hydroxy-4',6'-dimethoxyphenyl)prop-2-en-1-one (**2**)

IR spectrum of compound **2** is shown in Figure 4.83. The absorption bands observed at 3435 cm^{-1} and 1627 cm^{-1} corresponded to the hydroxyl (O-H) and carbonyl (C=O) group, respectively. Absorption bands elucidated in a range of 1439-1530 cm^{-1} and 2854-2924 cm^{-1} represented the aromatic ring (C=C) and aromatic proton (Ar C-H), respectively. Absorption bands produced in a range of 1154-1214 cm^{-1} and 1345-1347 cm^{-1} indicated the presence of (C-O) and tertiary amine (C-N), respectively (Mandge. et al., 2007; Syam. et al., 2012).

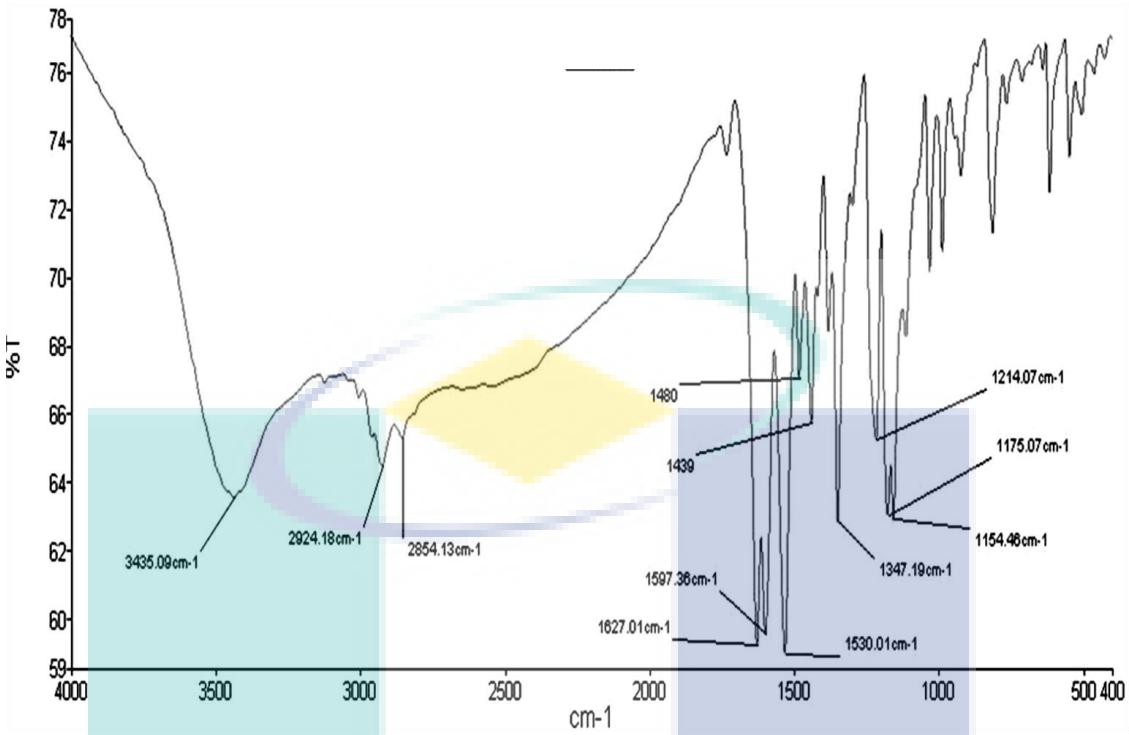

Figure 4.83 IR spectrum of (*E*)-3-(4-(dimethylamino)phenyl)-1-(2'-hydroxy-4',6'-dimethoxyphenyl)prop-2-en-1-one (**2**)

^{1}H-NMR spectrum (500 MHz, $CDCl_3$) of compound **2** is shown in Figure 4.84 (Appendix A10). Two doublets at δ 6.10 (d, *J* = 2.40 Hz) and 5.95 (d, *J* = 2.40 Hz) were assigned to the C-3' proton and C-5' proton, respectively. Two doublets that appeared at 7.53 (d, *J* = 8.75 Hz) and 7.51 (d, *J* = 8.75 Hz) were assigned to the C-2 and C-6 proton, respectively. Two doublets observed at 6.70 (d, *J* = 8.90 Hz) and 6.68 (d, *J* = 8.90 Hz) were assigned to the C-3 and C-5 proton, respectively. A singlet produced at 3.04 (s, 6H) was assigned to the proton of two methyl attached to nitrogen group, referred to dimethylamino substitute at C-4. A singlet that appeared at 3.83 (s, 3H) was assigned to the methoxy proton at C-4' and a singlet at 3.91 (s, 3H) was assigned to the methoxy proton at C-6'. A doublet that appeared at 7.75 (d, *J* = 15.40 Hz) was assigned to the proton at α-carbon and a doublet elucidated at 7.83 (d, *J* = 15.40 Hz) was assigned to the proton at β-carbon. The details of ^{1}H-NMR spectra is shown in Table 4.22.

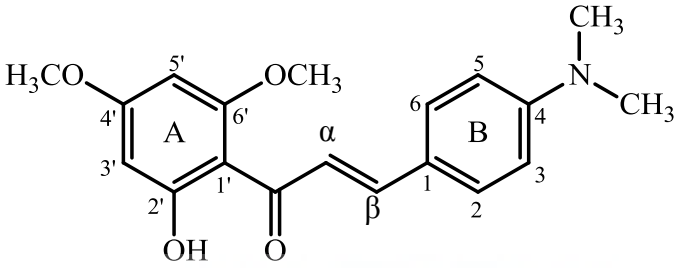

2

Figure 4.84 Structure of (*E*)-3-(4-(dimethylamino)phenyl)-1-(2'-hydroxy-4',6'-dimethoxyphenyl)prop-2-en-1-one (**2**)

Table 4.22 NMR data of (*E*)-3-(4-(dimethylamino)phenyl)-1-(2'-hydroxy-4',6'-dimethoxyphenyl)prop-2-en-1-one (**2**)

Carbon	**^{1}H (δ)**	**Multiplicity**	**Designation**
1'	-	-	-
2'	-	-	-
3'	6.10	(d, *J* = 2.40 Hz, 1H)	C3'-H
4'	-	-	-
5'	5.95	(d, *J* = 2.40 Hz, 1H)	C5'-H
6'	-	-	-
1	-	-	-
2	7.53	(d, *J* = 8.75 Hz, 1H)	C2-H
3	6.70	(d, *J* = 8.90 Hz, 1H)	C3-H
4			
5	6.68	(d, *J* = 8.90 Hz, 1H)	C5-H
6	7.51	(d, *J* = 8.75 Hz, 1H)	C6-H
α	7.75	(d, *J* = 15.40 Hz, 1H, H-α)	Cα-H
β	7.83	(d, *J* = 15.40 Hz, 1H, H-β)	Cβ-H
OCH_3 (C4')	3.83	(s, 3H)	OCH_3 (C4')
OCH_3 (C6')	3.91	(s, 3H)	OCH_3 (C6')
OH (C2')	-	(s, 1H)	OH (C2')
CH_3 (C4)	3.04	(s, 6H)	$(CH_3)_2$-N (C4)

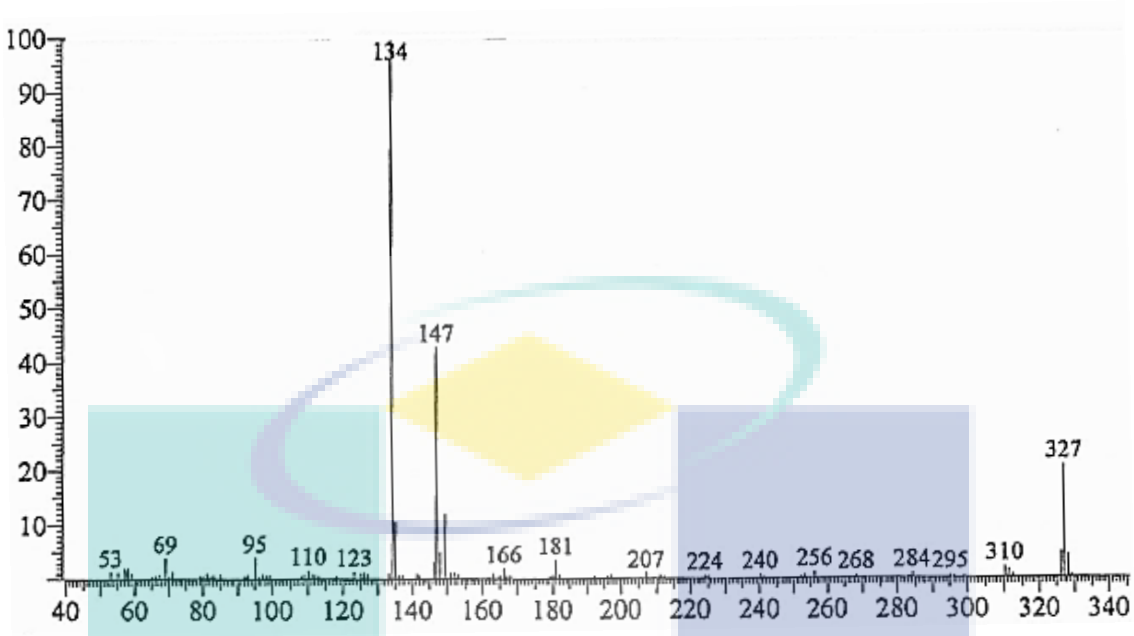

Figure 4.85 GC-MS spectrum of (*E*)-3-(4-(dimethylamino)phenyl)-1-(2'-hydroxy-4',6'-dimethoxyphenyl)prop-2-en-1-one (**2**)

GC-MS spectrum of compound **2** shown in Figure 4.85 displays the main fragment ions of a molecular structure at *m/z* = 327, 310, 283, 207, 181 and 147. The result obtained from this supports the tentative of synthesized compound **2**.

4.1.21 (*E*)-3-(5-bromo-2-hydroxyphenyl)-1-(2'-hydroxy-4',6'-dimethoxyphenyl)prop-2-en-1-one (90)

Flavokawain B derivative, (*E*)-3-(5-bromo-2-hydroxyphenyl)-1-(2'-hydroxy-4',6'-dimethoxyphenyl)prop-2-en-1-one (**90**) was synthesized via Claisen-Schmidt condensation of 2'-hydroxy-4',6'-dimethoxyacetophenone (1.00 mmol) and 5-bromosalicylaldehyde (1.00 mmol) diluted in 5 mL MeOH, catalyzed by 40% KOH and stirred at room temperature for 72 hr as described in page 38. The product was obtained in a form of yellow crystal with a yield of 76.2% and melting point in a range of 166-168°C (Srinivasarao et al., 2013).

Compound **90** absorbed UV light in the wavelength range of 300-400 nm, which corresponded to the conjugated α,β-unsaturated carbonyl (C=O) chromophore. The UV spectrum of compound **90** shown in Figure 4.86 shows that the maximum absorption occurred at a wavelength, λ_{max}, of 359 nm.

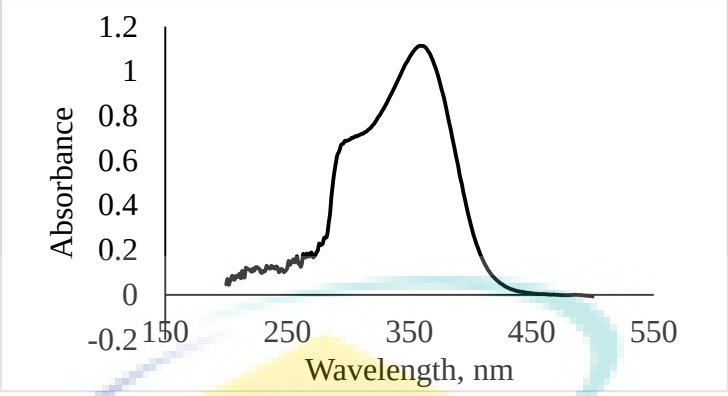

Figure 4.86 UV spectrum of (*E*)-3-(5-bromo-2-hydroxyphenyl)-1-(2'-hydroxy-4',6'-dimethoxyphenyl)prop-2-en-1-one (**90**)

IR spectrum of compound **90** is shown in Figure 4.87. The absorption bands observed at 3435 cm^{-1} and 1623 cm^{-1} corresponded to the hydroxyl (O-H) and carbonyl (C=O) group, respectively. Absorption band observed in a range of 1419-1590 cm^{-1} and 2945-2994 cm^{-1} represented the aromatic ring (C=C) and aromatic proton (Ar C-H), respectively. Absorption bands that appeared in a range of 1220-1221 cm^{-1} was referred to (C-O).

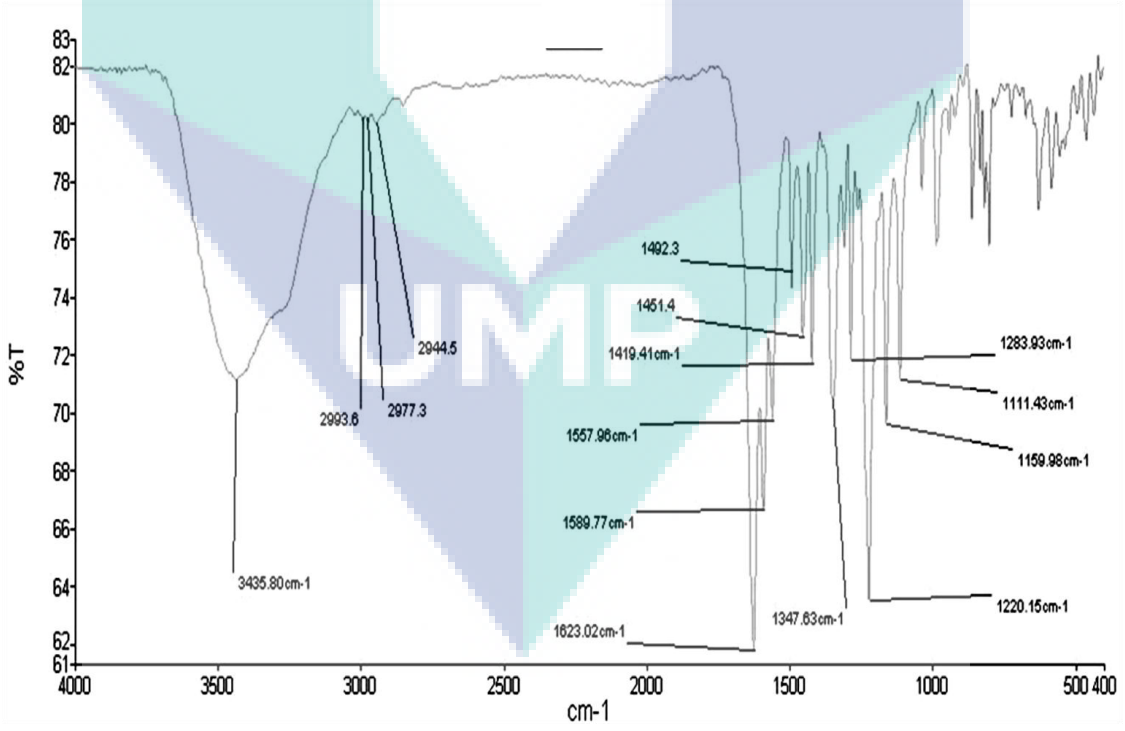

Figure 4.87 IR spectrum (*E*)-3-(5-bromo-2-hydroxyphenyl)-1-(2'-hydroxy-4',6'-dimethoxyphenyl)prop-2-en-1-one (**90**)

^{1}H-NMR spectrum (600 MHz, acetone) of compound **90** is shown in Figure 4.88 (Appendix A11). Two singlets at δ 3.88 and 3.98 were assigned to the methoxy proton at C-4' and C-6', respectively. Two broad singlets that appeared at 6.13 (brs, 1H) and 6.12 (brs, 1H) were assigned to the C-3' proton and C-5' proton, respectively. A doublet elucidated at 6.97 (d, *J* = 8.64 Hz) was assigned to the C-3 proton and a doublet at 7.39 (d, *J* = 8.70 Hz) was assigned to the C-4 proton. A broad singlet observed at 7.78 (brs, 1H) was assigned to the C-6 proton. A doublet that appeared at 8.01 (d, *J* = 15.70 Hz) was assigned to the proton at α-carbon proton and another doublet appeared at 8.12 (d, *J* = 15.70 Hz) was assigned to the proton at β-carbon. A singlet produced at 14.19 represented the hydroxyl proton at C-2', chelated to carbonyl group. The details of ^{1}H-NMR spectra is shown in Table 4.23.

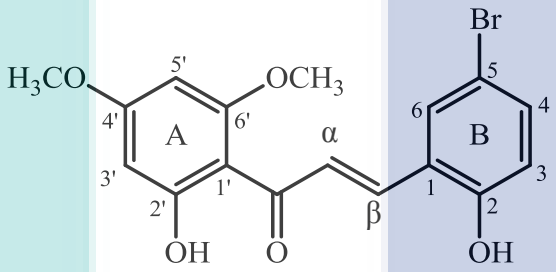

90

Figure 4.88 Structure of (*E*)-3-(5-bromo-2-hydroxyphenyl)-1-(2'-hydroxy-4',6'-dimethoxyphenyl)prop-2-en-1-one (**90**)

Table 4.23 NMR data of (*E*)-3-(5-bromo-2-hydroxyphenyl)-1-(2'-hydroxy-4',6'-dimethoxyphenyl)prop-2-en-1-one (**90**)

Carbon	^{1}H (δ)	Multiplicity	Designation
1'	-	-	-
2'	-	-	-
3'	6.13	(brs, 1H)	C3'-H
4'	-	-	-
5'	6.12	(brs, 1H)	C5'-H
6'	-	-	-
1	-	-	-
2	-	-	-
3	6.97	(d, *J* = 8.64 Hz, 1H)	C3-H
4	7.39	(d, *J* = 8.70 Hz, 1H)	C4-H
5	-	-	-
6	7.78	(brs, 1H)	C6-H
α	8.01	(d, *J* = 15.70 Hz, 1H, H-α)	Cα-H
β	8.12	(d, *J* = 15.70 Hz, 1H, H-β)	Cβ-H
OCH_3 (C4')	3.88	(s, 3H)	OCH_3 (C4')
OCH_3 (C6')	3.98	(s, 3H)	OCH_3 (C6')
OH (C2')	14.19	(s, 1H)	OH (C2')

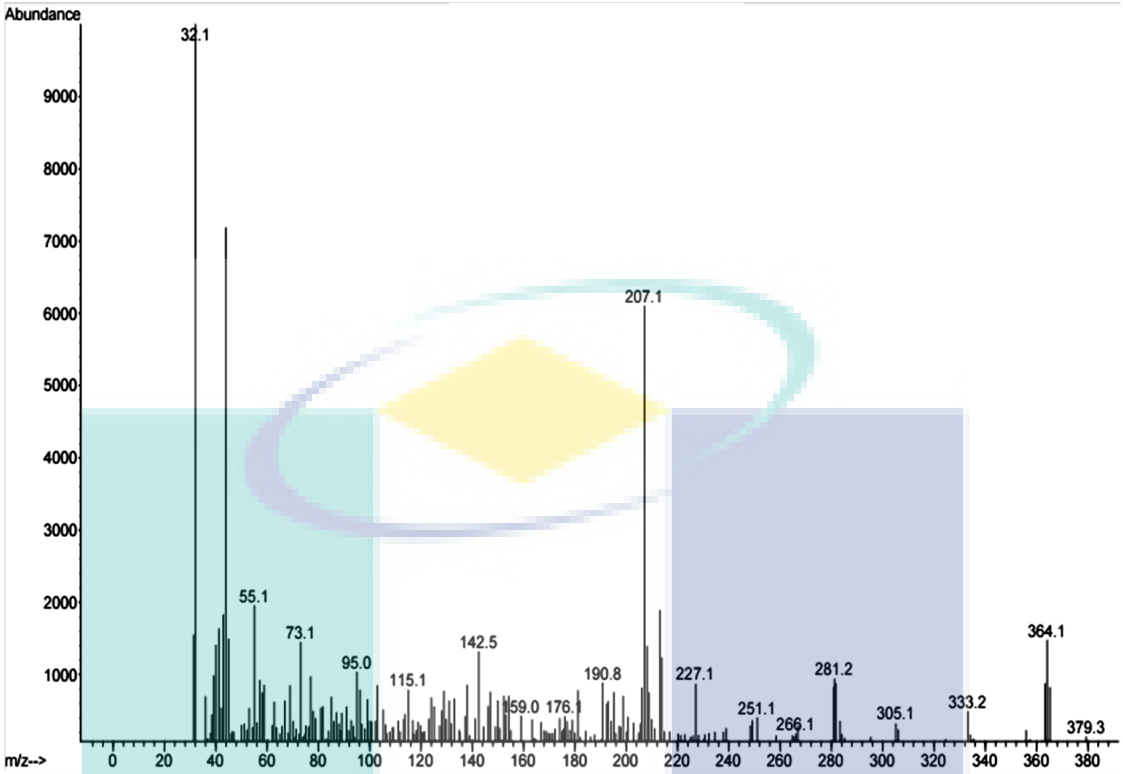

Figure 4.89 GC-MS spectrum of (*E*)-3-(5-bromo-2-hydroxyphenyl)-1-(2'-hydroxy-4',6'-dimethoxyphenyl)prop-2-en-1-one (**90**)

GC-MS spectrum of compound **90** shown in Figure 4.89 displays the main fragment ions of a molecular structure at *m/z* = 379, 364, 333, 305, 281, 251, 227, 214, 207, 191, 142, 115, 95 and 73. The result obtained from this analysis could supports the tentative of synthesized compound **90**.

4.1.22 (*E*)-3-(2-bromo-3-hydroxy-4-methoxyphenyl)-1-(2'-hydroxy-4',6'-dimethoxyphenyl)prop-2-en-1-one (91)

Flavokawain B derivative, (*E*)-3-(2-bromo-3-hydroxy-4-methoxyphenyl)-1-(2'-hydroxy-4',6'-dimethoxyphenyl)prop-2-en-1-one (**91**) was synthesized via Claisen-Schmidt condensation of 2'-hydroxy-4',6'-dimethoxyacetophenone (1.00 mmol) and 2-bromo-3-hydroxy-4-methoxybenzaldehyde (1.00 mmol) diluted in 5 mL MeOH, catalyzed by 40% KOH and stirred at room temperature for 72 hr as described in page 38. The product was obtained in a form of orange crystal with a yield of 85.6% and melting point in a range of 201-203°C.

Compound **91** absorbed UV light in the wavelength range of 300-415 nm, which corresponded to the conjugated α,β-unsaturated carbonyl (C=O) chromophore. The UV-Visible spectrum of compound **91** shown in Figure 4.90 shows that the maximum absorption occurred at wavelength, λ_{max}, in a range of 366-369 nm.

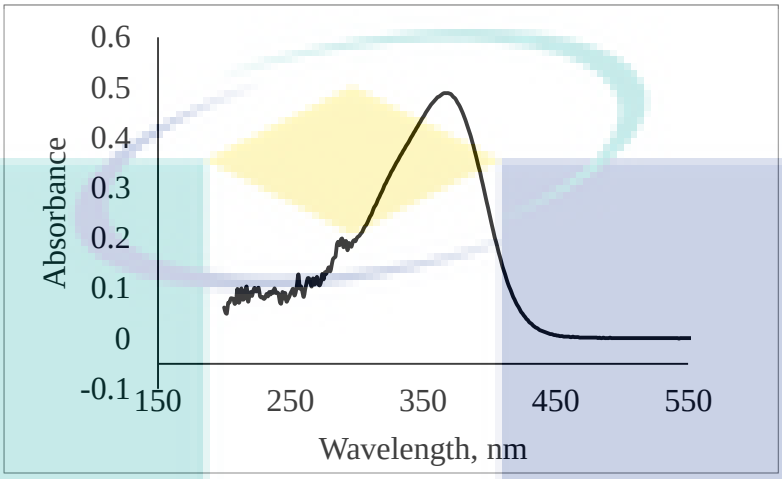

Figure 4.90 UV spectrum of (*E*)-3-(2-bromo-3-hydroxy-4-methoxyphenyl)-1-(2'-hydroxy-4',6'-dimethoxyphenyl)prop-2-en-1-one (**91**)

IR spectrum of compound **91** is shown in Figure 4.91. The absorption bands observed at 3425 cm^{-1} and 1634 cm^{-1} represented the hydroxyl (O-H) and carbonyl (C=O) group, respectively. Absorption bands produced in a range of 1496-1596 cm^{-1} and 2838-3014 cm^{-1} corresponded to the aromatic ring (C=C) and aromatic proton (Ar C-H), respectively. Absorption band that appeared in a range of 1213-1259 cm^{-1} corresponded to (C-O).

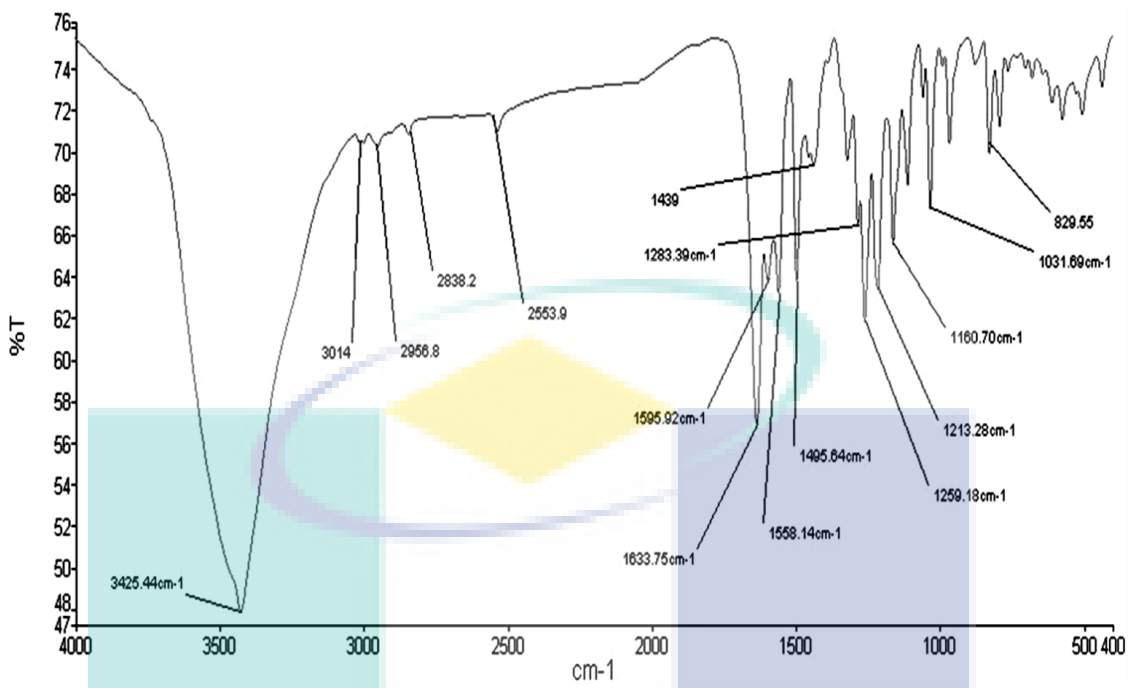

Figure 4.91 IR spectrum of (*E*)-3-(2-bromo-3-hydroxy-4-methoxyphenyl)-1-(2'-hydroxy-4',6'-dimethoxyphenyl)prop-2-en-1-one (**91**)

^{1}H-NMR spectrum (500 MHz, $CDCl_3$) of compound **91** is shown in Figure 4.92 (Appendix A11). The signal of singlet produced at δ 3.75 was assigned to the methoxy proton at C-4'; a singlet that appeared at 3.85 was assigned to the methoxy proton at C-6'; a singlet at 3.81 was assigned to the methoxy proton at C-4. A doublet elucidated at 5.88 (d, *J* = 2.35 Hz) represented the C-5' proton and a doublet appeared at 6.00 (d, *J* = 2.50 Hz) was assigned to the C-3' proton. A doublet that appeared at 6.78 (d, *J* = 8.55 Hz) was assigned to the C-5 proton and a doublet at 7.20 (d, *J* = 8.60 Hz) was assigned to the C-6 proton. A doublet observed at 7.67 (d, *J* = 15.45 Hz) was assigned to the proton at α-carbon and another doublet elucidated at 8.02 (d, *J* = 15.40 Hz) was assigned to the proton at β-carbon. The details of ^{1}H-NMR spectra is shown in Table 4.24.

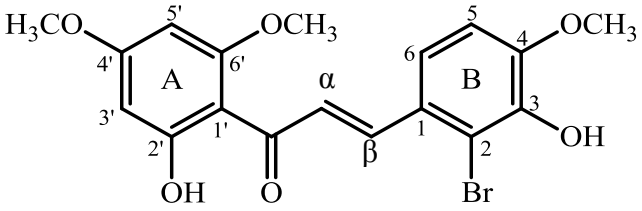

91

Figure 4.92 Structure of (*E*)-3-(2-bromo-3-hydroxy-4-methoxyphenyl)-1-(2'-hydroxy-4',6'-dimethoxyphenyl)prop-2-en-1-one (**91**)

Table 4.24 NMR data of (*E*)-3-(2-bromo-3-hydroxy-4-methoxyphenyl)-1-(2'-hydroxy-4',6'-dimethoxyphenyl)prop-2-en-1-one (**91**)

Carbon	^{1}H (δ)	Multiplicity	Designation
1'	-	-	-
2'	-	-	-
3'	6.00	(d, *J* = 2.50 Hz, 1H)	C3'-H
4'	-	-	-
5'	5.88	(d, *J* = 2.35 Hz, 1H)	C5'-H
6'	-	-	-
1	-	-	-
2	-	-	-
3	-	-	-
4	-	-	-
5	6.78	(d, *J* = 8.55 Hz, 1H)	C5-H
6	7.20	(d, *J* = 8.60 Hz, 1H)	C6-H
α	7.67	(d, *J* = 15.45 Hz, 1H, H-α)	Cα-H
β	8.02	(d, *J* = 15.40 Hz, 1H, H-β)	Cβ-H
OCH_3 (C4')	3.75	(s, 3H)	OCH_3 (C4')
OCH_3 (C6')	3.85	(s, 3H)	OCH_3 (C6')
OCH_3 (C4)	3.81	(s, 3H)	OCH_3 (C4)
OH (C2')	-	(s, 1H)	OH (C2')

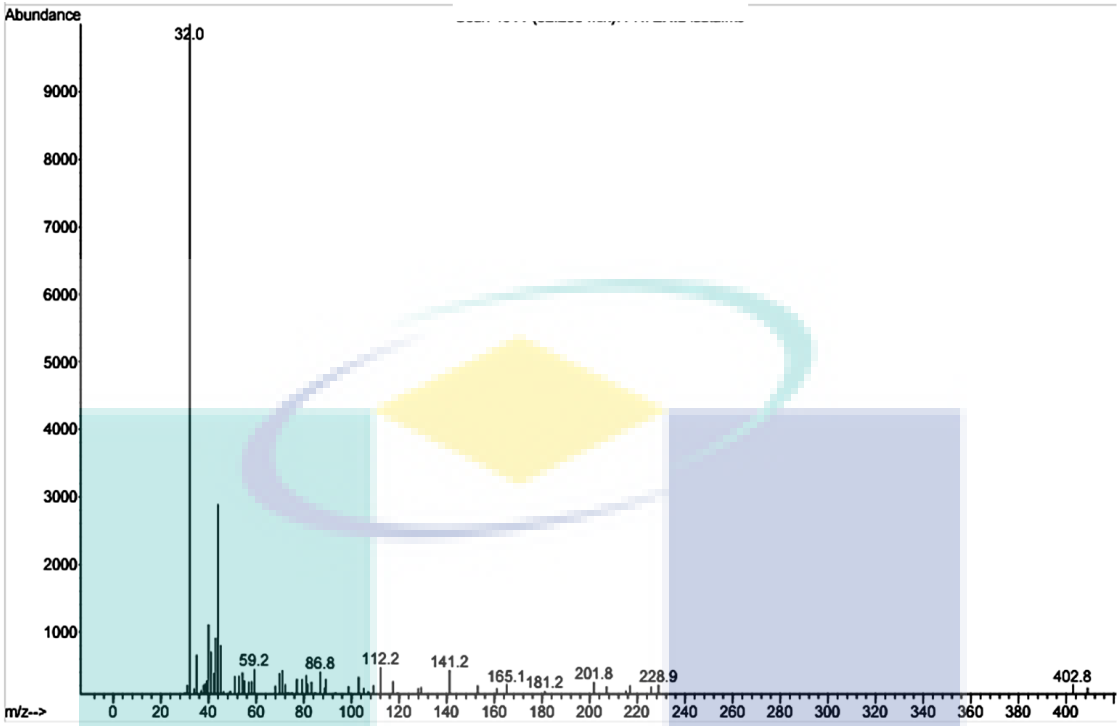

Figure 4.93 GC-MS spectrum of (*E*)-3-(2-bromo-3-hydroxy-4-methoxyphenyl)-1-(2'-hydroxy-4',6'-dimethoxyphenyl)prop-2-en-1-one (**91**)

GC-MS spectrum of compound **91** shown in Figure 4.93 shows the main fragment ions of a molecular structure at *m/z* = 409, 408, 403, 229, 207, 202, 181, 165, 141, 112, 87 and 59. The result obtained from this analysis could support the tentative of synthesized compound **91**.

4.2 Cytotoxic Effects of Flavokawain B Derivative against MCF-7 and MDA-MB-231 Breast Cancer Cell Line

3-(4,5-dimethylthiazol-2-yl)-2,5-diphenyltetrazolium bromide (MTT) assay was performed to screen the potential anti-cancer activity of the synthesized compounds against the breast cancer cell lines. Cytotoxicity of the synthesized compounds was studied by performing MTT assay in two human breast cancer cell lines that already well-documented study with different characteristics namely, MCF-7 and MDA-MB-231 for 72 hr (Moses et al., 2016).

Table 4.25 IC_{50} values of flavokawain B derivative in a cytotoxicity test against MCF-7 and MDA-MB-231 cell lines.

Compound	IC_{50} values (µg/mL)	
	MCF-7	MDA-MB-231
4	7.70 ± 0.30	5.90 ± 0.30
5	8.90 ± 0.60	6.80 ± 0.45
75	12.30 ± 1.40	18.10 ± 1.10
76	25.00 ± 1.80	21.10 ± 1.20
77	>30	>30
78	>30	>30
79	6.50 ± 0.40	4.12 ± 0.20
80	7.12 ± 0.80	4.04 ± 0.30
81	>30	9.50 ± 0.60
82	9.70 ± 0.70	8.30 ± 0.56
83	>30	>30
84	5.50 ± 0.35	5.50 ± 0.40
85	8.43 ± 0.40	7.22 ± 0.70
44	13.30 ± 3.10	17.10 ± 2.15
86	>30	>30
87	>30	>30
46	>30	>30
88	>30	>30
89	>30	27.00 ± 1.50
2	>30	20.50 ± 1.60
90	6.50 ± 0.35	14.16 ± 1.10
91	>30	>30
Doxorubicin	2.10 ± 0.10	5.05 ± 0.20

Table 4.25 shows the IC_{50} values of flavokawain B derivative when tested against MCF-7 and MDA-MB-231 using doxorubicin as the positive control and DMSO as the negative control; and the chart from Table 4.25 is shown in Appendix B. Compound **4**, **5**, **75**, **79**, **80**, **82**, **84**, **85**, **44** and **90** showed good cytotoxicity against all cell lines, whereas compound **81** exhibited better cytotoxicity against MDA-MB-231 compared to MCF-7. Compound **76** showed moderate cytotoxicity against MCF-7 and

MDA-MB-231 with an IC_{50} values of 25.00 ± 1.80 µg/mL and 21.10 ± 1.20 µg/mL, respectively. Compound **89** and **2** demonstrated moderate cytotoxicity against MDA-MB-231 with an IC_{50} values 27.00 ± 1.50 µg/mL and 20.50 ± 1.60 µg/mL, respectively. Compound **77**, **78**, **83**, **86**, **87**, **46**, **88** and **91** showed low cytotoxic effects on both MCF-7 and MDA-MB-231 cell lines, whereas compound **81**, **89** and **2** showed low cytotoxicity particularly against MCF-7 cancer cell line, rendering an IC_{50} values of more than 30 µg/mL, according to the rule established by the American National Cancer Institute (NCI) is in IC_{50} less than 30 µg/mL, the compound is considered exhibits good cytotoxicity (Zheng et al., 2000).

The results obtained from MTT assay were analyzed for structure-activity relationship study focus given on flavokawain B with heteroatom and methoxy substituents. Flavokawain B with halogen substituent in ring B has shown better biological activity than those with methoxy substituent. The results showed that the synthesized compound with chloro substituent at position 3 in ring B is more active against MCF-7 than those with chloro substituent at position 2. On the other hand, the synthesized compound with chloro substituent at 2-position in ring B are more potent against MDA-MB-231, than those with chloro substituent at position 3. Other than halogenated compounds, most chalcones with methoxy group substituent at position 2 or 3 in ring B have shown good anti-cancer activity against both cancer cell lines. In addition, it is well established that anti-cancer properties of chalcone are due to the presence of α,β-unsaturated ketone moieties and among the tested chalcone, the 2′-hydroxyl group in ring A is essential for the cytotoxicity, predominantly its anti-cancer properties.

Previous study reported that chalcones with halogen substituent at position 3 in ring B were more active than that of position 4 and improvement in inhibition of cell growth was observed when the ring B was substituted with chloro group compared to fluoro group in position 3 or 4 (Dias et al., 2013). The presence of electron-withdrawing and electron-donating group affects the α,β-unsaturated system which eventually affects the cytotoxicity (F. Jin et al., 2007). Generally, electron-donating group in ring A improves the cytotoxic properties, as it affects the acidity of the 2′-hydroxyl group in ring A, while electron donating group in ring B did not improve the IC_{50} values at 30 µg/mL. This is possibly due to the effects of electron-donating group on the α,β-

unsaturated system since α,β-unsaturated system becomes more nucleophile and the Michael receptor or protein cannot bind effectively therefore the activity decrease. In contrast, compound with electron-withdrawing groups in ring B possessing chloro and fluoro especially at position 2 and 3, have exhibited better cytotoxicity against breast cancer cell line (Mai et al., 2014). The presence of electron-withdrawing group pulled the electrons from α,β-unsaturated ketone make it more electrophilic, so the receptor (nucleophile) possibly creates a strong interation with the compound. The compound with electron-donating group such as methoxy group especially at position 3,4 or 3,5 and 2,4,6 could cause rich in nucleophilicity and resonate the α,β-unsaturated carbonyl (Nakhjiri et al., 2012), the structure become less effective eventually and binding with the Michael receptor (nucleophile) and the compounds reduce the cytotoxicity. (Bakar et al., 2018; Mai et al., 2014; Pouget et al., 2001)

The cytotoxicity results obtained from this study have proven the anti-cancer properties of flavokawain B derivative whereof chalcones with halogen substituent at position 2 and 3 in ring B have demonstrated the most potent anti-cancer activity against MCF-7 and MDA-MB-231 followed by chalcones with methoxy substituent.

CHAPTER 5

CONCLUSION

5.1 General conclusion

Chalcone and its derivative have many pharmacological properties as well as anti-cancer. Flavokawain B is a natural chalcone that can be extracted from the root of kava-kava plants and also can be synthesized by using several method. In this research project, twenty-two (**22**) flavokawain B derivative have been synthesized by reacting 2'-hydroxy-4',6'-dimethoxyacetophenone with different substituted benzaldehydes via Claisen-Schmidt condensation reaction and purification of products by column chromatography was conducted. The compounds were elucidated by using different spectroscopic techniques such as UV-Vis, FTIR, GC-MS and NMR. Among twenty-two (**22**) synthesized compounds, two compounds were found to be the new flavokawain B analogs, which are (*E*)-3-(2-fluorophenyl)-1-(2′-hydroxy-4′,6′-dimethoxyphenyl)prop-2-en-1-one (**80**) and (*E*)-3-(2-bromo-3-hydroxy-4-methoxy-phenyl)-1-(2'-hydroxy-4',6'-dimethoxyphenyl)prop-2-en-1-one (**91**). Previously, compound **80** was synthesized by Bandgar (2010) and used as the intermediate for the preparation of nitrogen-containing chalcones, however the data was not published (Bandgar et al., 2010b). All compounds were tested for their cytotoxicity against MCF-7 and MDA-MB-231.

Among the synthesized flavokawain B derivatives, compound **4** (7.70 ± 0.30 µg/mL), **5** (8.90 ± 0.60 µg/mL), **79** (6.50 ± 0.40 µg/mL), **80** (7.12 ± 0.80 µg/mL), **82** (9.70 ± 0.70 µg/mL), **84** (5.50 ± 0.35 µg/mL), **85** (8.43 ± 0.40 µg/mL) and **90** (6.50 ± 0.35 µg/mL) have demonstrated good anti-cancer activity against MCF-7 while compound **4** (5.90 ± 0.30 µg/mL), **5** (6.80 ± 0.45 µg/mL), **79** (4.12 ± 0.20 µg/mL), **80** (4.04 ± 0.30 µg/mL), **81** (9.50 ± 0.60 µg/mL), **82** (8.30 ± 0.56 µg/mL), **84** (5.50 ± 0.40

μg/mL) and **85** (7.22 ± 0.70 μg/mL) have demonstrated good anti-cancer activity against MDA-MB-231.

5.2 Recommendation

It is recommended that in future research, focus is given on compound **79** and **84** obtained in this study considering their huge potential as a good anti-cancer agent especially against breast cancer cell lines. It is also recommended to use tamoxifen as positive control in MTT assay and perform cytotoxicity test on normal cells derived from breast tissue to check on the compound selectivity.

More flavokawain B derivative should be synthesized to test on cancer cell. A mechanism study and more in depth study of structure-activity relationship between the compound derivatives and the respective anti-cancer activity should be conducted in future. Docking study and 3D QSAR study are possible to be conducted in the next study. These flavokawain B derivative can also be tested against other cancer cell line such as liver, lung, colon, prostate and many more cancer cell.

REFERENCES

Abu, N., Akhtar, M. N., Yeap, S. K., Lim, K. L., Ho, W. Y., Abdullah, M. P., Ho, C. L., Omar, A. R., Ismail, J., & Alitheen, N. B. (2016). Flavokawain B induced cytotoxicity in two breast cancer cell lines, MCF-7 and MDA-MB231 and inhibited the metastatic potential of MDA-MB231 via the regulation of several tyrosine kinases In vitro. *BMC Complementary and Alternative Medicine, 16*, 1-14. doi:10.1186/s12906-016-1046-8

Abu, N., Akhtar, M. N., Yeap, S. K., Lim, K. L., Ho, W. Y., Zulfadli, A. J., Omar, A. R., Sulaiman, M. R., Abdullah, M. P., & Alitheen, N. B. (2014). Flavokawain A induces apoptosis in MCF-7 and MDA-MB231 and inhibits the metastatic process in vitro. *PLoS One, 9*(10), 1-12. doi:10.1371/journal.pone.0105244

Abu, N., Ho, W. Y., Yeap, S. K., Akhtar, M. N., Abdullah, M. P., Omar, A. R., & Alitheen, N. B. (2013). The flavokawains: uprising medicinal chalcones. *Cancer Cell International, 13*(102), 1-7. doi:10.1186/1475-2867-13-102

Abu, N., Mohamed, N. E., Yeap, S. K., Lim, K. L., Akhtar, M. N., Zulfadli, A. J., Kee, B. B., Abdullah, M. P., Omar, A. R., & Alitheen, N. B. (2015). In Vivo Anti-Tumor Effects of Flavokawain A in 4T1 Breast Cancer Cell-Challenged Mice. *Anti-Cancer Agents in Medicinal Chemistry, 15*, 905-915.

Ahmad, M. R., Sastry, V. G., Bano, N., Anwer, S., & Kumaraswamy, G. (2011). Antioxidant and antibacterial activities of some novel chalcone derivatives and their synthesis by conventional and microwave irradiation methods. *Journal of Chemical and Pharmaceutical Research, 3*(5), 710-717.

Akhtar, M. N., Sakeh, N. M., Zareen, S., Gul, S., Lo, K. M., Ul-Haq, Z., Shah, S. A. A., & Ahmad, S. (2015). Design and synthesis of chalcone derivatives as potent tyrosinase inhibitors and their structural activity relationship. *Journal of Molecular Structure, 1085*, 97-103. doi:10.1016/j.molstruc.2014.12.073

Aksöz, B. E., & Ertan, R. (2011). Chemical and Structural Properties of Chalcones I. *FABAD Journal of Pharmaceutical Sciences, 36*, 223-242.

Al-Masum, M., Ng, E., & Wai, M. C. (2011). Palladium-catalyzed direct cross-coupling of potassium styryltrifluoroborates and benzoyl chlorides—a one step method for chalcone synthesis. *Tetrahedron Letters, 52*(9), 1008-1010. doi:10.1016/j.tetlet.2010.12.085

Ali, N. M., Akhtar, M. N., Ky, H., Lim, K. L., Abu, N., Zareen, S., Ho, W. Y., Alan-Ong, H. K., Tan, S. W., Alitheen, N. B., Ismail, J., Yeap, S. K., & Kamarul, T. (2016). Flavokawain derivative FLS induced G2/M arrest and apoptosis on breast cancer MCF-7 cell line. *Drug Design, Development and Therapy, 10*, 1897-1907. doi:10.2147/DDDT.S102164

Avupati, V. R., & Yejella, R. P. (2014). Chalcones: A Mini Review. *World Journal Of Pharmacy And Pharmaceutical Sciences, 3*(10), 1713-1742.

Bakar, A. A., Akhtar, M. N., Ali, N. M., Yeap, S. K., Quah, C. K., Loh, W.-S., Alitheen, N. B., Zareen, S., Ul-Haq, Z., & Shah, S. A. A. (2018). Design, Synthesis and Docking Studies of Flavokawain B Type Chalcones and Their Cytotoxic Effects on MCF-7 and MDA-MB-231 Cell Lines. *Molecules*, *23*(3), 1-14. doi:10.3390/molecules23030616

Bandgar, B. P., Gawande, S. S., Bodade, R. G., Totre, J. V., & Khobragade, C. N. (2010a). Synthesis and biological evaluation of simple methoxylated chalcones as anticancer, anti-inflammatory and antioxidant agents. *Bioorganic & Medicinal Chemistry*, *18*, 1364–1370. doi:10.1016/j.bmc.2009.11.066

Bandgar, B. P., Patil, S. A., Gacche, R. N., Korbad, B. L., Hote, B. S., Kinkar, S. N., & Jalde, S. S. (2010b). Synthesis and biological evaluation of nitrogen-containing chalcones as possible anti-inflammatory and antioxidant agents. *Bioorganic & Medicinal Chemistry Letters*, *20*(2), 730–733. doi:10.1016/j.bmcl.2009.11.068

Bassiouni, Y., & Faddah, L. (2012). Nanocarrier-Based Drugs: The Future Promise for Treatment of Breast Cancer. *Journal of Applied Pharmaceutical Science*, *2*(5), 225-232. doi:10.7324/japs.2012.2530

Boeck, P., Falcão, C. A. B., Leal, P. C., Yunes, R. A., Filho, V. C., Torres-Santos, E. C., & Rossi-Bergmann, B. (2006). Synthesis of chalcone analogues with increased antileishmanial activity. *Bioorganic & Medicinal Chemistry*, *14*, 1538–1545. doi:10.1016/j.bmc.2005.10.005

Boumendjel, A., Boccard, J., Carrupt, P.-A., Nicolle, E., Blanc, M., Geze, A., Choisnard, L., Wouessidjewe, D., Matera, E.-L., & Dumontet, C. (2008.). Antimitotic and Antiproliferative Activities of Chalcones: Forward Structure–Activity Relationship. *Journal of Medicinal Chemistry*, *51*(7), 2307–2310.

Cailleau, R., Olivé, M., & Cruciger, Q. V. J. (1978). Long Term Human Breast Carcinoma Cell Lines of Metastatic Origin: Preliminary Characterization. *In Vitro*, *14*(11), 911-915.

Carlo, G. D., Mascolo, N., Izzo, A. A., & Capasso', F. (1999). Minireview Flavonoids: Old And New Aspects of A Class of Natural Therapeutic Drugs. *Life Sciences*, *65*(4), 337-353.

Chauhan, S. S., Singh, A. K., Meena, S., Lohani, M., Singh, A., Arya, R. K., Cheruvu, S. H., Sarkar, J., Gayen, J. R., Datta, D., & Chauhan, P. M. S. (2014). Synthesis of novel β-carboline based chalcones with high cytotoxic activity against breast cancer cells. *Bioorganic & Medicinal Chemistry Letters*, *24*, 2820–2824. doi:10.1016/j.bmcl.2014.04.109

Chavez, K. J., Garimella, S. V., & Lipkowitz, S. (2010). Triple negative breast cancer cell lines: one tool in the search for better treatment of triple negative breast cancer. *Breast Disease*, *32*(1-2), 35-48. doi:10.3233/BD-2010-0307

Chen, Z.-H., Zheng, C.-J., Sun, L.-P., & Piao, H.-R. (2010). Synthesis of new chalcone derivatives containing a rhodanine-3-acetic acid moiety with potential anti-bacterial activity. *European Journal of Medicinal Chemistry, 45*, 5739-5743. doi:10.1016/j.ejmech.2010.09.031

Chiaradia, L. D., Mascarello, A., Purificação, M., Vernal, J., Cordeiro, M. N. S., Zenteno, M. E., Villarino, A., Nunes, R. J., Yunes, R. A., & Terenzi, H. (2008). Synthetic chalcones as efficient inhibitors of *Mycobacterium tuberculosis* protein tyrosine phosphatase PtpA. *Bioorganic & Medicinal Chemistry Letters, 18*, 6227–6230. doi:10.1016/j.bmcl.2008.09.105

Chinthala, Y., Thakur, S., Tirunagari, S., Chinde, S., Domatti, A. K., Arigari, N. K., K.V.N.S., S., Alam, S., Jonnala, K. K., Khan, F., Tiwari, A., & Grover, P. (2015). Synthesis, docking and ADMET studies of novel chalcone triazoles for anti-cancer and anti-diabetic activity. *European Journal of Medicinal Chemistry, 93*, 564-573. doi:10.1016/j.ejmech.2015.02.027

Choudhary, A. N., & Juyal, V. (2011). Synthesis of chalcone and their derivatives as antimicrobial agents. *International Journal of Pharmacy and Pharmaceutical Sciences, 3*(3), 125-128.

Comşa, Ş., Cîmpean, A. M., & Raica, M. (2015). The Story of MCF-7 Breast Cancer Cell Line: 40 years of Experience in Research. *Anticancer Research, 35*, 3147-3154.

Coşkun, D., Tekin, S., Sandal, S., & Coşkun, M. F. (2016). Synthesis, Characterization, and Anticancer Activity of New Benzofuran Substituted Chalcones. *Journal of Chemistry, 2016*, 1-8. doi:10.1155/2016/7678486

Detsi, A., Majdalani, M., Kontogiorgis, C. A., Hadjipavlou-Litina, D., & Kefalas, P. (2009). Natural and synthetic 2'-hydroxy-chalcones and aurones: synthesis, characterization and evaluation of the antioxidant and soybean lipoxygenase inhibitory activity. *Bioorganic & Medicinal Chemistry, 17*(23), 8073–8085. doi:10.1016/j.bmc.2009.10.002

Dhar, D. N. (1981). *The chemistry of chalcones and related compounds*: John Wiley & Sons.

Dharmaratne, H. R. W., Nanayakkara, N. P. D., & Khan, I. A. (2002). Kavalactones from *Piper methysticum*, and their ^{13}C NMR spectroscopic analyses. *Phytochemistry, 59*, 429–433. doi:http://dx.doi.org/10.1016/S0031-9422(01)00443-5

Dias, T. A., Duarte, C. L., Lima, C. F., Proença, M. F., & Pereira-Wilson, C. (2013). Superior anticancer activity of halogenated chalcones and flavonols over the natural flavonol quercetin. *European Journal of Medicinal Chemistry, 65*, 500-510. doi:10.1016/j.ejmech.2013.04.064

Doan, T. N., & Tran, D. T. (2011). Synthesis, Antioxidant and Antimicrobial Activities of a Novel Series of Chalcones, Pyrazolic Chalcones, and Allylic Chalcones. *Pharmacology & Pharmacy, 2*(4), 282-288. doi:10.4236/pp.2011.24036

Dyrager, C., Wickström, M., Fridén-Saxin, M., Friberg, A., Dahlén, K., Wallén, E. A. A., Gullbo, J., Grøtli, M., & Luthman, K. (2011). Inhibitors and promoters of tubulin polymerization: Synthesis and biological evaluation of chalcones and related dienones as potential anticancer agents. *Bioorganic & Medicinal Chemistry, 19*, 2659-2665. doi:10.1016/j.bmc.2011.03.005

Eddarir, S., Cotelle, N., Bakkour, Y., & Rolando, C. (2003). An efficient synthesis of chalcones based on the Suzuki reaction. *Tetrahedron Letters, 44*, 5359–5363. doi:10.1016/S0040-4039(03)01140-7

Feild, T. S., Lee, D. W., & Holbrook, N. M. (2001). Why Leaves Turn Red in Autumn. The Role of Anthocyanins in Senescing Leaves of Red-Osier Dogwood. *Plant Physiology, 127*(2), 566-574. doi:10.1104/pp.010063

Ferreyra, M. L. F., Rius, S. P., & Casati, P. (2012). Flavonoids: biosynthesis, biological functions, and biotechnological applications. *Frontiers in Plant Science, 3*, 1-15. doi:10.3389/fpls.2012.00222

Ghasemi, F., Rostami, S., Nabavinia, M. S., & Meshkat, Z. (2016). Developing Michigan Cancer Foundation 7 Cells with Stable Expression of E7 Gene of Human Papillomavirus Type 16. *Iranian Journal of Pathology, 11*(1), 41-46.

Go, M., Wu, X., & Liu, X. (2005). Chalcones: an update on cytotoxic and chemoprotective properties. *Current medicinal chemistry, 12*(4), 483-499.

Gopi, C., Dhanaraju, M. D., & Sastry, V. G. (2016). Synthesis and spectroscopic characterisation of novel bioactive molecule of 3-(2-substituted)-1H-indol-3-yl)-1-(thiophen-2yl)prop-2-en-1-one chalcone derivatives as effective anti-oxidant and anti-microbial agents. *Beni-Suef University Journal of Basic and Applied Sciences, 5*, 236–243. doi:10.1016/j.bjbas.2016.08.004

Gu, X., Ren, Z., Tang, X., Peng, H., Ma, Y., Lai, Y., Peng, S., & Zhang, Y. (2012). Synthesis and biological evaluation of bifendate–chalcone hybrids as a new class of potential P-glycoprotein inhibitors. *Bioorganic & Medicinal Chemistry, 20*, 2540–2548. doi:10.1016/j.bmc.2012.02.050

Gupta, S., Shivahare, R., Korthikunta, V., Singh, R., Gupta, S., & Tadigoppula, N. (2014). Synthesis and biological evaluation of chalcones as potential antileishmanial agents. *European Journal of Medicinal Chemistry, 81*, 359-366. doi:10.1016/j.ejmech.2014.05.034

Hans, R. H., Guantai, E. M., Lategan, C., Smith, P. J., Wan, B., Franzblau, S. G., Gut, J., Rosenthal, P. J., & Chibale, K. (2010). Synthesis, antimalarial and antitubercular activity of acetylenic chalcones. *Bioorganic & Medicinal Chemistry Letters, 20*, 942–944. doi:10.1016/j.bmcl.2009.12.062

Herencia, F., Lo, M. P., Ubeda, A., & Ferrándiz, M. L. (2002). Nitric oxide-scavenging properties of some chalcone derivatives. *Nitric oxide, 6*(2), 242-246.

Hufford, C. D., & Oguntimein, B. O. (1982). New dihydrochalcones and flavanones from uvaria angolensis. *Journal of Natural Products, 45*(3), 337-342. doi:http://pubs.acs.org/doi/pdf/10.1021/np50021a016

Jadhav, S. Y., Bhosale, R. B., Shirame, S. P., Sonawane, V. D., Hublikar, M. G., Sonawane, K. D., & Shaikh, R. U. (2013). Synthesis and Biological Evaluation of Fluoro-Hydroxy Substituted Pyrazole Chalcones as Anti-Inflammatory, Antioxidant And Antibacterial Agents. *International Journal of Pharma and Bio Sciences, 4*(2), 390-397.

Jayapal, M. R., & Sreedhar, N. Y. (2010). Anhydrous K_2CO_3 as Catalyst for the synthesis of Chalcones under Microwave Irradiation. *Journal of Pharmaceutical Sciences and Research, 2*(10), 644-647.

Jin, C., Liang, Y.-J., He, H., & Fu, L. (2013). Synthesis and antitumor activity of novel chalcone derivatives. *Biomedicine & Pharmacotherapy, 67*, 215–217. doi:10.1016/j.biopha.2010.12.010

Jin, F., Jin, X. Y., Jin, Y. L., Sohn, D. W., Kim, S.-A., Sohn, D. H., Kim, Y. C., & Kim, H. S. (2007). Structural Requirements of 2',4',6'-Tris(methoxymethoxy) chalcone Derivatives for Anti-inflammatory Activity: The Importance of a 2'-Hydroxy Moiety. *Archives of Pharmacal Research, 30*(11), 1359-1367.

Jordan, V. C. (1993). A current view of tamoxifen for the treatment and prevention of breast cancer. *British Journal of Pharmacology, 110*, 307-517.

Juvale, K., Stefan, K., & Wiese, M. (2013). Synthesis and biological evaluation of flavones and benzoflavones as inhibitors of BCRP/ABCG2. *European Journal of Medicinal Chemistry, 67*, 115-126. doi:http://dx.doi.org/10.1016/j.ejmech.2013.06.035

Kamal, A., Ramakrishna, G., Raju, P., Viswanath, A., Ramaiah, M. J., Balakishan, G., & Pal-Bhadra, M. (2010). Synthesis and anti-cancer activity of chalcone linked imidazolones. *Bioorganic & Medicinal Chemistry Letters, 20*, 4865–4869. doi:10.1016/j.bmcl.2010.06.097

Karthikeyan, C., Moorthy, N. S. H. N., Ramasamy, S., Vanam, U., Manivannan, E., Karunagaran, D., & Trivedi, P. (2015). Advances in Chalcones with Anticancer Activities. *Recent Patents on Anti-Cancer Drug Discovery, 10*, 97-115.

Kim, R. B. (2002). Drugs As P-Glycoprotein Substrates, Inhibitors, and Inducers. *Drug Metabolism Reviews, 34*(1&2), 47–54

Konieczny, M. T., Konieczny, W., Sabisz., M., Skladanowski, A., Wakieć, R., Augustynowicz-Kopeć, E., & Zwolska, Z. (2007). Acid-catalyzed synthesis of oxathiolone fused chalcones. Comparison of their activity toward various

microorganisms and human cancer cells line. *European Journal of Medicinal Chemistry, 42*, 729-733. doi:10.1016/j.ejmech.2006.12.014

Kraege, S., Stefan, K., Juvale, K., Ross, T., Willmes, T., & Wiese, M. (2016). The combination of quinazoline and chalcone moieties leads to novel potent heterodimeric modulators of breast cancer resistance protein (BCRP/ABCG2). *European Journal of Medicinal Chemistry, 117*, 212-229. doi:10.1016/j.ejmech.2016.03.067

Kumar, R., Mohanakrishnan, D., Sharma, A., Kaushik, N. K., Kalia, K., Sinha, A. K., & Sahal, D. (2010). Reinvestigation of structure-activity relationship of methoxylated chalcones as antimalarials: Synthesis and evaluation of 2,4,5-trimethoxy substituted patterns as lead candidates derived from abundantly available natural β-asarone. *European Journal of Medicinal Chemistry, 45*, 5292-5301. doi:10.1016/j.ejmech.2010.08.049

Lee, A. V., Oesterreich, S., & Davidson, N. E. (2015). MCF-7 cells-changing the course of breast cancer research and care for 45 years. *Journal of the National Cancer Institute, 107*(7), 1-4. doi:10.1093/jnci/djv073

Li, M., Tse, L. A., Chan, W.-c., Kwok, C.-h., Leung, S.-l., Wu, C., Yu, W.-c., Yu, I. T.-s., Yu, C. H.-T., & Wang, F. (2016). Evaluation of breast cancer risk associated with tea consumption by menopausal and estrogen receptor status among Chinese women in Hong Kong. *Cancer epidemiology, 40*, 73-78.

Lin, J. H., & Yamazaki, M. (2003). Role of P-Glycoprotein in Pharmacokinetics: Clinical Implications. *Clinical Pharmacokinetics, 42*(1), 59-98.

Lin, Y.-M., Zhou, Y., Flavin, M. T., Zhou, L.-M., Nie, W., & Chen, F.-C. (2002). Chalcones and flavonoids as anti-tuberculosis agents. *Bioorganic & Medicinal Chemistry, 10*(8), 2795-2802.

Liu, H., Zang, C., Fenner, M. H., Possinger, K., & Elstner, E. (2003a). PPARγ ligands and ATRA inhibit the invasion of human breast cancer cells in vitro. *Breast Cancer Research and Treatment, 79*, 63–74.

Liu, M., Wilairat, P., Croft, S. L., Tan, A. L.-C., & Go, M.-L. (2003b). Structure–Activity Relationships of Antileishmanial and Antimalarial Chalcones. *Bioorganic & Medicinal Chemistry, 11*(13), 2729-2738. doi:10.1016/s0968-0896(03)00233-5

Liu, M., Wilairat, P., & Go, M. (2001). Antimalarial alkoxylated and hydroxylated chalcones [corrected]: structure-activity relationship analysis. *Journal of Medicinal Chemistry, 44*(25), 4443. doi:10.1021/jm0101747

Loganathan, R., Radhakrishnan, A. K., Selvaduray, K. R., & Nesaretnam, K. (2015). Selective anti-cancer effects of palm phytonutrients on human breast cancer cells. *Royal Society of Chemistry, 5*(3), 1745-1753. doi:10.1039/c4ra12343c

Luo, Y., Song, R., Li, Y., Zhang, S., Liu, Z. J., Fu, J., & Zhu, H. L. (2012). Design, synthesis, and biological evaluation of chalcone oxime derivatives as potential immunosuppressive agents. *Bioorganic & Medicinal Chemistry Letters, 22*(9), 3039-3043. doi:10.1016/j.bmcl.2012.03.080

Mai, C. W., Yaeghoobi, M., Abd-Rahman, N., Kang, Y. B., & Pichika, M. R. (2014). Chalcones with electron-withdrawing and electron-donating substituents: Anticancer activity against TRAIL resistant cancer cells, structure-activity relationship analysis and regulation of apoptotic proteins. *European Journal of Medicinal Chemistry, 77*, 378-387. doi:10.1016/j.ejmech.2014.03.002

Mandge, S., Singh, H. P., Gupta, S. D., & Moorthy, N. S. N. (2007). Synthesis and Characterization of Some Chalcone Derivatives. *Trends in Applied Sciences Research, 2*(1), 52-56.

Moses, S. L., Edwards, V. M., & Brantley, E. (2016). Cytotoxicity in MCF-7 and MDA-MB-231 Breast Cancer Cells, Without Harming MCF-10A Healthy Cells. *Journal of Nanomedicine & Nanotechnology, 7*(2), 1-11. doi:10.4172/2157-7439.1000369

Mosmann, T. (1983). Rapid colorimetric assay for cellular growth and survival: Application to proliferation and cytotoxicity assays. *Journal of Immunological Methods, 65*(1), 55-63. doi:http://dx.doi.org/10.1016/0022-1759(83)90303-4

Mukherjee, S., Kumar, V., Prasad, A. K., Raj, H. G., Bracke, M. E., Olsen, C. E., Jain, S. C., & Parmar, V. S. (2001). Synthetic and biological activity evaluation studies on novel 1, 3-diarylpropenones. *Bioorganic & Medicinal Chemistry, 9*(2), 337-345.

Nakhjiri, M., Safavi, M., Alipour, E., Emami, S., Atash, A. F., Jafari-Zavareh, M., Ardestani, S. K., Khoshneviszadeh, M., Foroumadi, A., & Shafie, A. (2012). Asymmetrical 2,6-bis(benzylidene)cyclohexanones: Synthesis, cytotoxic activity and QSAR study. *European Journal of Medicinal Chemistry, 50*, 113-123. doi:10.1016/j.ejmech.2012.01.045

Narender, T., & Reddy, K. P. (2007). A simple and highly efficient method for the synthesis of chalcones by using borontrifluoride-etherate. *Tetrahedron Letters, 48*, 3177–3180. doi:10.1016/j.tetlet.2007.03.054

Nowakowska, Z. (2007). A review of anti-infective and anti-inflammatory chalcones. *European Journal of Medicinal Chemistry, 42*, 125-137. doi:10.1016/j.ejmech.2006.09.019

Ogawa, D., Hyodo, K., Suetsugu, M., Li, J., Inoue, Y., Fujisawa, M., Iwasaki, M., Takagi, K., & Nishihara, Y. (2013). Palladium-catalyzed and copper-mediated cross-coupling reaction of aryl- or alkenylboronic acids with acid chlorides under neutral conditions: efficient synthetic methods for diaryl ketones and chalcones at room temperature. *Tetrahedron, 69*, 2565-2571. doi:10.1016/j.tet.2013.01.058

Park, C.-S., Ahn, Y., Lee, D., Moond, S. W., Kim, K. H., Yamabe, N., Hwang, G. S., Jang, H. J., Lee, H., Kang, K. S., & Lee, J. W. (2015). Synthesis of apoptotic chalcone analogues in HepG2 human hepatocellular carcinoma cells. *Bioorganic & Medicinal Chemistry Letters, 25*, 5705–5707. doi:10.1016/j.bmcl.2015.10.093

Petrov, O., Ivanova, Y., & Gerova, M. (2008). $SOCl_2$/EtOH: Catalytic system for synthesis of chalcones. *Catalysis Communications, 9*(2), 315-316. doi:10.1016/j.catcom.2007.06.013

Pouget, C., Lauthier, F., Simon, A., Fagnere, C., Basly, J.-P., Delage, C., & Chulia, A.-J. (2001). Flavonoids: Structural Requirements for Antiproliferative Activity on Breast Cancer Cells. *Bioorganic& Medicinal Chemistry Letters, 11*, 3095–3097.

Prasad, Y. R., Kumar, P. R., Smiles, D. J., & Babu, P. A. (2008a). QSAR studies on chalcone derivatives as antibacterial agents against *Bacillus pumilis*. *ARKIVOC, xi*, 266-276.

Prasad, Y. R., Rao, A. L., & Rambabu, R. (2008b). Synthesis and Antimicrobial Activity of Some Chalcone Derivatives. *Journal of Chemistry, 5*(3), 461-466. doi:http://dx.doi.org/10.1155/2008/876257

Rahman, M. (2011). Chalcone: A Valuable Insight into the Recent Advances and Potential Pharmacological Activities. *Chemical Sciences Journal, 29*, 1-16.

Rao, Y. K., Fang, S.-H., & Tzeng, Y.-M. (2004). Differential effects of synthesized 2'-oxygenated chalcone derivatives: modulation of human cell cycle phase distribution. *Bioorganic & Medicinal Chemistry, 12*(10), 2679-2686. doi:10.1016/j.bmc.2004.03.014

Rapado, L. N., Freitas, G. C., Polpo, A., Rojas-Cardozo, M., Rincón, J. V., Scotti, M. T., Kato, M. J., Nakano, E., & Yamaguchi, L. F. (2014). A Benzoic Acid Derivative and Flavokawains from Piper species as Schistosomiasis Vector Controls. *Molecules, 19*, 5205-5218. doi:10.3390/molecules19045205

Reddy, M. V. B., Su, C.-R., Chiou, W.-F., Liu, Y.-N., Chen, R. Y.-H., Bastow, K. F., Lee, K.-H., & Wu, T.-S. (2008). Design, synthesis, and biological evaluation of Mannich bases of heterocyclic chalcone analogs as cytotoxic agents. *Bioorganic & Medicinal Chemistry, 16*, 7358–7370. doi:10.1016/j.bmc.2008.06.018

Rivera-Guevara, C., & Camacho, J. (2011). Tamoxifen and its new derivatives in cancer research. *Recent Patents on Anti-Cancer Drug Discovery, 6*(2), 237-245.

Rojas, J., Payá, M., Dominguez, J. N., & Ferrándiz, M. L. (2002). The Synthesis and Effect of Fluorinated Chalcone Derivatives on Nitric Oxide Production. *Bioorganic & Medicinal Chemistry Letters, 12*, 1951–1954. doi:http://dx.doi.org/10.1016/S0960-894X(02)00317-7

Roman, B. I., Ryck, T. D., Dierickx, L., Vanhoecke, B. W. A., Katritzky, A. R., Bracke, M., & Stevens, C. V. (2012). Exploration of the SAR of anti-invasive chalcones: Synthesis and biological evaluation of conformationally restricted analogues. *Bioorganic & Medicinal Chemistry, 20,* 4812–4819. doi:10.1016/j.bmc.2012.05.069

Roussaki, M., Lima, S. C., Kypreou, A.-M., Kefalas, P., Silva, A. C. d., & Detsi, A. (2012). Aurones: a promising heterocyclic scaffold for the development of potent antileishmanial agents. *International Journal of Medicinal Chemistry, 2012,* 1-8. doi:10.1155/2012/196921

Ruiz, C., Haddad, M., Alban, J., Bourdy, G., Reategui, R., Castillo, D., Sauvain, M., Deharo, E., Estevez, Y., Arevalo, J., & Rojas, R. (2011). Activity-guided isolation of antileishmanial compounds from Piper hispidum. *Phytochemistry Letters, 4*(3), 363-366. doi:10.1016/j.phytol.2011.08.001

Sabzevari, O., Galati, G., Moridani, M. Y., Siraki, A., & O'Brien, P. J. (2004). Molecular cytotoxic mechanisms of anticancer hydroxychalcones. *Chemico-Biological Interactions, 148*(1-2), 57-67. doi:10.1016/j.cbi.2004.04.004

Sekizaki, H. (1988). Synthesis of 2-Benzylidene -3(2H)-benzofuran-3-ones (Aurones) by oxidation of 2'-Hydroxychalcone with Mercury(II) Acetate. *Bulletin of the Chemical Society of Japan, 61,* 1407-1409.

Seo, Y. H., & Oh, Y. J. (2013). Synthesis of Flavokawain B and its Anti-proliferative Activity Against Gefitinib-resistant Non-small Cell Lung Cancer (NSCLC). *Bulletin of the Korean Chemical Society, 34*(12), 3782-3786. doi:10.5012/bkcs.2013.34.12.3782

Sharma, G. N., Dave, R., Sanadya, J., Sharma, P., & Sharma, K. K. (2010). Various types and management of breast cancer: an overview. *Journal of advanced pharmaceutical technology & research, 1*(2), 109-126.

Shenvi, S., Kumar, K., Hatti, K. S., Rijesh, K., Diwakar, L., & Reddy, G. C. (2013). Synthesis, anticancer and antioxidant activities of 2,4,5-trimethoxy chalcones and analogues from asaronaldehyde: Structureeactivity relationship. *European Journal of Medicinal Chemistry, 62,* 435-442. doi:10.1016/j.ejmech.2013.01.018

Siegel, R. L., Miller, K. D., & Jemal, A. (2016). Cancer statistics, 2016. *CA: A Cancer Journal for Clinicians, 66*(1), 7-30. doi:10.3322/caac.21332

Siegel, R. L., Miller, K. D., & Jemal, A. (2017). Cancer Statistics, 2017. *CA: A Cancer Journal for Clinicians, 67*(1), 7-30. doi:10.3322/caac.21387

Singh, A. K., & Gupta, B. (2015). A Novel Approach for Breast Cancer Detection and Segmentation in a Mammogram. *Procedia Computer Science, 54,* 676-682. doi:10.1016/j.procs.2015.06.079

Srinivas, K. V. N. S., Koteswara Rao, Y., Mahender, I., Das, B., Rama Krishna, K. V. S., Hara Kishore, K., & Murty, U. S. N. (2003). Flavanoids from Caesalpinia pulcherrima. *Phytochemistry*, *63*(7), 789-793. doi:10.1016/s0031-9422(03)00325-x

Srinivasarao, V., Krishna, C. R., Ramesh, M., & Parthasarathy, T. (2013). Synthesis, in vitro anticancer activity evaluation and docking investigations of novel aromatic chalcones. *Modern Chemistry, 1*(1), 1-7. doi:10.11648/j.mc.20130101.11

Syam, S., Abdelwahab, S. I., Al-Mamary, M. A., & Mohan, S. (2012). Synthesis of Chalcones with Anticancer Activities. *Molecules, 17*, 6179-6195. doi:10.3390/molecules17066179

Tadigoppula, N., Korthikunta, V., Gupta, S., Kancharla, P., Khaliq, T., Soni, A., Srivastava, R. K., Srivastava, K., Puri, S. K., & Raju, K. S. R. (2012). Synthesis and insight into the structure–activity relationships of chalcones as antimalarial agents. *Journal of Medicinal Chemistry, 56*(1), 31-45.

Tiwari, B., Pratapwar, A. S., Tapas, A. R., Butle, S. R., & Vatkar, B. S. (2010). Synthesis and Antimicrobial Activity of Some Chalcone Derivatives. *International Journal of ChemTech Research, 2*(1), 499-503.

Tran, T. D., Nguyen, T. T., Do, T. H., Huynh, T. N., Tran, C. D., & Thai, K. M. (2012). Synthesis and antibacterial activity of some heterocyclic chalcone analogues alone and in combination with antibiotics. *Molecules, 17*(6), 6684-6696. doi:10.3390/molecules17066684

Truong, V. V., Nam, T. D., Hung, T. N., Nga, N. T., Quan, P. M., Chinh, L. V., & Jung, S.-H. (2015). Synthesis and anti-proliferative activity of novel azazerumbone conjugates with chalcones. *Bioorganic & Medicinal Chemistry Letters, 25*, 5182–5185. doi:10.1016/j.bmcl.2015.09.069

Unoh, Y., Hirano, K., Satoh, T., & Miura, M. (2013). Palladium-Catalyzed Decarboxylative Arylation of Benzoylacrylic Acids toward the Synthesis of Chalcones. *The Journal of Organic Chemistry, 78*, 5096−5102. doi:10.1021/jo400716e

Valdameri, G., Gauthier, C., Terreux, R., Kachadourian, R., Day, B. J., Winnischofer, S. M. B., Rocha, M. E. M., Frachet, V., Ronot, X., Pietro, A. D., & Boumendjel, A. (2012). Investigation of chalcones as selective inhibitors of the breast cancer resistance protein: critical role of methoxylation in both inhibition potency and cytotoxicity. *Journal of Medicinal Chemistry, 55*(7), 3193-3200. doi:10.1021/jm2016528

Weldon, D. J., Saulsbury, M. D., Goh, J., Rowland, L., Campbell, P., Robinson, L., Miller, C., Christian, J., Amis, L., Taylor, N., Dill, C., Jr., W. D., Evans, S. L., & Brantley, E. (2014). One-pot synthesis of cinnamylideneacetophenones and their *in vitro* cytotoxicity in breast cancer cells. *Bioorganic & Medicinal Chemistry Letters, 24*, 3381–3384. doi:10.1016/j.bmcl.2014.05.089

Won, S.-J., Liu, C.-T., Tsao, L.-T., Weng, J.-R., Ko, H.-H., Wang, J.-P., & Lin, C.-N. (2005). Synthetic chalcones as potential anti-inflammatory and cancer chemopreventive agents. *European Journal of Medicinal Chemistry, 40*, 103–112. doi:10.1016/j.ejmech.2004.09.006

Yerragunta, V., T.Kumaraswamy, D.Suman, V.Anusha, Patil, P., & T. Samhitha. (2013). A review on Chalcones and its importance. *PharmaTutor, 1*(2), 54-59.

Zheng, Z., Zeng, W., Huang, Y., Yang, Z., Li, J., Cai, H., & Su, W. (2000). Detection of antitumor and antimicrobial activities in marine organism associated actinomycetes isolated from the Taiwan Strait, China. *FEMS Microbiology Letters, 188*, 87-91. doi:10.1111/j.1574-6968.2000.tb09173.x

Zwaagstra, M. E., Korthouwer, R. E. M., Timmerman, H., & Zhang, M.-Q. (1998). Synthesis of 3- and 5'-substituted flavone-8-carboxylic acids as 'three-armed' leukotriene *$CysLT_1$* receptor antagonists. *European Journal of Medicinal Chemistry, 33*, 95-102. doi:https://doi.org/10.1016/S0223-5234(98)80034-2

APPENDIX A1

(*E*)-1-(2'-hydroxy-4',6'-dimethoxyphenyl)-3-phenylprop-2-en-1-one (**4**)

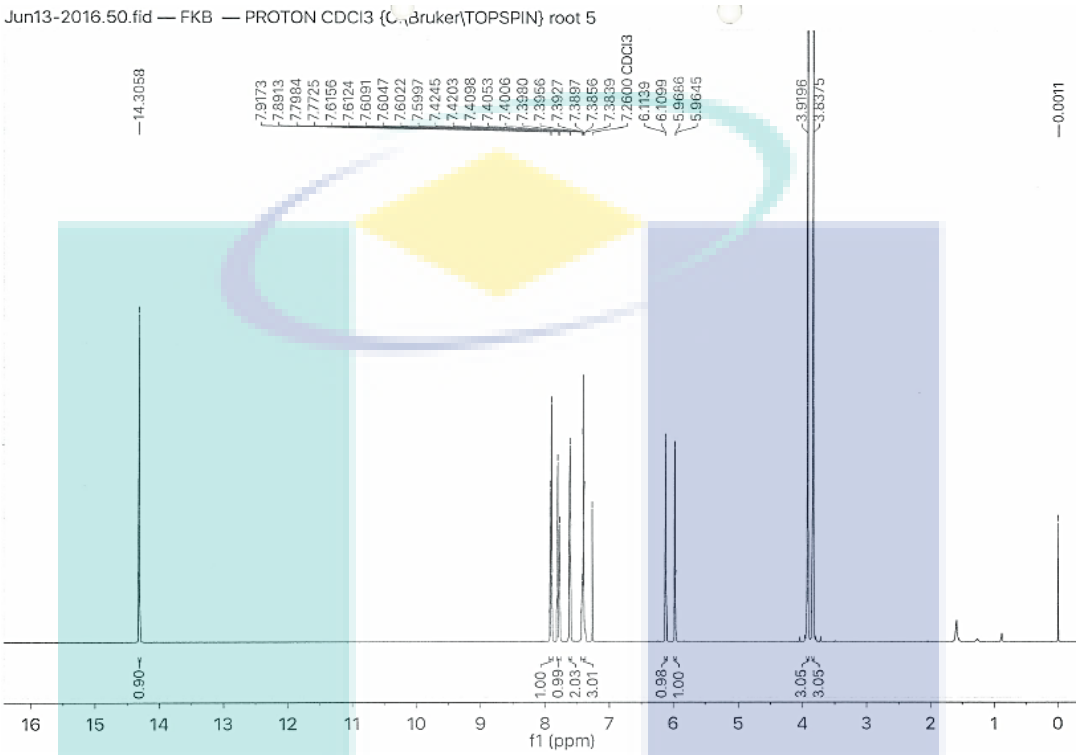

(*E*)-1-(2'-hydroxyl-4',6'-dimethoxyphenyl)-3-(4-methoxyphenyl)prop-2-en-1-one (**5**)

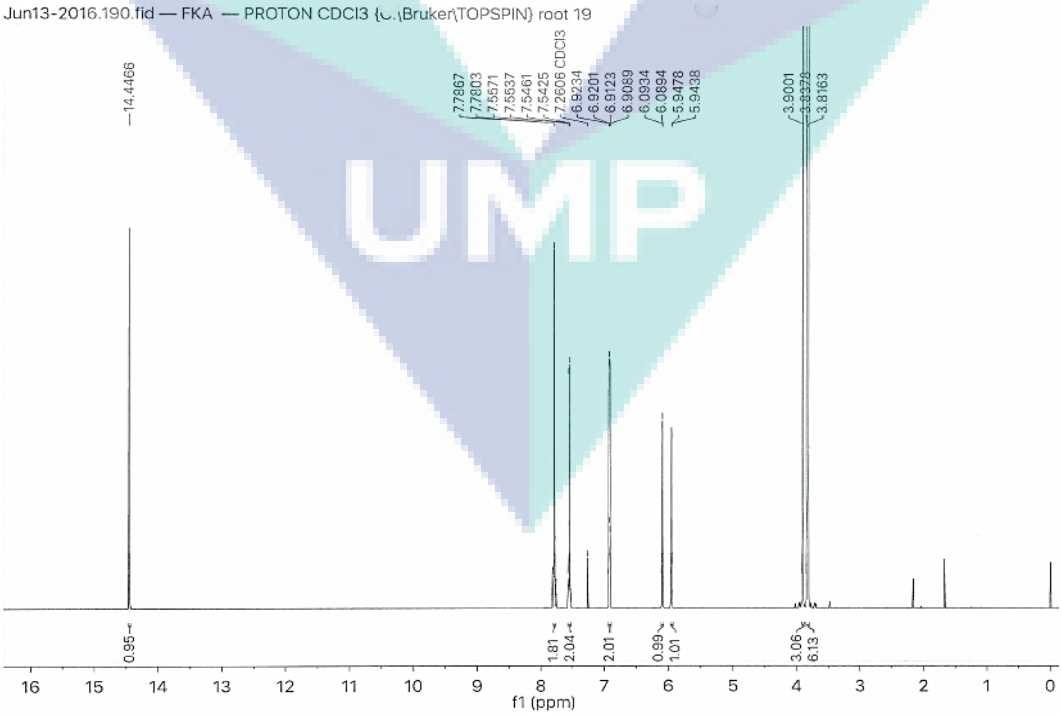

APPENDIX A2

(*E*)-1-(2'-hydroxy-4',6'-dimethoxyphenyl)-3-(4-(methylthio)phenyl)prop-2-en-1-one (**75**)

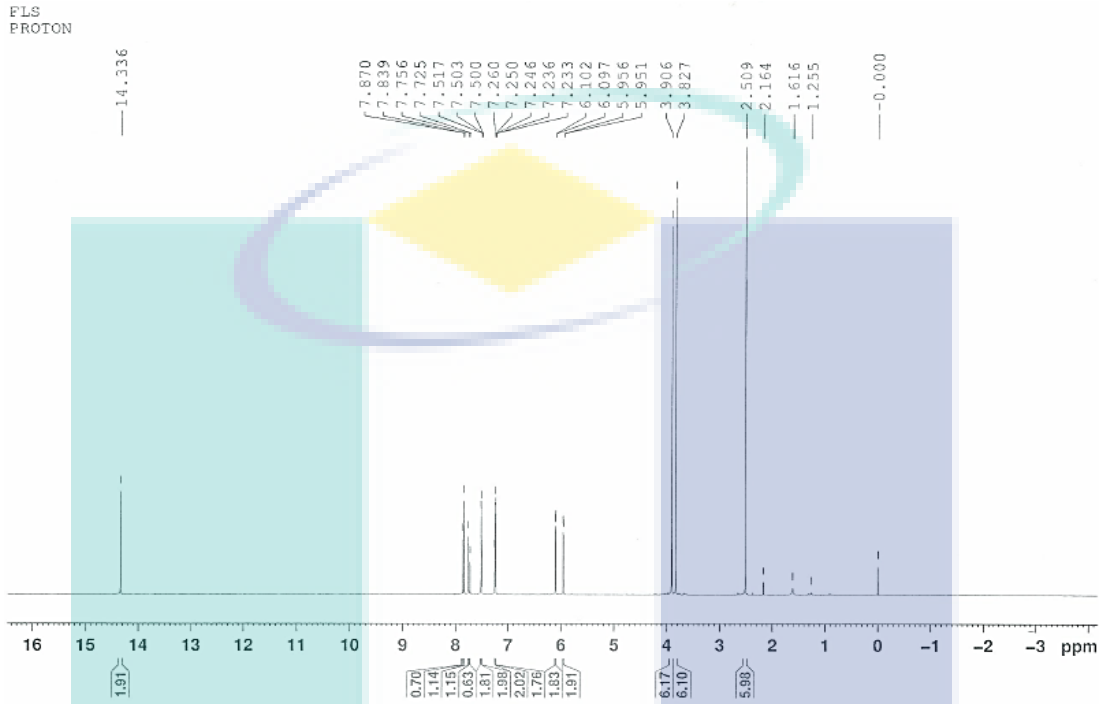

(*E*)-3-(2,3-dimethoxyphenyl)-1-(2'-hydroxy-4',6'-dimethoxyphenyl)prop-2-en-1-one (**76**)

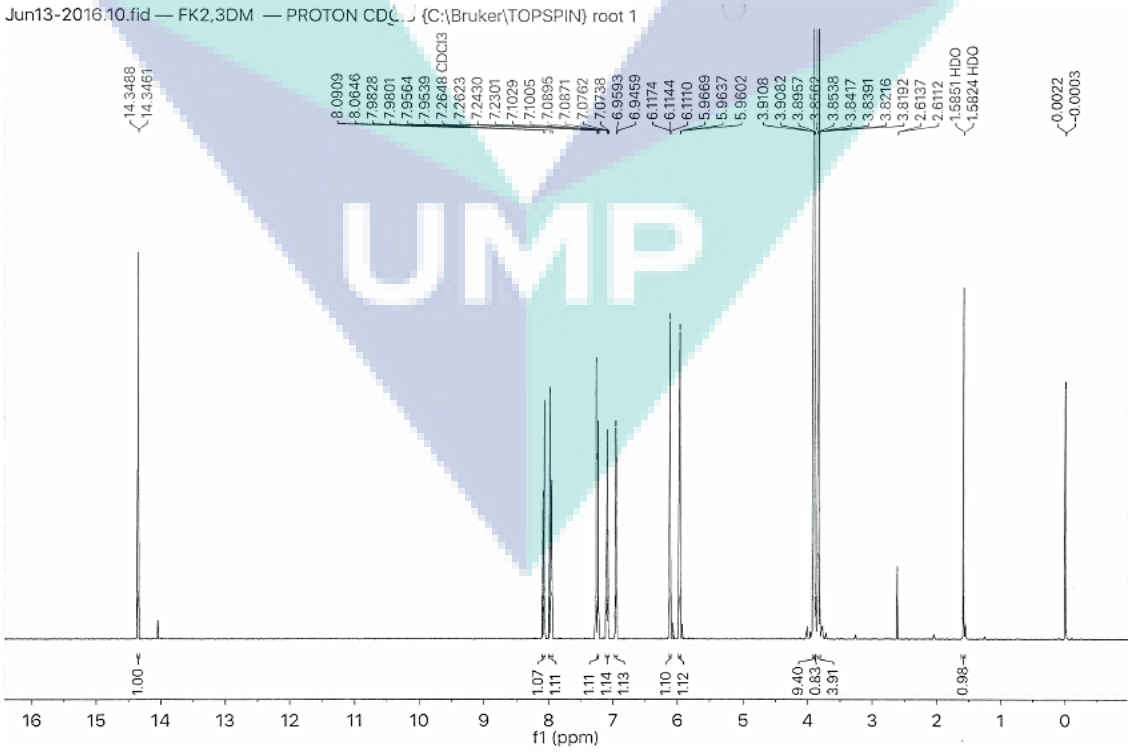

APPENDIX A3

(*E*)-1-(2'-hydroxy-4',6'-dimethoxyphenyl)-3-(2,4,6-trimethoxyphenyl)prop-2-en-1-one (**77**)

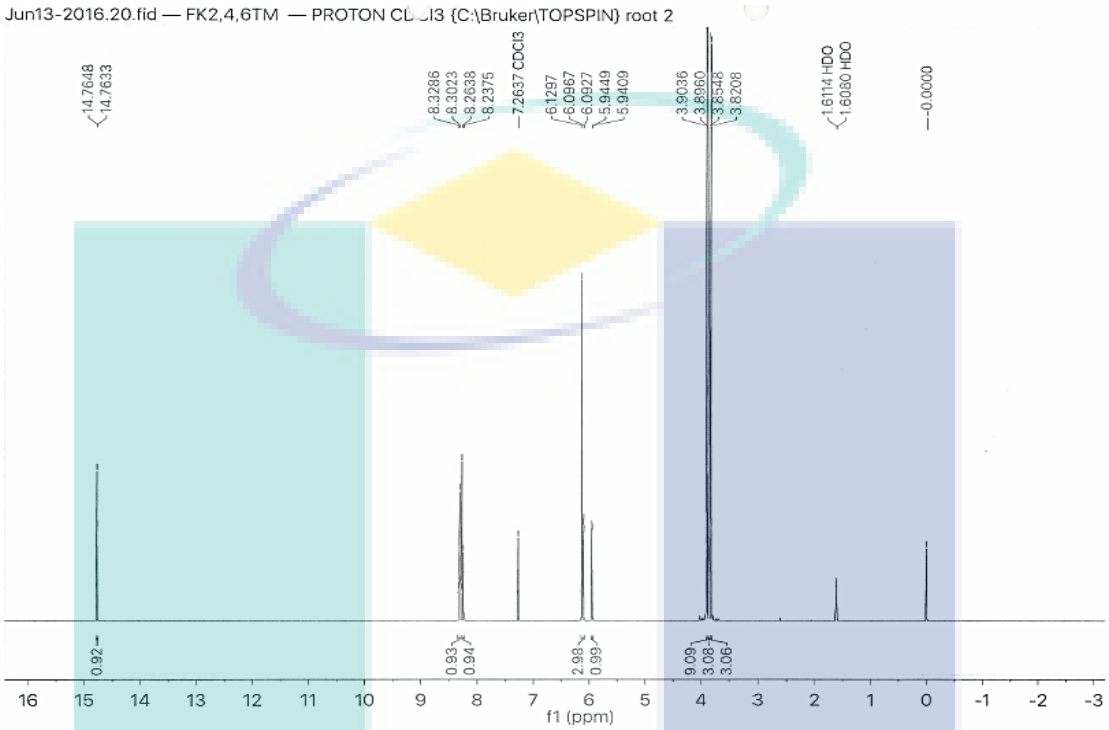

(*E*)-3-(2,4-dimethoxyphenyl)-1-(2'-hydroxy-4',6'-dimethoxyphenyl)prop-2-en-1-one (**78**)

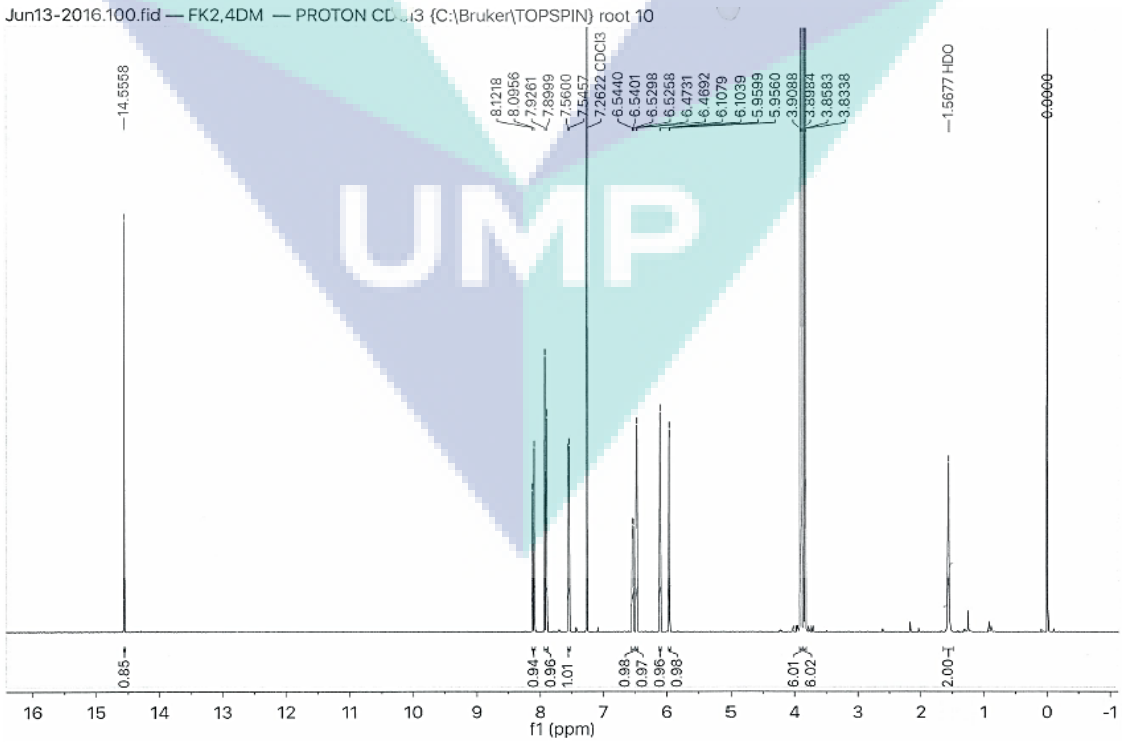

APPENDIX A4

(*E*)-3-(2-chlorophenyl)-1-(2'-hydroxy-4',6'-dimethoxyphenyl)prop-2-en-1-one (**79**)

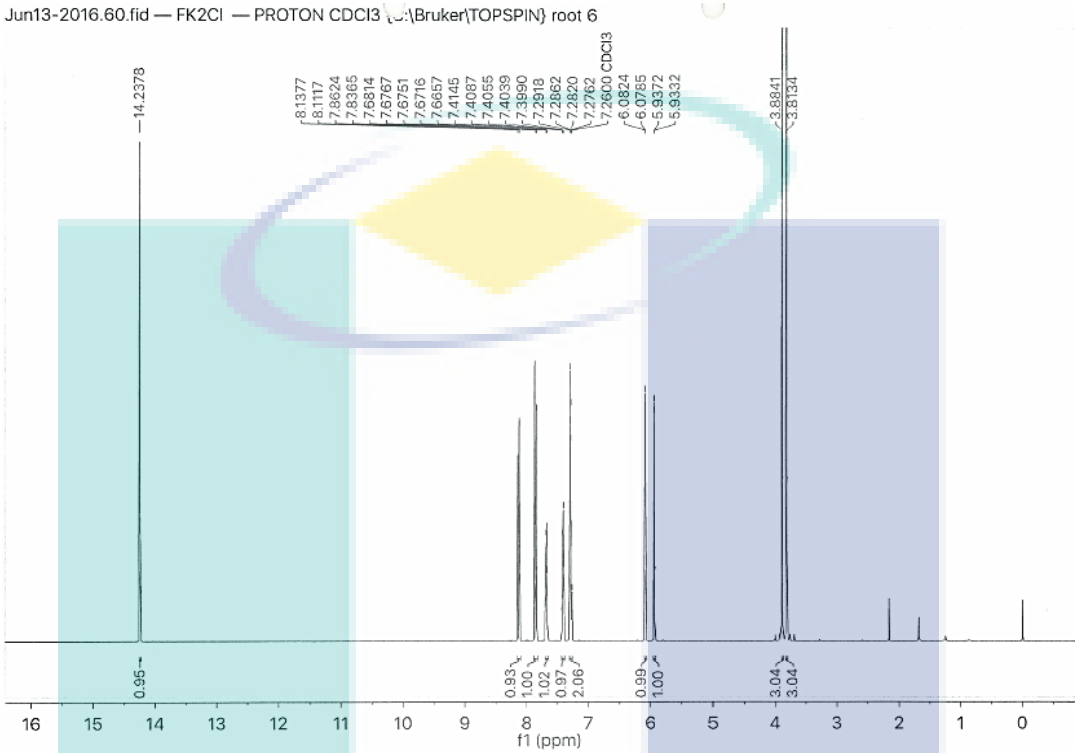

(*E*)-3-(2-fluorophenyl)-1-(2'-hydroxy-4',6'-dimethoxyphenyl)prop-2-en-1-one (**80**)

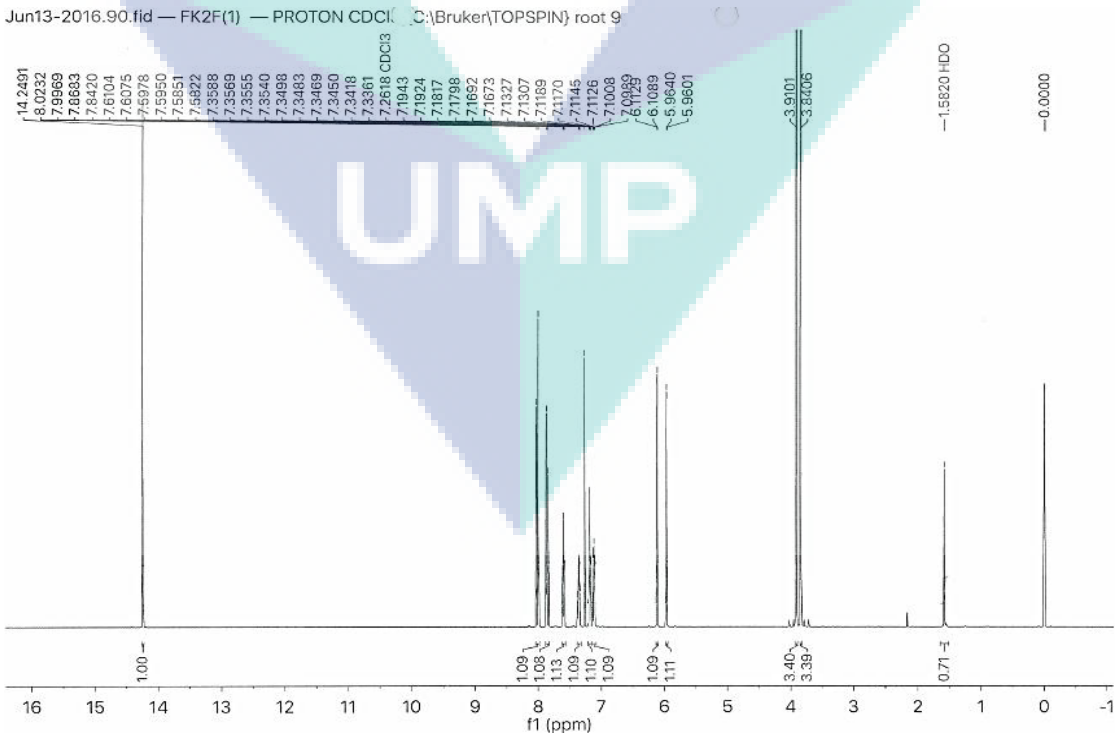

APPENDIX A5

(*E*)-1-(2'-hydroxy-4',6'-dimethoxyphenyl)-3-(2-methoxyphenyl)prop-2-en-1-one (**81**)

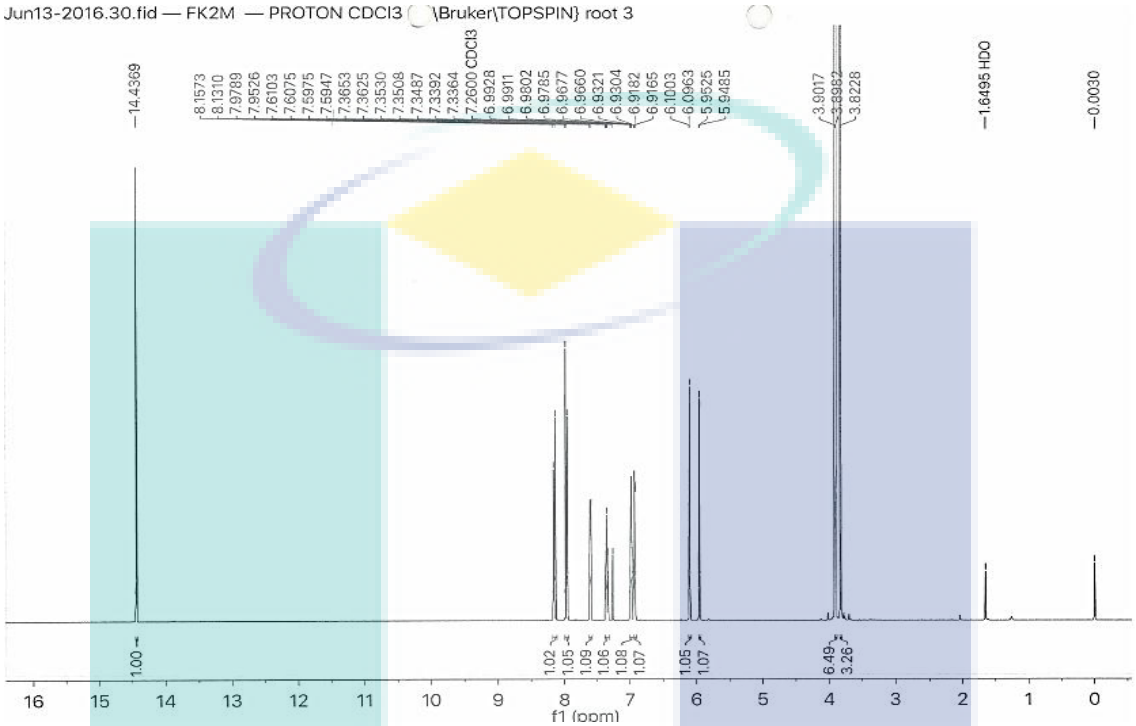

(*E*)-3-(3,4-dimethoxyphenyl)-1-(2'-hydroxy-4',6'-dimethoxyphenyl)prop-2-en-1-one (**82**)

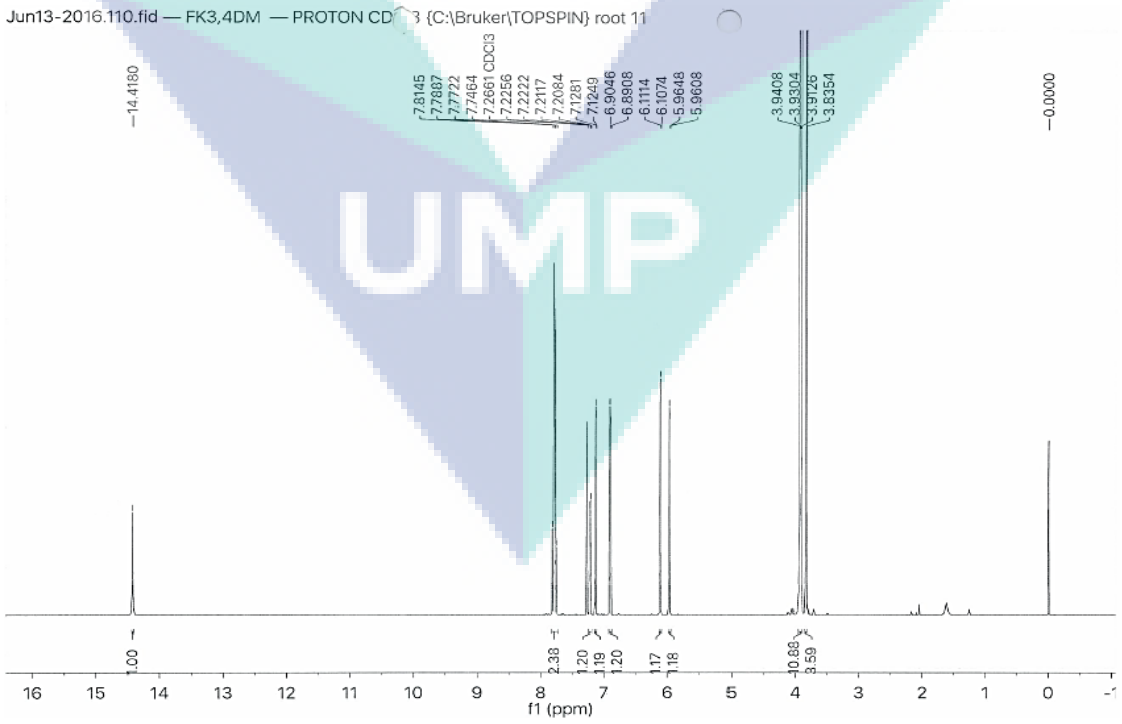

APPENDIX A6

(*E*)-3-(3,5-dimethoxyphenyl)-1-(2'-hydroxy-4',6'-dimethoxyphenyl)prop-2-en-1-one (**83**)

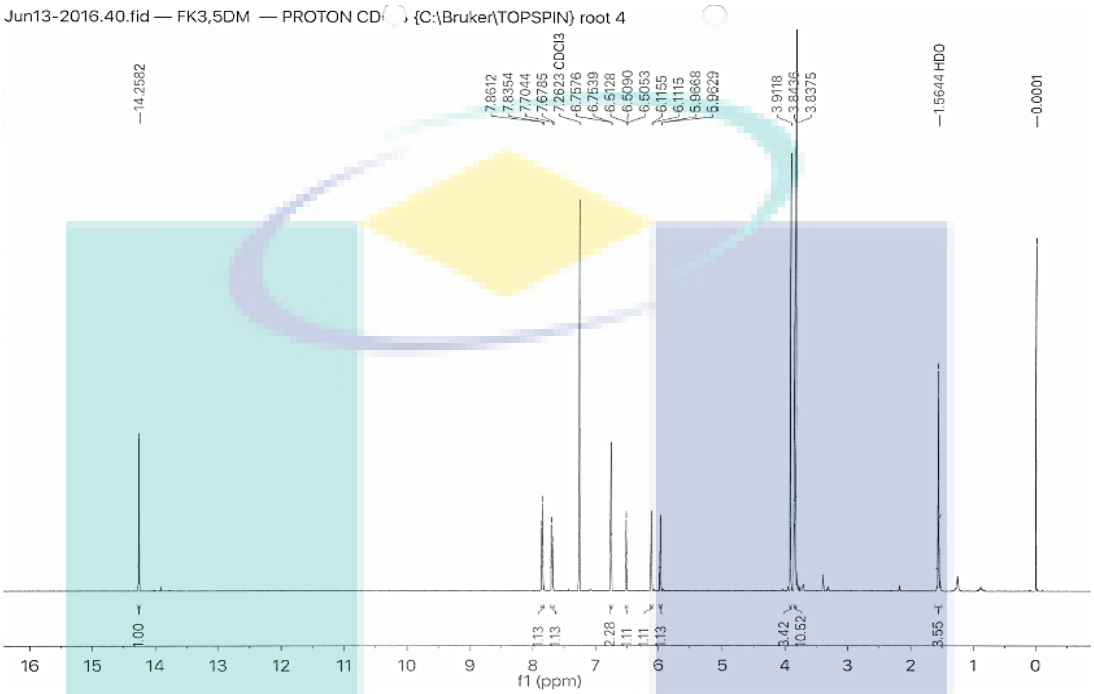

(*E*)-3-(3-chlorophenyl)-1-(2'-hydroxy-4',6'-dimethoxyphenyl)prop-2-en-1-one (**84**)

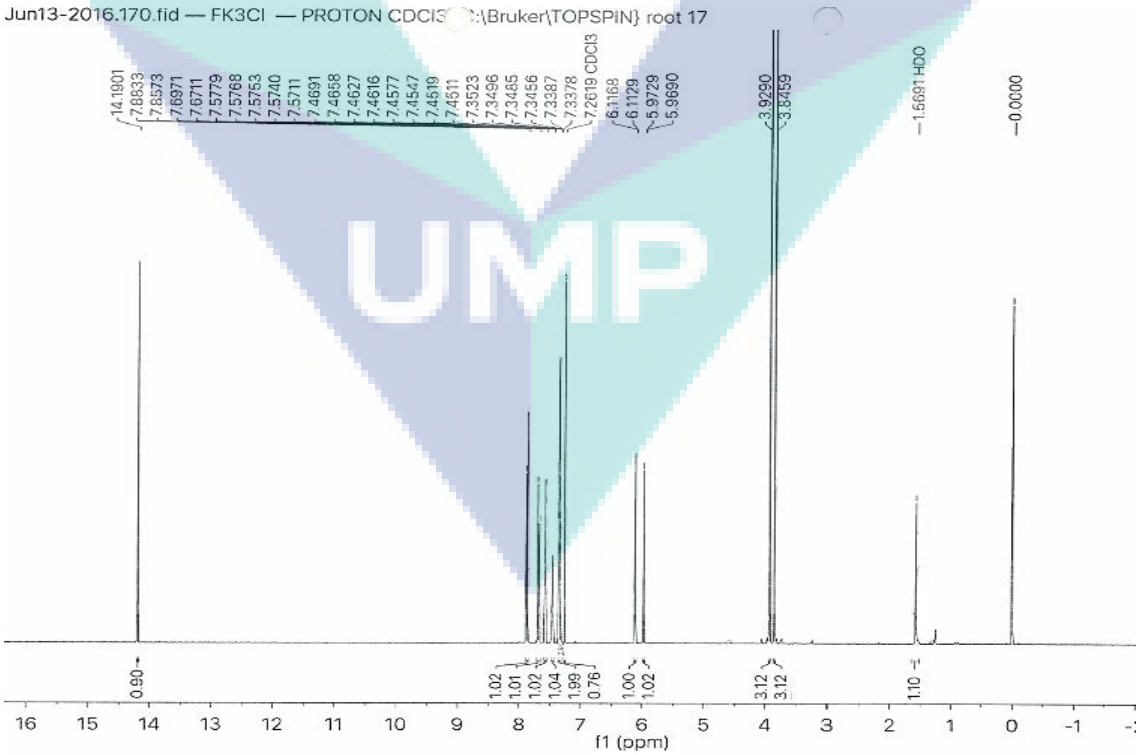

APPENDIX A7

(*E*)-1-(2'-hydroxy-4',6'-dimethoxyphenyl)-3-(3-methoxyphenyl)prop-2-en-1-one (**85**)

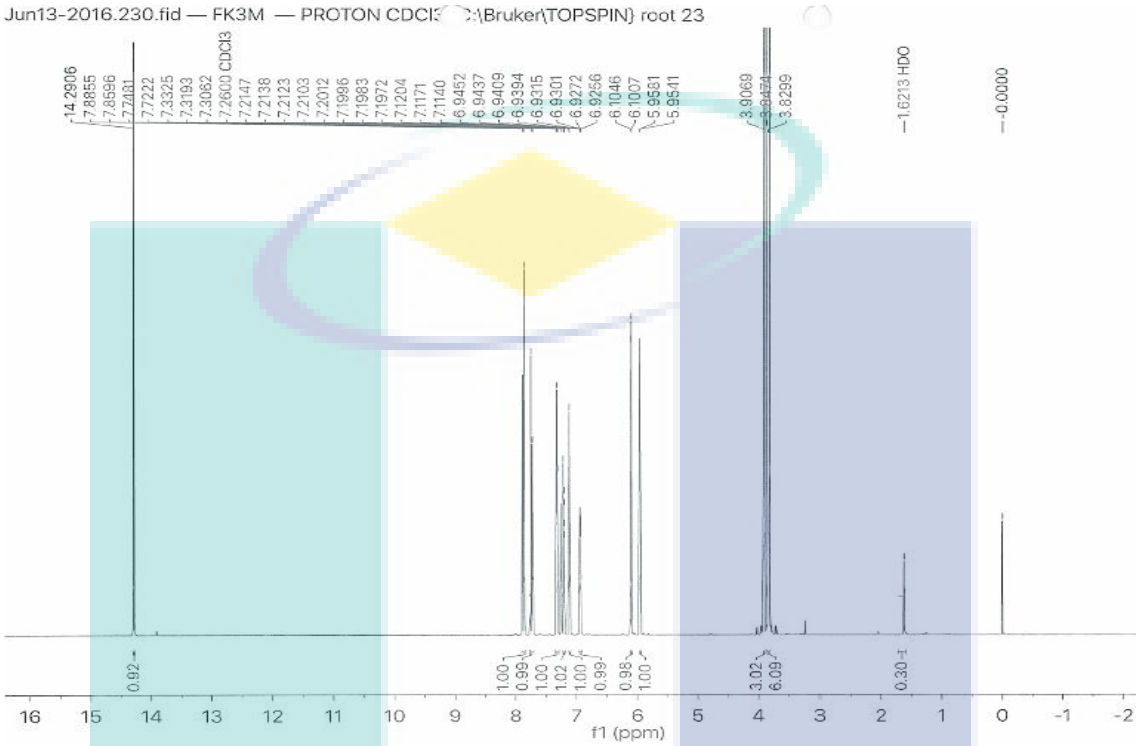

(*E*)-1-(2'-hydroxy-4',6'-dimethoxyphenyl)-3-(3-nitrophenyl)prop-2-en-1-one (**44**)

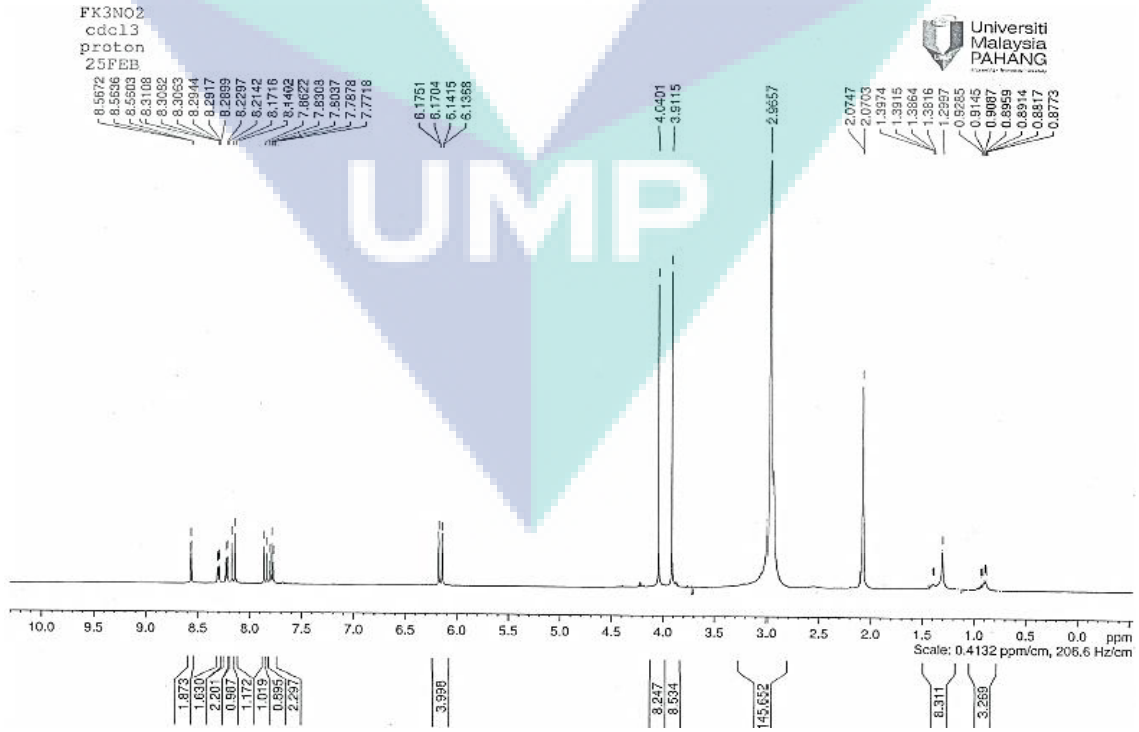

APPENDIX A8

(*E*)-3-(4-bromophenyl)-1-(2'-hydroxy-4',6'-dimethoxyphenyl)prop-2-en-1-one (**86**)

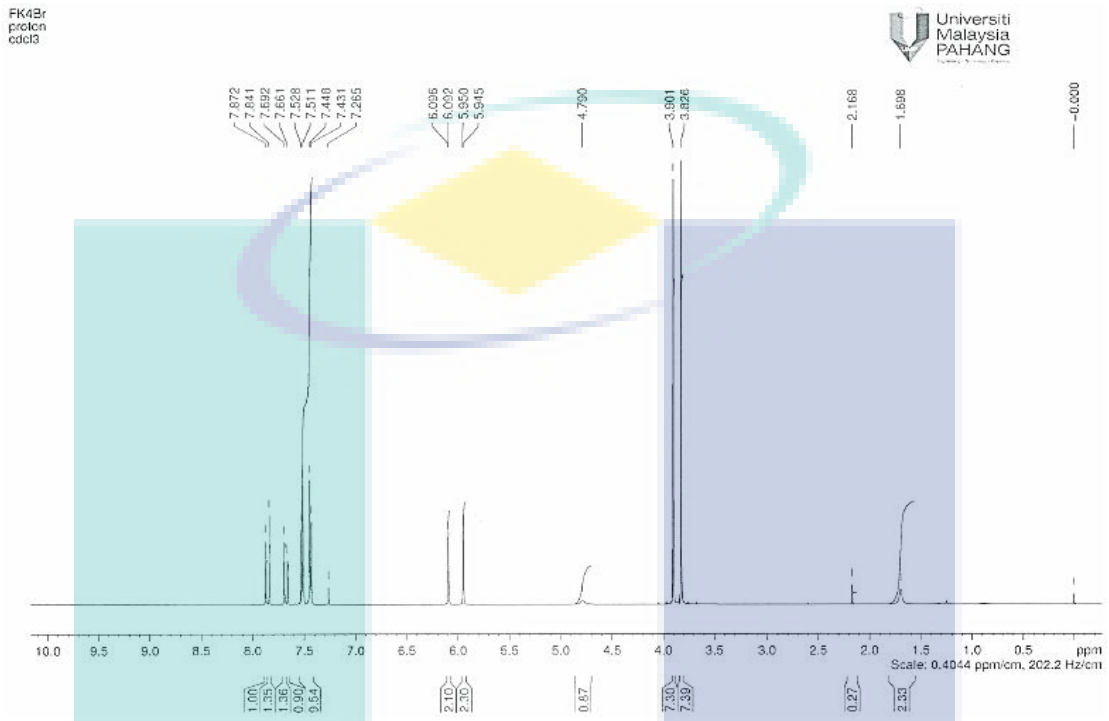

(*E*)-3-(4-chlorophenyl)-1-(2'-hydroxy-4',6'-dimethoxyphenyl)prop-2-en-1-one (**87**)

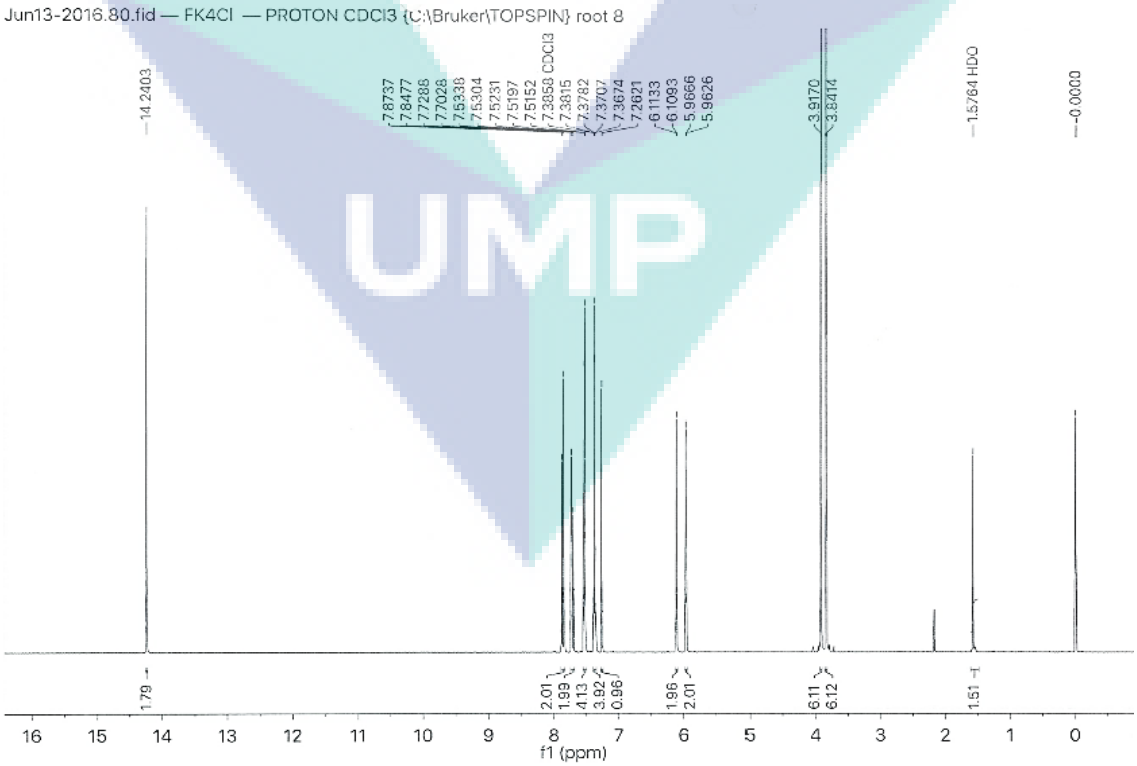

APPENDIX A9

(*E*)-3-(4-fluorophenyl)-1-(2'-hydroxy-4',6'-dimethoxyphenyl)prop-2-en-1-one (**46**)

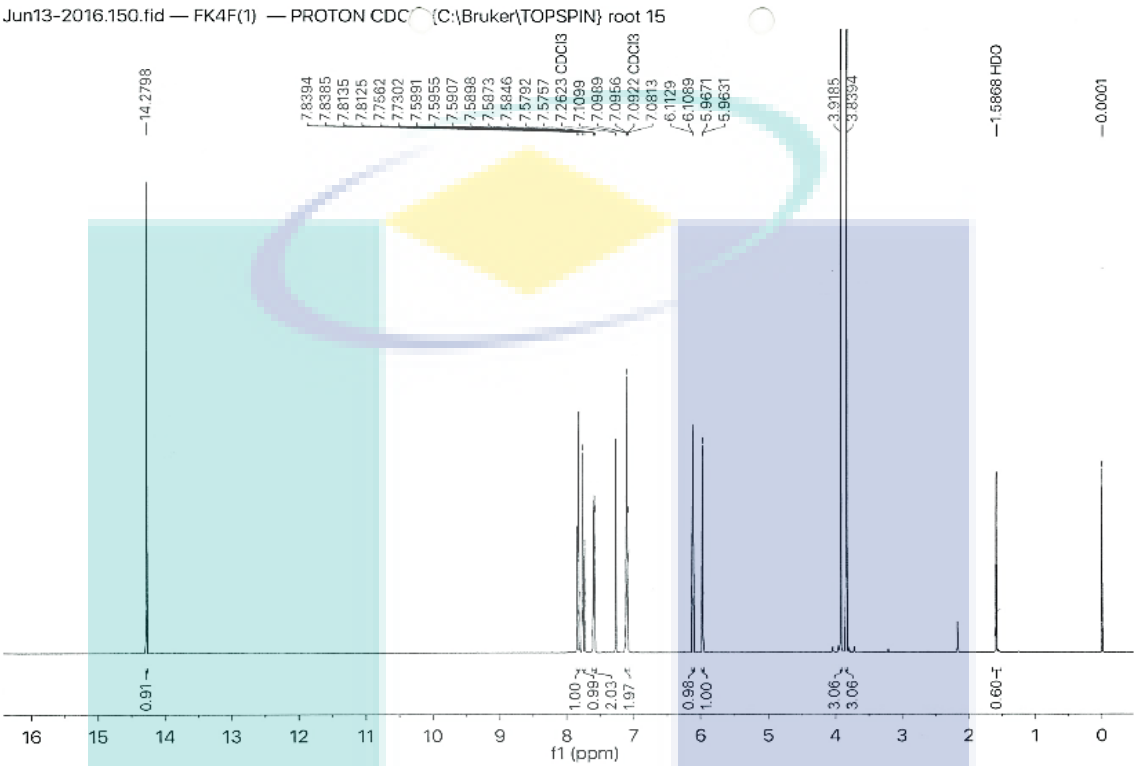

(*E*)-1-(2'-hydroxy-4',6'-dimethoxyphenyl)-3-(p-tolyl)prop-2-en-1-one (**88**)

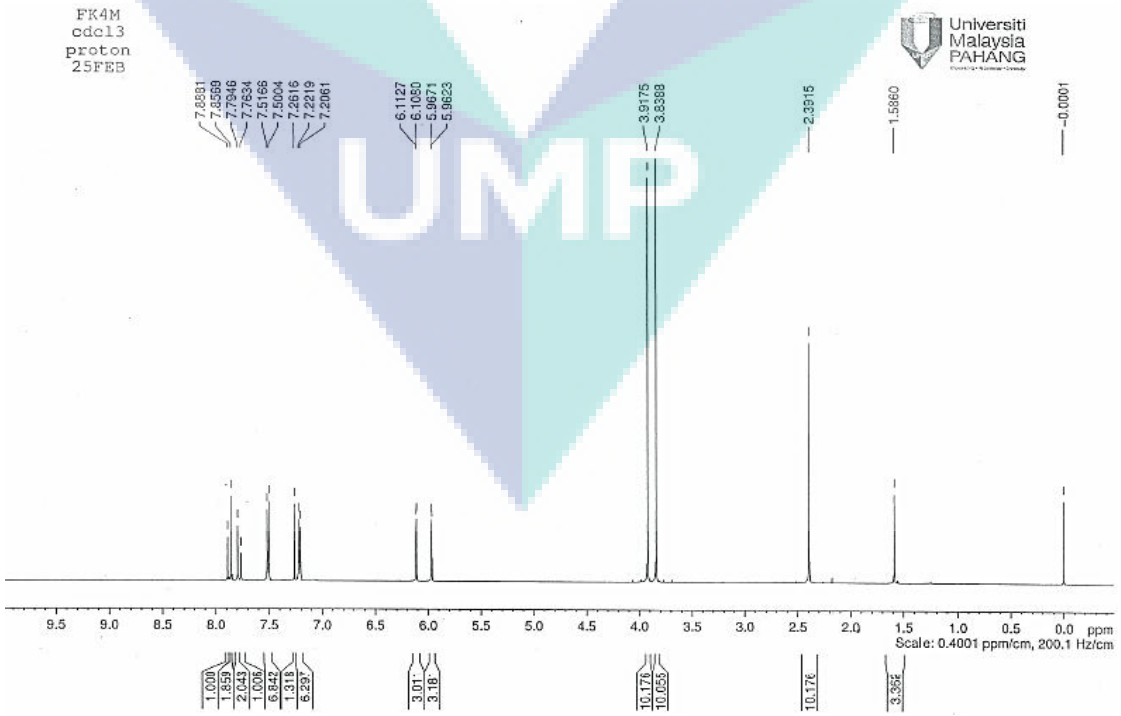

APPENDIX A10

(*E*)-3-(4-hydroxy-3-methoxyphenyl)-1-(2'-hydroxy-4',6'-dimethoxyphenyl)prop-2-en-1-one (8**9**)

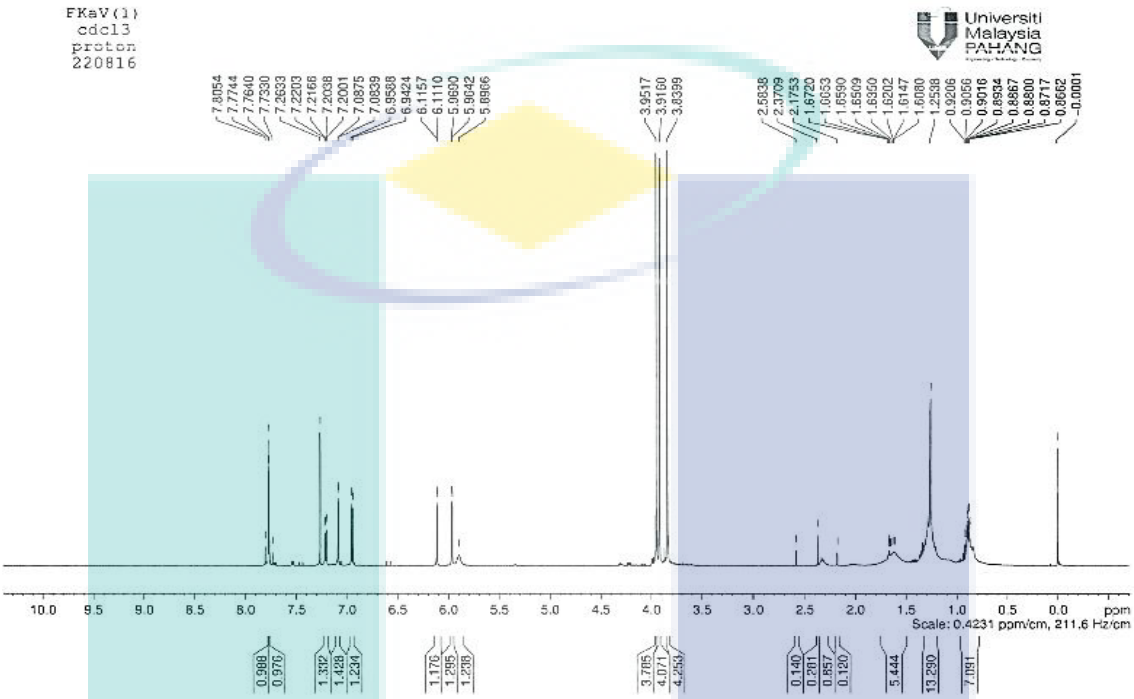

(*E*)-3-(4-(dimethylamino)phenyl)-1-(2'-hydroxy-4',6'-dimethoxyphenyl)prop-2-en-1-one (**2**)

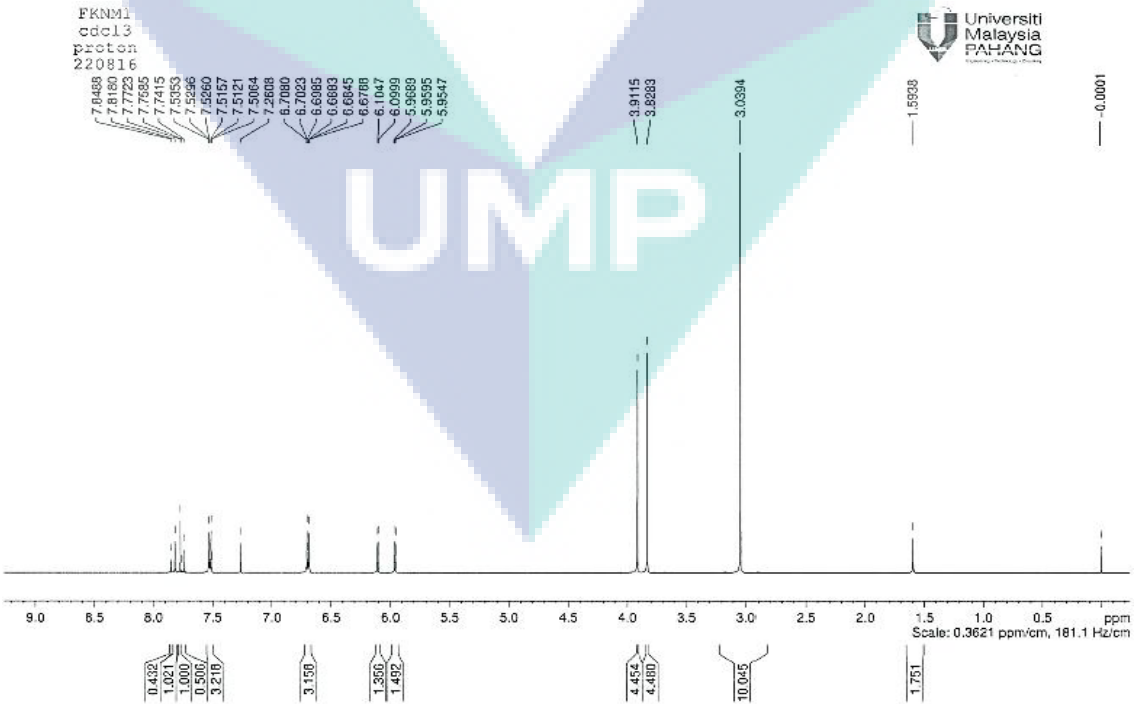

APPENDIX A11

(*E*)-3-(5-bromo-2-hydroxyphenyl)-1-(2'-hydroxy-4',6'-dimethoxyphenyl)prop-2-en-1-one (**90**)

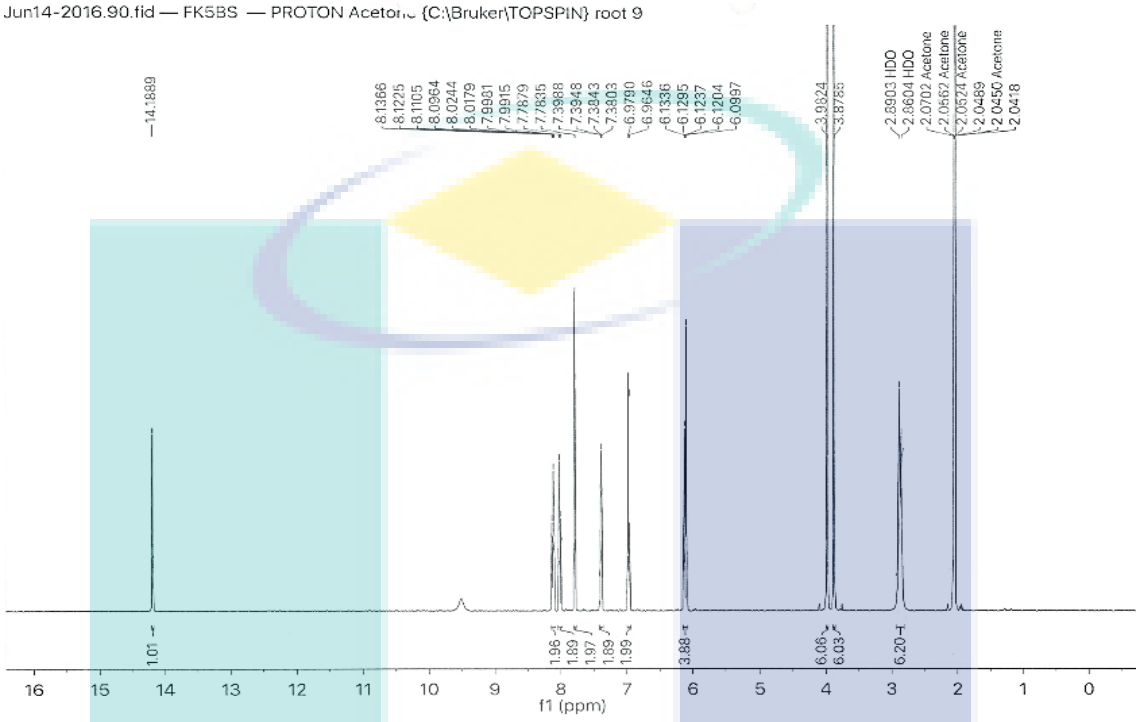

(*E*)-3-(2-bromo-3-hydroxy-4-methoxyphenyl)-1-(2'-hydroxy-4',6'-dimethoxyphenyl)prop-2-en-1-one (**91**)

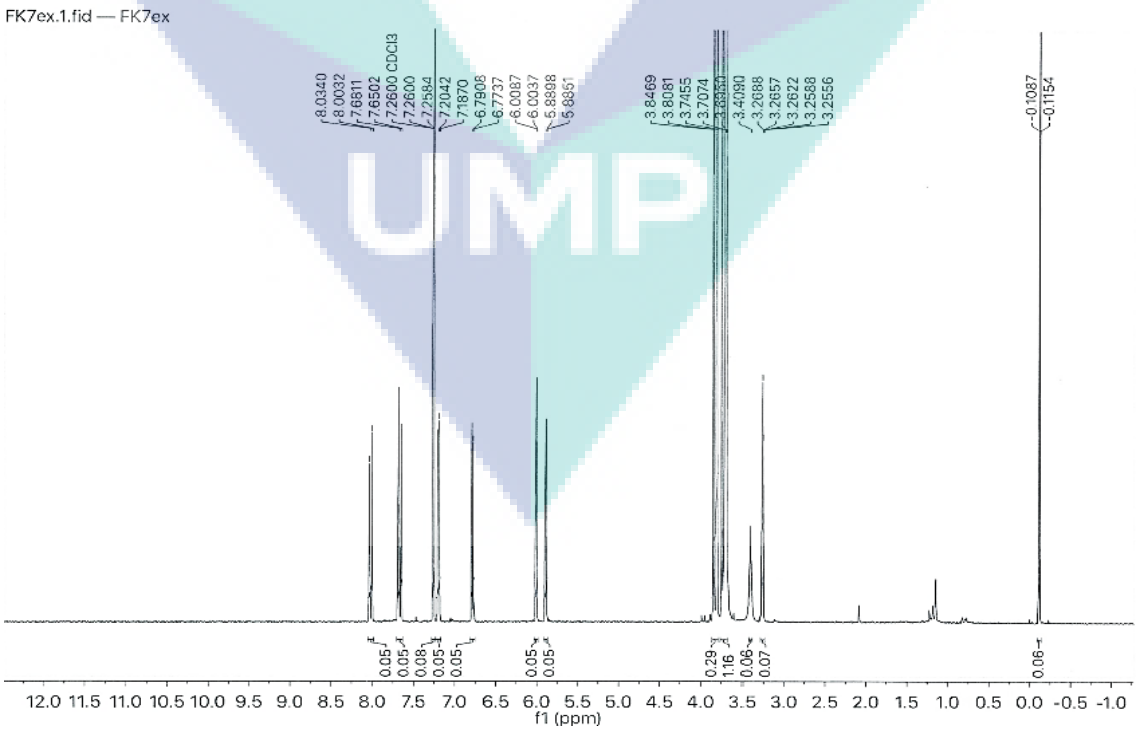

APPENDIX B

Chart of IC_{50} values of Flavokawain B derivative in a cytotoxicity test against MCF-7.

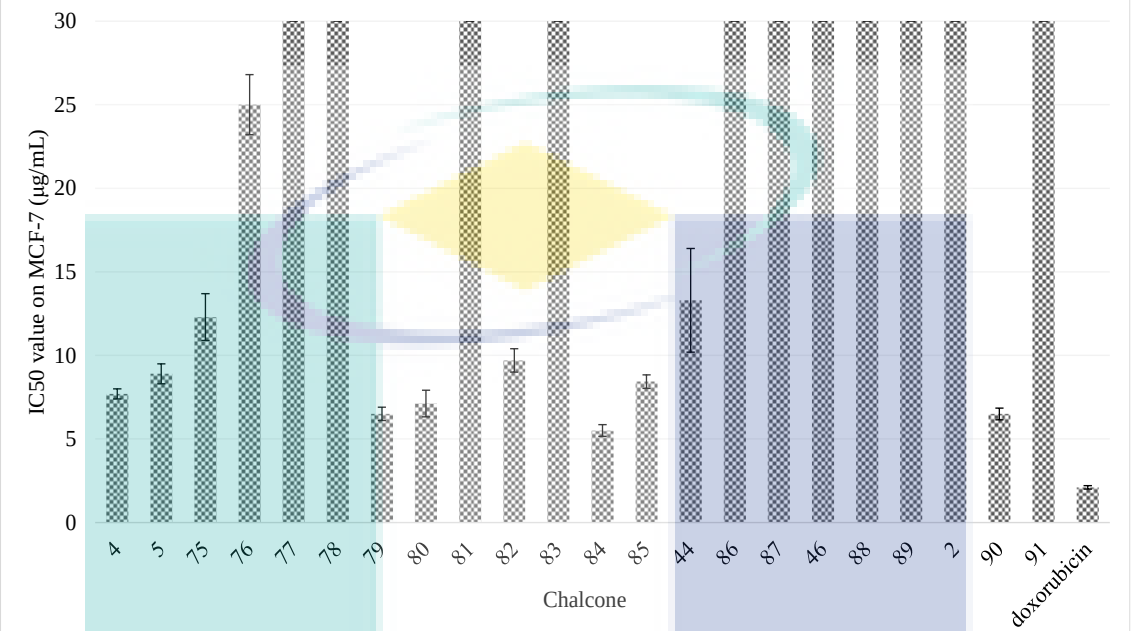

- Chalcone 77, 78, 81, 83, 86, 87, 46, 88, 89, 2, 91 have >30 µg/mL IC_{50} value on MCF-7

Chart of IC_{50} values of Flavokawain B derivative in a cytotoxicity test against MDA-MB-231.

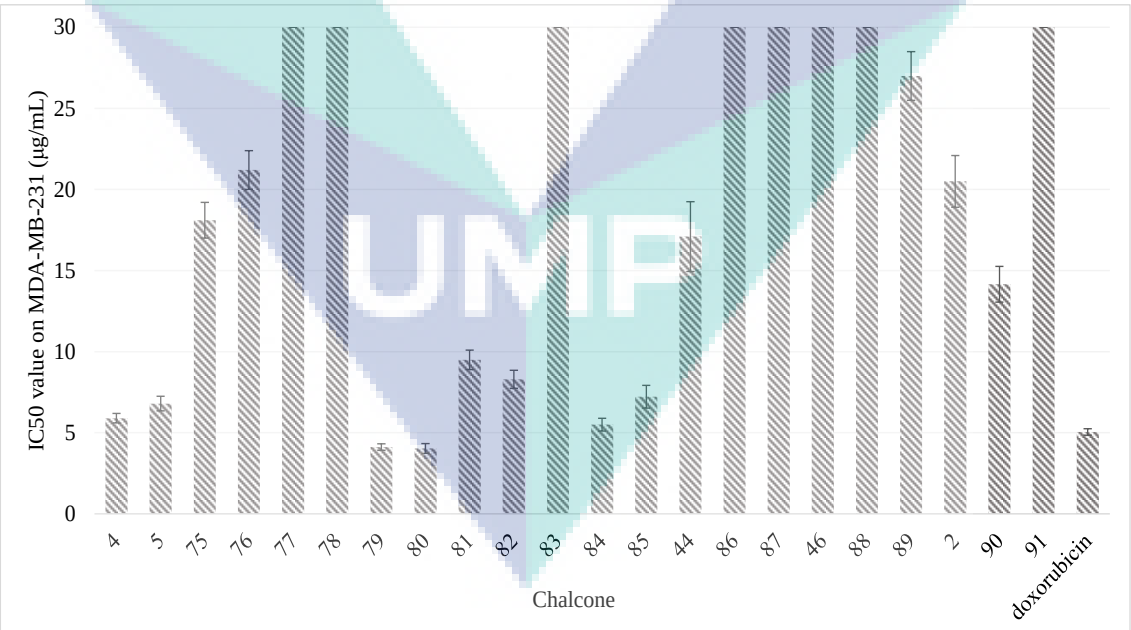

- Chalcone 77, 78, 83, 86, 87, 46, 88, 91 have >30 µg/mL IC_{50} value on MDA-MB-231

APPENDIX C

Appendix C1: List of Publications

1. Bakar, A.A., Akhtar, M.N., Ali, N.M., Yeap, S.K., Quah, C.K., Loh, W.S., Alitheen, N.B., Zareen, S., Ul-Haq, Z. and Shah, S.A.A. 2018. Design, Synthesis and Docking Studies of Flavokawain B Type Chalcones and Their Cytotoxic Effects on MCF-7 and MDA-MB-231 Cell Lines. Molecules, 23, 1-14.
2. Akhtar, M.N., Salim, L.Z.A., Yeap, S.K., Abu, N., Zareen, S., Lo, K.M. and Bakar, A.A. 2017. Synthesis and cytotoxic effects of (E)-3-(2,3-dimethoxyphenyl)-1-(5-methylfuran-2-yl)prop-2-en-1-one in MDA-MB-231 and MCF-7 breast cancer cell lines. Phytochemistry Letters, 19, 145-150.

Appendix C2: List of Conference

1. International Conference in Organic Synthesis 2016, (ICOS 2016). Synthesis of flavokawain A derivatives and their effects on breast cancer MCF-7 and MDA-MB-231 cell lines, Kuching, Sarawak. 21st-24th August 2016. Oral Presentation.

Appendix C3: List of Award

1. Synthesis of Flavokawain B Type Cytotoxic Products for the Breast Cancer Cell Lines. Creation Innovation Technology & Research Exposition (Citrex 2017). Universiti Malaysia Pahang, Kuantan. **(Bronze Medal)**